AD-A054 193 UNIVERSITY OF BOTSWANA LESOTHO AND SWAZILAND ROMA (L--ETC F/G 20/14
TRANS-EQUATORIAL TRANSMISSIONS AT VERY HIGH FREQUENCY.(U)
SEP 73 E H CARMAN, M P HEERAN F61052-67-C-0003
UNCLASSIFIED RADC-TR-73-383 NL

1 OF 2
AD A054193

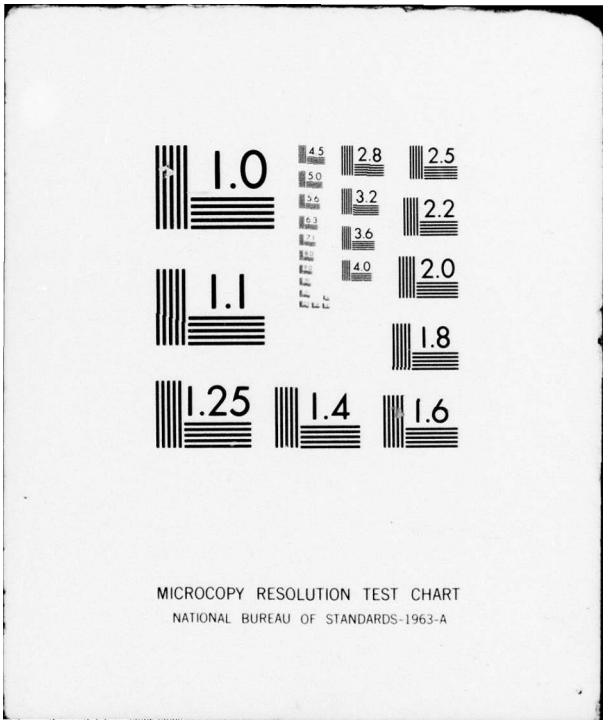
1.0
1.1
1.25
1.4
1.6
1.8
2.0
2.2
2.5
2.8
3.2
3.6
4.0
4.5
5.0
5.6
6.3
7.1
MICROCOPY RESOLUTION TEST CHART
NATIONAL BUREAU OF STANDARDS-1963-A

1974

RADC-TR-73-383
Final Technical Report
September 1973

TRANSEQUATORIAL TRANSMISSIONS AT VERY HIGH FREQUENCY

University of Botswana

Rome Air Development Center
Air Force Systems Command
Griffiss Air Force Base, New York

TRANSEQUATORIAL TRANSMISSIONS AT VERY HIGH FREQUENCY

E. H. Carman
M. P. Heeran
with

An Appendix by M. A. Anastassiadis & D. Antoniadis

University of Botswana

TRANS-EQUATORIAL TRANSMISSIONS

AT VERY HIGH FREQUENCY

APPROVED: Marvin R. Clinch

MARVIN R. CLINCH
Project Engineer

APPROVED: Franz H. Dettmer

FRANZ H. DETTMER
Colonel, USAF
Chief, Intel & Recon Div

FOR THE COMMANDER: Carlo P. Crocetti

CARLO P. CROCETTI
Chief, Plans Office

ABSTRACT

Long range VHF transequatorial propagation (TEP) experiments between Greece and Southern Africa on 34, 40 and 45.1 MHz, in progress since 1967, have an equinoctial character regarding occurrence and strength. Studies of fading characteristics and topside electron density profiles lead to the conclusions that phase coherent signals are most likely at least 2-hop great-circle F-transmissions, while other afternoon and evening types, including flutter signal, which is strongly related to equatorial spread-F, are off great-circle supermodes involving two reflections from the F-layer without intermediate ground reflection. The transmissions have a strong solar-geophysical relationship with a close sunspot number dependence. Correlation with sudden ionospheric disturbances indicates periodic solar dependent defocussing of TEP signal by the lower ionosphere. The combined effects of neutral winds and the position of the magnetic equator control seasonal behaviour.

TABLE OF CONTENTS

LIST OF FIGURES

ACKNOWLEDGMENTS

The Authors express their sincere gratitude to Professor Michael A. Anastassiadis for providing personnel and facility in the operation of the transmitting equipment for the present contract effort. Professor Anastassiadis was a co-principal investigator for the project. However, the analysis presented in this Report is the work of the present Authors except where indicated below. A related experiment, carried out by Anastassiadis and Antoniadis[1] outside the contract effort, already reported is reproduced in Appendix I.

The Authors are indebted to Dr. G.E.K. Lockwood, Dr. J.G. Caldwell and Mrs. E. Hewens of the Communications Research Centre, Ottawa, Canada for their generous production of electron density profiles.

Mr. J. Rottger of Max Planck Institute, Lindau, Germany collaborated in the experiments and analysis of Chapter 4.3.

The preliminary airglow data presented in Chapter 7 resulted from a collaboration between the present authors, Professor N.J. Skinner and Professor R.W.H. Stevenson.

1. INTRODUCTION

1.1 Experimental Program

A series of long range VHF transequatorial propagation (TEP) experiments between Europe and Southern Africa began in 1967. The program consists of (i) CW transmissions beginning each hour of the day for a period of five minutes from Athens, Greece (lat. 37.7°N, long. 24.0°E) at 34 and 45.1 MHz, the signals being recorded at Roma, Lesotho (lat. 29.7°S, long. 27.7°E), (ii) two-way pulse transmission between Athens and Roma at 34 and 45 MHz (see acknowledgment page (ix) of this Report, (iii) continuous monitoring at Roma of the 40 MHz FM Police network in Greece, (iv) monitoring in Southern Africa at Pretoria (lat. 26.0°S, long. 28.2°E) and Port Elizabeth (lat. 34.0°S, long. 25.6°E) of the 40 MHz FM Police network in Greece for a period of one year, (v) continuous transmissions near 14 MHz from Tsumeb, South West Africa (lat. 19.1°S, long. 17.4°E) to Lindau, Germany (lat. 47.3°N, long. 9.4°E) and Lindau to Roma, together with 34 MHz from Athens to Roma, covering the period of equatorial sunset.

In Chapter 2 below attention is drawn to the importance of monitoring existing commercial transmitters. One of the advantages is that such transmitters usually operate on a reliable, conservative schedule whereas research equipment tends to be operated at the limit of its performance capability. The 40 MHz Greek Police network has this kind of reliability and the continuous monitoring of that system in Southern Africa for six years has provided data which would be difficult to obtain otherwise. A disadvantage of the 40 MHz network is absence of prolonged signal of more than a few seconds. This has restricted observations to long term synoptic investigation of signal presence and strength. For the more detailed study of short time behaviour such as fading including the effect of irregularities, the 34 and 45.1 MHz CW transmissions from the experimental transmitters proved to be of special significance. The restrictions here have been due to technical failure of equipment requiring careful logging of actual transmission and reception. It was only possible to operate the experimental equipment for two years.

1.2 Transmitting and Receiving Sites

Fig. 1 shows the TEP paths joining the transmitting and receiving sites while Fig. 2 shows the spread in latitude of the 40 MHz receiving

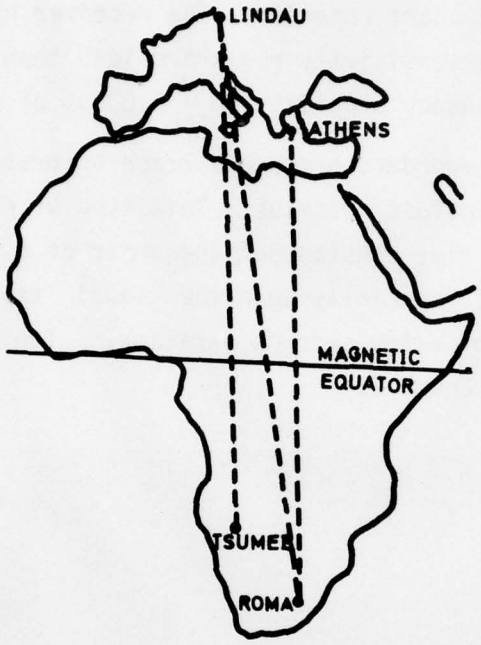

Fig. 1 – European-Southern African TEP Paths

sites. The principal TEP circuit was from Athens to Roma which are almost magnetically conjugate and are separated by a 7490 km path nearly at right angles to the dip equator.

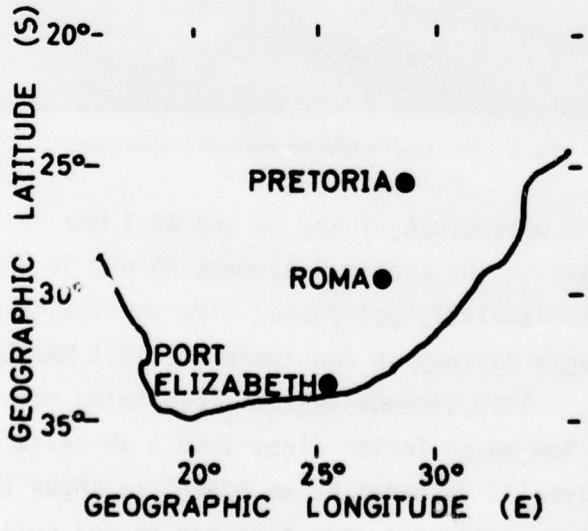

Fig. 2 – 40 MHz TEP Receiving Sites

1.3 Instrumentation and Data Collection

To record the 40 MHz signal a standard 25-50 MHz "Sensicon A" FM Motorola receiver is coupled to an omnidirectional cardioid vertical whip antenna and Rustrak chart recorder. The receiver has a selectivity of ± 30 kHz (-100 db), a sensitivity requiring less than 0.4 microvolt for 20 db quieting and a frequency stability to ± 0.0005% of reference frequency.

Rustrak recorders produce a trace on pressure sensitive paper by percussion action against a stylus. This type of recording has limitations. A relatively large time constant of the order of a second or so causes damping of signal level especially when the signal itself is characteristically only of the order of a few seconds duration. Typical Rustrak recordings are illustrated in Chap. 5.

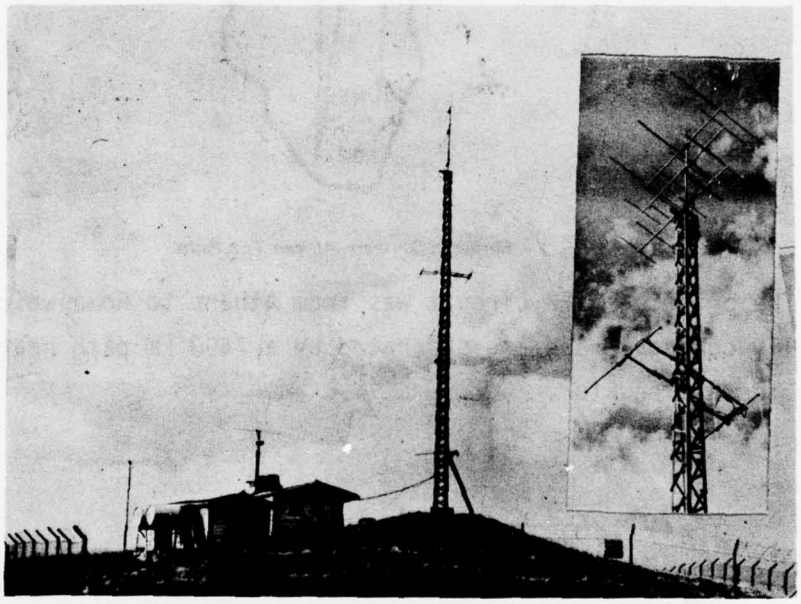

Fig. 3 – Receiving Facility and Antenna Arrangement

Fig. 3 is a photograph of the 34 and 45.1 MHz receiving antennas. At the top of the mast is the single 4-element 50 ohm 34 MHz Yagi with a gain of about 6 db horizontally polarised. The vertically polarised twin stacked 3-element Yagis halfway up the tower are 45.1 MHz 50 ohm arrays with a gain of 8 db. Both antenna systems feed Telco model SR twin channel receivers with very low noise factor (less than 3 db below 70 MHz). The output of each receiver is recorded by an Esterline Angus twin A602C. This system is designed for continuous operation but is not suitable for a study of rapidly varying characteristics. For such a study a "Sefram Rapidgraph"

with a time constant less than 0.02 seconds and a range of chart speeds up to 100 mm s^{-1} is employed. Typical Sefram recordings are illustrated in Chap. 5. Signal strength was determined by periodic calibration against a Hewlett Packard Model 606A Signal generator.

Two 200 W output-power base station transmitters coupled with 5-element Yagi antennas were installed at the transmitting site in Athens. For the experimental program transmissions were started at the beginning of each hour of the day and continued for five minutes. For identification purposes the transmissions were interrupted for one second every minute and were terminated by a series of one second pulses.

2. REVIEW

2.1 Synoptic Observations

The first observations of transequatorial propagation were by radio amateurs during the 1947-48 solar maximum. Signals at frequencies significantly above path MUFs and over paths too long for single hop transmission were received by U.S. and Mexican amateurs from South American sources and by Northern Australian amateurs from Hawaiian and Asian sources. Notable among IGY amateur experiments in the Americas, the Far East and the European-African region were those reported by Cracknell[2] and Southworth[3]. McCue and Fyfe[4] point out in a review that nearly all VHF circuits longer than 1-hop are transequatorial circuits. Experimental investigations of such paths have been made by back-scatter techniques and by forward propagation. Back-scatter experiments have the advantages of a single experimental site and the opportunity for azimuthal scanning. Villard et al[5], Dueno[6] and Thomas[7] observed 5000 to 12000 km ground range back-scatter echoes occurring mainly during the equinoxes between 1500 and 2100 hours. Back-scatter signals occur more often at lower frequencies, slant ranges tend to be constant for fixed frequency and echoes have a lower occurrence probability than corresponding forward propagation signals. Although forward propagation investigations require at least two widely spaced experimental sites, they have the added significance already referred to over back-scatter observations of the possibility of investigating path characteristics, together with simulation of potential commercial modes.

Even monitoring of existing commercial transmitters can produce useful data difficult to obtain by other methods. Systematic investigations include monitoring in North Queensland of 44-48 MHz Korean sources by Carman et al[8] and Gibson-Wilde and Carman[9], Cracknell and Whiting's[10] observations in Rhodesia of 29 MHz signals from Cyprus and Nielson's[11] Cook Islands recordings of 54-66 MHz Hawaiian transmissions. Australian-Far Eastern and Hawaiian-Cook Islands circuits differ markedly in seasonal behaviour; the former have a complete absence of signal in the June solstice while in the latter case signal disappears in the December solstice. Signal has highest occurrence during equinoxes for both circuits.

The most recent of the more significant experiments are forward propagation projects involving experimental transmitters and receivers at several frequencies. Washburn et al[12], Bowen et al[13], Nielson[11], and McNamara[14] investigating TEP paths in the Americas, Far East and Pacific observed a maximum frequency of 102 MHz. This latter frequency was observed over a 4800 km path[14] [15] while frequencies as high as 50 MHz have been observed over an 8000 km path[8] [9].

In a review presented at the Fourth International Symposium on Equatorial Aeronomy, Ibadan, Nigeria (1972) Nielson and Crochet[16] point out that the highest TEP frequencies, apart from those centred about the equatorial E_s belt, are observed on circuits that place all reflection points in the vicinity of the maxima of the equatorial anomaly. This type of reflection occurs if transmitting and receiving sites are conjugately related and lie 1000 km or more northwards or southwards of the anomaly maxima[4] [12] [17], or from circuits where reflection occurs at a single anomaly maximum[18].

High signal strengths have been reported on most TEP circuits [12] [13] [17] [19] [20]. Carman et al[20] and Fyfe[21] show that signal strength variation is similar to occurrence with maxima appearing at the equinoxes. In the 30-50 MHz range signals sometimes approach[22] or exceed[20] free space attenuated values; for example, for 45.1 MHz Carman et al[20] observed signal strength during the September 1970 equinox many times greater than the free space attenuated value.

2.2 Doppler and Time-Delay Experiments

Nielson and Crochet[16] also discuss evening broadening of spectra and time-delay profiles as distinct from daytime TEP which almost always has a width less than 1 to 2 Hz. The broadening at first attributed by Osborne[23] and Yeh and Villard[24] to substantial Doppler shifts of some propagating rays was subsequently shown by Calvert et al[25] to have a filamentary, often continuous power over many hertz. Examples of both

kinds of broadening are shown in Fig. 4 taken from Davies and Chang[26] and result from regions within the equatorial zone that drift eastwards at about 100 m s^{-1}. Broadening up to 15 or 20 Hz is not uncommon.

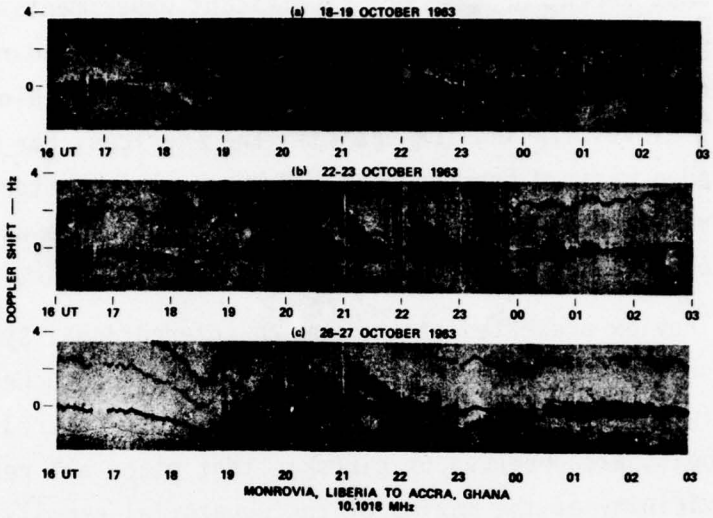

Fig. 4 — Examples of Swoopers, October 1963 (from ref. 26)

Fig. 5 is an example of similar observations of time discrete VHF spectra taken from reference 11. Both Doppler and time spreads have maxima near 2000 to 2200 local time and depend upon the presence of multiple ray paths involving reflections from ionospheric irregularities.

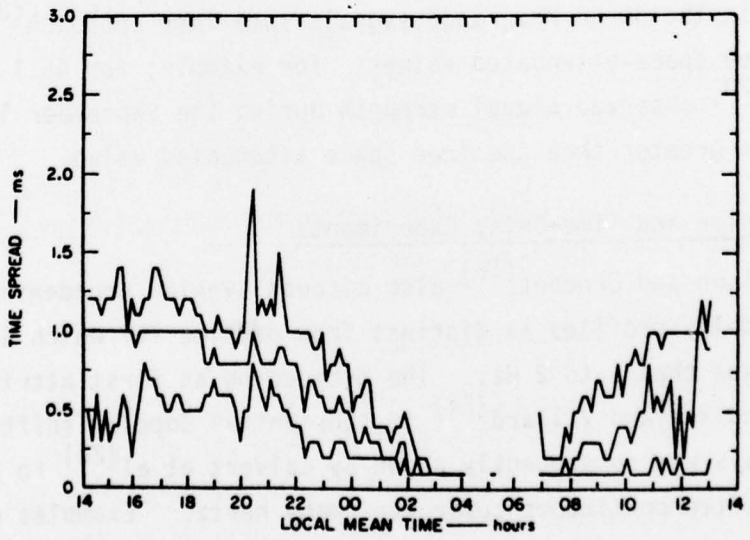

Fig. 5 — Median and Quartile Values of Maximum Time-Delay Spread for Raratonga-Oahu Path for March 1968—36 to 40 MHz (from ref. 11)

Results from Nielson's[11] Oahu-Raratonga path appear in Figs. 6 and 7. He finds that the major peaks in Fig. 6 move with ordered motion. This together with excess Doppler spread near 2200 LMT indicates horizontal and downward motion of the reflecting surface. Individual peaks correspond to discrete spatially separated patches apparently drifting with almost the same velocity. Here a patch is not necessarily the physical boundary of a group of smaller scale irregularities but can be thought of as a volume through which irregularities drift; it may be a tilted front and ripples in the tilt are the irregularities. Patches have short term stability as can be seen from Fig. 8[16] which shows spectra selected at 10 second and

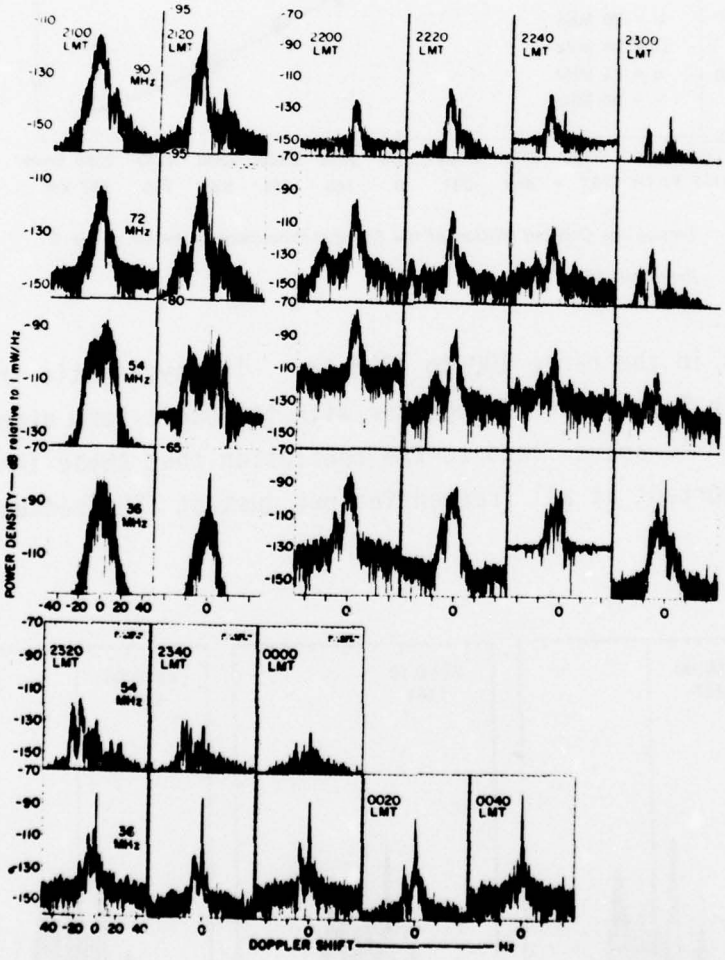

Fig. 6 — Multiple Frequency Doppler Spectra for 25 March 1968 LMT, taken on Hawaii-Raratonga Path (from ref. 11)

2 minute intervals from a sequence taken at 10 second intervals. The group features remain almost constant over a 2 minute interval even though the detailed structure within each group varies during a 10 second interval. As with data obtained by other methods[27-33] such as fixed frequency monostatic radar and HF flutter, TEP data shows[16] that irregularity patches

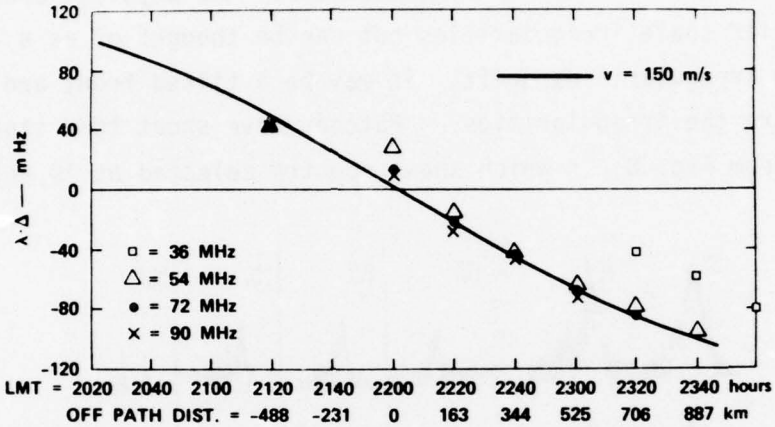

Fig. 7 — Testing the Ordered Motion of the Spectral Prominences Shown in Fig. 6 (from ref. 16)

have dimensions in the range 100 to 1000 km. The systematic frequency shift evident in Figs. 6 and 7 together with the short term stability of patches referred to above, lead to the conclusion that these irregularity patches are important at all frequencies not just at TEP frequencies.

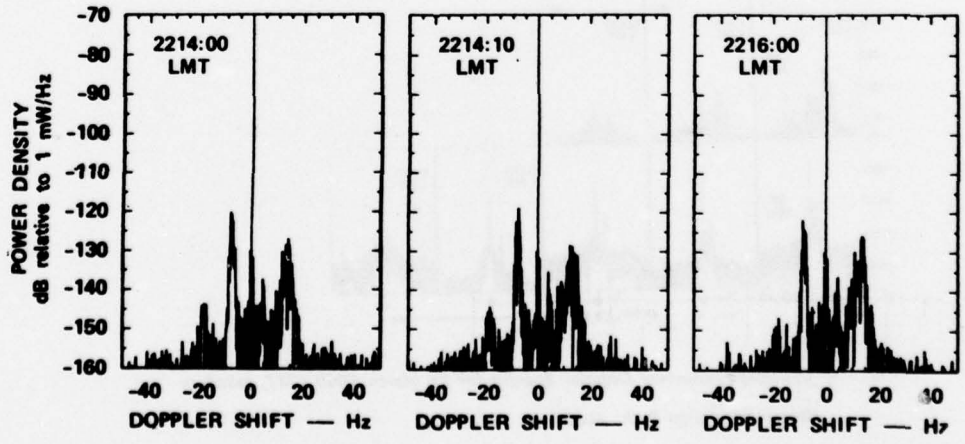

Fig. 8 — Samples of the Spectra of a 72 MHz Signal Propagated between Raratonga and Hawaii (from ref. 16)

Other workers[34-39] have explored the equatorial ionosphere at sites remote from the equatorial zone using HF. Fig. 9 is an example taken from reference 38 which illustrates the existence of irregularity patches on several off great-circle paths between Lindau and Tsumeb. Röttger[39] finds a median transverse size for the patches of about 400 km. In a similar experiment between Valensole (lat. 43.5°N, long. 5.6°E) and Grahamstown (lat. 33.2°S, long. 26.3°E) Crochet [34] [35] also found irregularity patches leading to off great-circle TEP. Both workers obtained a correlation between TEP off great-circle modes and equatorial spread-F.

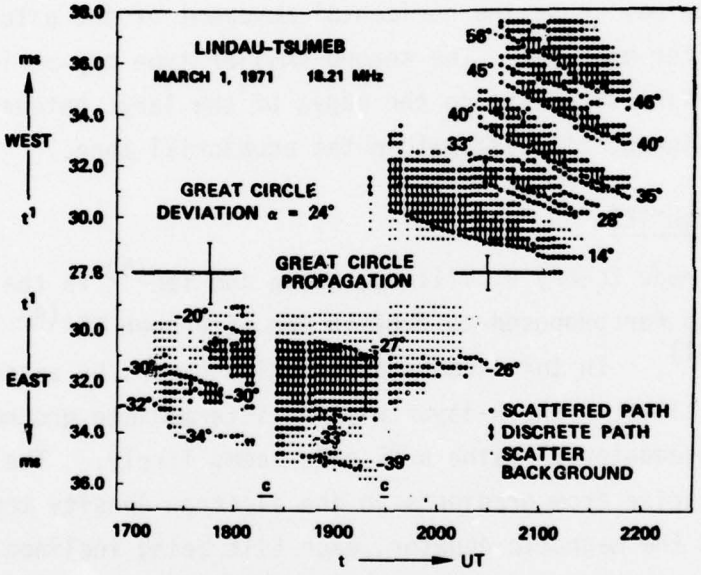

Fig. 9 – Multiple Echoes from the Equatorial Zone Showing Eastward Drift on the Lindau-Tsumeb Path (from ref. 38)

Nielson and Crochet[16] point to the difficulty in attempting to explain frequency dependent signal level because a given operating frequency may have simultaneous scattering from either under-dense or over-dense patches. Furthermore TEP frequency ranges include both the background and irregularity plasma frequencies. But the plasma density must have spatially local maxima within a patch to account for the total VHF data of Fig. 6. Plasma frequencies of the order of 15 to 20 MHz must be reached even under ideal conjugate ionosphere-to-ionosphere reflection to explain 72 MHz data.

The same authors summarise the important role played by irregularities in producing evening TEP: weakness of background plasma at times of TEP indicates that the propagation is supported by irregularities; Doppler and time-delay experiments show that these irregularities present many reflecting surfaces, the resulting signal occurs only at night-time and correlates with spread-F (see, however, Chap. 4 of this Report). They suggest a possible explanation of TEP observations in terms of (a) large-scale and (b) medium and small-scale irregularity patches. The large scale patches (100-1000 km in longitude) form and begin to move eastward and downwards after the evening F-layer height rises; they may exist simultaneously at different longitudes and have large horizontal gradients of ionisation on their boundaries. Electromagnetic drift from large scale electric fields or wavelike motion may cause the horizontal movement of the patches which disappear soon after midnight. The second smaller type may be in the form of a fine ripple-like structure on the edges of the large patches and are possibly field aligned, at least within the equatorial zone.

2.3 Afternoon TEP

The ^{n}F mode theory of Villard, Stein and Yeh[5] is the most widely accepted theory so far proposed to explain the afternoon TEP[4] [9] [13] [17] [22] [40] [41]. In this theory propagation occurs by successive reflections from tilts in the F-layer without intermediate ground reflections. For transequatorial paths a ^{2}F mode seems likely. The necessary tilts (up to 6^{o}) arise from gradients in the electron density more or less symmetrical about the magnetic equator, each tilt being inclined towards the equator. The recent time-delay measurements of Anastassiadis and Antoniadis[1] are consistent with this theory but do not rule out a normal 2-hop propagation mode. The large peak densities on the crests of the anomaly, necessary to explain afternoon TEP, occasionally occur following sunset and may continue to influence the total reflection process even when irregularities are present.

3. SYNOPTIC DATA

Data recorded at Roma from 1 September 1969 to 31 August 1970 appears in Appendix III. These figures show the maximum signal strength in dBm occurring each hour throughout the year for 34 and 45.1 MHz, and each half hour for 40 MHz. The data of Appendix III considered along with similar data of Reports 1[55], 2[56] and 3[57] constitutes almost four years of continuous recording at Roma and one year of recording at Pretoria. Variation of signal strength over the four year period is discussed in Section 3.2. For two years of transmission at 34 and 45.1 MHz complete transmitting and receiving schedules appear in Appendix II.

3.1 Occurrence of Signal

In Fig. 10 histograms show the presence probability or proportion of days of the month when signal was recorded at Roma during each hour of the day. Maximum presence occurs during the equinoxes for all three frequencies. The 40 and 45.1 MHz signal almost vanishes during the June solstice and 40 MHz reaches a much less marked minimum during the December solstice. The 34 MHz signal decreases less during the solstices compared with the higher frequencies. In January and February 1971 the presence

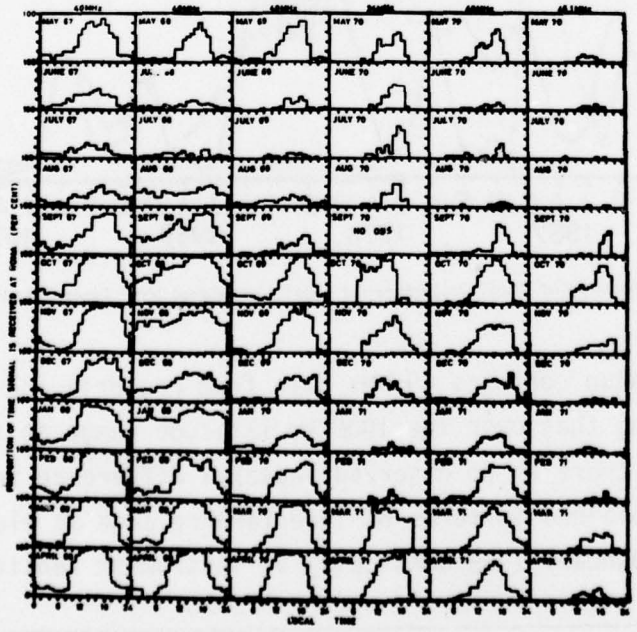

Fig. 10 – Histograms Showing Proportion of Time 34, 40 and 45.1 MHz Signal is Reiceved at Roma

probability of 34 MHz signal appears to be lower than 40 MHz. However, it is known that signal was lost during those months due to antenna preamplifier failure and the data is unreliable. The December histogram indicates the general behaviour for that solstice. Nielson[11] points out that TEP transmissions between Oahu and Raratonga near 50 MHz show a marked difference between the two solstices with higher reception occurring in June. However, Fig. 11 shows that the difference in the two solstices is not as marked as with the Roma-Athens 40 MHz circuit; furthermore, the effect is reversed, higher reception occurring in December at Roma. This difference will be discussed later in Section 6.3. Seasonal behaviour of Roma 40 MHz further illustrated in Chap. 6 (Fig. 25) shows that the above mentioned significant difference between the two solstices is evident only in afternoon and evening TEP.

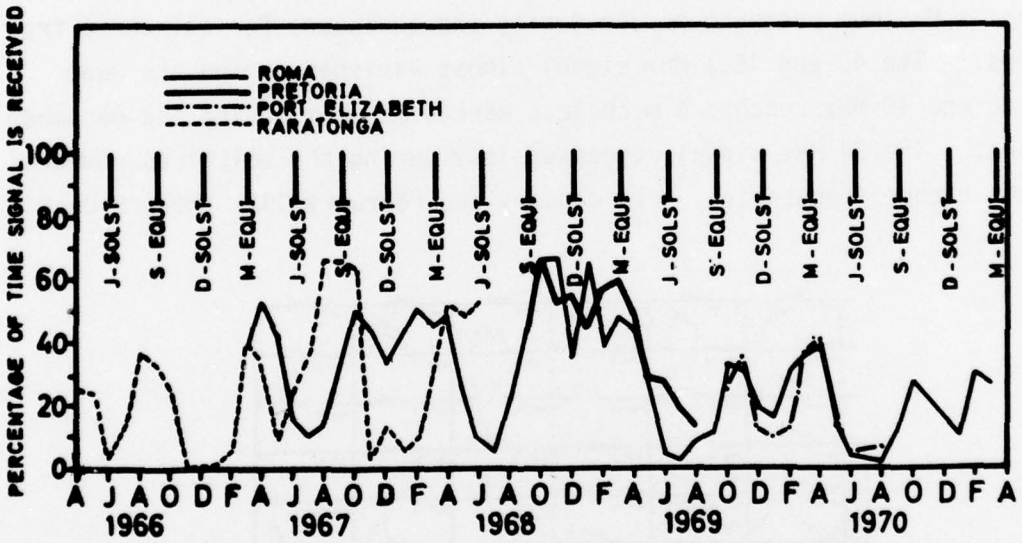

Fig. 11 – The Seasonal Variation of Signal Occurrence for Two Long Range VHF Transequatorial Circuits*

Fig. 11 also contains 40 MHz data from Pretoria and Port Elizabeth (see Fig. 2) showing that over the 1000 km latitude range at the receiving end of the circuit there is no observed seasonal difference in occurrence which cannot be explained in terms of interference such as electrical storms (e.g. see Fig. 11 January 1969 Roma data) or instrument sensitivity.

---

* The Raratonga data have been adopted from Nielson[11] (Fig. 10) and have been normalised to the maximum of the Roma data.

The growth of 40 MHz TEP during morning hours and decay during evening hours are illustrated in Fig. 12. Between 1200 and 2000 hours the curves almost coincide. Significant differences in occurrence during June and December solstices already shown in Fig. 11 are evident in all the curves for particular hours excepting the morning hours from March 1967 to June 1968. For 21 of the 36 months plotted signal before 1200 hours is present for less than 20% of the days of the month suggesting low presence probability before noon excepting near sunspot maximum (see Fig. 10).

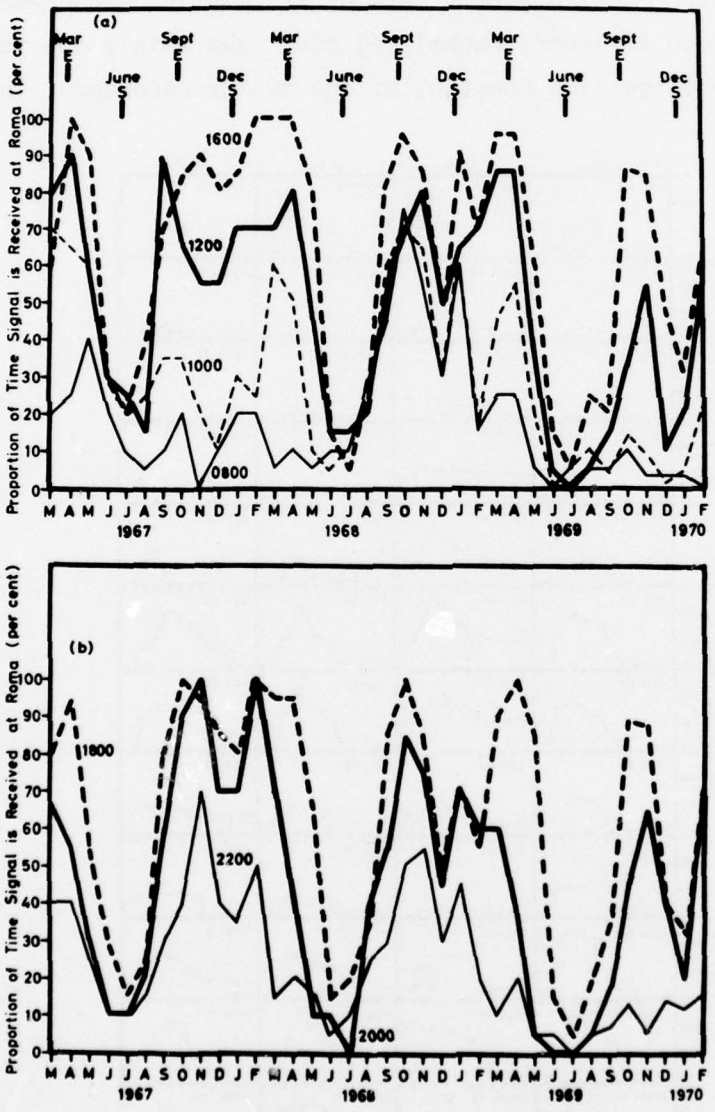

Fig. 12 – (a) Diurnal Development and (b) Diurnal Decay of 40 MHz TEP Reception at Roma during 36 Months

3.2 Signal Strength

Diurnal variation of signal strength is shown in Fig. 13 for 40 MHz and in Fig. 14 for 34 and 45.1 MHz. Here all days of the month were included in the averaging process irrespective of whether signal was present or not. For the four years shown, the behaviour of 40 MHz signal strength is similar to occurrence (Fig. 10) with maxima appearing at the equinoxes, April being greater than October. 40 MHz behaviour differs from the other two frequencies in that signal strength almost disappears at the June solstice but relatively high signal strength is evident even at the solstices on 34 and 45.1 MHz. This apparent lack of systematic dependence on frequency is partly due to lower transmitted power but mainly due to damping by the relatively large time constant of the 40 MHz recorder. This is also

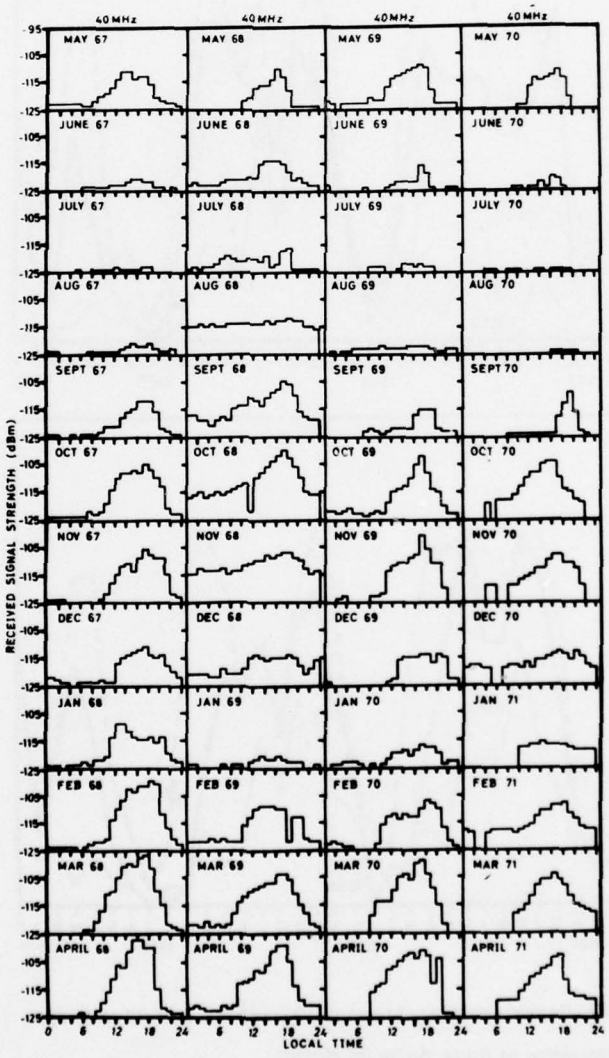

Fig. 13 – Diurnal Variation of Signal Strength for 40 MHz

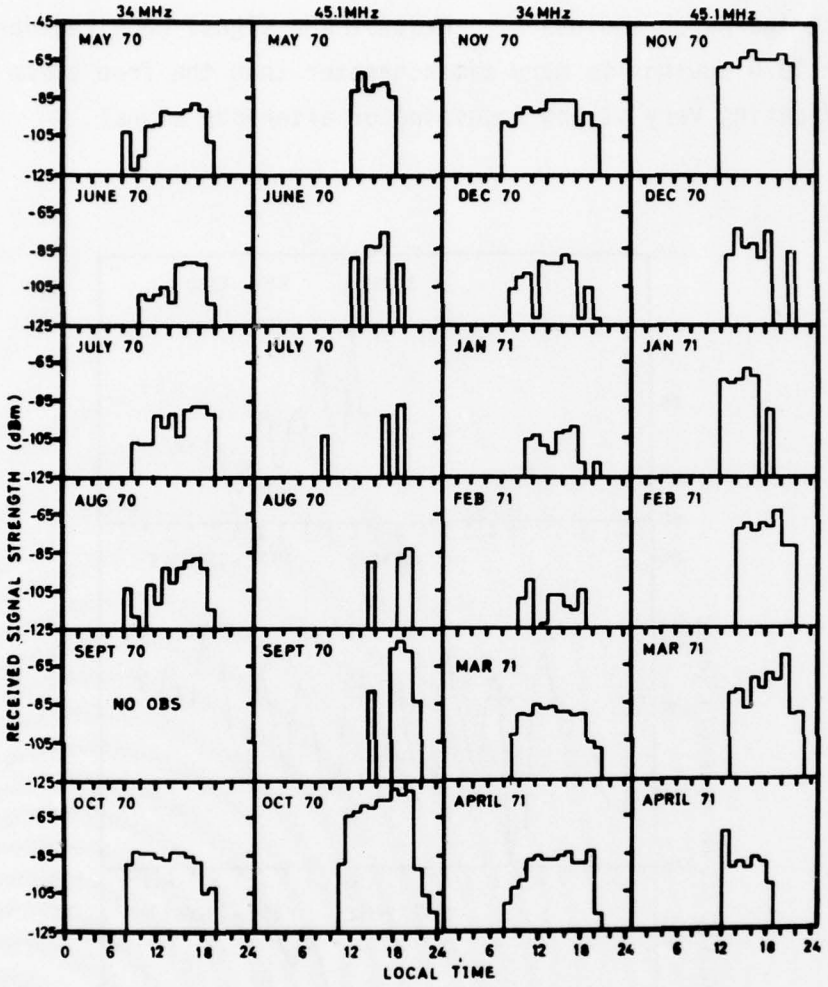

Fig. 14 – Diurnal Variation of Signal Strength for 34 and 45.1 MHz

evident in Fig. 15 where seasonal behaviour of signal strength is shown. Here the plotted points were obtained by averaging over each month for those days on which signal was present during the respective daily time intervals indicated in the figure. This figure shows the equinoctial maximum, June minimum and December sub-minimum characteristics of the 40 MHz particularly well. For the year shown 45.1 MHz follows a similar maximum and minimum pattern, but preamplifier failure evident also in the 34 MHz signal strength for February 1971 makes comparison difficult for that frequency. 40 MHz

signal strength is usually less than the free space attenuated value excepting at the March equinoxes. At 45.1 MHz signal received during the September 1970 equinox is many times greater than the free space attenuated value indicating very strong focussing of afternoon signal.

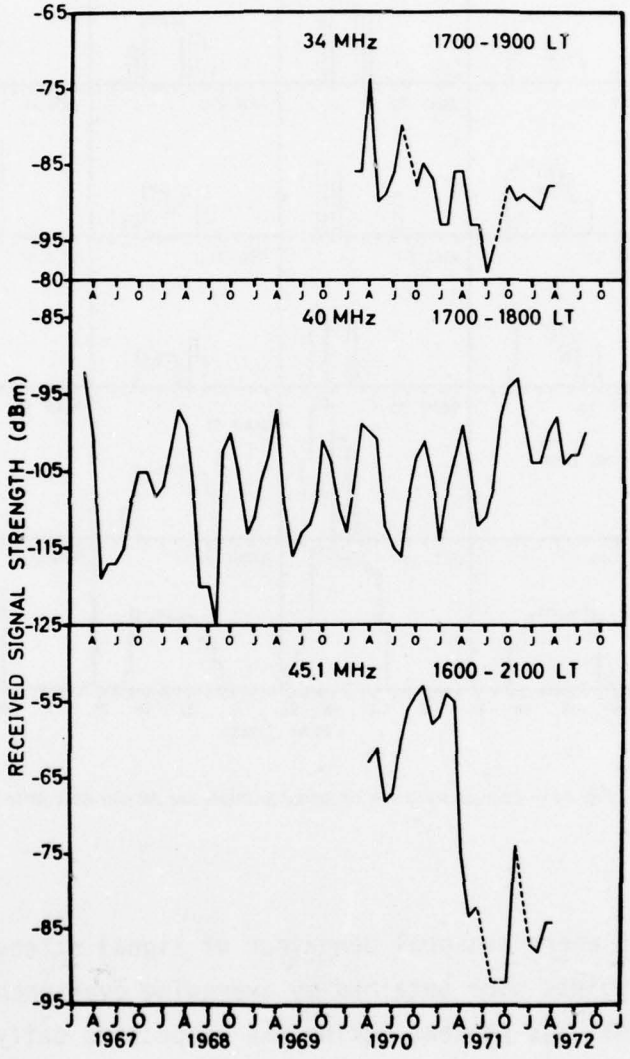

Fig. 15 — Seasonal Variation of Received Signal Strength for the Frequencies Shown Averaged over each Month for the Time Intervals Indicated

4. SIGNAL FADING

4.1 Classification

Representative samples of the types of fading observed on 34 and 45.1 MHz are reproduced in Fig. 16. There are three groups. Group A contains three types which all tend to have irregular periods and have less than twenty fades per minute. Group B contains periodic signal with 20-30 fades per minute and includes the double periodic type. Flutter or scatter signal which has been observed in the range 0.5 to 2 Hz forms Group C.

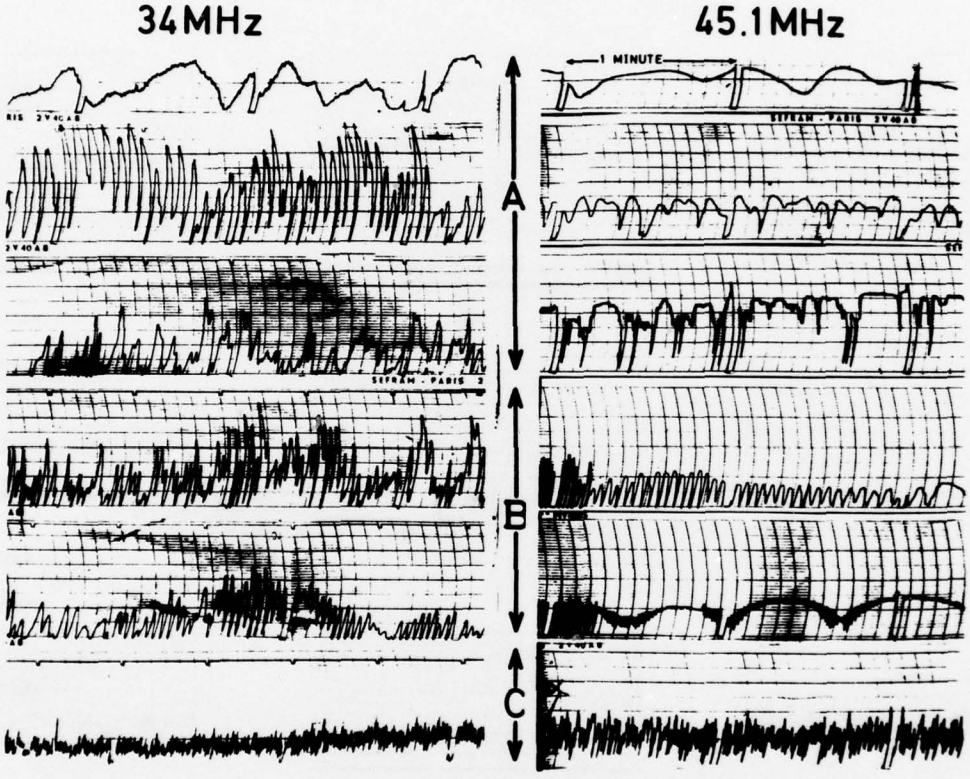

16 — Typical Examples of the Types of Fading Occurring on the Athens-Roma TEP Path. The Signal is Identified by a Two Second Break Every Minute

The three groups have distinctive diurnal characteristics which can be related to multipath, phase coherent interference and the evening equatorial ionosphere. For instance, Davies[42] has described double periodic fading similar to the Group B type of Fig. 16. He suggests that the shorter period fade results from beating between the high and low rays while the longer fade comes from the ordinary and extraordinary waves. On the other hand, Lockwood[43] suggests the fast fading is due to the O-wave and the X-wave. From samples of Roma records Lockwood also notes (i) that when double periodic occurs the operating frequency is well below the maximum

observed frequency (MOF) for oblique propagation while flutter fading probably occurs when the MOF falls below the operating frequency, (ii) the occurrence of double periodic implies a high angle and low angle ray and hence at least a 2-hop path since a 1-hop path has no low angle ray. Caldwell and Lockwood[44] suggest that the Group A signals which include slow periodic and random fading could result from off great-circle propagation but the phase coherence of double periodic makes off great-circle transmission of this type unlikely because of the scatter nature of ground reflection in the former case.

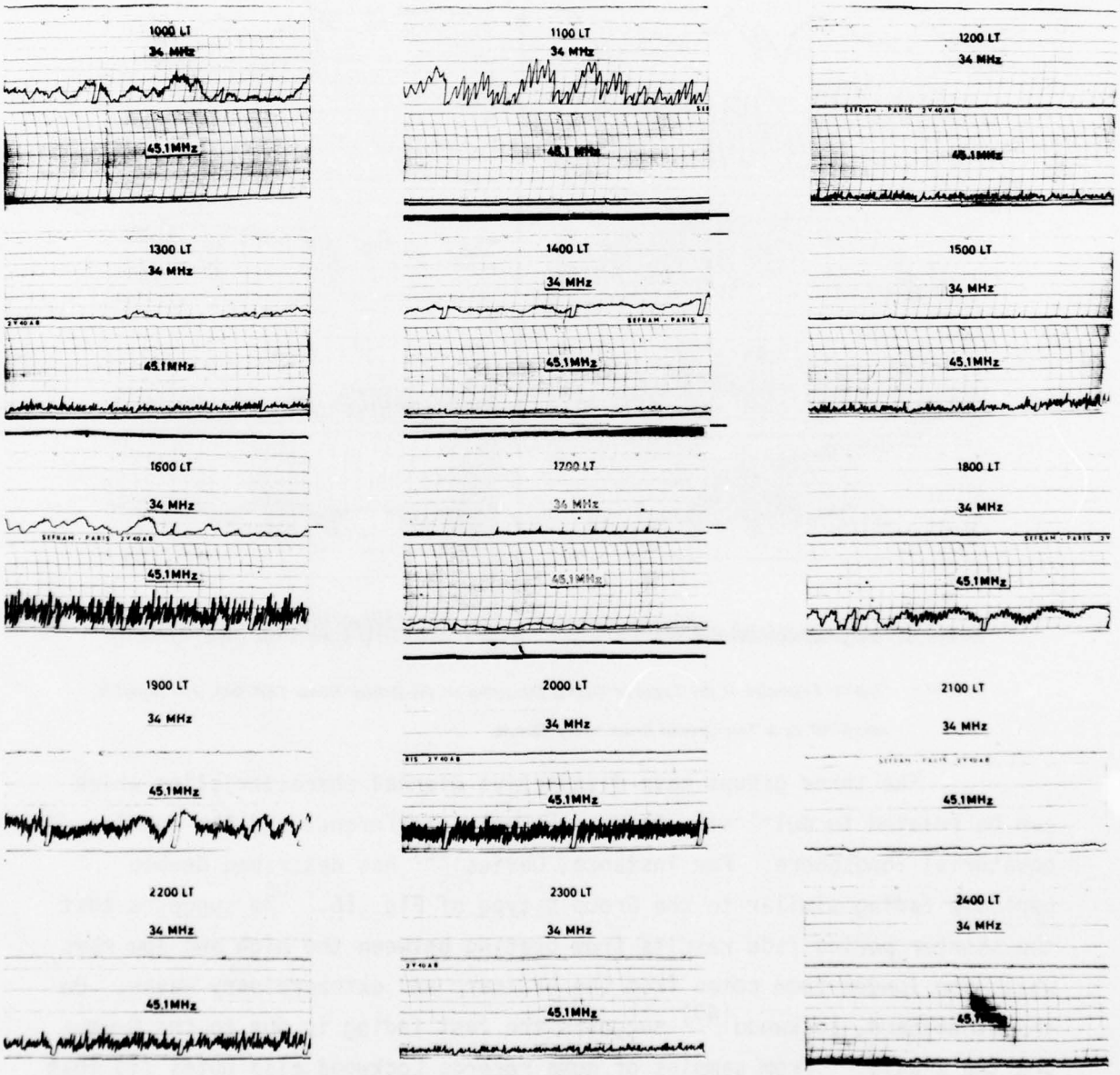

Fig. 17 – Recordings of 34 and 45.1 MHz Signal at Roma for 27 October 1970

Fig. 17 shows a complete day's reception of 34 and 45.1 MHz for times when signal was present. This day, 27 October 1970, is of particular interest because flutter fading of 45.1 MHz signal occurs very early in the day - 1200 LT, disappears and reappears in the evening. The transition from phase coherent (double periodic) signal to scatter (flutter type fading) signal occurs at 1900 LT.

4.2 Spread-F

Since October 1970 was a month of outstanding 45.1 MHz occurrence, the rate of fading is shown in Fig. 18 for the evening hours for this month.

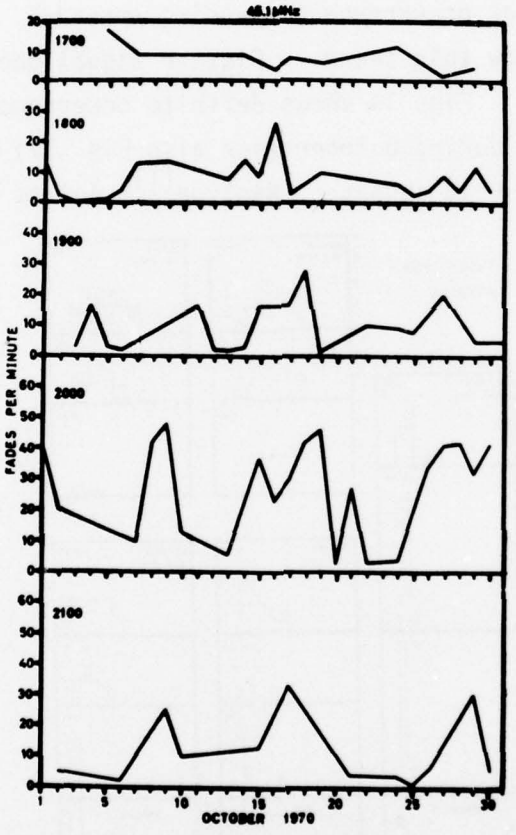

Fig. 18 – Fading Rates at the Local Times shown for October 1970 for 45.1 MHz

The three or four days centred on 17 October are of special interest because they show that an enhanced fading rate persists over a period of four hours. Moreover, there is a tendency for the rate of fading to increase from Group

B to Group C type towards evening as one would expect because this is the time of approach to equatorial sunset and onset of spread-F. However, the occurrence of this behaviour over a period of a few days with a distinct absence of high fade rates persisting for some hours over the same sunset period for the days before and after the days centred on the 17th is difficult to explain. The diurnal behaviour for three months September-November is much easier to interpret. In Fig. 19 the fading rate of the three groups of signals at 34 and 45.1 MHz are compared with equatorial spread-F. Evening spread-F correlates well with 45.1 MHz flutter signal with rates greater than 30 fades per minute. The diurnal behaviour for 45.1 MHz is similar to the behaviour indicated in Fig. 18 for certain days in that the occurrence peak moves to a progressively later hour with increasing fade rate until it coincides with the peak occurrence of evening spread-F. Peak occurrence of 34 MHz does not show this trend. Flutter signal does not only occur in the evening hours. Fig. 19 shows definite occurrence of flutter fading on 45.1 MHz at midday during October (see also Fig. 17) and November 1970 at a time when spread-F is absent. Nielson[11] points out and the results

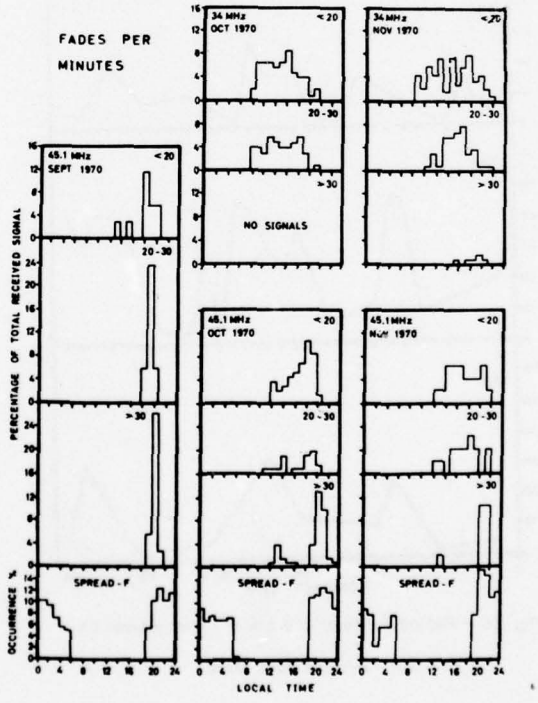

Fig. 19 – Histograms Showing how Fading Rate Increases towards Equatorial Sunset and then Coincides with Evening Occurrence of Spread-F. The Spread-F Occurrences are Percentage of Total Spread-F Appearing at the Various Hours for Fort Archaubault

of Fig. 19 confirm that spread-F occurs at times when TEP is absent and therefore spread-F is not a sufficient condition for TEP. However, since flutter type signals which are usually associated with spread-F are shown here to occur in the absence of spread-F, it must be concluded that spread-F is also not a necessary condition for flutter type TEP.

Analysis of flutter fading for the year May 1970 through April 1971 appearing in Fig. 20 shows that the maximum occurrence for 45.1 MHz was in August 1970 and for that month 50% of all 45.1 MHz received signal was flutter signal, another maximum of less than 25% occurred in March 1971. The maximum for 34 MHz was 15% in April 1971. Maximum spread-F for the year was in June 1970 coinciding with a period when TEP was almost

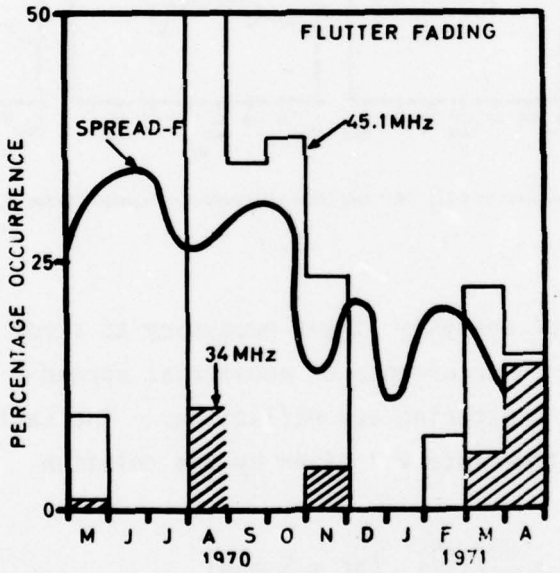

Fig. 20 – Comparison of Flutter Fading on 34 and 45.1 MHz with the Occurrence of Spread-F for the Year May 1970 to April 1971

absent. The seasonal pattern of TEP with very low occurrence in the solstices makes meaningful comparison with seasonal spread-F difficult. However, the coincidence of a maximum in spread-F with the well defined maximum in 45.1 MHz flutter fading is probably significant.

4.3 Fading Rates Observed on the Paths Lindau-Roma and Tsumeb-Lindau - Preliminary Results

J. RÖTTGER* E.H. CARMAN M.P. HEERAN

Simultaneous CW transmissions at 14.0 MHz from Tsumeb to Lindau and at 14.7 MHz from Lindau to Roma, together with 34 MHz from Athens to Roma were made for a few evenings covering the period of equatorial sunset during April 1972. Fig. 1 of Chap.1 shows the great-circle paths while Fig. 21 shows the observed fading rates.

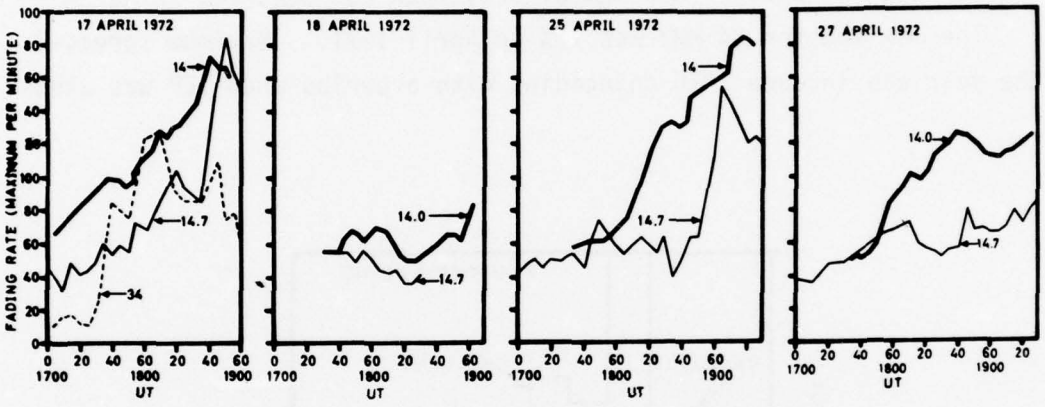

Fig. 21 – Simultaneous Transmissions at 14.0, 14.7 and 34.0 MHz between Tsumeb-Lindau, Lindau-Roma and Athens-Roma

For detailed analysis it was necessary to study variation in fading rate in relation to occurrence of equatorial spread-F irregularity patches causing side scattering and reflection. The variation in fading rate during a fixed time interval given by the relation

$$\bar{v} = \frac{\Delta N}{\Delta t} / \left|\frac{\Delta N}{\Delta t}\right| \quad (\Delta t = 5 \text{ min})$$

was evaluated during the entire period of observations. $\bar{v}$ gives the relative number of events when an increase or decrease is observed simultaneously on both paths. In the present case two of the frequencies (14.0 and 14.7 MHz) are sufficiently close to permit a comparison and the results appear in Table I.

* Max Planck Institute for Aeronomy, Lindau-Harz, Western Germany

TABLE I

	14.0 - 14.7 MHz
17 April 1972	0.67
18 April 1972	0.50
25 April 1972	0.50
27 April 1972	0.71

It is evident that $\overline{v} = 0.50$ means that there is only statistical dependence ($\frac{\Delta N}{\Delta t} = 0$ is not considered in this case). To determine the significance limits of $\overline{v}$ a series of random numbers was tested to find the standard error σ_v of $\overline{v}$. This error was found to be $\sigma_v = 0.104$. Assuming that $\overline{v}$ estimated by means of random errors has a normal distribution, the 2σ - limits give the 5% boundaries of significance. All values exceeding $\overline{v} + 2\sigma$ (= 0.708) are 95% significant, i.e. the probability that these values are statistical is lower than 5%. In the present case Table I shows that there is good correlation between 14 and 14.7 MHz fading rate variations on 27 April when the significance is 95%. On 17 April correlation is 90% significant which is still relevant. There is no correlation on 18 and 25 April.

The quasi-simultaneous occurrence of intermediate maxima on the 17 and 27 April indicates that the propagation path is not in a discrete plane but that off great-circle propagation occurs throughout the whole period of the observation. The intermediate maxima on both paths may be caused simultaneously by the same patch of irregularity. If the propagation was in a great-circle plane, the maxima would occur at different times coinciding with the times the patches crossed the great-circle plane.

This preliminary result indicates the occurrence of off great-circle propagation caused by irregularity patches. It appears necessary to investigate further cases and to expand the work to include a study of equatorial spread-F.

5. TEP AND TOPSIDE SOUNDING

5.1 Electron Density Profiles

Sixteen passes of the Alouette satellites were compared with broadly representative samples of 40 MHz reception at Roma from May 1967

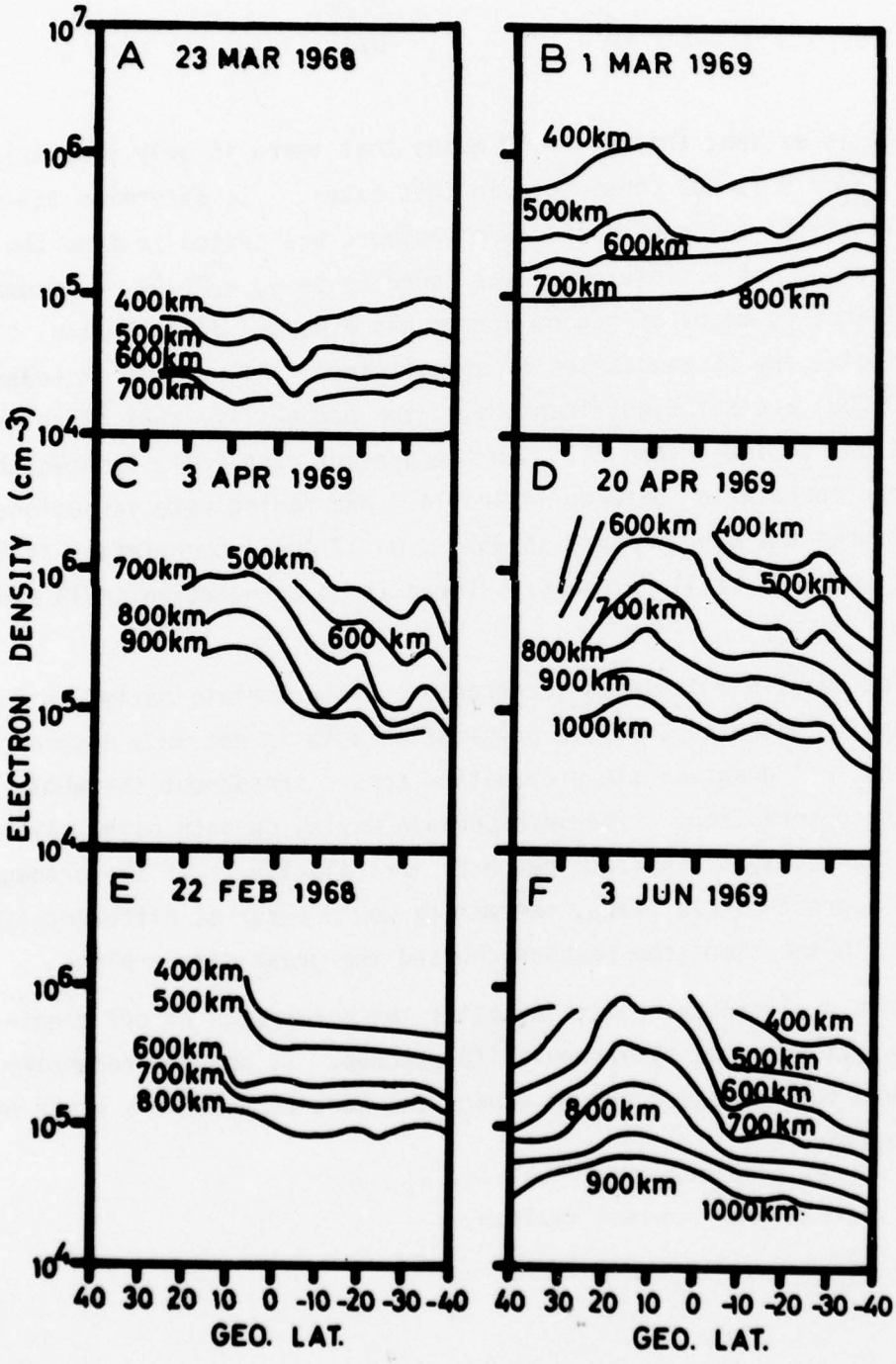

Fig. 22 – (a) Electron Density Profiles Obtained from Alouettes I and II Topside Sounding

through June 1969. 34, 40 and 45.1 MHz were compared with twenty seven passes of Alouette II and Isis II from May 1970 through June 1971. Exam-

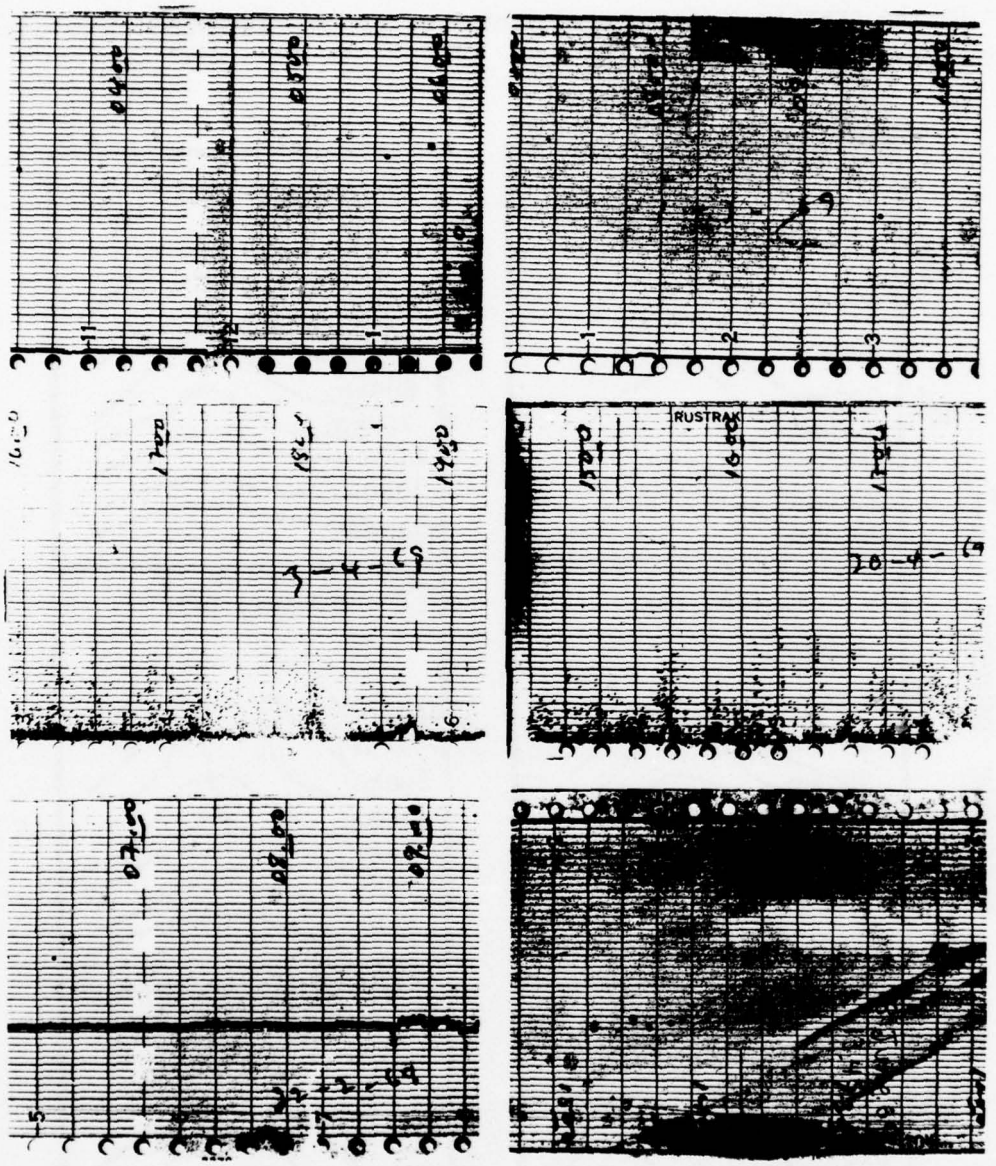

Fig. 22 (b) Signals on 40 MHz corresponding to the Electron Density Profiles of Fig. 22 (a)

ples of electron density profiles prepared from satellite data provided by the Communications Research Centre, Ottawa, Canada, appear in Figs. 22 and 23 along with corresponding samples of TEP recordings from Roma. Fig. 22 illustrates typical equinoctial and solstitial data at different times of the day. Here it is evident that the equatorial anomaly over Africa in the equinoctial period is absent in the early morning, begins to develop at

about 0800 LT, is well developed at 1700 LT and shows signs of decline at about 1900 LT. This corresponds with reported behaviour[45] [46] for the American region. Mid-latitude fluctuations in electron density are also evident in the profiles. The solstitial data indicates a weaker development of the anomaly. The profiles of Fig. 23 show afternoon development of the anomaly.

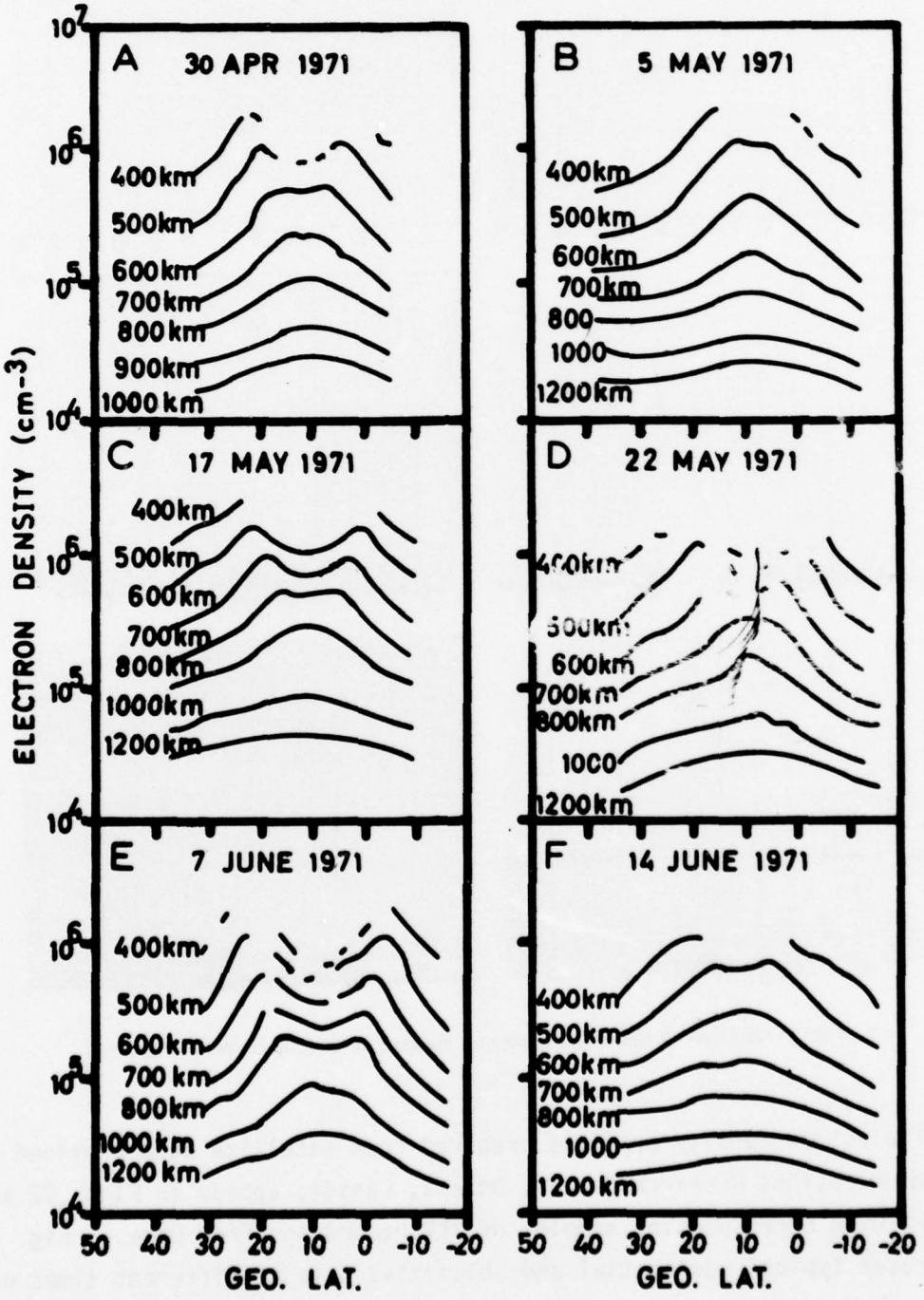

Fig. 23 – (a) Electron Density Profiles Obtained from Alouette II and Isis II Topside Sounding

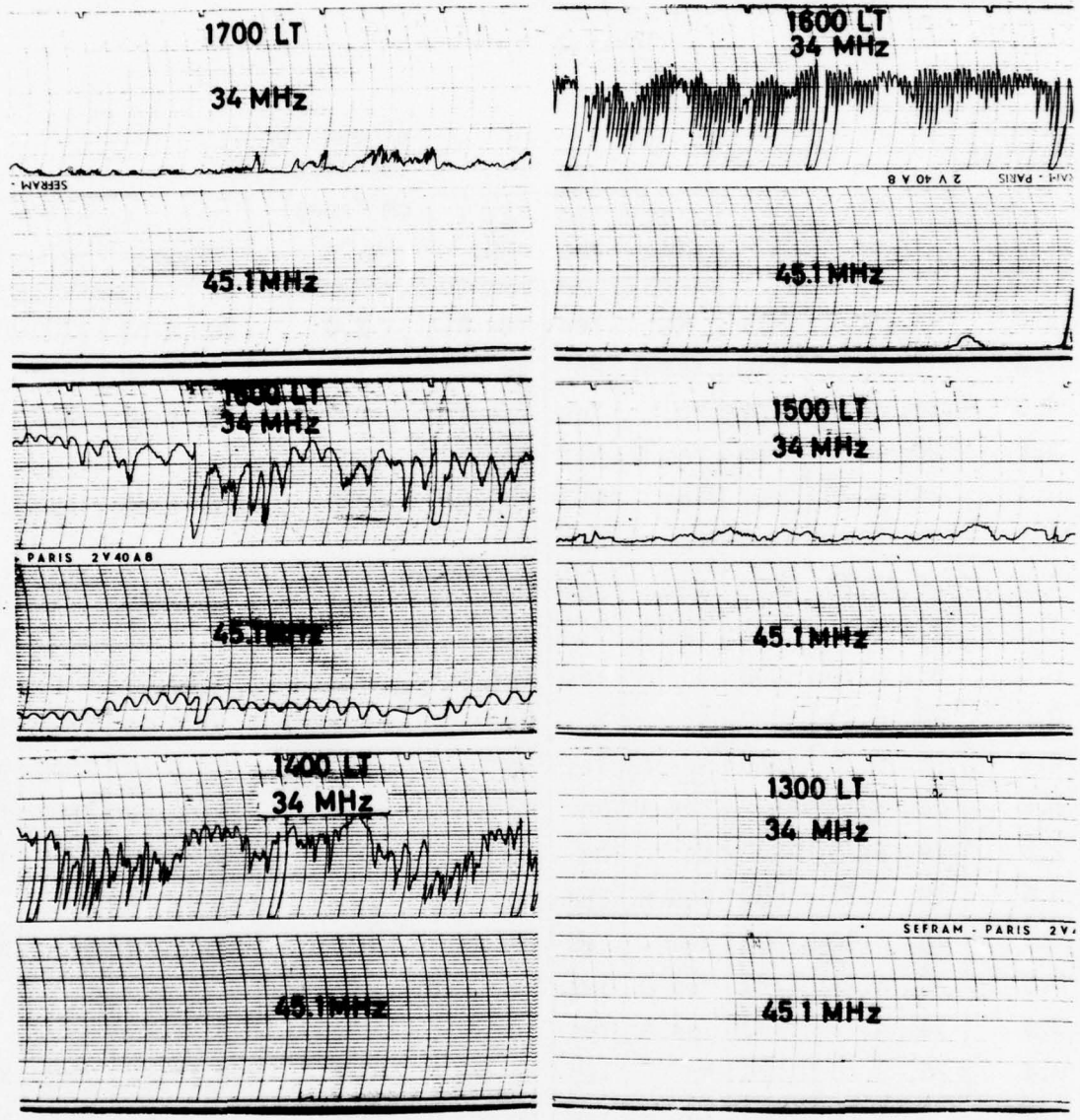

Fig. 23 (b) Signals on 34 and 45.1 MHz corresponding to the Electron Density Profiles of Fig. 23 (a)

5.2 Gradients

Although double maxima do not always occur in the data of Figs. 22 and 23 in cases where the anomaly is developed gradients exist near the magnetic equator. The existence of these gradients is essential to the theory of Villard, Stein and Yeh[5]. Gradients have been obtained from all available profiles in the latitude range 0 through -5 degrees (geographic) and are arranged in decreasing order in Table 2 alongside occurrence of TEP.

TABLE 2

e^- density gradient cm^{-3} deg^{-1} x 10^5	Date	LT	TEP 34 MHz	TEP 40 MHz	TEP 45.1 MHz	e^- density gradient cm^{-3} deg^{-1} x 10^5	Date	LT	TEP 40 MHz
2.2	14.10.70	1400	No	Yes	Yes A	2.0	20. 4.69	1730	Yes
1.4	7. 6.71	1400	Yes A	No	No	1.7	3. 4.69	1830	Yes
1.3	15. 9.70	1800	No	Yes	Yes A	0.9	16. 4.69	1700	Yes
1.2	20. 4.71	1600	Yes A	No	No				
1.1	20. 6.70	1600	Yes	No	No	0.8	21. 5.69	1400	No
1.1	30. 4.71	1700	Yes	No	No				
1.0	5.12.70	2000	Yes	Yes	No	0.6	13.11.68	1330	Yes
1.0	17. 5.71	1600	Yes A	No	Yes A	0.5	18. 3.69	1730	Yes
0.9	31. 8.70	1900	No	Yes	Yes B	0.5	1. 3.69	0900	No
0.8	20. 5.70	1900	No	No	No	0.4	3. 6.69	1430	No
0.8	25. 5.70	1900	Yes A	Yes	No	0.4	7. 5.68	1200	No
0.8	22. 5.71	1500	Yes A	No	No	0.4	22. 2.68	1800	No
0.6	14. 6.71	1300	No	No	No	0.2	28. 2.68	0800	Yes
0.6	19. 4.71	1600	Yes A	Yes	No				
0.6	16. 3.70	1500	Yes	Yes	No obs	0.2	26.10.68	0400	No
0.5	10. 4.71	1700	Yes A	Yes	No				
0.5	14. 4.71	1600	Yes A	Yes	Yes A				
0.4	26. 3.70	1400	No	Yes	No obs	0.2	28.11.68	0000	Yes
0.4	5. 5.71	1600	Yes B	Yes	No	0.1	4. 5.67	0800	No
0.3	17. 4.71	1600	Yes A	Yes	No				
0.3	2. 5.71	1400	Yes C	No	No				
0.02	11.12.70	0700	No	No	No	0	7.10.68	0530	Yes
0	5. 7.70	1100	Yes A	No	No	0	23. 3.68	0600	No
0	13. 5.70	2000	No	No	No				
0	18. 5.70	2000	No	No	No				
0	26. 5.70	1900	No	Yes	No				
0	29. 3.71	1800	Yes B	No	No				

Columns 4 and 6 indicate the type of TEP in terms of the classification of 4.1 Fig. 16 for 34 and 45.1 MHz signal (excepting for the four cases where the signal was too weak to permit classification). As already mentioned in Section 1.1 the recorder used for 40 MHz signal reception did not produce fading characteristics and hence classification of signal was not possible. The data of Table 2 is summarised in Table 3. Here an arbitrary value of electron density gradient ($0.5 \times 10^5 cm^{-3} deg^{-1}$) has been taken to divide the data into two distinct classes.

TABLE 3

e density gradient $cm^{-3} deg^{-1}$	Signal Occurrence					
	34 MHz		40 MHz		45.1 MHz	
	Yes	No	Yes	No	Yes	No
$\geq 0.5 \times 10^5$	12	5	14	10	5	11
$< 0.5 \times 10^5$	5	5	7	12	0	9

It is clear from the table that the lower gradients correspond to low occurrence probability - about 32% and only half of this is afternoon or evening TEP. Thus the evidence strongly supports absence of afternoon or evening TEP in cases where electron density gradients tend to be absent. For higher gradients the probability of TEP is somewhat higher than 50% and Table 2 shows that these high gradients occur mainly in the afternoon or evening. Thus TEP occurrence and high electron density gradients tend to coincide in the afternoon or evening corresponding with the time of maximum development of the equatorial anomaly. This supports a supermode involving two reflections from the F-layer without intermediate ground reflection (^2F supermode) as an important mechanism for TEP at that time of day. However, as Fig. 19 shows, there is also a significant probability for propagation of Group B (20-30 fades per minute) signal during the afternoon. In 4.1 it was shown that this type of signal is phase coherent and results from at least a 2-hop great-circle mode. Analysis of flutter fading with regard to electron density gradients has not been possible presumably due to presence of spread-F on ionograms. Hence the absence of evening Group C TEP in Table 2.

6. SOLAR-GEOPHYSICAL INFLUENCE

6.1 Sunspot Number

Variation of presence probability of signal with sunspot number is illustrated in Fig. 24. This is a composite figure comparing 48 MHz data recorded at Townsville (lat. 19.3°S, long. 146.8°E) from FM transmitters at Seoul, Korea (Gibson-Wilde and Carman[9]) with the 40 MHz signal recorded at Roma. The dashed lines show the envelopes of maximum signal during equinoxes and minimum signal during December and June solstices. The envelope of maximum signal follows the curve of sunspot number sufficiently closely to reflect the sub-minimum and sub-maximum of 1971/72 in the latter curve. Since all three envelopes are converging to a minimum one can predict that the 40 MHz signal will almost, if not completely, vanish during the next solar minimum.

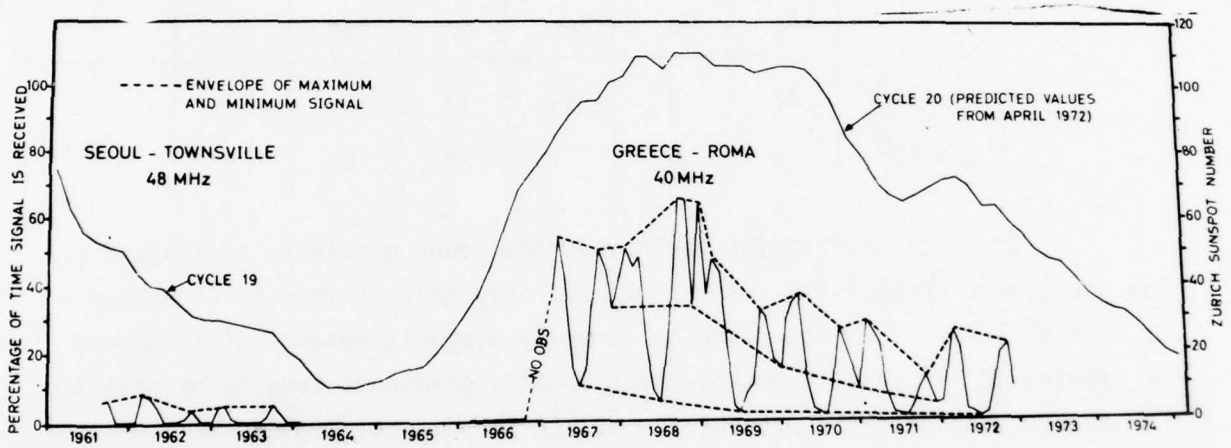

Fig. 24 – Transequatorial Propagation Compared with Zurich Sunspot Number during 12 Years. The Figure Shows Equinoctial Maxima and Solstitial Minima for Far-Eastern and African Circuits

Fig. 25 shows that the solar influence is different at different periods of the day. The evening (1800-2300 LT) 40 MHz occurrence has much the same form as plots for the whole day shown in Fig. 24. Morning and afternoon transmissions follow a somewhat different pattern - especially the afternoon where there is no definite dependence on sunspot number. The morning TEP peaks rather sharply near sunspot maximum.

The strong dependence of evening TEP on sunspot number so clearly evident in Figs. 24 and 25 leads to the conclusion that the solar control is a general characteristic of this kind of transmission.

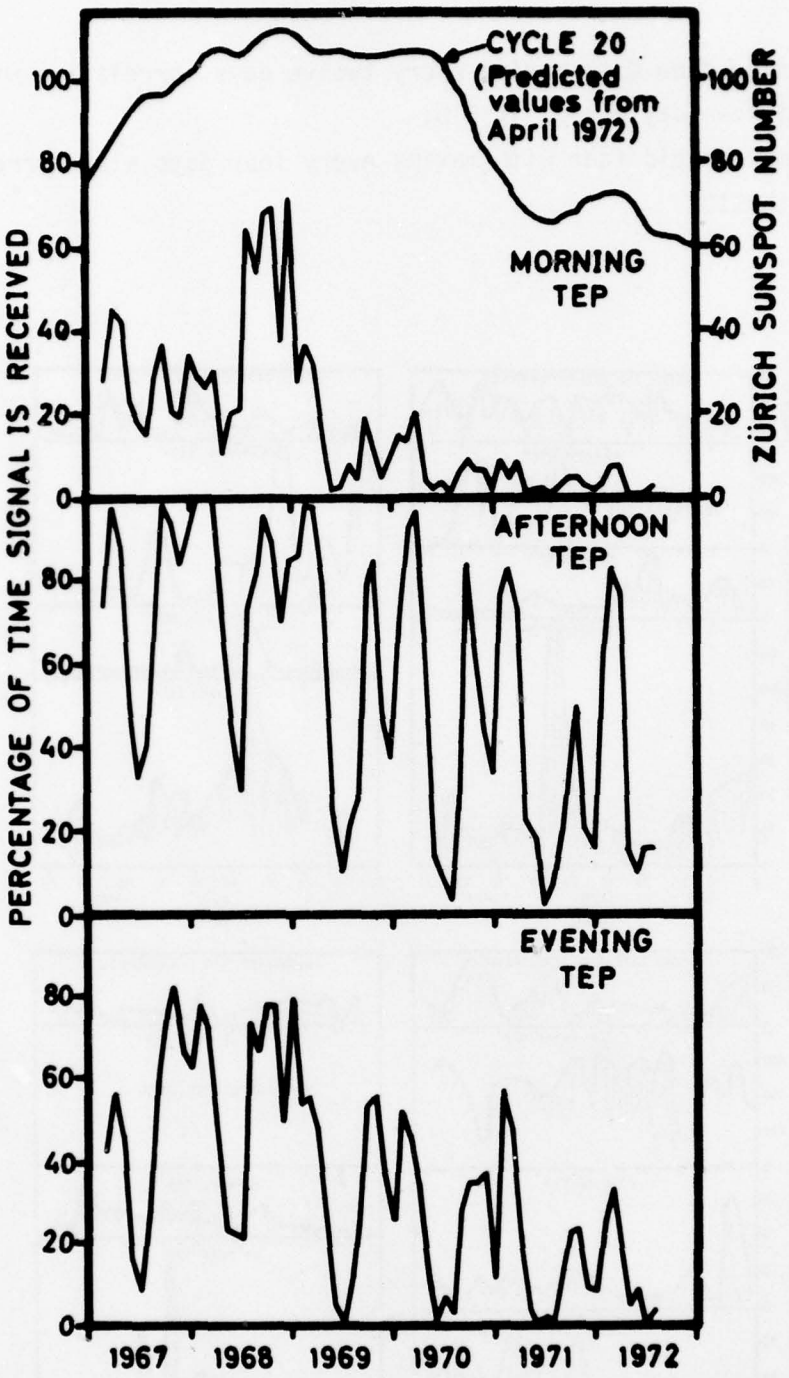

Fig. 25 - Seasonal Variation of Signal Occurrence of 40 MHz TEP for Morning (0000–1100 LT), Afternoon (1200–1700 LT) and Evening (1800–2300 LT) Hours

6.2 Sudden Ionospheric Disturbances

In Fig. 26 the average signal strength for each day for four equinoctial periods is compared with the occurrence of sudden ionospheric disturbances (SID). This leads to the interesting result that two distinctive periodic variations in TEP signal strength closely related to solar activity can be distinguished:

(i) a slow fade with maxima every twelve days correlating with thirteen-day maxima in SID;

(ii) a more rapid fade with maxima every four days also correlating with SID.

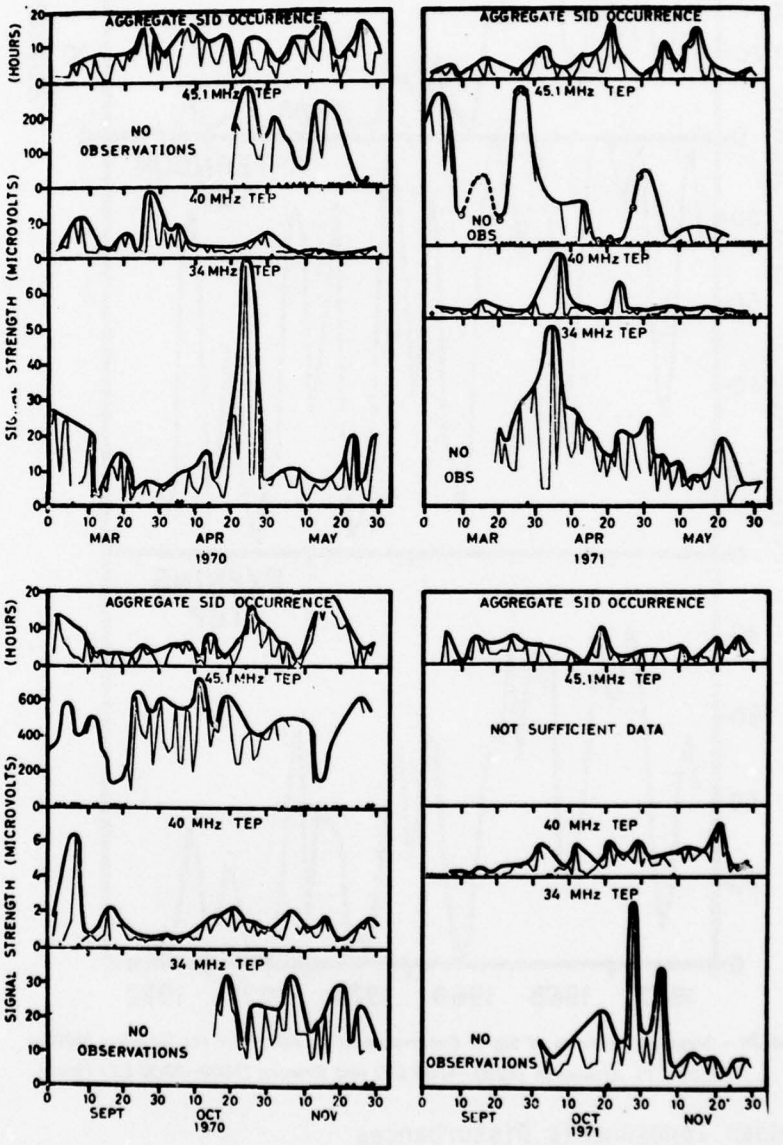

Fig. 26 – Characteristics of Sudden Ionospheric Disturbances Compared with Fading of Transequatorial Propagation Signal Strength. The Figure Illustrates Correlation between Fading of SID and TEP of Two Periodicities, 12–13 Day and 4 Day

The twelve-day fades in signal strength have been compared with maxima in SID. In a first simple analysis coincidence of maxima in signal strength were compared with minima in SID, and vice versa, for the four three-month equinoctial seasons of 1970 and 1971. In 43% of 280 comparisons maxima coincided with maxima and minima with minima. There is thus a definite probability that TEP signal is lowest when SID is greatest. There was no marked variation from season to season or dependence on frequency.

A similar analysis was done for signal occurrence during September 1970 equinox. The signal occurrences had maxima which coincided with SID maxima in 55% of all cases. These are in phase with signal strength fading in only 32% of all cases.

Correlation between the period of the short four-day fades in SID and TEP is remarkable. During 366 days the average period for SID was 3.5 days and for 679 days of TEP the average was 3.6 days indicating a strong relationship.

Sudden ionospheric disturbances are caused by X-rays from solar flares increasing the ionisation in the lower ionosphere. They are characterised by increased absorption of short-wave radio signals resulting in short-wave fade-outs (SWF). For detailed discussion of ionospheric disturbances see, for example, Reid[47].

The large scale effects of solar flares produce the periodicity in SID evident in Fig. 26. One might look for an explanation of the thirteen-day fades by studying the passage of active regions across the sun's disc. However, that TEP signal strength follows very nearly the same periodicity is by no means to be expected from synoptic behaviour so far reported.

Such a correlation, and especially an <u>inverse</u> correlation could only arise from two causes, either from absorption or from defocussing in the lower ionosphere. To determine which of these predominates, it is necessary to consider the correlation between SID and signal occurrence mentioned above. The strong inverse correlation between fading of occurrence and strength of signal suggests that increased ionisation in the lower ionosphere produces a lower signal strength at a <u>fixed</u> receiver site

accompanied by a greater probability of occurrence. Clearly this points to a defocussing mechanism in the lower ionosphere.

6.3 Seasonal Behaviour

For the seasonal variation Gibson-Wilde[40] showed there was a relationship between the symmetry in the equatorial anomaly (see Rao[48], Lyon[49]. for example) during equinoxes and the occurrence of the Townsville TEP of Fig. 24. The decreased TEP during the solstices could likewise be related to asymmetry in the positions and magnitudes of the anomaly peaks. Fig. 27 shows a similar behaviour for the European-African circuit. Here monthly median values of f_0F2 published by C.R.P.L. for the months indicated are plotted for that circuit.

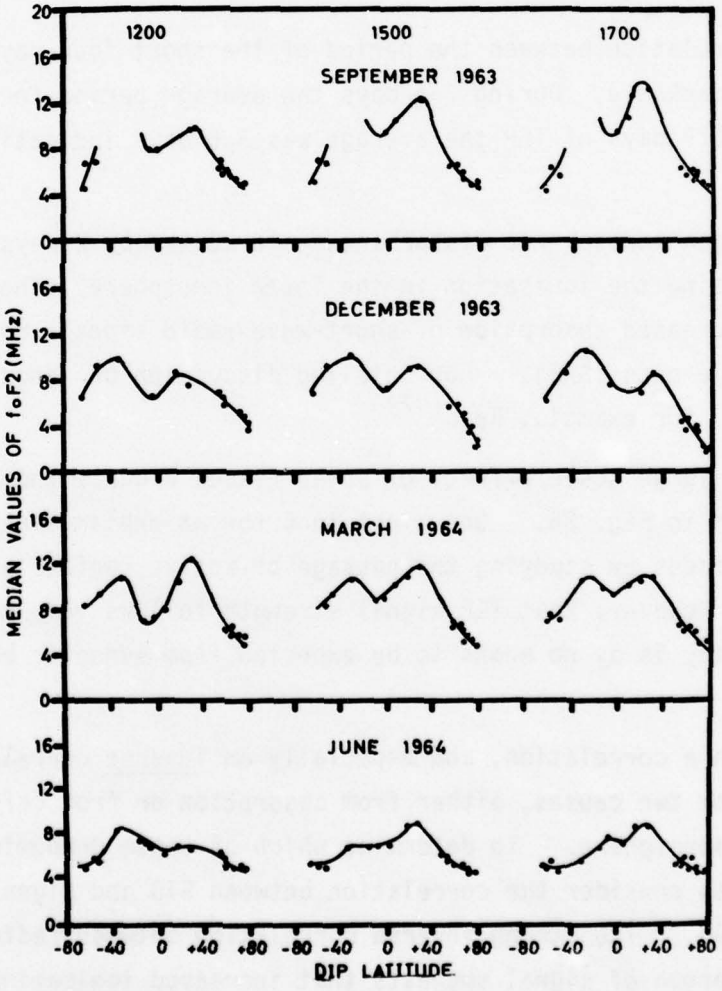

Fig. 27 – Variation of Monthly Median Values of f_0F2 with Dip Latitute for Three Afternoons Hours

The concentrations of electron density on either side of the magnetic equator are well developed during the equinoxes and December solstice, but in the latter case some asymmetry occurs. On the other hand, during the June solstice, the anomaly peaks are weakly developed and rather more asymmetrical in position and magnitude. This must be regarded as a general characteristic of the equatorial ionosphere influencing TEP for African and Far-Eastern circuits.

In Fig. 11 TEP transmissions from Oahu to Raratonga were compared with the Athens-Roma circuit and it was noted that Nielson's[11] reported higher reception in June than December is reversed and more marked for the latter circuit. That the Pacific and African circuits have reversed solstitial reception can be explained in terms of relative positions of the magnetic and geographic equators. But for an explanation of how the difference in reception is greater for the African circuit, it is necessary to introduce a further factor.

Fig. 28 illustrates how the north-south neutral wind described by Hanson and Moffett[50] is such a factor. Vertical electrodynamic forces remove electrons from the neighbourhood of the magnetic equator and subsequent downward diffusion results in symmetrical enhancements to the north and south of the magnetic equator. When the sub-polar point lies to the north of the magnetic equator as during the June solstice, this increases

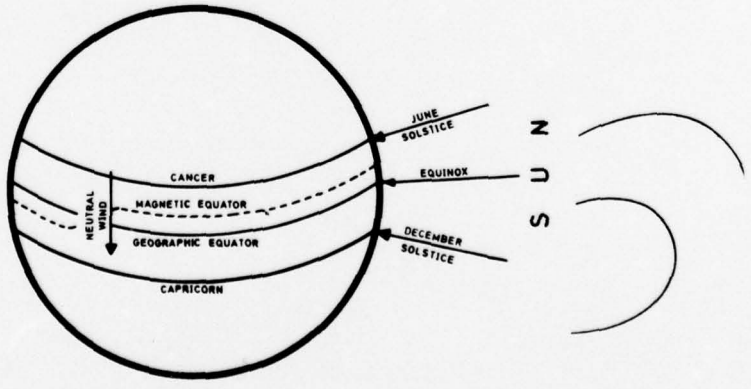

Fig. 28 – Geophysical Factors Influencing Transequatorial Propagation

the northern ionisation, but the neutral wind moves this excess of ionisation south tending to fill the trough over the equator. During the December solstice neutral wind and increased ionisation due to the southern track of the sub-polar point combine to produce increased enhancement south of the magnetic equator as is evident from Fig. 27. This explains the behaviour for the African circuit. For the Pacific circuit the southward position of the magnetic equator and the southward direction of the neutral wind combine to produce the reverse effect.

7. OPTICAL INVESTIGATIONS

7.1 Airglow and the Equatorial Anomaly

A study of optical emissions from the night-time F-region has considerable potential as a means for investigating the equatorial anomaly and hence TEP. There are three tropical emissions resulting from a charge transfer process :-

$$O^+ + O_2 \rightarrow O + O_2^+$$

and

$$O^+ + NO \rightarrow O + NO^+$$

followed by dissociative recombination :-

$O_2^+ + e \rightarrow O + O + 6.96$ eV (5577, 6300-6364 Å)

and $NO^+ + e \rightarrow N + O + 2.76$ eV (5199-5201 and possibly 6300 Å).

Barbier[51] has deduced a semi-empirical relationship between the intensity of 6300 Å emission and the ionospheric parameters h'F and f_0F2. The dependence of these parameters on the number density of electrons and the concentration of O_2^+ should thus make it possible to study variations of plasma frequency evident as irregularity patches by observing the 6300 Å emission from the patches and surrounding background in the form of isophote sky maps.

Barbier et al[52] [53] observed large enhancements in 6300 Å emission which were described as "intertropical arcs" because of their appearance as broad arc-like bands on either side of the magnetic equator. King[54] has shown that these arcs are closely related to the equatorial anomaly.

An airglow experiment designed to cover the southern part of the Athens-Roma TEP path was planned from the beginning of the project. Development of photometers and the establishment of observing sites has proved to be a long task reaching maturity only during the final stages of the TEP program. However, the preliminary results at present available and which are introduced below are sufficiently promising to form the basis of planning for a new combined Airglow-TEP experiment.

The data of Fig. 29 was collected by employing intercalibrated photometers for simultaneous observations at three stations: Roma, Ewanrigg (17.5°S, 31.0°E) and Olorgesailie (1.5°S, 36.5°E). Plotted 6300 Å intensity values, appearing in Fig. 29 were taken from isophote sky maps of the kind illustrated in Fig. 30. The composite data covers about 40 degrees of latitude corresponding to the southern half of the present TEP path.

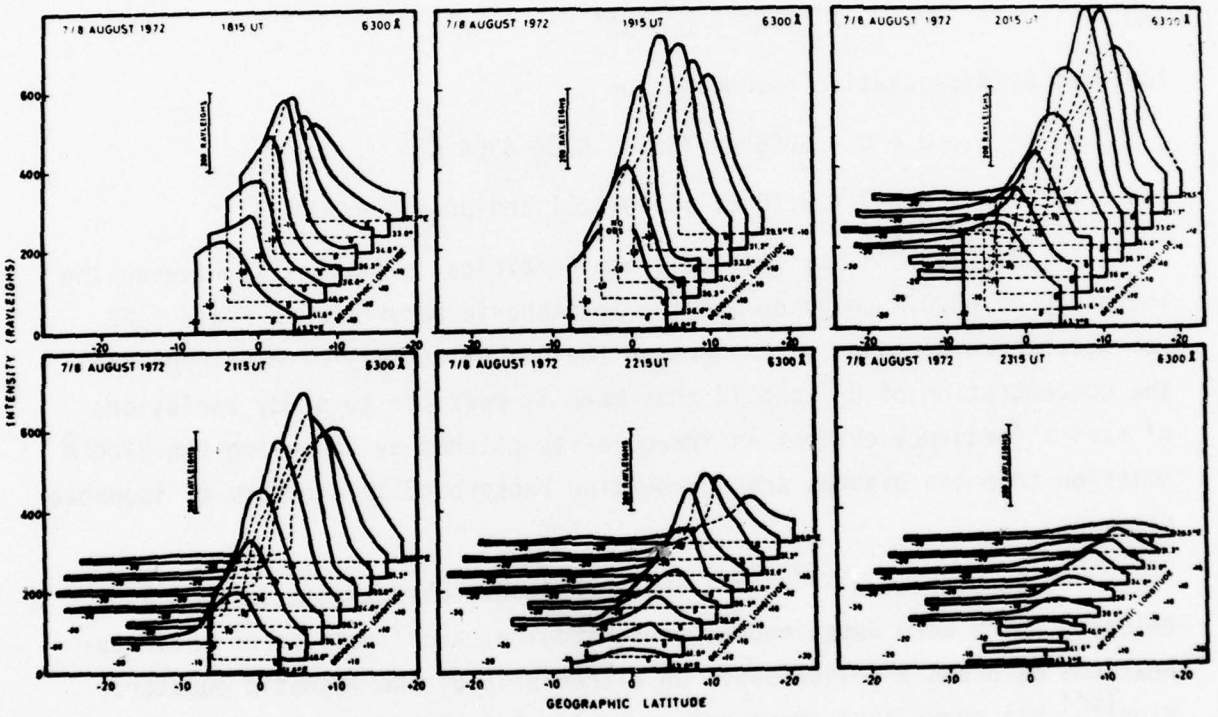

Fig. 29 – Overlays Showing the Development and Decay of an "Intertropical Red Arc" during the night of 7/8 August 1972

Figs. 29 and 30 show by both overlay and contour representation how the intertropical arc has a stable diurnal character. Development and decay of the main tropical enhancement has a time variation similar to the equatorial anomaly. There are longitudinal fluctuations in the tropical region that also appear to be stable. The intensity peak slightly west of the centre of the northern field has been observed on many occasions and appears to be related to local geophysical factors still to be investigated rather than diurnal influence of the equatorial anomaly. This peak is the dominant feature of the contour map but the overlays of Fig. 29 show that the peak is a detail in the general enhancement of the intertropical arc.

Fig. 30 –Latitute Variation of 6300 Å Airglow Intensity at 2015 UT for the night of 7/8 August 1972. Intensities are in Rayleighs and broken contours are interpolated values.

Airglow photometry as a means of studying night-time ionospheric morphology is a sensitive technique with considerable dynamic range. It is possible from the one set of data to investigate structural features such as intensity enhancements or depressions, or the movement of contours which

might be orders of magnitude apart in values of their intensities. Much of the structure shown in Fig. 29 is not relevant to TEP and therefore detailed interpretation of the higher latitude features is outside the scope of the present report. However, one interesting feature is the movement of the tropical intensity peak of Figs. 29 and 30. Fig. 31 (a) shows how the position of the peak systematically changes through the night. Movement towards the dip equator until about local midnight is accompanied by an increase to maximum intensity. The motion is further illustrated in Fig. 31 (b) where it is evident that the peak undergoes a systematic velocity change throughout the night. The range of velocities decreases from 2.6 deg hr^{-1} towards the dip equator in the premidnight period to 1 deg hr^{-1} away from the dip equator at 0030 LT; it then increases again to about 1 deg hr^{-1} towards the dip equator at 0200 LT. Movement of intertropical arcs north of the equator with velocities of the same order have been deduced by King[54] from Barbier

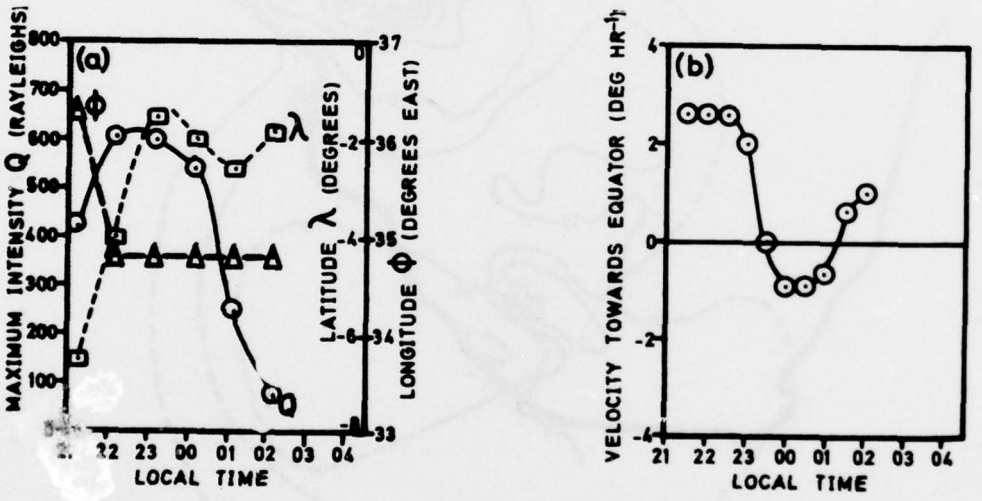

Fig. 31 – (a) Location in Latitute and Longitude of the Peak Intensity of 6300 Å Airglow throughout the night of 7/8 August 1972 -

(b) Velocity of Intensity Peak of Fig. 31 (a) Nothwards (i.e. towards both geographic and dip equators)

et al's[52] observations. However, the present results do not support King's[54] deduction that the movement ceases at about 0200 or 0300 LMT. Furthermore, Fig. 31 (a) shows that the southern peak of the arc does not approach closer to the magnetic equator than 12^{o} as compared with the reported[54] 5^{o} limit to the southern excursion of the northern peak. Clearly further analysis of observational results is necessary.

Observations such as this have opened up a promising new field

for investigating large scale irregularities in both tropical and midlatitude regions.

7.2 Evening TEP and the Sunspot Cycle

It is perhaps unfortunate that TEP experiments programmed to coincide with the solar maximum of 1968 have not synchronized with airglow programs proceeding during the same period. At the time of writing the present report the immediate future for a combined TEP-Airglow investigation is unfavourable. Evening signals are becoming increasingly rare and prospects for copious signal after sunset will not increase until after the next solar minimum in 1975.

LIST OF REFERENCES

(1) Anastassiadis, M.A. and Antoniadis, D. "Time Delay Measurements in the Athens (Greece)-Roma (Lesotho) VHF Transequatorial Propagation Circuit", J. Atmos. Terr. Phys., 34, 1972,1215.

(2) Cracknell, R.G. "Transequatorial Propagation of VHF Signals", QST, 43, Dec. 1959, 11.

(3) Southworth, M.P. "Night Time Equatorial Propagation at 50 Mc/s", Final results from an IGY amateur observing program, Stanford Electronics Labs., Final Report, contract AF-19-604-5235, May 1960.

(4) McCue, C.C. and Fyfe, D.F. "Transequatorial Propagation: Task Bridger Introductory Review", Proc. I.R.E.E., Australia, Jan. 1965, 1.

(5) Villard, O.G., Stein, S. and Yeh, K.C. "Studies of Transequatorial Propagation by the Scatter Sounder Method", J. Geophys. Res., 62, 1957, 399.

(6) Dueno, B. "Peculiarities and Seasonal Variations of Transequatorial Backscatter echoes as observed at Mayaguez, Puerto Rico", J. Geophys. Res., 65, 1960, 1691.

(7) Thomas, J.A. "Transequatorial Backscatter Observations of Magnetically Controlled Ionisation", Nature, 191, 1961, 792.

(8) Carman, E.H., Gibson-Wilde, B.C. and Conway, R.J. "Anomalous VHF Transequatorial Ionospheric Propagation Recorded at Townsville", Aust. J. Phys. 16, 1963, 171.

(9) Gibson-Wilde, B.C. and Carman, E.H. "Further Studies of Long Range Transequatorial VHF Radio Signals at Townsville", J. Atmos. Terr. Phys., 26, 1964, 1231.

(10) Cracknell, R.G. and Whiting, R.A. 1965 RSGB Bulletin, 367.

(11) Nielson, D.L. "Long-Range VHF Propagation across the Geomagnetic Equator", Stanford Research Institute Research Report, March 1969.

(12) Washburn, C.L., Olin, R.P., Johnson, F.H. and Woronka, W. "Transequatorial F-layer Propagation Study", ITT Fed. Laboratories Final Report, contract AF-30-602-2506 June 1963.

(13) Bowen, E.D., Fay, W.J. and Heritage, J.L. "Transequatorial F-layer Propagation Study", J. Geophys. Res. 73, 1968, 2469.

(14) McNamara, L.F. "Comparison of Observations and Predictions on two Japan-Townsville circuits", IPS-15, Ionospheric Prediction Service, Darlinghurst, N.S.W., Australia, Nov. 1970.

(15) McNamara, L.F. "Evening-type Transequatorial Propagation in the Far-East", IPS-16, Ionospheric Prediction Service, Darlinghurst, N.S.W., Australia, Nov. 1971.

(16) Nielson, D.L. and Crochet, M. "HF and VHF Transequatorial Propagation", Fourth International Symposium on Equatorial Aeronomy, Ibadan, Nigeria, Sept. 1972.

(17) Nielson, D.L. "Oblique Sounding of a Transequatorial Path" in Spread-F and its effects on Radiowave Propagation, AGARDOGRAPH 95, (W. & J. Mackay Co., Ltd. London) 1966, 467.

(18) Davies, K. and Barghausen, A. "The Effect of Spread-F on the Propagation of Radiowaves near the Magnetic Equator", in Scatter Propagation of Radiowaves, AGARD Conf. Proc. 37, 1968.

(19) Yamaoka, M., et al. "The Experimental Results on the Transequatorial Path between Australia and Japan in VHF band", Inst. Elect. Commun. Engr., Japan, Res. Note A-P, Oct. 1966.

(20) Carman, E.H., Heeran, M.P. and Anastassiadis, M.A. "Investigation of a VHF Transequatorial Path between Europe and Southern Africa", J. Atmos. Terr. Phys. (in press) 1972.

(21) Fyfe, D.F. "Observations of Transequatorial Propagation from 1964 to 1968", Tech. Note CPD(T) 174, Dept. of Supply, Weapons Research Establishment, Salisbury, South Australia, July 1969.

(22) Nielson, D.L. "A Review of VHF Transequatorial Propagation" in Scatter Propagation of Radiowaves, AGARD Conf. Proc. 37, 1968.

(23) Osborne, B.W. J. Atmos. Terr. Phys., 2, 1951, 66.

(24) Yeh, K.C. and Villard, O.G. "A New Type of Fading Observable on High-Frequency Radio Transmissions Propagated over Paths crossing the Magnetic Equator", Proc. I.R.E., 46, 1958, 1968.

(25) Calvert, W. et al. "Equatorial Spread-F Motions", in Proc. Intl. Conf. on the Ionosphere (Physical Society, London), 1963, 316.

(26) Davies, K. and Chang, N. "Radio Doppler Observations of the Ionosphere near the Magnetic Equator" in Scatter Propagation of Radiowaves, AGARD Conf. Proc., 37, 1968.

(27) Clemesha, B.R. "An Investigation of the Irregularities in the F-region associated with Equatorial Type Spread-F", J. Atmos. Terr. Phys., 26, 1964, 91.

(28) Kelleher, R.F. and Skinner, N.J. "Studies of F-region Irregularities at Nairobi. II - By Direct backscatter at 27.8 MHz", Ann. Geophys., 27, 1971, 195.

(29) Cohen, R. and Bowles, K.L. "On the nature of Equatorial Spread-F", J. Geophys. Res., 66, 1961, 1081.

(30) Calvert, W. and Cohen, R. "The Interpretation and Synthesis of certain Spread-F Configurations appearing on Equatorial Ionograms", J. Geophys. Res., 66, 1961, 3125.

(31) Pitteway, M. and Cohen, R. "A Waveguide Interpretation of Temperate Latitude Spread-F on Equatorial Ionograms", J. Geophys. Res., 66, 1961, 3141.

(32) Krishamurthy, B. and Rao, B. "Variation of Spread-F Index with Frequency in pre- and post- midnight periods at Waltair", J. Atmos. Terr. Phys., 26, 1964, 783.

(33) Huang, C. "F-Region Irregularities that cause Scintillations and Spread-F Echoes at Low Latitude", J. Geophys. Res., 75, 1970, 4833.

(34) Crochet, M. "Contribution a l'étude de l'influence des Inhomogeneites Ionosphériques sur la Propagation des Ondes Décamétriques á Longue Distance", Thesis, Physics Department, University of Paris, 1969.

(35) Crochet, M. "Propagation Transéquatoriale en Dehors du Grand Circle en Ones Décamétriques", Parts I & II, Ann. de Geophys., 28, 1972, 27.

(36) Röttger, J. "Einflüsse des Äquatorialen Spread-F auf die Kurzwellenausbreitug", Kleinheubacher Berichte, 14, 1971a, 269.

(37) Röttger, J. "An Application of the Monte-Carlo Method to Remote Sensing Systems", AGARD Conf. Proc. 49, 1971b.

(38) Röttger, J. "Bestimmung von Parametern des Äquatorialen Spread-F aus Schrägubertragungsmessungen aut der Strecke Lindau-Tsumeb", Kleinheubacher Berichte, 15, 1972a, 77.

(39) Röttger, J. "Some Effects of Atmospheric Gravity Waves Observed on a Transequatorial Radio Path", Proc. AGARD Conf. 1972b.

(40) Gibson-Wilde, B.C. "The Equatorial Anomaly in the Australian Zone during Sunspot Minimum", J. Atmos. Terr. Phys., 28, 1967, 1269.

(41) Tao, K. et al "Experimental Results of VHF Transequatorial Propagation", J. Radio Res. Lab. 17, 1970, 83.

(42) Davies, K. "Ionospheric Radio Propagation" (Dover Pub. Inc., N.Y.), 1966, 245.

(43) Lockwood, G.E.K. Private communication, 1971.

(44) Caldwell, J.D. and Lockwood, G.E.K. Private communication, 1972.

(45) Wright, J.W. "Cortes Verticales de la Ionósfera a Través del Ecuador Geomagnético", NBS Tech. Note 138, 1962, 34.

(46) Lockwood, G.E.K. and Nelms, G.L. "Topside Sounder Observations of the Equatorial Anomaly in the 75°W Longitude Zone", J. Atmos. Terr. Phys. 26, 1964, 569.

(47) Reid, G.C. "Physics of Geomagnetic Phenomena", (edited by S. Matsushita and W.H. Campbell) Academic Press, N.Y., 2, 1967, 627.

(48) Rao, C.S.R. and Malthora, P.L. "A Study of the Geomagnetic Anomaly during IGY", J. Atmos. Terr. Phys., 26, 1964, 1075.

(49) Lyon, A.J. "The Geomagnetic Anomaly", Proc. Int. Conf. on the Ionosphere, Physical Society, London, 1963, 88.

(50) Hanson, W.B. and Moffett, R.J. "Ionisation Transport Effects in the Equatorial F-region", J. Geophys. Res., 71, 1966, 5559.

(51) Barbier, D. "La Lumiere du Ciel Nocturne en Ete a Tamanrasset", Compt. Rend., 245, 1957, 1559.

(52) Barbier, D., Weill, G. and Glaume, J. Ann. Geophys., 17, 1961, 305.

(53) Barbier, D. J. Phys. Soc. Japan, 17, 1962, 255.

(54) King, J.W. "Airglow Observations and the Decay of the Ionospheric Equatorial Anomaly", J. Atmos. Terr. Phys., 30, 1968, 391.

(55) Carman, E.H., Anastassiadis, M.A. and Heeran, M.P. "Transequatorial Transmissions at Very High Frequency" RUAL Report No. 5, Contract 61052-67-C-0003, 1967.

(56) Carman, E.H., Anastassiadis, M.A. and Heeran, M.P. "Transequatorial Transmissions at Very High Frequency" RUAL Report No. 9, Contract 61052-67-C-0003, 1968.

(57) Carman, E.H., Heeran, M.P. and Anastassiadis, M.A. "Transequatorial Transmissions at Very High Frequency" RUAL Report No. 16, Contract 61052-67-C-0003, 1969.

APPENDIX I

Time delay measurements in the Athens (Greece)–Roma (Lesotho) VHF trans-equatorial propagation circuit

M. ANASTASSIADIS and D. ANTONIADIS
University of Athens, Greece

(*Received* 9 *August* 1971)

Abstract—An experimental approach is made to the problem of determining absolute time delays in the transequatorial propagation path (TEP) of 7500 km Athens (Greece)–Roma (Lesotho). On the basis of the experimental results obtained, different suggested mechanisms of TEP were investigated. The most consistant is the $^1F2$ mode without excluding completely also $2F2$ under specific conditions. Multipath, flutter fading and pulse stretching observable in several cases, are discussed. Further measurements during equinoxial periods to come, will complete the above first conclusions.

TRANS-EQUATORIAL *propagation is defined as a long range ionospheric* propagation over a path that is more or less bisected by the magnetic equator, using frequencies that are substantially higher than those used in conventional short-wave radio. In the remainder of this paper the initials TEP will be used to denote this kind of propagation.

The usual criterion for distinguishing a given class of propagation is the basic reflection mechanism that returns the wave to the Earth. In late 1956, fixed frequency 23–46 MHz backscatter equipment was operated by Stanford University from a site in the Virgin Islands (64°45 long., 17°45 lat.). Usually long range backscatter echoes observed there by VILLARD *et al.* (1957) prompted their suggestion of ionosphere to ionosphere reflections from the large horizontal gradients of the equatorial anomaly. Long-range backscatter echoes in Japan similar to those observed by Villard led OBAYASHI (1959) to predict an exospheric field-guided mode of VHF propagation wherein the radio wave becomes trapped between field-aligned *irregularities.*

In 1962 WASHBURN *et al.* (1963) conducted a multifrequency (30–75 MHz) experiment between Panama and Chile (magnetic conjugates) and observed unusually large signal strengths relative to scatter and both the rapid and slow flutter fading characteristics. An oblique sounder circuit operating between Kauai and Rarotonga by NIELSON (1966) during the summer of 1962 showed a remarkable regularity of VHF propagation up to 64 MHz. These terminals are both magnetic and geographic *conjugates and a rate of occurrence unequalled before or since was observed.*

The long range trans-equatorial circuit, Athens (Greece)–Roma (Lesotho) has been under investigation since 1967 (CARMAN *et al.*, 1967, 1968, 1969). At first the Greek police network on 40 MHz was monitored and recorded in Roma. Very useful information on the seasonal and diurnal dependence of received signals were collected and, since early 1970 and for the same purpose, the experiment was organized in a much more systematic way. Athens transmitting centre started to radiate *CW* signals following a definite code on 34 MHz, 45·1 MHz and 72 MHz each hour day and night. This is the typical experimental setup for monitoring the occurrence, signal strength and fading characteristics of forward propagation signals, on the above frequencies.

Roughly, the occurrence and the signal strength over the three years of monitoring the Greek police FM network on 40 MHz, has shown the pattern that has been reported by several workers in the TEP field (SOUTHWORTH, 1960), for circuits in the Americas (WASHBURN *et al.*, 1963; DUENO, 1960), Pacific Ocean (THOMAS *et al.*, 1962) and the Far East–Australia (CARMAN *et al.*, 1963; GIBSON-WILDE and CARMAN, 1964). This pattern is characterized by an enhancement of more or less both, occurrence and signal strength during equinoxes, with minima during solstices.

Since March 1971, duplex pulse transmission has been introduced in the investigation of the above TEP European–African circuit by installing two pulse reproduction units on 33·6 MHz and 45·0 MHz of the authors' design at the receiving end in Roma–Lesotho. The mission of such a pulse reproduction unit is to transmit a pulse of definite shape and amplitude, on either of the above mentioned frequencies, a definite time after the reception of the triggering pulse sent from Athens, on either 34 or 45·1 MHz respectively. This new experiment aims to obtain absolute time delay measurements, as well as pulse propagation characteristics, in order to determine the actual path followed by the signals over the TEP circuit.

Villard's *et al.* and Obayashi's theoretical considerations are based on experimental results obtained through the backscatter technique. Other techniques are used rather to investigate signal strength and/or occurrence, seasonal and diurnal variations. The concept of the backscatter technique forms a good method for the determination of time delays for the paths followed by the signal, but however, it presents at least two shortcomings: (a) The exact earth surface location of the echo's origin (scattering area) is not known (MCCUE and FYFE 1965); and (b) owing to the very nature of ground backscatter transmissions it is reasonable to assume that echoes are at times uncertain to occur even though conditions might permit it (DUENO, 1960).

The technique used in our experiment is thought to overcome the above uncertainties and also given that the shape and amplitude of the transmitted pulses from Roma are definitely known it has been possible to investigate the various distortions suffered by the signal in its path. In the present experiment by sacrificing the flexibility of the backscatter technique a high accuracy of path delay measurements has been achieved for signals propagated between the above mentioned terminals.

DESCRIPTION OF THE EQUIPMENT AND EXPERIMENTATION

Two channels have been used in this experiment. On one channel the frequency of 34·0 MHz is used for transmission from Athens and 33·6 MHz for transmission from Roma.

On the other channel transmission on 45·1 MHz is used in Athens and 45·0 MHz in Roma.

On both channels the experimental setup includes two modified pulse transmitters and two receivers on the appropriate frequencies at the transmitting end (Athens) and two receivers coupled to the pulse reproduction units at the receiving end (Roma). The antennas at the transmitting end consist of two horizontal five-element Yagis for the transmission on 34·0 MHz and 45·1 MHz, a vertical cardioidal for reception at 33·6 MHz and a two-element Yagi antenna for 45·0 MHz. The antennas at the receiving end consist of a three-element Yagi for reception on

34 MHz and stacked twin three-element Yagis for reception on 45·1 MHz. For transmission on 33·6 MHz and 45·0 MHz a three-element Yagi and a four-element Yagi are used respectively. Each of the pulse reproduction units that have been installed in Roma consists of a combination of a triggered pulse generator and a fixed frequency low powered (120 W) pulse transmitter. They possess a controllable muting delay period that permits the locking on the triggering repetition rate and helps avoiding the problems of random shot noise in cases of small signals. It also solves automatically the problem of direct feedback between receiver and transmitter. The block diagram of the complete pulse reproduction setup at the receiving end (Roma) is given in Fig. 1.

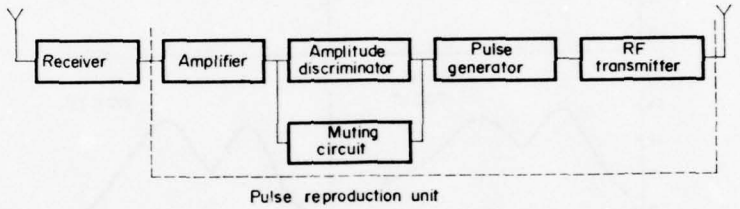

Fig. 1. Block diagram of the complete pulse reproduction setup on one channel.

The two pulse transmitters at the transmitting end, are driven by a single pulse generator which is triggered externally by a standard frequency generator. At the same transmitting end, the outputs of the receivers are connected to a 556 Tektronix Oscilloscope which is used on the delayed sweep mode (Fig. 2). With a pulse width of 160 μs this arrangement provides time delay measurements accurate to ± 50 μs. This accuracy is determined by the resolution that can be achieved with the receiver bandwidth of 8 kHz and a sweep rate of 0·5 ms cm^{-1}. The overall experimental error increases because the triggering delay at the receiving end depends on signal conditions. This introduces an error of approx ± 20 μs. Thus maximum overall error is ± 70 μs, for the double path delay of the order of 50 ms. The one-way path delay is half the total time delay.

Experimental Results

In order to make the interpretation of time delay measurements as reliable as possible, the period of experimentation was selected carefully. It is becoming increasingly evident that the TEP mode bears a close relationship to the equatorial anomaly. By inspecting the distribution of the *F2*-layer electron density on either side of the magnetic equator for all periods of the year given by the C.R.P.L. predictions, we found that the anomaly is well developed and symmetrical throughout the afternoon hours during the equinox (Fig. 3). TEP occurrence and signal strength during March equinoctial period are the highest and consequently any kind of interference is of least significance, during this period.

Time delay data collected up to now cover the spring equinoctial period of 1971 (March–April). Measurements were performed on both 34 and 45 MHz. Propagation conditions however were much better on 34 than on 45 MHz. Though the following characteristics refer mostly to the observations on the channel of 34 MHz they are also very descriptive of the behaviour on 45 MHz as well.

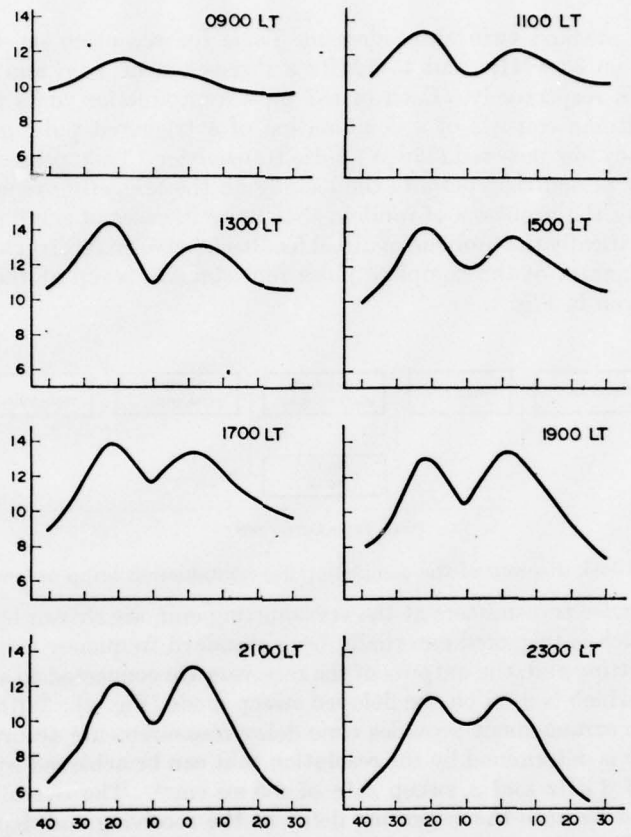

Fig. 3. Distribution of f_0F2 around the magnetic equator vs. local time for 19 March 1971 from the C.R.P.L. predictions.

The major characteristics of the return 'echoes' can be summarized as follows. By 'echo' it is referred here the triggered pulse sent from Roma:

(1) Time delays from 25·70 ms to 26·20 ms have been measured with a tendency for the lower time delay signals to be of higher strength.

(2) Time delay shows an almost continuous change throughout any day (Fig. 4).

(3) Multipath propagation can be identified in many cases during any day. It seems to be associated with rapid flutter fading and is most prevalent at times when signal strength builds up or decays (Fig. 5). It was seldomly observed during periods of strong, close to free space, signal propagation. Delay between first and last received pulse (echoes) never exceeded 600 μs. The pulse width, amplitude and multipath characteristics changed very rapidly as a function of time (Figs. 4 and 5).

(4) Pulse stretching occurred in many cases and its appearance is closely associated with that of multipath propagation which may be considered as its primary cause.

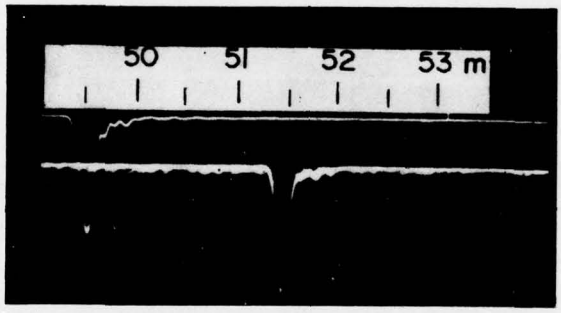

Fig. 2. Undistorted 33·6 MHz 'echo' with rapid fading present observed in Athens. The upper pulse gives the time delay and enables distortion to be evaluated by comparison of pulse shapes. Sweep rate 0·5 ms cm. Trace rate 1 trace/100 ms. Exposure 1·2 s.

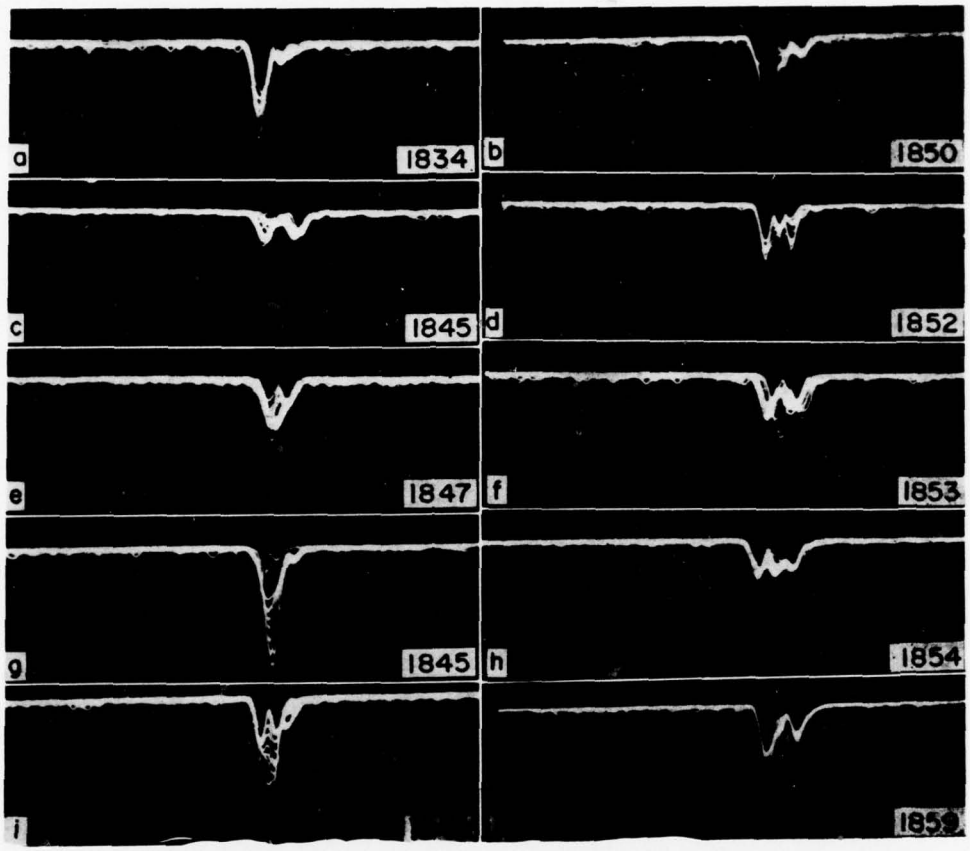

Fig. 5. A sequence of typical 'echoes' observed near sunset on 24 March 1971. Multipath propagation is present associated with flutter fading. Pulse broadening is clearly observable on most of these pictures. Sweep rate 0·5 ms/cm. Trace rate 1 trace/100 ms. Exposure 1·2 s.

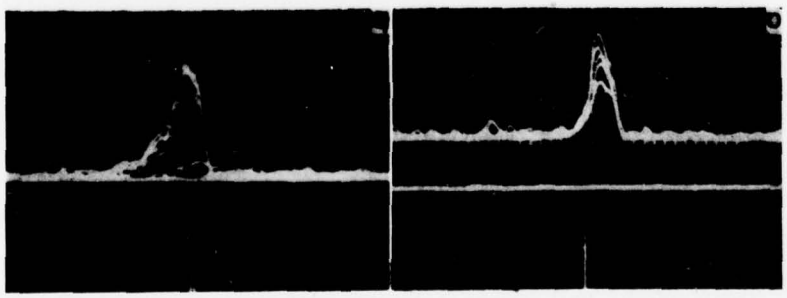

Fig. 6. Similar distortion characteristics, 'echoes' on 34 MHz (left) and 45 MHz (right) observed simultaneously.

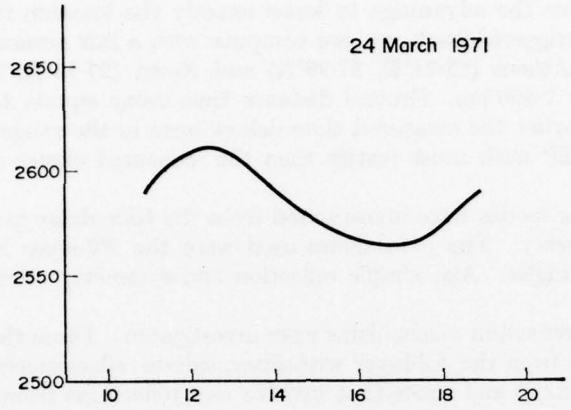

Fig. 4. Time delays measured (24 March 1971) vs. local time.

(5) Pulse characteristics appear to be similar for the 34 and 45 MHz signals (Fig. 6).

Discussion

On the basis of the above experimental results it is now possible to examine closely various theories proposed to explain TEP mechanism. Because direct ionospheric data along this European–African path are missing and consequently tracing of ray path is not possible, we are obliged to assume paths and propagation mechanisms consistent with time delays already measured.

The exospheric ducting theory proposed by Obayashi does not seem to account at all for the observed phenomenon since the time delay expected from this mode of propagation is about twice that actually observed. At this point it should be noted that in addition to the theoretical calculations by Booker (1962) that prove guiding unlikely above 10 MHz, a significant list of published experimental data (Dueno, 1960; Gallet and Utlaut, 1961; Thomas *et al.*, 1962; Nielson, 1969) are also inconsistent with the exospheric ducting mode.

The most widely accepted theory of TEP is the "*F* theory proposed by Villard *et al.* (1957). According to this theory successive reflections on the ionosphere without intermediate ground reflections can account for long range propagation when the necessary tilts for the production of these reflections exist in the *F*-layer. The necessary tilts arise because horizontal gradients in the electron density are more or less symmetrical about the magnetic dip equator, as in the well known equatorial anomaly.

Some observations on long distance circuits suggested that single hop propagation at unusually high frequencies can take place on high angle rays (Pedersen) without having to invoke ionospheric tilts (Fulton *et al.*, 1960). Most of these observations refer to non-trans-equatorial and rather short distance circuits. An attempt (Muldren and Maliphant, 1962) to explain TEP by this without tilts mechanism must be considered with reserve.

Because we have the advantage to know exactly the location from where the return pulses are triggered back, we can compute with a fair accuracy the ground distance between Athens (23·74°E, 37·99°N) and Roma (27·75°E, 29·42°S). This distance is exactly 7·490 km. Ground distance time delay equals 24·97 ms. As it was pointed out earlier the measured time delays were in the range from 25·70 to 26·20 ms. Any TEP path must justify then the measured excess delay range of 0·73 to 1·23 ms.

Various possible modes were investigated from the time delay point of view by using simple geometry. The parameters used were the *F2*-layer height and the arrival and firing angles. Also simple reflection and symmetry of the circuit were assumed.

Three possible reflection mechanisms were investigated: Those that involve two or three reflections from the *F2*-layer with intermediate reflections from the ground (denoted by $2F2$, $3F2$) and those that involve two reflections from the layer, but without intermediate reflection from the ground (the 'chorded hop' mode denoted by ${}^2F2$). The minimum time delay of 25·70 ms as well as the most common measured delay of 25·90 ms are not consistent with the $3F2$ mechanism which would give a minimum time delay of 26·35 ms (for $hF2 = 300$ km) lying completely out of the range of measured time delays.

On the other hand $2F2$ mode would give at minimum a time delay of 25·80 ms (for $hF2 = 300$ km) which lies within the measured range of time delay. Additionally ${}^2F2$ mechanism for the circuit under consideration gives a time delay of 25·83 ms under the same height conditions. It is thus obvious that, it is not possible to discriminate, the actual mechanism, among these two models, by the use of only simple geometry. On the other hand the observed multipath fading may arise from mutual interference between ${}^2F2$ and $2F2$ modes.

At this point a much more elaborate technique for ray tracing is required. This has been done graphically by Villard *et al.* and recently by Nielson (1969), who used typical latitudinal profiles of f_0F2 and layer heights of an afternoon equatorial ionosphere during equinox, in order to calculate oblique ionograms, through a computer program, for various circuit lengths. While the time delay resulting from the above mentioned program for a trans-equatorial circuit of 7·780 km is 26·5 ms the complete absence of the $2F2$ mode of propagation at any frequency from 16 to 52 MHz is very striking. This can be qualitatively understood (Villard *et al.*, 1957; McCue and Fyfe, 1965) if one considers that at the time of a well developed equatorial anomaly the *F2*-layer is not concentric with the Earth, but exhibits a tilted shape in the equatorial region. Thus rays for a given circuit length cannot be returned to Earth at the necessary region in order to produce $2F2$ mode, through only one reflection from the ionosphere.

However, at this point it should be pointed out that some morning signals (0900–1000 LT) of reduced field strength on 34 MHz, at times when the equatorial anomaly is not well developed could be attributed to the $2F2$ propagation mode. In contrary, the strong (commonly above free space) steady and of short time delay signals on 34 and 45 MHz observed in the afternoon (1300–1900 LT) when the equatorial anomaly is well developed should definitely be attributed to the ${}^2F2$ mechanism. Following the geometry of Athens–Roma path, elevation angle for

$^2F2$ propagation mode is less than 10°. As indicated by THOMAS and MCINNES (1962) for these angles ray focusing occurs leading to strong and steady 'echo' configuration, often observed in our experiment.

As it was pointed out earlier in this paper, multipath propagation was observed many times. This multipath is characteristic of periods of the day, with more or less small signals and is also associated with the phase of signal strength built up to the steady and strong with no multipath or stretching condition, or with the decaying phase from these conditions.

Figure 5 is an excellent example of the signal decaying phase. At 1905 of this day the signal had completely disappeared and was not observed, any more, during the same day. It can be seen that a very rapid fading exists and also the shape of the signal is violently changing (notice individual sweeps in each picture).

It is thought that this condition of the signal, very characteristic of its evening disappearance, arises from the breaking of the equatorial anomaly after sunset CARMAN *et al.* (1963).

The present experiment must be considered as a first approach to the problem of the determination of the exact mechanism of trans-equatorial propagation by absolute time delay measurements. Further measurements to be performed in the next equinoctial and solstitial periods will support or modify the above statements.

Acknowledgement—The authors express their many thanks to Professor ERIC CARMAN and Dr. M. HEERAN for their assistance and all the offered facilities for the installation of the time delay measuring equipment in Roma–Lesotho.

This work was supported by the University of Athens under research grant, the National Research Foundation and the Greek Atomic Energy Commission 'Demokritos' in Athens.

REFERENCES

BOOKER H. G.	1962	*J. geophys. Res.* **67,** 4135.
CARMAN E. H., GIBSON-WILDE B. C. and CONWAY R. J.	1963	*Aust. J. Phys.* **16,** 171.
DUENO B.	1960	*J. geophys. Res.* **65,** 1961.
FULTON B., SANDOZ O. and WARREN E.	1960	*J. geophys. Res.* **65,** 177.
GALLET R. M. and UTLAUD W. F.	1961	*Phys. Rev. Lett.* **6,** 591.
GIBSON-WILDE B. C. and CARMAN E. H.	1964	*J. Atmosph. Terr. Phys.* **26,** 1231.
MCCUE and FYFE D. F.	1965	*Proc. IREE Aust.* (Jan. 1965), 1.
MULDREW D. B. and MALIPHANT R. G.	1962	*J. geophys. Res.* **67,** 1805.
NIELSEN D. L.	1966	*Spread-F and its effects on Radiowave Propagation*, Agardograph 95, pp. 467–490. Mackay, London.
OBAYASHI T.	1959	*J. Radio Res. Lab. Japan* **6,** 303.
VILLARD O. G., STEIN S. and YEH K. C.	1957	*J. geophys. Res.* **62,** 399.

Reference is also made to the following unpublished material:

CARMAN E. H., ANASTASSIADIS M. A. and HEERAN M. P.	1967	Transequatorial Transmissions at Very High Frequency. Annual Progress Report No. 1. Contract 61052-67-C-0003.

CARMAN E. H., ANASTASSIADIS M. A. and HEERAN M. P.	1968	Transequatorial Transmissions at Very High Frequency. Annual Progress Report No. 2. Contract 61052-67-C-0003.
CARMAN E. H., HEERAN M. P. and ANASTASSIADIS M. A.	1969	Transequatorial Transmissions at Very high Frequency. Annual Progress Report No. 3. Contract 61052-67-C-0003.
NIELSON D. L.	1969	Long-range VHF Propagation across the geomagnetic equator. Research Report Stanford Research Institute (March 1969).
SOUTHWORTH M. P.	1960	Night time equatorial propagation at 50 Mc/s. Final results from an J.G.Y. amateur observing program. Stanford Electronic Labs Final Report, Contract AF-19-604-5235, May 1960.
THOMAS J. A. and MCINNES B. A.	1963	Transequatorial propagation analysis: Ray tracing and mode analysis. University of Queensland Scientific Report No. 10. Contract AF-64-(500)-9 (1962)
THOMAS J. A., MCINNES B. A. and CROUCHLEY J.	1962	Exospheric Propagation Experiments. Univ. of Queensland Scientific Report No. 11, Contract AF-64-500-9.
WASHBURN C. L., OLIN R. P., JOHNSON F. H. and WORONKA W.	1963	Transequatorial *F*-layer propagation study. ITT Federal Labs final Report Contract AF30 (602)-2506.

APPENDIX II

SIGNAL RECEIVED

34 MHz

Date	Time (Local time)
26. 1.70	1600
	1700
27. 1.70	0900
	1200, 1300
	1500
	1700 - 2000
28.1.70	1000
	1400
	1600, 1700
	2000, 2100
29. 1.70	1200
	No obs. 1600 on 29.1.70 to 0800 on 30.1.70
30. 1.70	1000 - 1200
	1600
	1700
	2000
31. 1.70	1100
	1300 - 1600
	1700
	2000
1. 2.70	1200
	1600, 1700
2. 2.70	1600, 1700
	2000
3. 2.70	1500
	1800
	2000 - 2200
4. 2.70	1200 - 1300
	1500, 1600
	1700 - 1145 on 5.2.70 No obs.
5. 2.70	1200 - 1800
	2000
6. 2.70	0900 - 1500
	1600 on 6.2.70 to 0900 on 7.2.70 No obs.
7. 2.70	1200
	1300 - 1800 No obs.

34 MHz

Date	Time (Local time)
8. 2.70	1100 - 1600 1900 - 2100
9. 2.70	1000 1200 1400, 1500 1800 - 2100
10. 2.70	1100 1400 1600 - 1800 2000, 2100
11. 2.70	1200 2000, 2100
12. 2.70	1100, 1200 1400, 1500 1800
13. 2.70	1100 1300 - 1800
14. 2.70	1000 1200, 1600, 1700 2000 - 2100 2300
15. 2.70	No obs
16. 2.70	1700 1800 - 1400 on 17.2.70 No obs.
17. 2.70	1500, 1600
18. 2.70	1100 1300 1600 1800
19. 2.70	0900 - 1700
20.2. 70	1500 - 1800
21. 2.70	0700 1100 - 1300 1500, 1600 1900 - 2300 No obs.
22. 2.70	0900 - 2100
23. 2.70	0900 - 1800 2000

34 MHz

Date	Time (Local time)
24. 2.70	0900 - 1400, 1600, 1700 2000
25. 2.70	0900 - 1400 1600 - 2000
26. 2.70	0900, 1000 1200 - 1400 1800
27. 2.70	1400, 1600 2000
28. 2.70	0800 - 1000 1200, 1300 1500 - 1800
1. 3.70	0900 - 1100 1300, 1500 - 2000
2. 3.70	0900 - 1200
3. 3.70	0900 - 1200 1500 - 1700
4. 3.70	0900 1200 1500 1700
5. 3.70	0900 1200 1500 1700
6. 3.70	0800, 0900 1600, 1700
7. 3.70	1700
8. 3.70	0900 1100 1500 1700
9. 3.70	1100 1500 1700
10. 3.70	1200 1500, 1600
11. 3.70	1500
12. 3.70	1000

34 MHz

Date	Time (Local time)
14. 3.70	1000, 1200 1400 1600
15. 3.70	1700 2000 on 15.3.70 to 0900 on 16.3.70 No obs.
16. 3.70	1200, 1500, 1700
17. 3.70	1100 - 1600
18. 3.70	1200 1500, 1600
19. 3.70	0900, 1100, 1200 1500, 1700
20. 3.70	1500, 1600
22. 3.70	0900
24. 3.70	1500
26. 3.70	1100 1300, 1700
27. 3.70	0900 1100, 1200 1900 on 27.3.70 to 2200 on 28.3.70 No obs.
30. 3.70	0900
31. 3.70	1600, 1700
1. 4.70	1500, 1700
2. 4.70	1400 - 1700
3. 4.70	0900, 1000 1200 1500 - 1700 1900
4. 4.70	0900, 1000 1200 1600, 1700 0000 on 5.4.70 to 1600 on 7.4.70 No obs.
7. 4.70	1700
8. 4.70	1500 1700
9. 4.70	0900, 1000 1500 1700

34 MHz		45.1 MHz	
Date	Time (Local time)	Date	Time (Local time)
10. 4.70	0800 - 1100 1700	Observations commenced on 20.4.70	
11. 4.70	1200, 1500 1700, 1800		
12. 4.70	1500 - 1700		
13. 4.70	0800, 0900 1500 - 1700		
14. 4.70	0900		
15. 4.70	1200 - 1500 1700		
16. 4.70	0800 - 0900 1100 - 1300 1400, 1600		
17. 4.70	1300 1500 - 1800		
18. 4.70	1200 1500 1700		
19. 4.70	1500 1700		
20. 4.70	0900 1100, 1600, 1700	20. 4.70	1700
21. 4.70	1200, 1300 1500, 1600	21. 4.70	1200 1400 - 1800, 2000
22. 4.70	1400 - 1600	22. 4.70	1000 1200 - 1800
23. 4.70	0800, 0900 1100 - 1500	23. 4.70	1300 - 1800
		24. 4.70	1200 1300, 1500 - 1700
25. 4.70	1100 1400 - 1700	25. 4.70	1200, 1300
26. 4.70	0900 1200 - 1700	26. 4.70	1200 - 1500
27. 4.70	1300 - 1600	27. 4.70	1300, 1400 1700
28. 4.70	1200, 1500, 1700	28. 4.70	1400, 1500

34 MHz		45.1 MHz	
Date	Time (Local time)	Date	Time (Local time)
29. 4.70	1200, 1500 - 1800	29. 4.70	1400 - 1800
30. 4.70	1500 - 1700		
1. 5.70	1100 1300, 1400, 1600	1. 5.70	1400, 1600
2. 5.70	1100, 1200 1500 - 1800	2. 5.70	1900
3. 5.70	1300 1600 - 1800		
4. 5.70	1200- 1400 1600	4. 5.70	1300 1500 - 1700
5. 5.70	0800, 1300 1600 - 1800		
6. 5.70	1000, 1200 1400 - 1700 1900	6. 5.70	1300 - 1400
7. 5.70	1200 1400 1600, 1700		
8. 5.70	1200, 1300 1600 - 1800		
9. 5.70	1400 - 1900		
10. 5.70	1200 1500 - 1800		
11. 5.70	1500	11. 5.70	1400 1500
12. 5.70	1100, 1500 1600, 1800, 1900		
13. 5.70	1100, 1200 1400 - 1700	13. 5.70	1300 - 1800
14. 5.70	1100, 1200 1400 - 1700	14. 5.70	1600
15. 5.70	1100 - 1300 1600	15. 5.70	1400 1600
16. 5.70	1200, 1300	16. 5.70	1400
17. 5.70	1300 - 1800		
18. 5.70	1400 - 1600		

34 MHz		45.1. MHz	
Date	Time (Local time)	Date	Time (Local time)
19. 5.70	1200, 1300, 1700		
20. 5.70	0800 1600, 1700		
21. 5.70	1200, 1300 1500 1700, 1800		
22. 5.70	1200, 1400, 1700, 1800		
23. 5.70	1700, 1800		
24. 5.70	1400 1700		
25. 5.70	1200 1900	25. 5.70	1000 on 25.5.70 to 1200 on 26.5.70 No obs.
26. 5.70	1600 - 1800		
29. 5.70	1300 1600, 1700		
30. 5.70	1600		
31. 5.70	1100 - 2000 No obs.		
1. 6.70	1500 - 1600		
2. 6.70	1000 - 1300 1500 - 1700		
3. 6.70	1300 - 1500 1800		
4. 6.70	1200 - 1400	4. 6.70	1300, 1400
5. 6.70	1300 - 1500, 1700	5. 6.70	1400, 1500, 1700
6. 6.70	1700, 1800	6. 6.70	1900
7. 6.70	No obs.	7. 6.70	No obs.
8. 6.70	1500 - 1800		
9. 6.70	1300 1500 1800, 1900		
10. 6.70	1400 - 1600	11. 6.70	1500
12. 6.70 to 16.6.70 No obs		12. 6.70 to 16.6.70 No obs.	
17. 6.70	1800		
18. 6.70	1600		

34 MHz		45.1 MHz	
Date	Time (Local time)	Date	Time (Local time)
19. 6.70	1600		
20. 6.70	1600 1800		
21. 6.70	1600 - 1800		
22. 6.70	1000, 1700, 1800		
23. 6.70	1700	23. 6.70	1700, 1800
24. 6.70	1100 - 1300 No obs. 1500 - 1700	24. 6.70	1100 - 1300 No obs. 1600, 1700
25. 6.70	1200 - 1500 No obs. 1700, 1800	25. 6.70	1200 - 1200 on 26.6.70 No obs.
26. 6.70	1200 - 1100 on 29.6.70 No obs.	26. 6.70	No obs.
29. 6.70	0000 - 1100 No obs. 1600, 1800		
30. 6.70	1100 - 1400 No obs. 1500 - 1700	30. 6.70	1100 - 1400 No obs.
1. 7.70	1600, 1700		
2. 7.70	1600 - 1800		
3. 7.70	1400 1600		
4. 7.70 and 5.7.70 No obs		4. 7.70 and 5.7.70 No obs.	
6. 7.70	1200 1700 - 1900		
7. 7.70	1200 1400 1600 1800		
8. 7.70	1000 1700, 1800		
9. 7.70	1600 - 1800	9. 7.70	0900
10. 7.70	1000 - 1200 1400 1700, 1900		
11. 7.70	1200 1500 1700, 1800		

34 MHz		45.1 MHz	
Date	Time (Local time)	Date	Time (Local time)
12. 7.70	1400 1600, 1700 1800		
13. 7.70	1700 1900		
15. 7.70	1800		
16. 7.70	1500 - 1700		
19. 7.70	1800		
20. 7.70	0900		
21. 7.70	0800 - 1000 No obs.	21. 7.70	0800 - 1000 No obs.
22. 7.70	0200 - 1100 No obs.	22. 7.70	0200 - 1100 No obs.
23. 7.70	1800		
24. 7.70	1600, 1700 1900		
25. 7.70	1300, 1400 1600 - 1800		
26. 7.70	0900 1200 - 1400 1600 - 1900		
27. 7.70	1200 - 1200 on 28.7.70 No obs.		
28. 7.70	1700 - 1900		
29. 7.70	1300, 1400 1600 - 1900		
30. 7.70	1700 - 1900		
31. 7.70	1600 - 1900		
1. 8.70	0800, 0900 1300, 1400 1800, 1900		
2. 8.70	1500, 1600 1900		
5. 8.70	1700		
9. 8.70	1300, 1400 1600 1900		
11. 8.70	1300 - 1700		

34 MHz

Date	Time (Local time)
12. 8.70	1500 - 1700
15. 8.70	1700
17. 8.70	1600, 1700
18. 8.70	1300 - 1700
19. 8.70	1100 - 1300 1500 - 1700
20. 8.70	1300 1600, 1700
21. 8.70	1400 1600 - 1800
22. 8.70 to 31.8.70	No obs
1. 9.70 to 30.9.70	No obs

45.1 MHz

Date	Time (Local time)
30. 8.70	2000
31. 8.70	1900
1. 9.70	1800
5. 9.70	1900
9. 9.70	1900 - 2100
10. 9.70	1900, 2000
11. 9.70	1000 - 1400 No obs 1900
12. 9.70 and 13.9.70	No obs
14. 9.70	1500
15. 9.70	1800 - 2000
16. 9.70	1900, 2000
17. 9.70 to 21.9.70	No obs.
22. 9.70	2000
23. 9.70	2000
24. 9.70	1900, 2000
25. 9.70	1900, 2000
26. 9.70	1800 2000
27. 9.70	1800
28. 9.70	1800 2000
29. 9.70	1300, 1900, 2000
30. 9.70	1800 - 2000

34 MHz		45.1 MHz	
Date	Time (Local time)	Date	Time (Local time)
1.10.70 to 15.10.70	No obs.	1.10.70	1800 2100
		2.10.70	1600 1800 2000, 2100
		3.10.70	1800 - 2000
		4.10.70	2000
		5.10.70	1700 - 1900
		6.10.70	1800 - 2100
		7.10.70	1400 - 1800 2000 - 2200
		8.10.70	1900, 2000
		9.10.70	1800 - 2100
		10.10.70	1900 - 2100
		11.10.70	1900
		12.10.70	1700, 1900, 2000
		13.10.70	1300, 1400 1500 - 1600 No obs 1700 - 2000
		14.10.70	1200 - 2000
		15.10.70	1300 - 1600 1700 - 2200
16.10.70	1100 - 1900	16.10.70	1700 - 2100
17.10.70	0900 - 1700	17.10.70	1200 1500 - 2100
18.10.70	0800 1100 - 1500 1700	18.10.70	1100, 1200 1400 1500 1900 2000
19.10.70	0800 - 1600	19.10.70	1600 - 2100
20.10.70	0900 - 1600	20.10.70	1600, 1800 - 2000
21.10.70	0900 - 1600	21.10.70	1900 - 2100
22.10.70	0900 - 1700 1900, 2100	22.10.70	1200 1900 - 2100

34 MHz		45.1 MHz	
Date	Time (Local time)	Date	Time (Local time)
23.10.70	0800 - 1000 1300 - 1500 1600	23.10.70	1300 - 1600
24.10.70	0800 - 1000 No obs. 1100 - 1600	24.10.70	0800 - 1000 No obs. 1300 - 2100
25.10.70	0900 - 1700	25.10.70	1800 1900 2100
26.10.70	0800 - 1100 1400 - 1700	26.10.70	1800 - 2300
27.10.70	1000 1100 1300 - 1600	27.10.70	1200 - 2400
28.10.70	0800, 0900 1100 - 1400 1600 1700	28.10.70	1800 - 2200
29.10.70	0900 1300 - 1700	29.10.70	1200 - 2100
30.10.70	0900 1100 1300 - 1500 1700	30.10.70	1200 - 1400 1800 - 2100
31.10.70	0800 - 1700 1900	31.10.70	1200 - 1400 1900 - 2000
1. 11.70	0800 - 1500 1700 - 1900	1.11.70	1300 1800 - 2100
2.11.70	1000 - 1900	2.11.70	1200 1400 1900 - 2100
3.11.70	1000 1500, 1600 1900	3.11.70	1500 - 1800 2000, 2100
4.11.70	1100 - 1900 2000		
5.11.70	0800, 1100 - 1600	5.11.70	1600 - 1800 2100
6:11.70	0800, 1100 1400 - 1700	6.11.70	1500 - 1900

34 MHz		45.1 MHz	
Date	Time (Local time)	Date	Time (Local time)
7.11.70	1200, 1400 - 1900		
8.11.70	0800 - 1600 1800 2000		
9.11.70	0800 - 1000 1200 - 1800		
10.11.70	1100 - 1700 1900 2000		
11.11.70	1000 - 1300 1500 - 1700		
12.11.70	0900 1100 - 1700	12.11.70	1200 - 2100
13.11.70	0800, 0900 1200 - 1400, 1700 2100	13.11.70	2000
14.11.70	1000 1300 - 1500 1700, 1800		
15.11.70	1600 1900	15.11.70	2000
16.11.70	1000, 1300, 1400 1600 1700		
17.11.70	1500, 1600, 1900	17.11.70	1500, 1900 - 2100
18.11.70	1000 1200 1400 1600 - 1800 2100		
20.11.70	1400 1700, 1800 2000, 2100		
21.11.70	1400 1600 1700		
22.11.70	1600		
23.11.70	1100 - 1200 1400, 1700, 1800		

34 MHz		45.1 MHz	
Date	Time (Local time)	Date	Time (Local time)
25.11.70	1100 1300, 1500 - 1700 1900		
26.11.70	0900, 1000, 1200 1500, 1600	26.11.70	1300 - 1800 2000
27.11.70	1600	27.11.70	2100
28.11.70	0800 - 1200 on 30.11.70 No obs.	28.11.70	0800 - 1200 on 30.11.70 No obs
30.11.70	1400 - 1700 2000	30.11.70	2100
1.12.70	1000 - 1400 1600, 1800	2.12.70	2100
3.12.70	1000 - 1700		
4.12.70	1000, 1100 1300 - 1600 1800		
5.12.70	1100, 1200 1500 - 1900		
6.12.70	0900, 1400 1600 1700 - 1900		
7.12.70	1300 - 1700	7.12.70	1700- 1900 2100
8.12.70	0900, 1200 - 1400 1600 1900 - 2100	8.12.70	1400 - 1600 2100
9.12.70	1300 1400, 1500 1700, 2000		
10.12.70	1100 - 1500	10.12.70	1600
11.12.70	0000 - 1600 on 14.12.70 No obs.	12.12.70	1600 - 1800
14.12.70	1700		
15.12.70	0900, 1300, 1600, 1700		
16.12.70	0900, 1400, 1600, 2000		
17.12.70	1100, 1300 1400 - 1300 on 18.12.70 No obs.	17.12.70	0000 - 1300 on 18.12.70 No obs.

34 MHz		45.1 MHz	
Date	Time (Local time)	Date	Time (Local time)
19.12.70	1600		
20.12.70	2000		
21.12.70	1600		
23.12.70	1200		
24.12.70	1200, 1300, 1500		
25.12.70	1300		
26.12.70	1200, 1400		
27.12.70	1200, 1300	27.12.70	1300
28.12.70	1100, 1200		
29.12.70	1200		
31.12.70	1200, 1300	31.12.70	1400
1. 1.71	1100 - 1300	1. 1.71	1200 - 1600
2. 1.71	1500		
3. 1.71	1200, 1500, 2000		
6. 1.71	1300 - 1800		
9. 1.71	2000		
11. 1.71	1100		
12. 1.71	1500, 2000		
13. 1.71	1200 - 1400 No obs. 1500	13. 1.71	1200 - 1300 No obs. 1400 1500
16. 1.71	1500	16. 1.71	1400
19. 1.71	1100 1600 - 2000 No obs.	19. 1.71	1600 - 2000 No obs.
		21. 1.71	1600, 1800
22. 1.71	1000 No obs 1600	22. 1.71	1000 No obs
23. 1.71	1300, 1400 1600, 1800		
25. 1.71	1000 - 1200 No obs.	25. 1.71	1000 - 1200 No obs. 1500
2. 2.71	0900 - 1200 on 3.2.71 No obs.	2. 2.71	0900 - 1200 on 3.2.71 No obs.
4. 2.71	1300, 1400 and 1600 No obs.	4. 2.71	1300, 1400 and 1600 No obs.

34 MHz		45.1 MHz	
Date	Time (Local time)	Date	Time (Local time)
5.2. 71	1400 and 1600 No obs.	5. 2.71	1400 and 1600 No obs.
11. 2.71	1700	11. 2.71	1900
16. 2.71	1500	16. 2.71	1900
18. 2.71	1100 - 1900 No obs.	18. 2.71	1100 - 1900 No obs.
20. 2.71	1500		
21. 2.71	1500		
22. 2.71	1000 1100 - 1500 No obs.	22. 2.71	1100 - 1500 No obs.
23. 2.71	1300, 1400 1500, 1800	23. 2.71	1400 - 2000
24. 2.71	1000, 1100 1300 No obs.	24. 2.71	1000 No obs. 1800
25. 2.71	1000, 1100, 1400, 1600		
26. 2.71	No obs.		
27. 2.71	1500, 1600	27. 2.71	1900, 2000
28. 2.71	1500, 1600	28. 2.71	1900
1. 3.71	1300 - 1500	1. 3.71	1700 1900, 2000
2. 3.71	1500	2. 3.71	1600 2000 2200
3. 3.71	No obs		
4. 3.71	No obs	4. 3.71	1900 - 2000
5. 3.71	1000 - 1600 No obs.	5. 3.71	1800 - 2000
6. 3.71	1500, 1600	6. 3.71	2000
8. 3.71	2000 - 1800 on 9.3.71 No obs.	7. 3.71	1900, 2000
11. 3.71	0800 1300	9. 3.71	1600, 1800, 1900
		10. 3.71	1200
12. 3.71	1000 - 1200 on 13.3.71 No obs.	12. 3.71	1300 - 1900
14. 3.71	1200, 1300		
15. 3.71	0900 - 1600	15. 3.71	1000 1600 - 1700
16. 3.71	1100 - 1400 1600	16. 3.71	1300, 1800

34 MHz		45.1 MHz	
Date	Time (Local time)	Date	Time (Local time)
17. 3.71	1000 - 1300 1500, 2000	17. 3.71	1800, 1900
18. 3.71	1100, 2000	18. 3.71	1600 - 2000
19. 3.71	1100, 1400 - 2000		
20. 3.71	0800 - 2000	20. 3.71	1300, 1400 1900
21. 3.71	0900 - 1500 1900, 2000		
22. 3.71	0900 - 2000	22. 3.71	2000
23. 3.71	1100 - 2000		
24. 3.71	1100 - 2000		
25. 3.71	1000 - 1400 1600, 1700 1900, 2000	25. 3.71	1200, 1400 - 1700 1900, 2000
26. 3.71	1200 - 1900		
27. 3.71	1000 - 2000	27. 3.71	1300 - 1800
28. 3.71	No obs.	28. 3.71	No obs.
29. 3.71	1100 - 1600 1800, 2000	29. 3.71	1300 - 1700
30. 3.71	1100 - 1800	30. 3.71	1300 - 1700
31. 3.71	1000, 1100 1300 - 1800		
1. 4.71	0900 - 1900		
2. 4.71	1300 - 1900		
3. 4.71	1100, 1300 - 1500, 1700 - 1900		
4. 4.71	0800 - 1200 1400 - 2000		
5. 4.71	1200 - 1900		
6. 4.71	1000, 1100 1800	6. 4.71	1500 - 1700
7. 4.71	0900 - 1900	7. 4.71	1400, 1500, 1700 1900
8. 4.71	0900 - 1900		
9. 4.71	0800, 0900, 1300 - 1800 2000		

34 MHz		45.1 MHz	
Date	Time (Local time)	Date	Time (Local time)
10. 4.71	1000 - 1100 1500 - 1700 1900		
11. 4.71	0900 1100 - 1900	11. 4.71	1300 1600
12. 4.71	0800 1000 - 1100 1300 - 1900	12. 4.71	1100, 1300
13. 4.71	1000 - 1900	13. 4.71	1200, 1300 1600 - 1800
14. 4.71	1100 - 1800	14. 4.71	1200 - 1400 1600
15. 4.71	1800		
16. 4.71	0900 - 1900	16. 4.71	1100, 1200
17. 4.71	0900 1100 - 1900		
18. 4.71	0900 - 1300 1500 - 1900		
19. 4.71	1000 - 1800 2000	19. 4.71	1400 1700
20. 4.71	1100, 1300 - 1900		
21. 4.71	1200 - 2000	21. 4.71	1600, 1800
22. 4.71	1000 - 1800	22. 4.71	1100 - 1600
23. 4.71	0800 1200, 1300 1600 - 1800	23. 4.71	1700, 1800
24. 4.71	1200 - 1600 1800		
25. 4.71	1200 - 1400 1600, 1800		
26. 4.71	1200 1400 - 1800	26. 4.71	1700 - 1800
27. 4.71	1300 - 1900		
28. 4.71	1200 - 1800	28. 4.71	1600 - 1700
29. 4.71	1200 - 1700 No obs.		
30. 4.71	1200 - 1800		

34 MHz		45.1 MHz	
Date	Time (Local time	Date	Time (Local time)
1. 5.71	1300 - 1800		
2. 5.71	1000 - 1800	2. 5.71	1700
3. 5.71	1000, 1100 1300 - 1800		
4. 5.71	0800 - 1700	4. 5.71	1200
5. 5.71	1300 - 1800	5. 5.71	1700
6. 5.71	1200 - 1800	6. 5.71	1600
7. 5.71	1100, 1300 - 1600 1800, 1900	7. 5.71	1400 1600 - 1800
8. 5.71	0900 1100 - 1800		
9. 5.71	1200 - 1700		
10. 5.71	1100 - 1700		
11. 5.71	1200 - 1500 1700	11. 5.71	1300
12. 5.71	1200 - 1800 2000	12. 5.71	1500, 1700 2100
13. 5.71	1100 - 1400 1600, 1700		
14. 5.71	1200 - 1800		
15. 5.71	1300 - 1700		
16. 5.71	1200 - 1800 2000	16. 5.71	1700, 1800 2000
17. 5.71	1300 - 1800	17. 5.71	1600, 1800
18. 5.71	1100 - 1600 1800, 1900	18. 5.71	1800
19. 5.71	1100 - 1800	19. 5.71	1700
20. 5.71	1000 - 1800	20. 5.71	1500 - 1600
21. 5.71	1300 - 1500	21. 5.71	1800
22. 5.71	1500 - 1700		
23. 5.71	1600, 1700		
No obs. 1800-1130 on 24.5.71			
24. 5.71	1300 - 1700	24. 5.71	1500
25. 5.71	1300, 1700, 1800		

34 MHz		45.1 MHz	
Date	Time (Local time)	Date	Time (Local time)
26. 5.71	1500, 1800, 1900		
27. 5.71	1600		
30. 5.71	1400, 1500 - 1900		
31. 5.71	1300, 1500, 1600		
1. 6.71	1600		
2. 6.71	0900, 1600, 1700 1900		
3. 6.71	1200 - 1600 1900, 2000		
4. 6.71	1000, 1100 1300 - 1800	4. 6.71	1600
5. 6.71	1000, 1300 1400, 1600 1800, 1900		
6. 6.71	1200 - 1700 2000		
7. 6.71	1200 - 1800		
8. 6.71	1100 - 2400		
10. 6.71	No obs.		
11. 6.71	1500 No obs.	10. 6.71	1500 No obs.
14. 6.71	1600, 1700		
18. 6.71	1700, 1800		
19. 6.71	1500		
20. 6.71	1800		
23. 6.71	1200, 1400 - 1600		
26. 6.71	1500 - 1700		
27. 6.71	1800		
28. 6.71	1400		
30. 6.71	1700		
1. 7.71	1500 - 1700		
2. 7.71	1800		
4. 7.71	1800		
6. 7.71	1600		

34 MHz		45.1 MHz	
Date	Time (Local time)	Date	Time (Local time)
9. 7.71	1300, 1500		
10. 7.71	1500		
13. 7.71	1100		
23. 7.71	1300, 1600, 1800		
25. 7.71	1400		
29. 7.71	1800		
31. 7.71	1600, 1700		
2. 8.71	1500, 1700, 1800		
3. 8.71	1600, 1700		
4. 8.71	1800		
5. 8.71	1100	20. 8.71	1700
19. 9.71	0500 - 1100 on 2.10.71 No obs.	19. 9.71	0500 - 1900 on 6.10.71 No obs.
2.10.71	1100 - 1500 1700		
3.10.71	1200 - 1500 1700 - 1800		
4.10.71	1000, 1100, 1800 1400 No obs.		
5.10.71	1200		
5.10.71	1300 - 1700 on 6.10.71 No obs.		
6.10.71	1700 - 1800 2000		
7.10.71	1000 - 1800		
8.10.71	0900, 1000 1400 - 2000		
9.10.71	1200 - 1300 1500 - 1800		
10.10.71	1200 1400 - 1700 1800 - 2000		
11.10.71	1600 - 1800		
12.10.71	1300 - 2000		
13.10.71	1100 - 1500 1700, 1800	13.10.71	1800, 1900

34 MHz		45.1 MHz	
Date	Time (Local time)	Date	Time (Local time)
14.10.71	1400 - 1900		
15.10.71	1000 - 1300 1500 - 1700		
16.10.71	1100 - 2000		
17.10.71	1400 - 1800 2000		
18.10.71	0900 1300 - 1700		
19.10.71	1100 - 1700 1900		
20.10.71	1300 - 1600		
21.10.71	1200 - 1500 1900 - 2000		
22.10.71	1600, 1700 1900		
23.10.71	1200 - 1700 1900 - 2200		
24.10.71	1300 - 1400 1600 1800, 1900		
25.10.71	1200 - 2000		
26.10.71	1100 - 1500		
27.10.71	1200 1400 - 1600 1800 - 2100		
28.10.71	1100- 1200 1400 - 1600 1900		
29.10.71	0900 - 1000 1200 - 1500 2000, 2100		
30.10.71	0800, 1400 - 1600 1900, 2000		
31.10.71	1300 - 1700 2000		
1.11.71	1600, 1700 1900 - 2100		

34 MHz		45.1 MHz	
Date	Time (Local time)	Date	Time (Local time)
2.11.71	1300 - 1800 2100		
3.11.71	1200, 1300 1500 - 1900		
4.11.71	1100 - 1800 2000		
5.11.71	1100 - 2000		
6.11.71	1200 - 1700 1900 - 2100		
7.11.71	1400 - 1600 1800, 2000, 2100		
8.11.71	1200 - 1400		
9.11.71	1000 - 1600 1800, 2000		
10.11.71	1100, 1200, 1400 1600, 1900, 2100		
11.11.71	0800, 1100 1200 - 1700 1900 - 0900 on 12.11.71 No obs.		
12.11.71	1000 - 1700 1900, 2100	12.11.71	1800
13.11.71	1000 - 1700 1900		
14.11.71	1100 - 1500 1700, 2000		
15.11.71	1200 - 1700		
16.11.71	1100 - 1900, 2100		
17.11.71	1100 - 1400 1800, 2100		
18.11.71	1100 - 1400		
19.11.71	1100 - 1400, 1600, 1800, 2100		
20.11.71	1000, 1600, 1800 1900, 2100	20.11.71	1600
21.11.71	1300 - 2100	21.11.71	1900

34 MHz		45.1 MHz	
Date	Time (Local time)	Date	Time (Local time)
22.11.71	1000 1200 - 1400 1800		
23.11.71	0900 1600 - 2000		
25.11.71	1600 1800 - 2000		
26.11.71	1900, 2000		
27.11.71	1100 - 1900 2100		
28.11.71	1100 - 1700 1900 - 2100		
29.11.71	1200 - 1400 1700, 1800		
30.11.71	1400, 1600, 1700 1900, 2100		
1.12.71	1400 - 1800 2000, 2100		
2.12.71	1100, 1300 - 1600		
3.12.71	1100 - 2000		
4.12.71	1300 - 1900		
5.12.71	1000 - 1700		
6.12.71	1300 - 1800		
7.12.71	1100, 1200 1600 - 1800		
8.12.71	1300, 1500, 2100		
9.12.71	1300, 1400, 1600		
10.12.71	1200, 1300, 1800		
11.12.71	1100 - 1300 1500, 1700, 1800		
12.12.71	1300 No obs 1400, 1500, 1700, 1900		
13.12.71	1600, 1700, 1900		
14.12.71	1400, 1700, 2100		
15.12.71	1300 - 1800 2000, 2100		

34 MHz		45.1 MHz	
Date	Time (Local time)	Date	Time (Local time)
16.12.71	1500, 1800 2100, 2200		
17.12.71	1200 1700 - 2100, 2300		
19.12.71	1600, 1700		
20.12.71	1200; No obs at 1300 1400 - 1800 2100, 2300		
21.12.71	1400 - 1900 2100, 2200		
22.12.71	1300 - 1600		
23.12.71	1300, 1400 1600 - 1900, 2100		
24.12.71	1300 - 1500 1700, 2000, 2100		
25.12.71	1300 - 1500 1700		
26.12.71	1300 - 1500 1800, 2100		
27.12.71	1400, 2100, 2200		
28.12.71	1600 - 1800 2100		
29.12.71	1000, 1200, 1300 1500, 1600 1800 - 2000		
31.12.71	1400, 1500		
2. 1.72	1300		
3. 1.72	1200 - 1400		
4. 1.72	1300, 1400		
5. 1.72	1100 - 1400		
8. 1.72	1500, 1600		
9. 1.72	1200, 1400, 1500		
10. 1.72	1200, 2100		
12. 1.72	1100, 1300, 1600		
13. 1.72	1100 - 1300, 1500		

34 MHz		45.1 MHz	
Date	Time (Local time)	Date	Time (Local time)
14. 1.72	1200, 1300, 1600 - 2100		
15. 1.72	1200 - 1700		
16. 1.72	1200, 1300, 1500, 1600		
17. 1.72	1300, 1400		
18. 1.72	1500, 1800		
19. 1.72	1300, 1400		
20. 1.72	1400, 1500		
21. 1.72	1300, 1400, 1600		
22. 1.72	1400, 1600, 2000		
23. 1.72	1100 - 1500, 1900		
24. 1.72	1000 - 1400, 1600 1900 - 2200		
25. 1.72	1200 - 1900		
26. 1.72	1000 - 1500, 1700 - 2300		
27. 1.72	1100 - 2000, 2200		
28. 1.72	1100 - 2200		
29. 1.72	1200 - 1700, 1900, 2000		
30. 1.72	1200 - 2100		
31. 1.72	1000 - 2100		
1. 2.72	1100 - 1500, 1700, 1900 - 2100		
2. 2.72	1000, 1100, 1300 - 1700, 2100		
3. 2.72	1200, 1300, 1500 - 1700		
4. 2.72	1200 - 1700, 1900		
5. 2.72	1100 - 1700, 2000, 2100		
6. 2.72	1400 - 1700, 2100, 2200		
7. 2.72	1300 - 1700, 1900, 2100		
8. 2.72	1300 - 1500, 1700, 1900, 2100		
9. 2.72	1200 - 1900		

34 MHz		45.1 MHz	
Date	Time (Local time)	Date	Time (Local time)
10. 2.72	1500, 1600, 1800		
11. 2.72	1300 - 1900		
12. 2.72	1200 - 2000		
13. 2.72	1300 - 1600, 1800, 1900, 2100		
14. 2.72	0900, 1200, 1500, 1800 - 2100		
15. 2.72	1600 - 2000		
16. 2.72	1100 - 1500, 1800, 1900, 2100		
17. 2.72	1000 - 1800	17. 2.72	1300, 1400
18. 2.72	1100 - 1700		
19. 2.72	0900 - 1900		
20. 2.72	1200 - 2100	20. 2.72	1300, 1400
21. 2.72	1100 - 2100		
22. 2.72	1000 - 2200		
23. 2.72	1200 - 1800, 2000	23. 2.72	1300, 2000
24. 2.72	0900 - 1900		
25. 2.72	0800 - 2000		
26. 2.72	0800, 1000 - 2000	26. 2.72	1200
27. 2.72	0800 - 2200	27. 2.72	1200, 2000
28. 2.72	0900 - 2100	28. 2.72	1200
29. 2.72	1000 - 2100	29. 2.72	1200, 1300, 1700 1800
1. 3.72	0900 - 2000	1. 3.72	1200, 1300
2. 3.72	0800 - 1500, 1700 - 2000		
3. 3.72	1000 - 1400, 1600 - 1800	3. 3.72	1400
4. 3.72	0900 - 1700, 1900 - 2100		
5. 3.72	0800 - 1800, 2000		
6. 3.72	1400 - 1700		
7. 3.72	1000 - 2000		
8. 3.72	0900 - 1200, 1400, 1500 1700 - 2000		

34 MHz		45.1 MHz	
Date	Time (Local time)	Date	Time (Local time)
9. 3.72	0800 - 2000		
10. 3.72	0900 - 1100, 1300, 1400, 1700, 1900, 2000		
11. 3.72	1000 - 2100	11. 3.72	2000
12. 3.72	0900 - 1400, 1600 - 1900	12. 3.72	1900
13. 3.72	0900 - 1400, 1600 - 2200	13. 3.72	2000
14. 3.72	1000 - 1900		
15. 3.72	1200 - 2100	15. 3.72	1300, 1400, 1600-1800 2000, 2100
16. 3.72	1200 - 2000	16. 3.72	1900
17. 3.72	1000 - 1900 2000 on 17.3.72 to 1800 on 19.3.72 No obs.	17. 3.72	2000 to 1800 on 19.3.72 No obs.
19. 3.72	1800 - 2300	19. 3.72	1900, 2000
20. 3.72	0700 - 2200		
21. 3.72	1000 - 2200	21. 3.72	1800
22. 3.72	0800 - 2000		
23. 3.72	0800 - 1800, 2100, 2300		
24. 3.72	0900 - 1800	24. 3.72	1600, 1800
25. 3.72	1000 - 2000		
26. 3.72	0900 - 2100	26. 3.72	1900, 2000
27. 3.72	0800 - 2100	27. 3.72	1500, 1800, 1900
28. 3.72	0900 - 2200	28. 3.72	1700 - 2000
29. 3.72	0900 - 2000	29. 3.72	1700
30. 3.72	1000 - 2100	30. 3.72	1800
31. 3.72	0900 - 1700		
1. 4.72	0800 - 1100, 1300 - 1900		
2. 4.72	0900 - 2000	2. 4.72	1200, 1500, 1600
3. 4.72	1100 - 1900	3. 4.72	1500
4. 4.72	1100 - 1900	4. 4.72	1700
5. 4.72	0800 - 1900		

34 MHz		45.1 MHz	
Date	Time (Local time)	Date	Time (Local time)
6. 4.72	1000 - 1900	6. 4.72	1300, 1500 - 1700
7. 4.72	1100 - 1900		
8. 4.72	1000 - 1900, 2100	8. 4.72	1400, 1500, 1700, 1900
9. 4.72	1100 - 2000	9. 4.72	1600, 1800, 1900
10. 4.72	1100 - 1900	10. 4.72	1900
11. 4.72	0800, 1000, 1200 - 2000		
12. 4.72	0800 - 1900	12. 4.72	1300 - 1700
13. 4.72	1000 - 1300, 1500 - 1800	13. 4.72	1200
14. 4.72	0800 - 1700	14. 4.72	1200, 1300, 1500, 1600
15. 4.72	No obs	15. 4.72	No obs
16. 4.72	No obs	16. 4.72	No obs
17. 4.72	1000 - 1800		
18. 4.72	0900, 1200 - 2000		

APPENDIX III

SIGNAL STRENGTH AND OCCURRENCE DATA

Data recorded in the period 1 September 1969 to 31 August 1970, at Roma (Lesotho), appear in this Appendix. Crosshatched areas refer to times of no observations due to equipment failure.

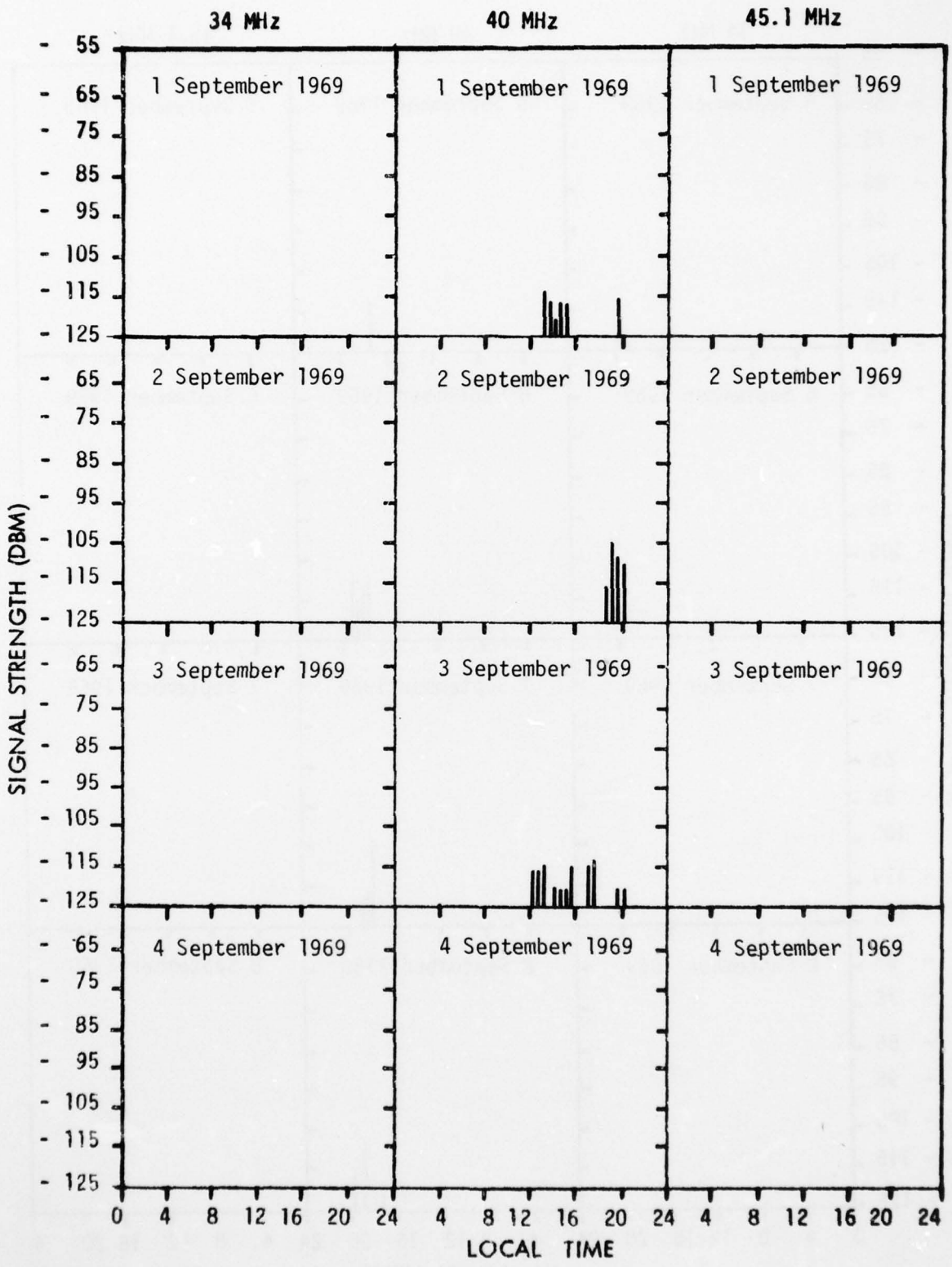

Fig. 32.– 34, 40 and 45.1 MHz Reception at Roma

AD-A054 193 UNIVERSITY OF BOTSWANA LESOTHO AND SWAZILAND ROMA (L--ETC F/G 20/14
TRANS-EQUATORIAL TRANSMISSIONS AT VERY HIGH FREQUENCY.(U)
SEP 73 E H CARMAN, M P HEERAN F61052-67-C-0003
UNCLASSIFIED RADC-TR-73-383 NL

2 OF 2
AD
AD54193

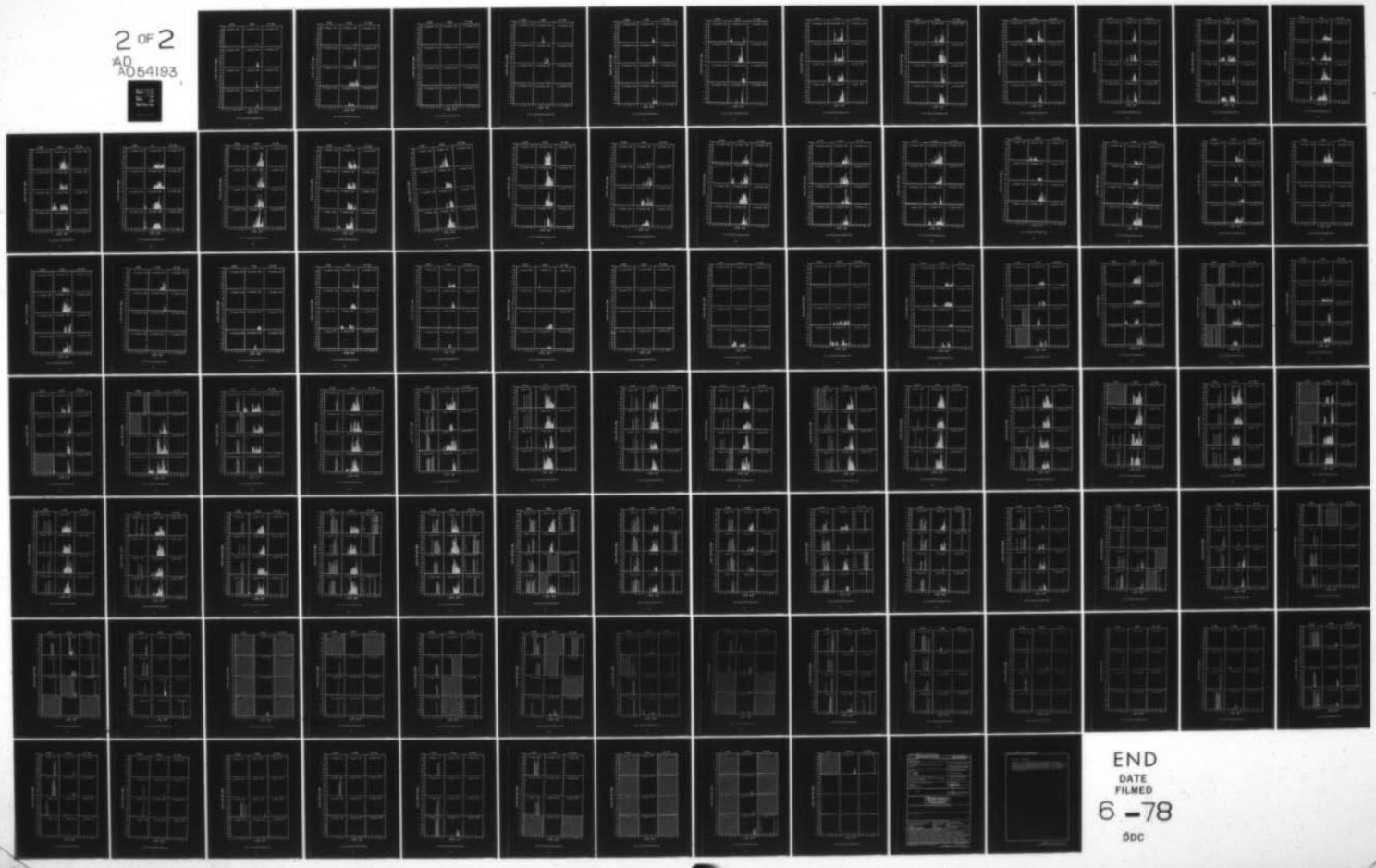

END
DATE FILMED
6-78
DDC

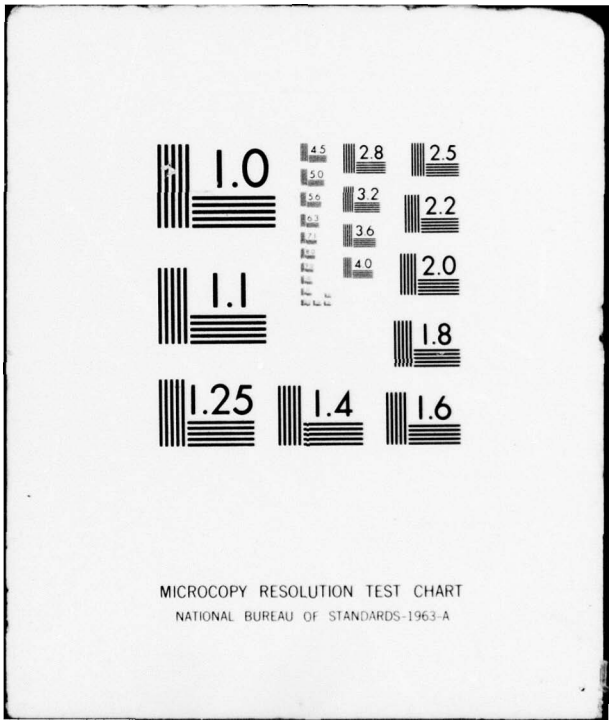
1.0
1.1
1.25
1.4
1.6
1.8
2.0
2.2
2.5
2.8
3.2
3.6
4.0
4.5
5.0
5.6
6.3
7.1
8.0
9.0
MICROCOPY RESOLUTION TEST CHART
NATIONAL BUREAU OF STANDARDS-1963-A

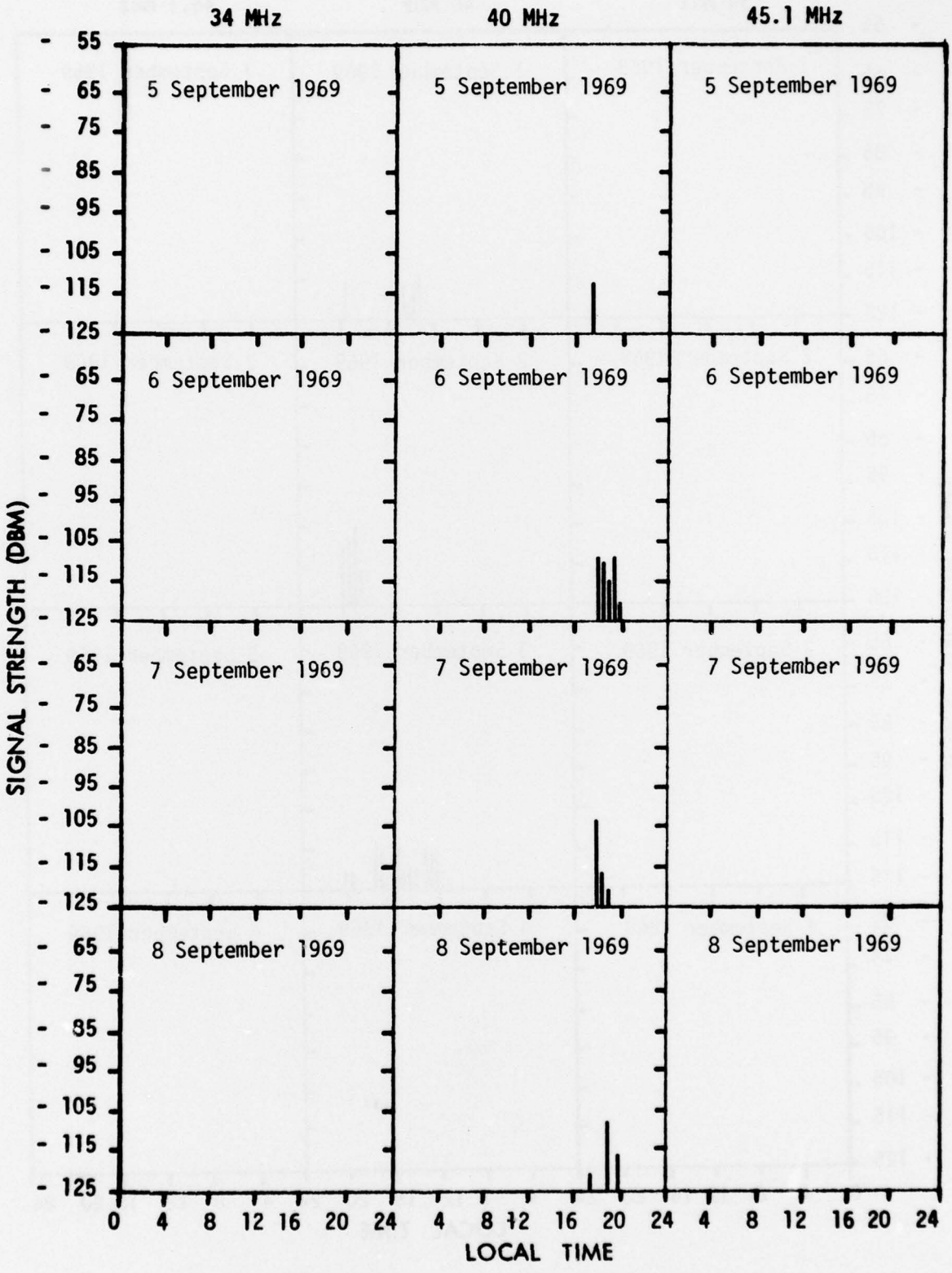

Fig. 33 – 34, 40 and 45.1 MHz Reception at Roma

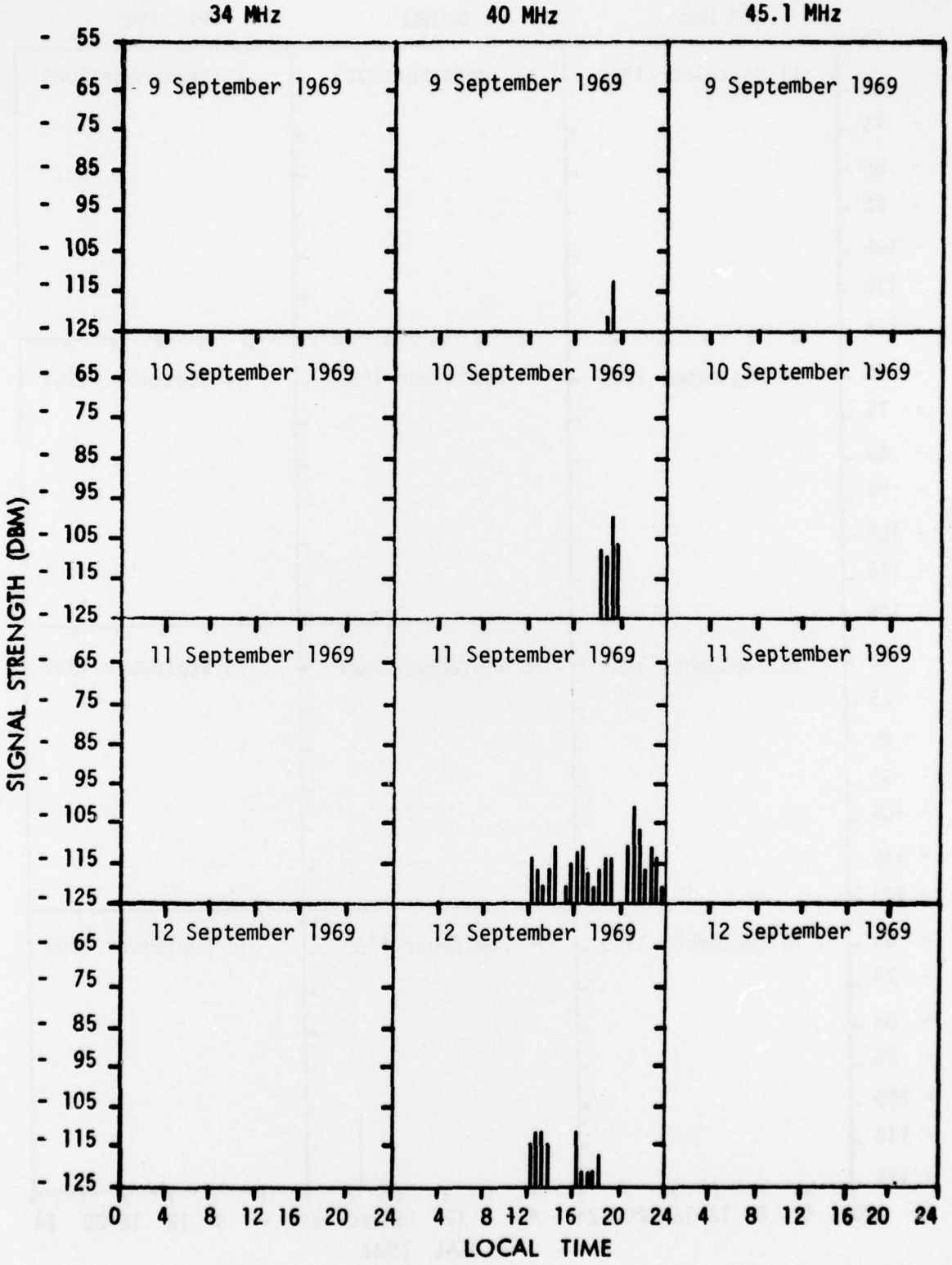

Fig. 34 – 34, 40 and 45.1 MHz Reception at Roma

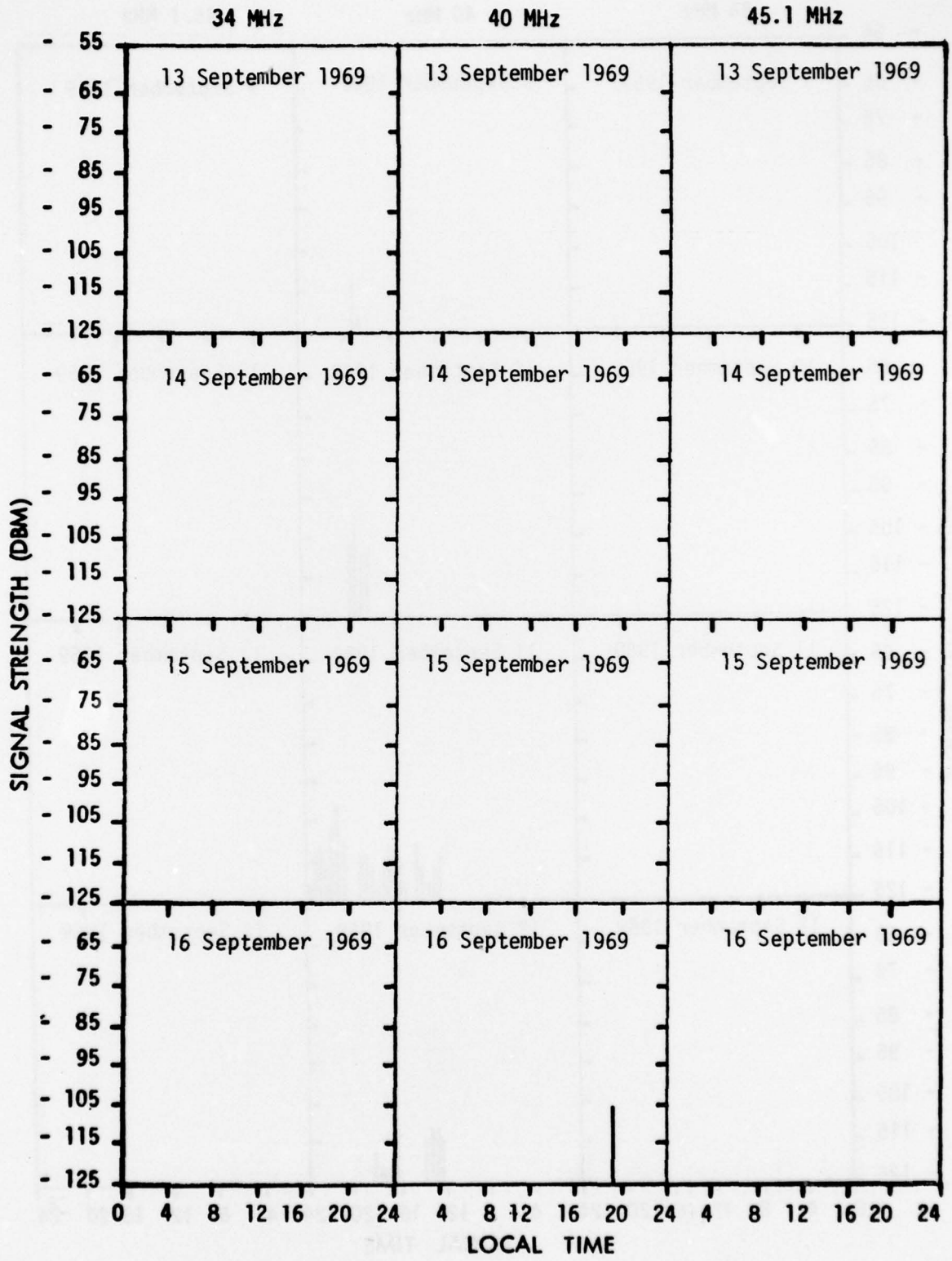

Fig. 35 – 34, 40 and 45.1 MHz Reception at Roma

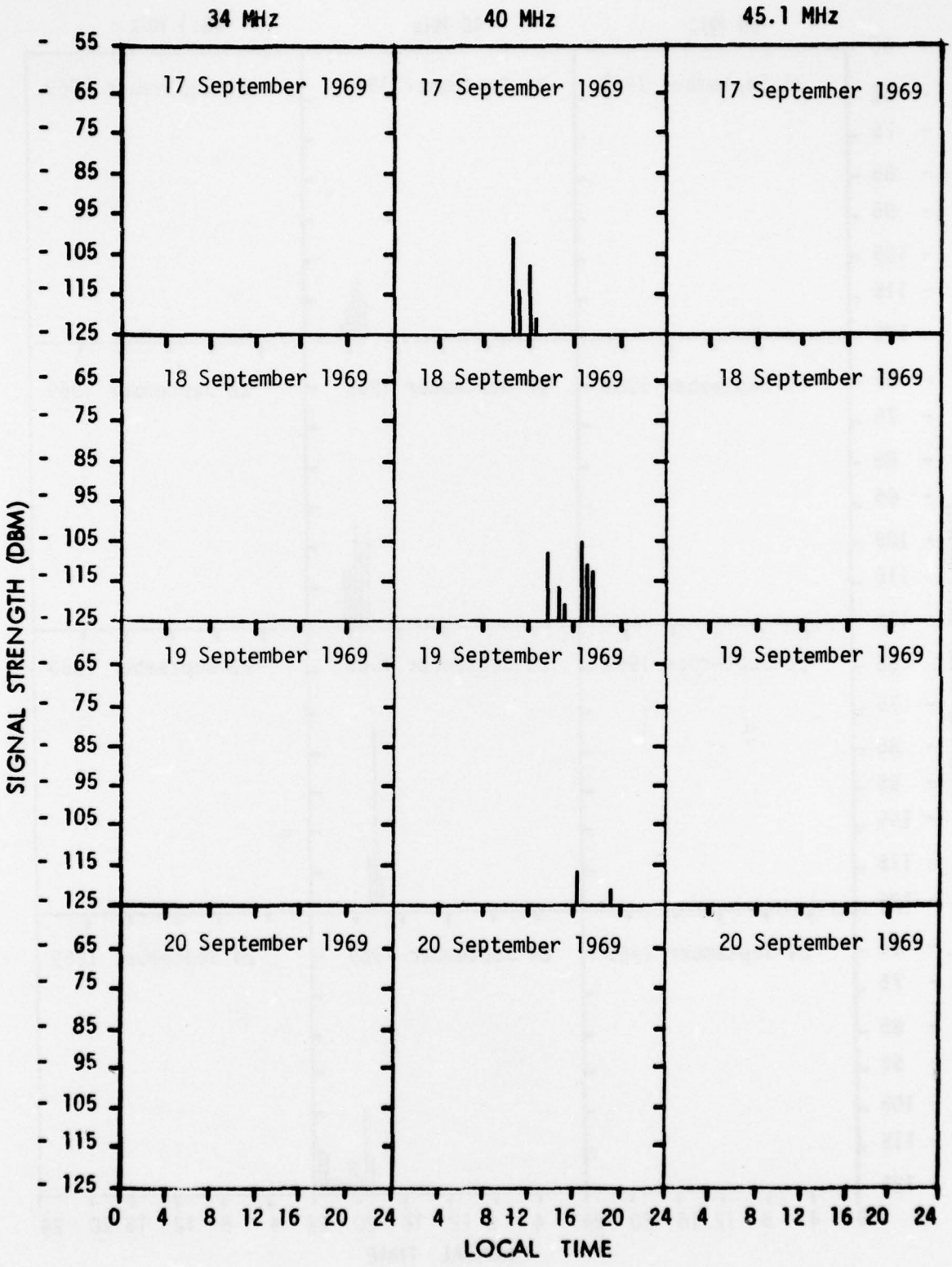

Fig. 36 – 34, 40 and 45.1 MHz Reception at Roma

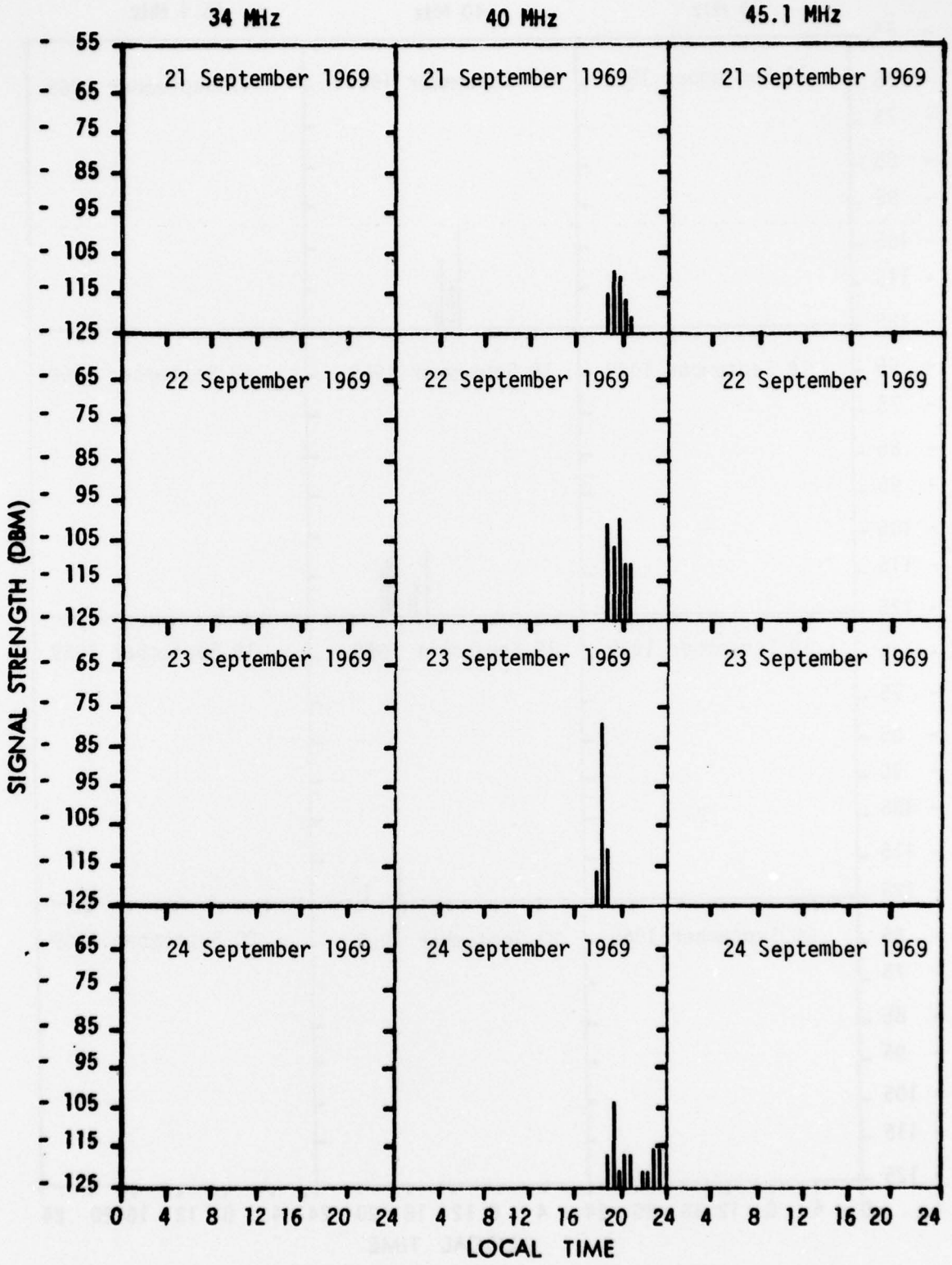

Fig. 37 – 34, 40 and 45.1 MHz Reception at Roma

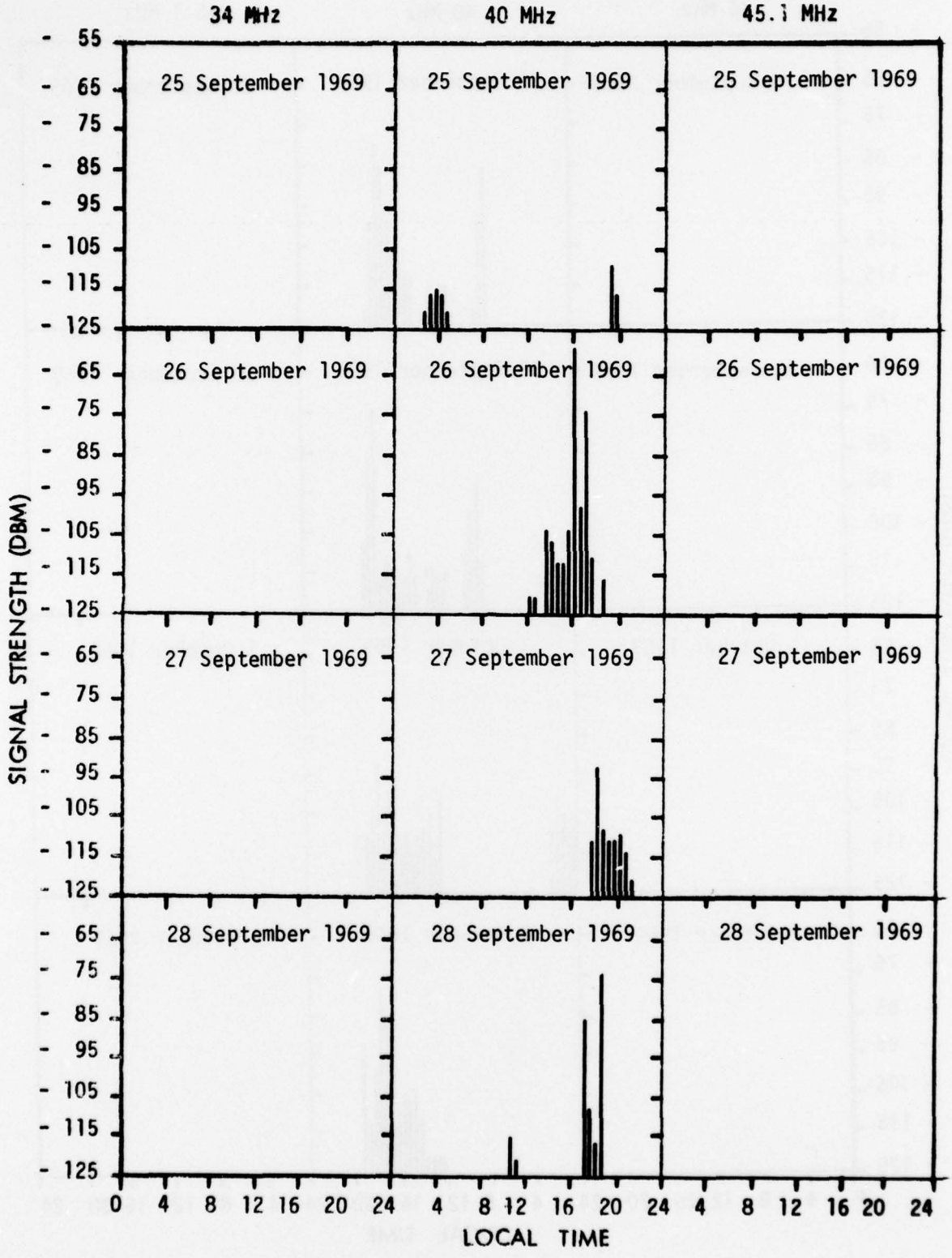

Fig. 38 – 34, 40 and 45.1 MHz Reception at Rome

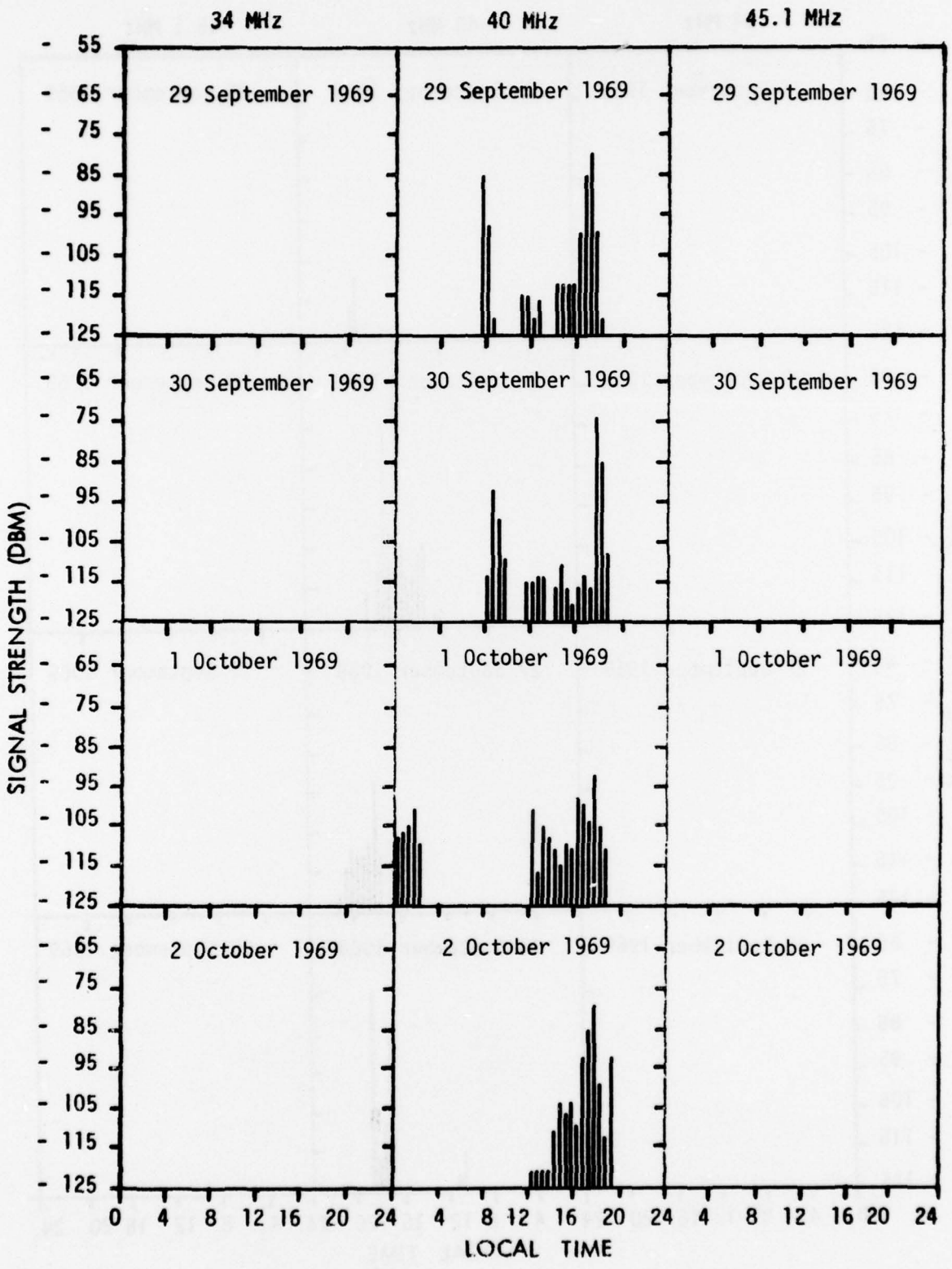

Fig. 39 – 34, 40 and 45.1 MHz Reception at Roma

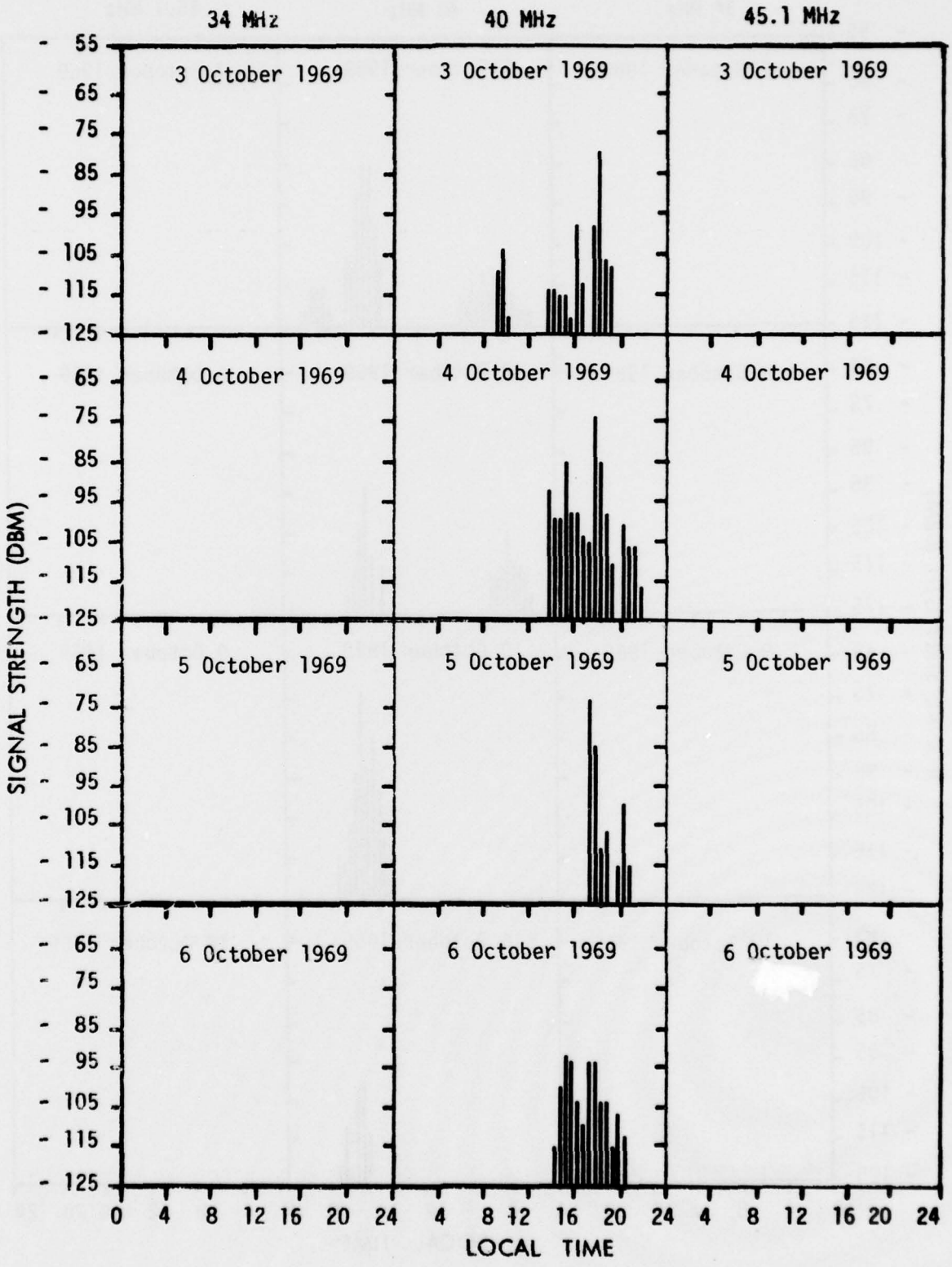

Fig. 40 – 34, 40 and 45.1 MHz Reception at Roma

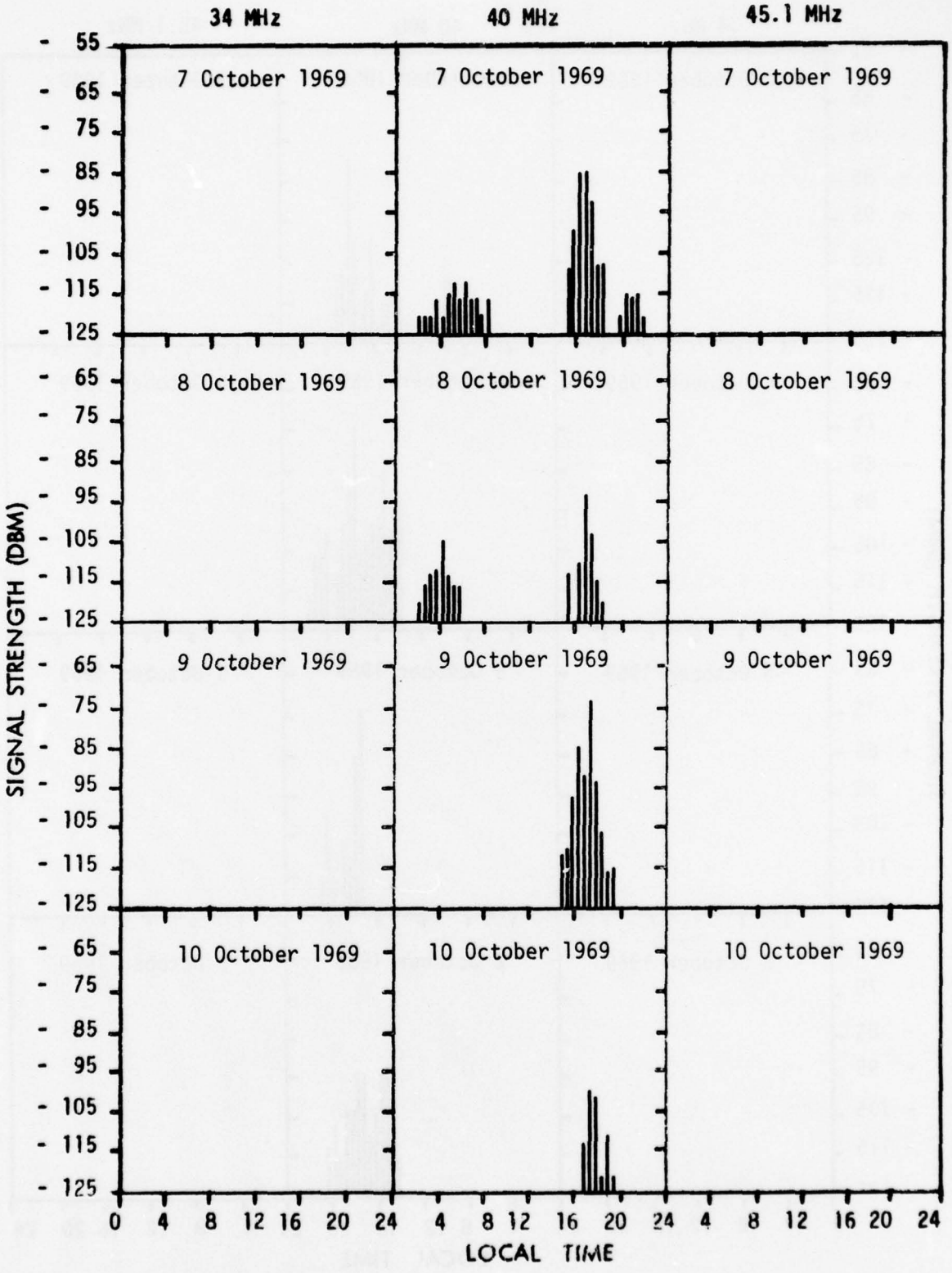

Fig. 41 – 34, 40 and 45.1 MHz Reception at Rome

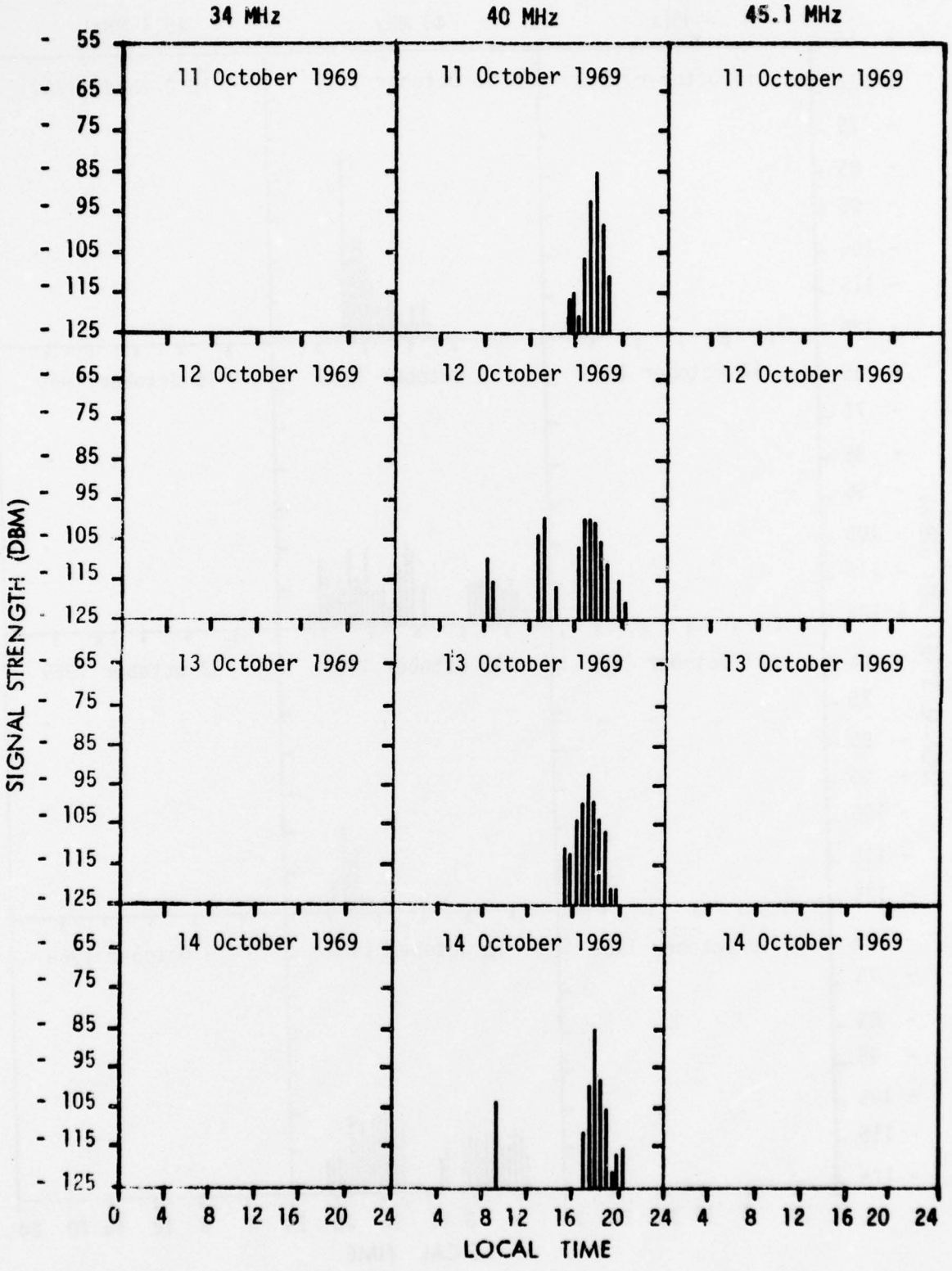

Fig. 42 – 34,40 and 45.1 MHz Reception at Rome

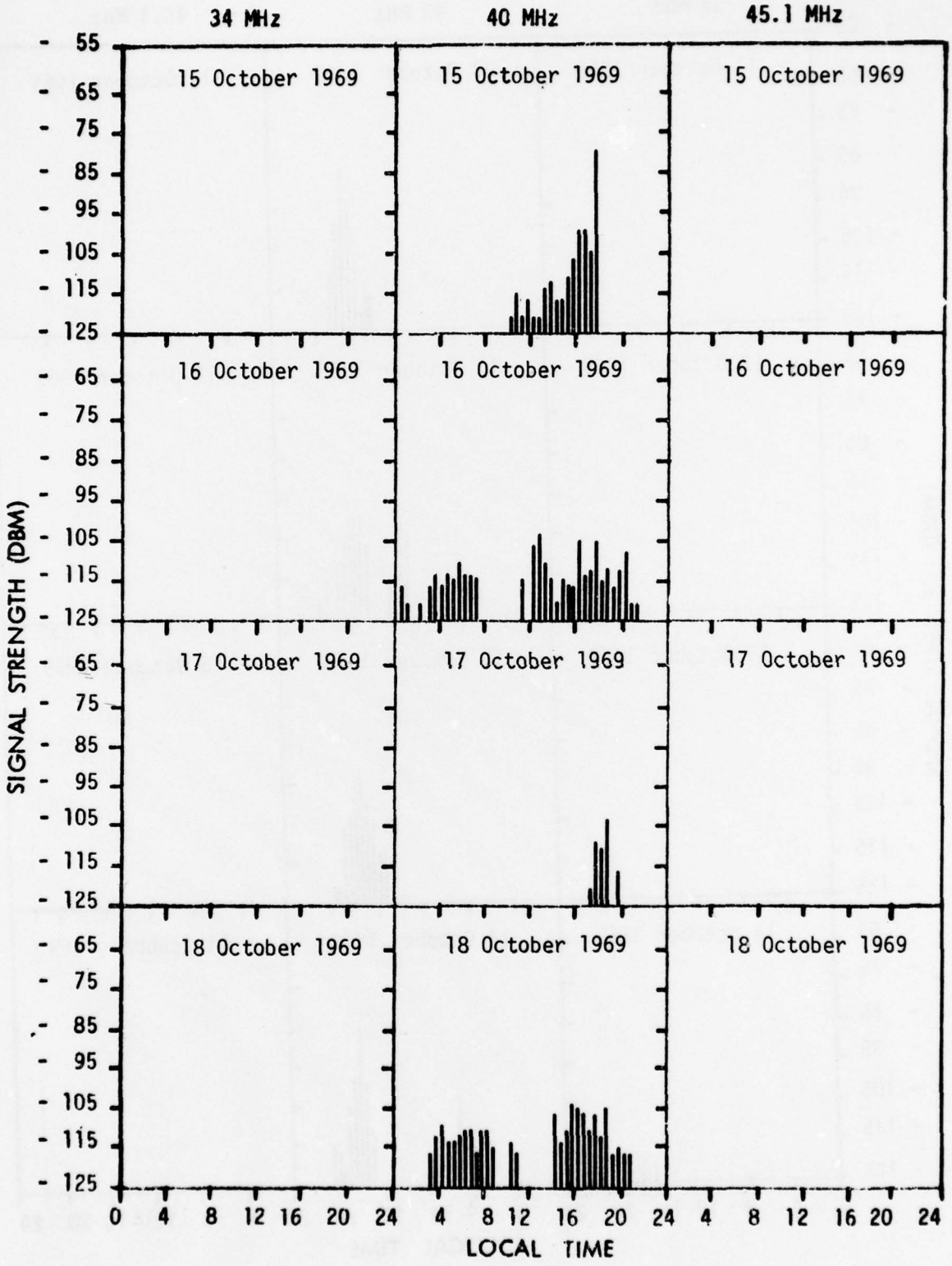

Fig. 43 – 34, 40 and 45.1 MHz Reception at Roma

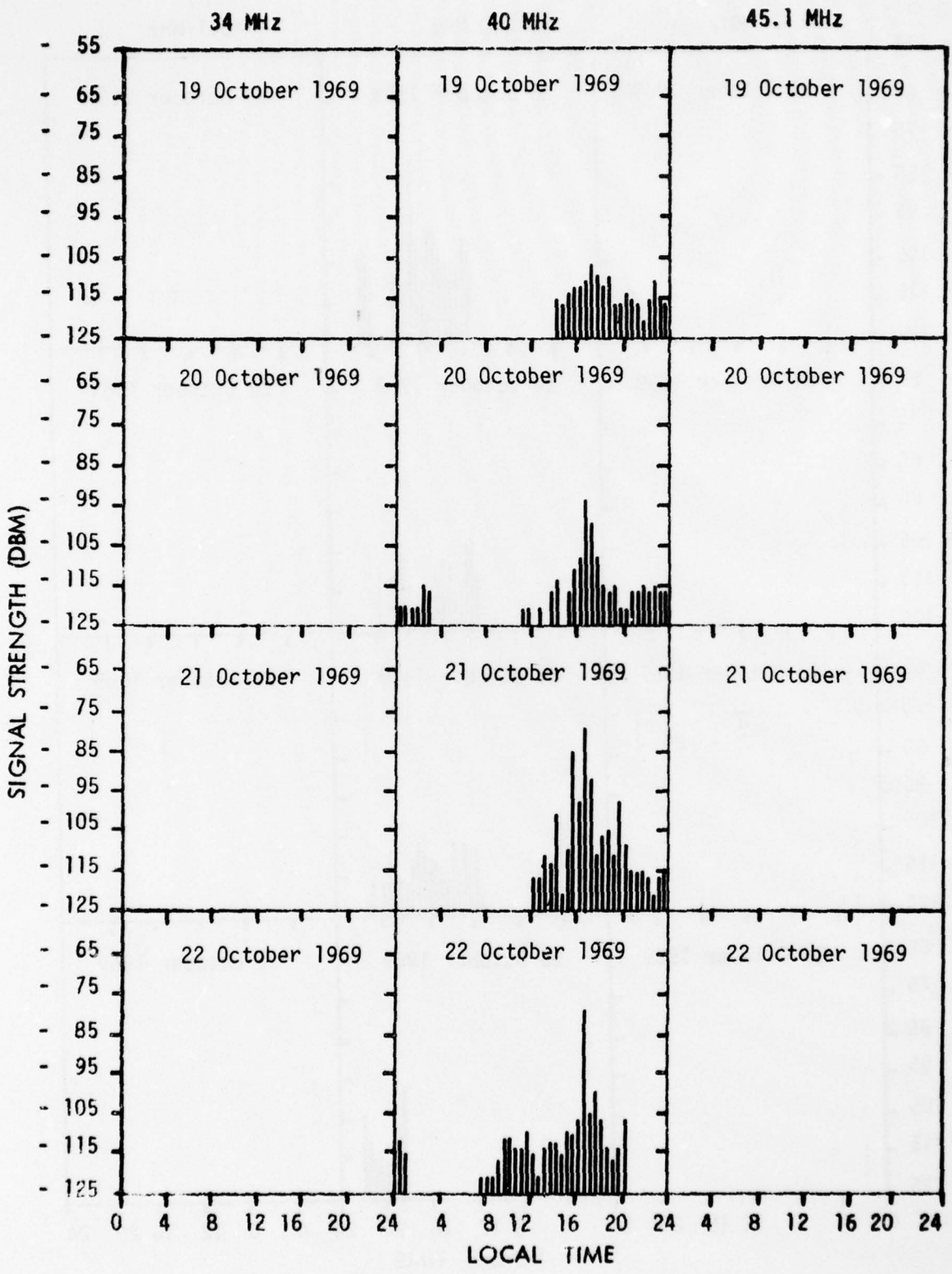

Fig. 44 – 34, 40 and 45.1 MHz Reception at Roma

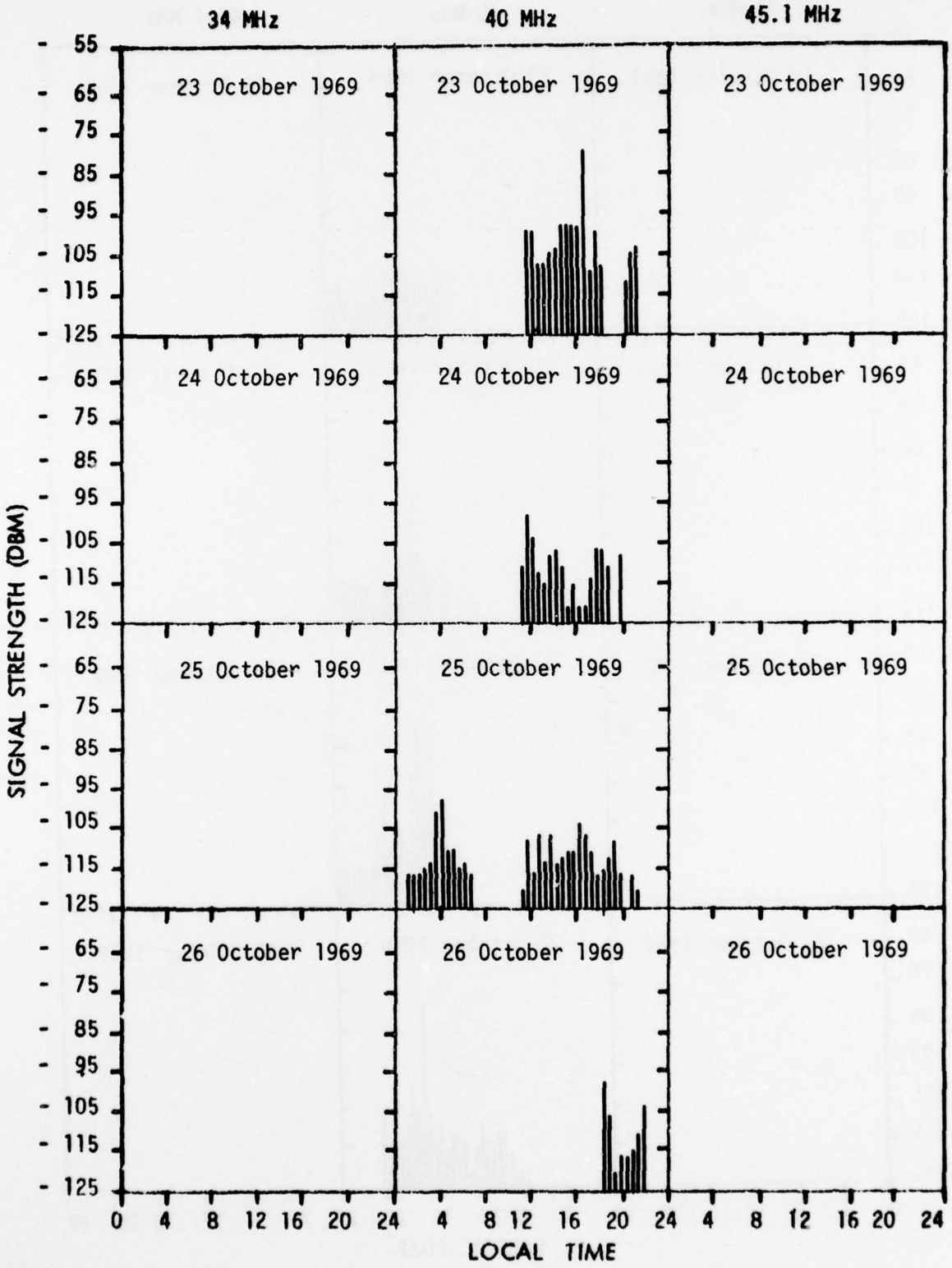

Fig. 45 – 34, 40 and 45.1 MHz Reception at Rome

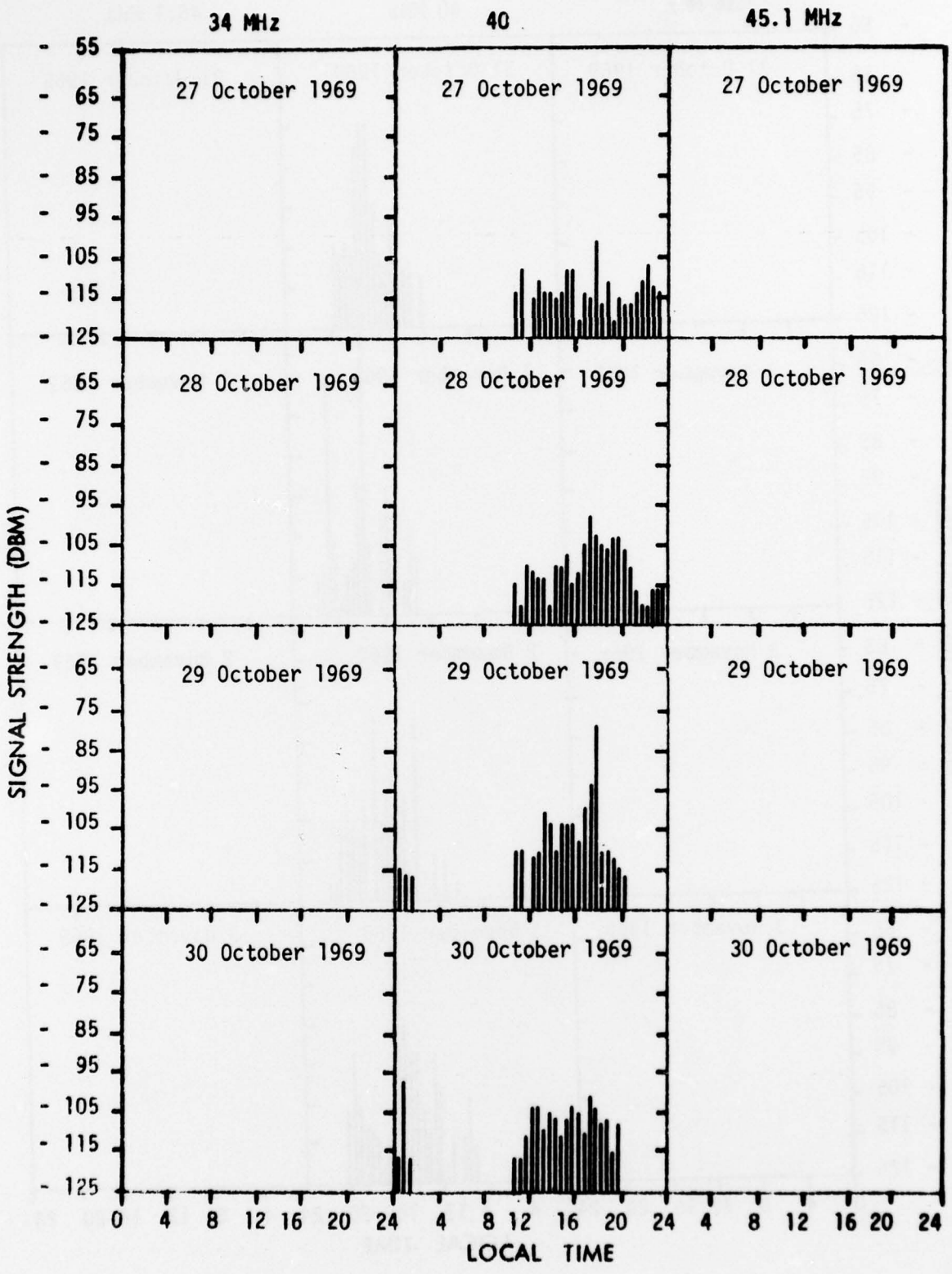

Fig. 46 – 34, 40 and 45.1 MHz Reception at Rome

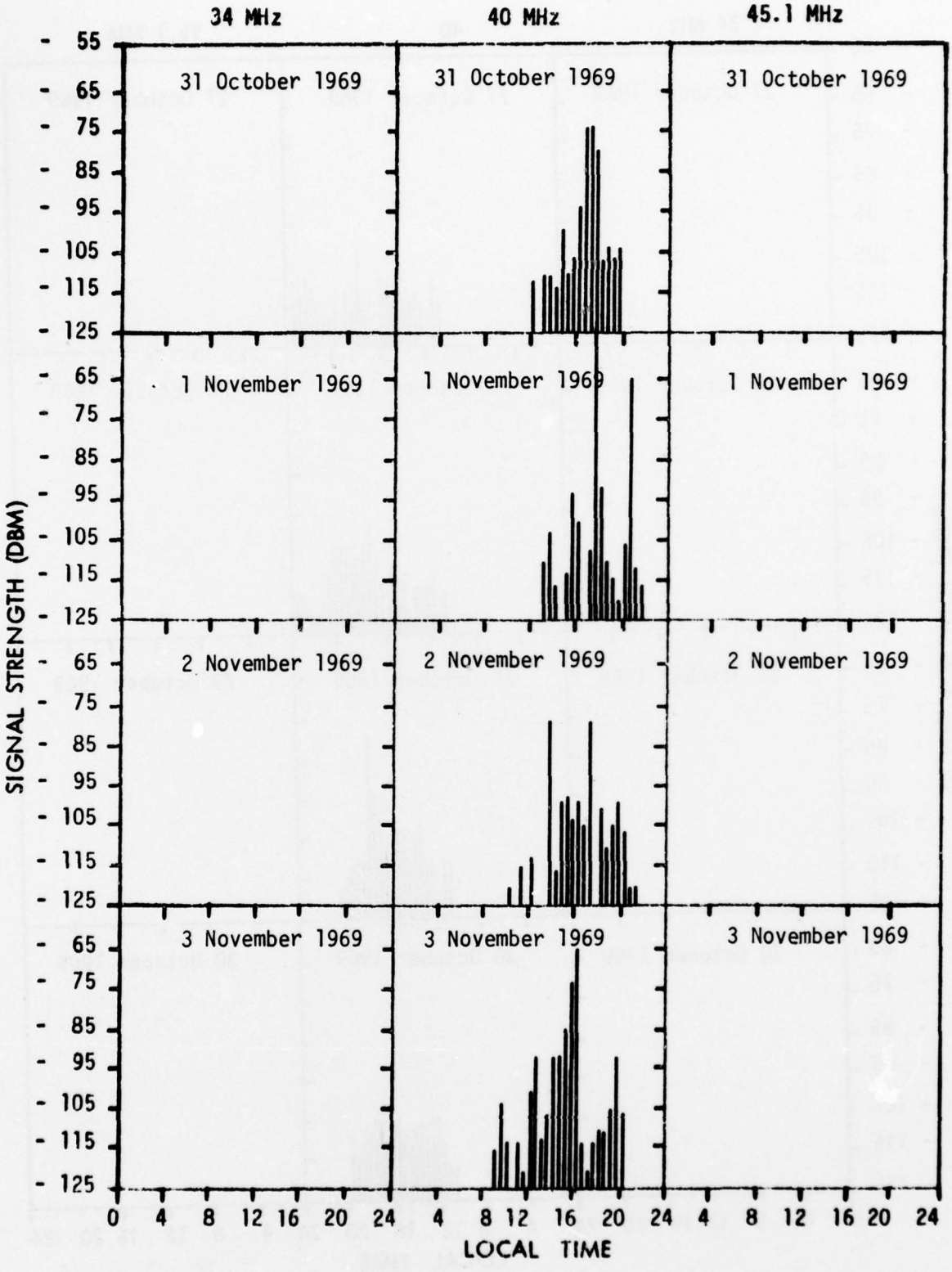

Fig. 47 – 34, 40 and 45.1 MHz Reception at Roma

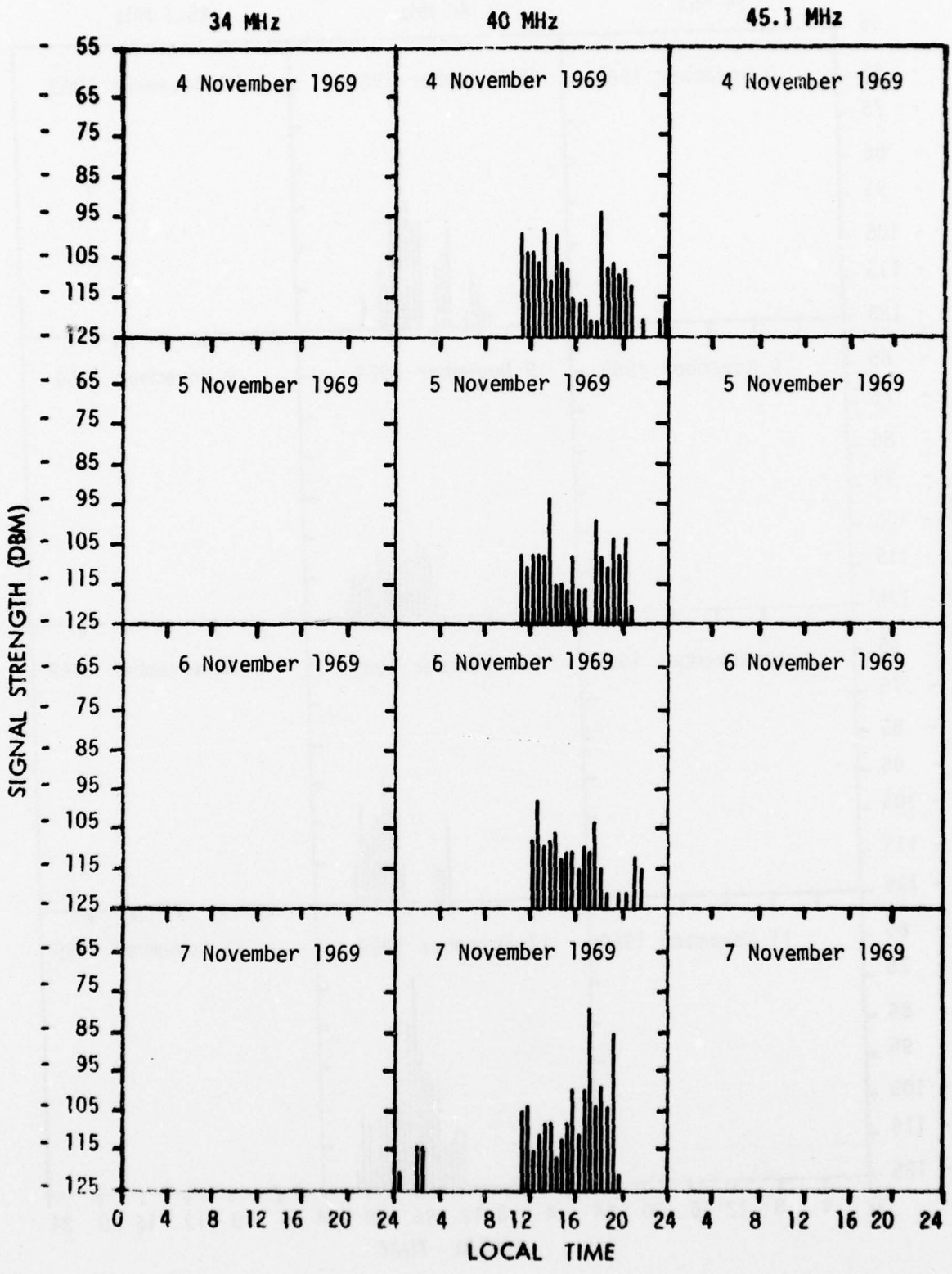

Fig. 48 – 34, 40 and 45.1 MHz Reception at Roma

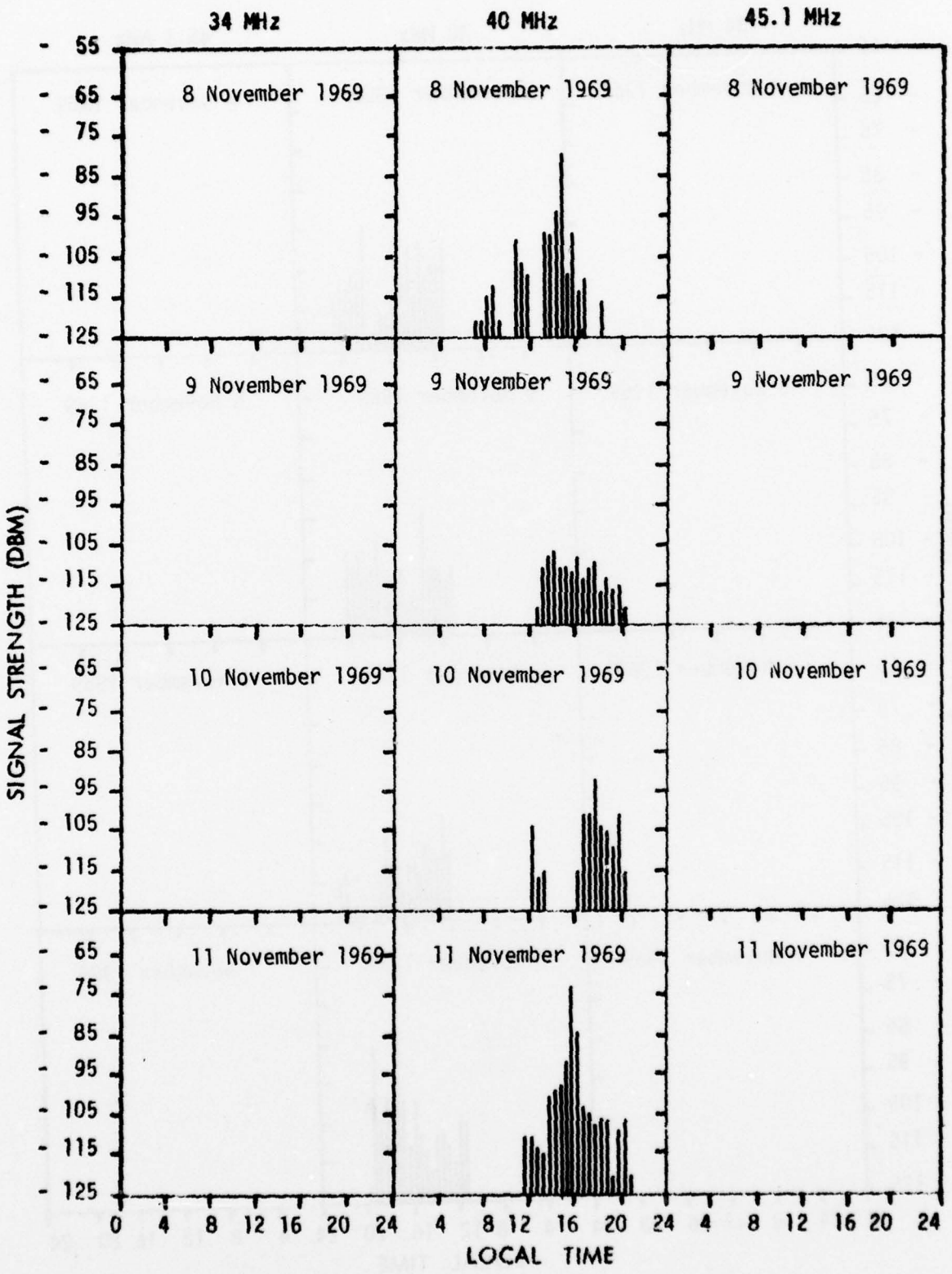

Fig. 49 – 34, 40 and 45.1 MHz Reception at Roma

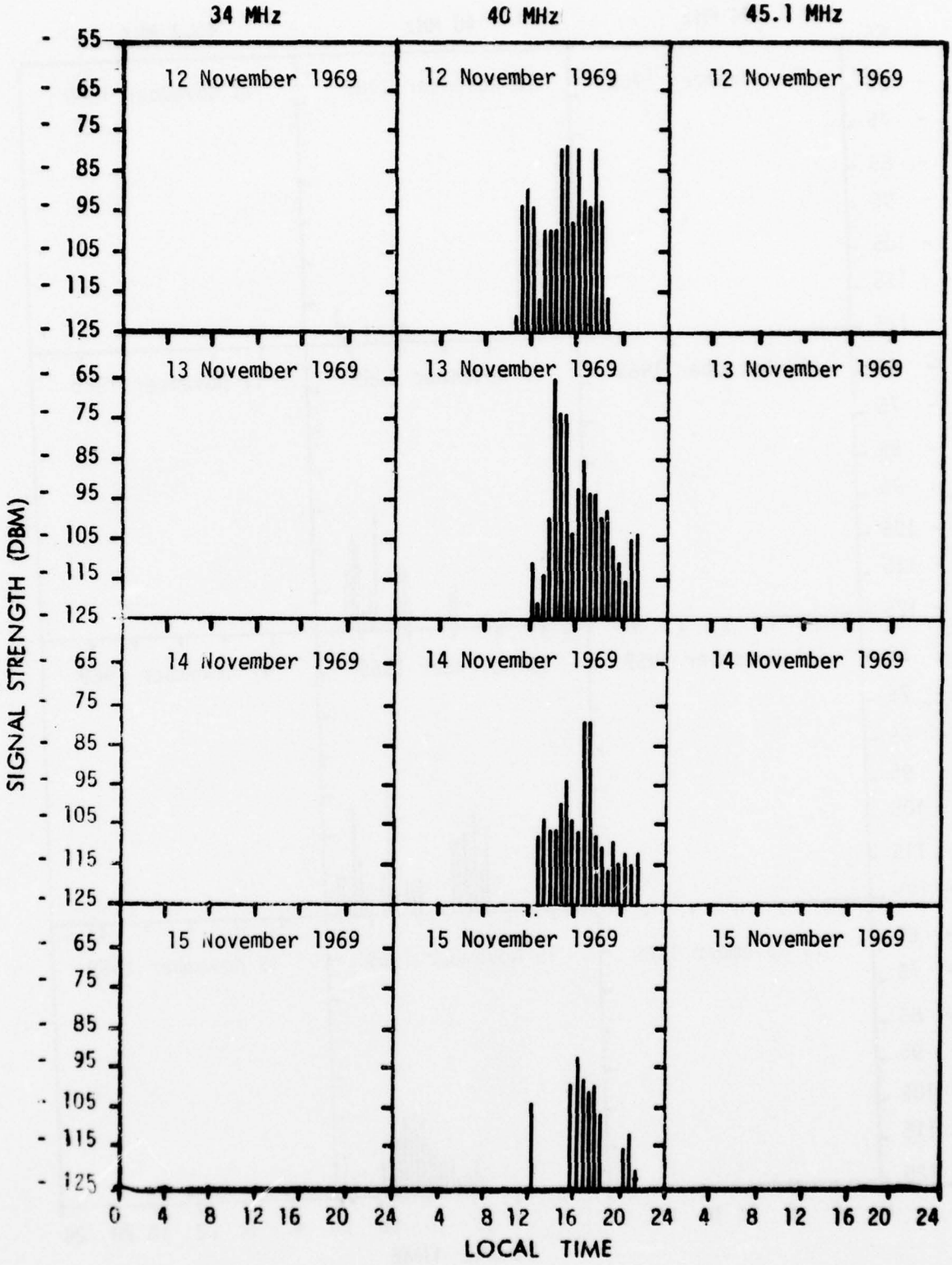

Fig. 50 – 34, 40 and 45.1 MHz Reception at Roma

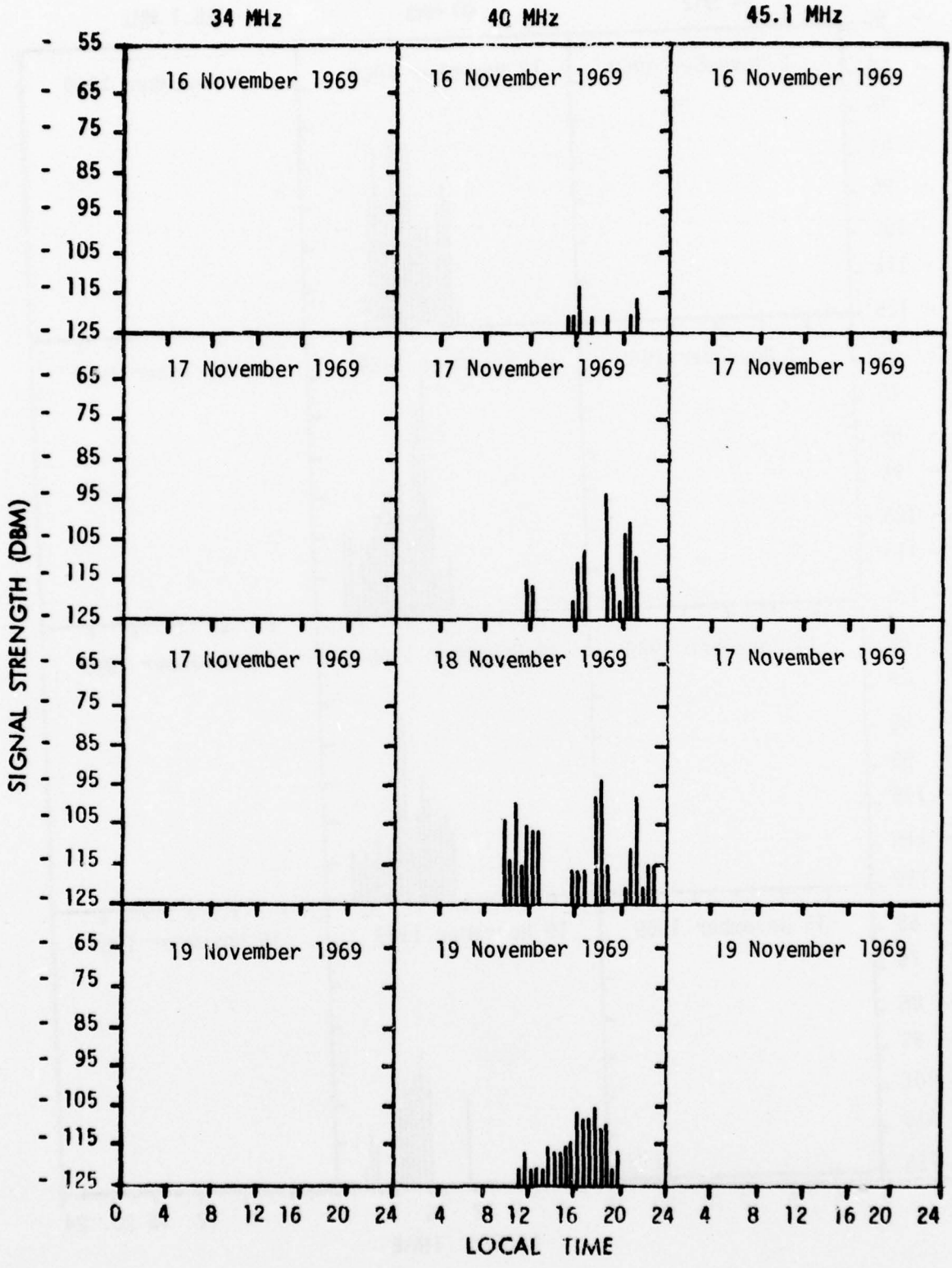

Fig. 51 – 34, 40 and 45.1 MHz Reception at Roma

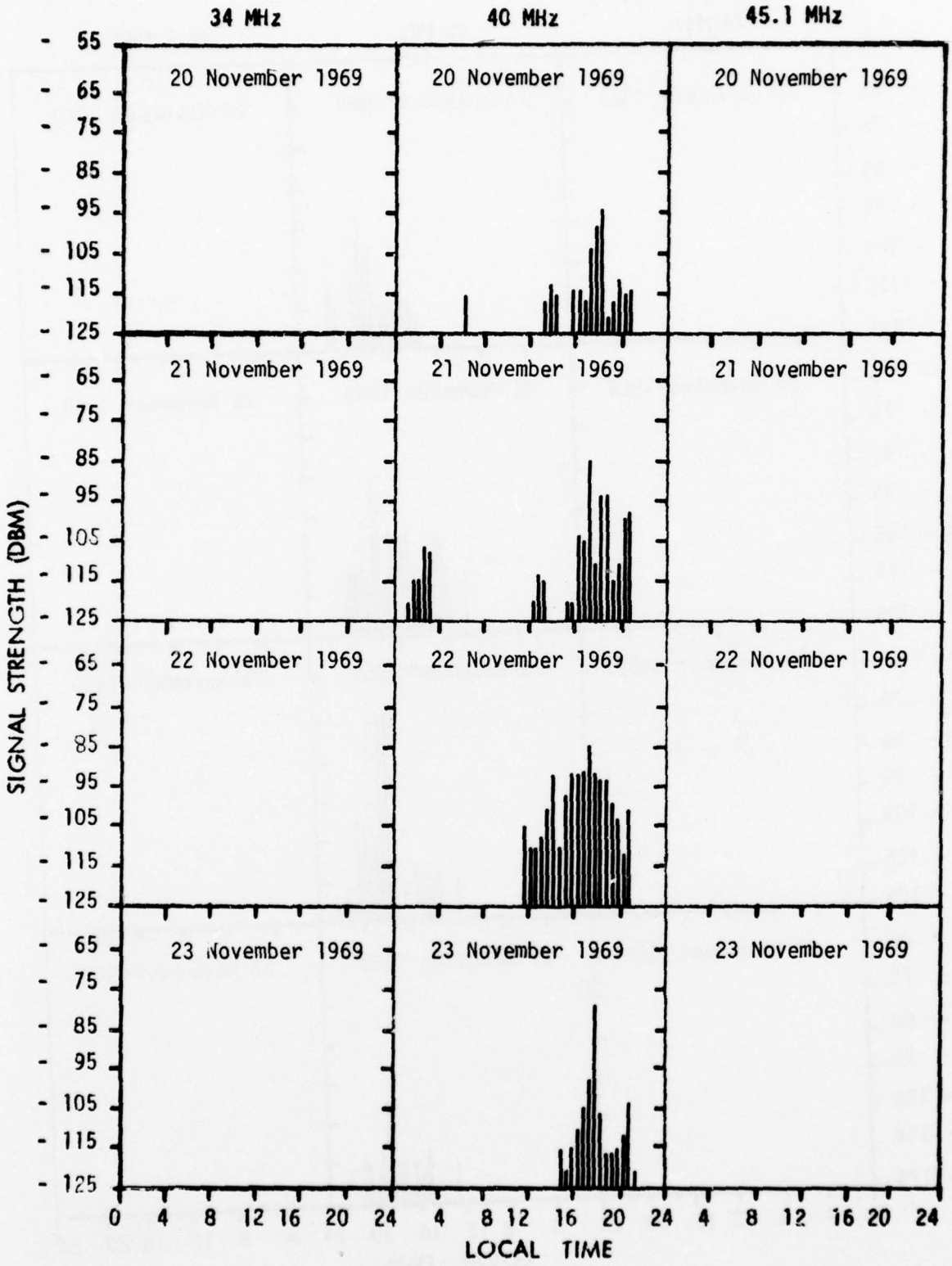

Fig. 52 – 34, 40 and 45.1 MHz Reception at Roma

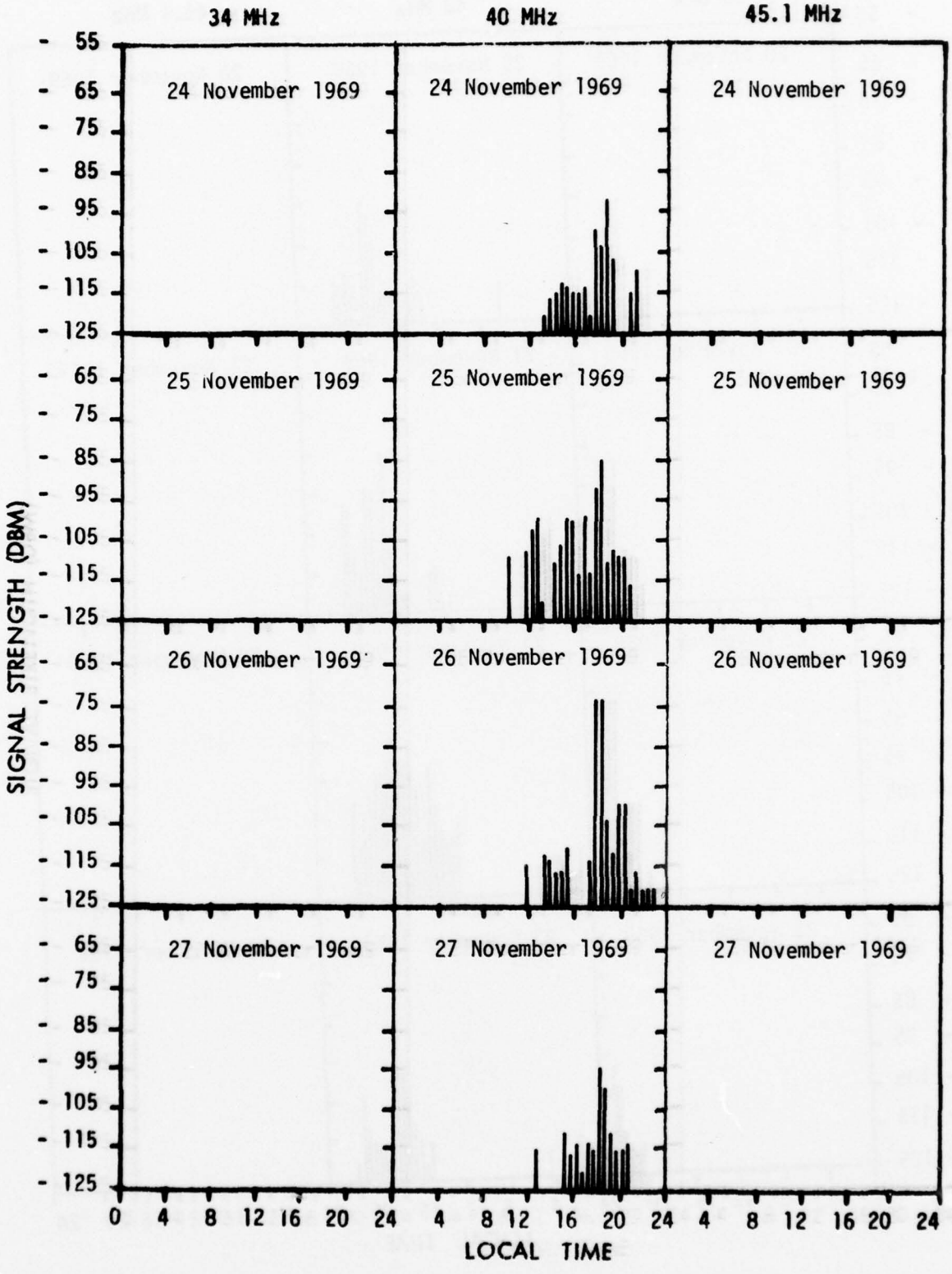

Fig. 53 – 34, 40 and 45.1 MHz Reception at Roma

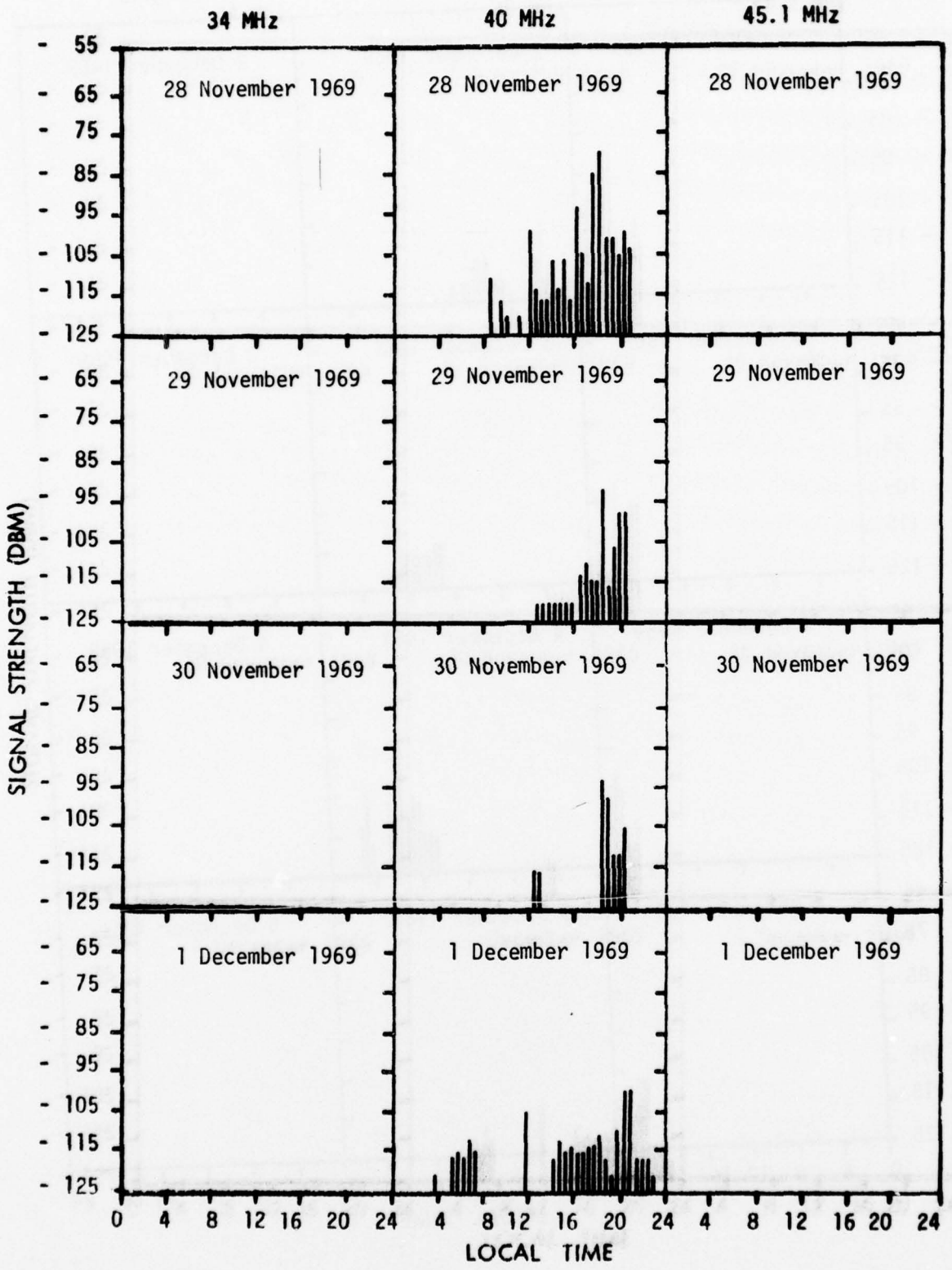

Fig. 54 – 34, 40 and 45.1 MHz Reception at Rome

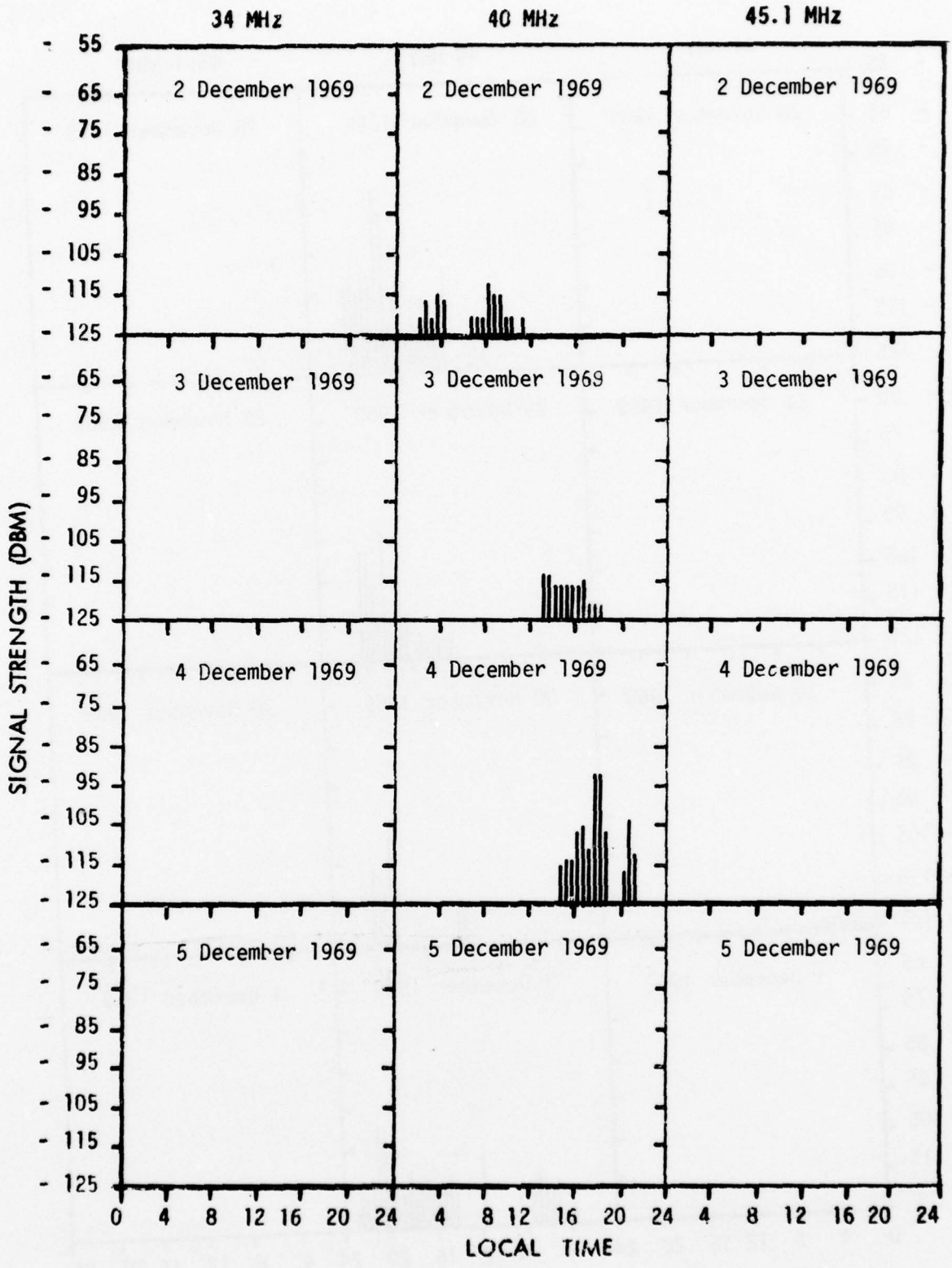

Fig. 55 – 34, 40 and 45.1 MHz Reception at Roma

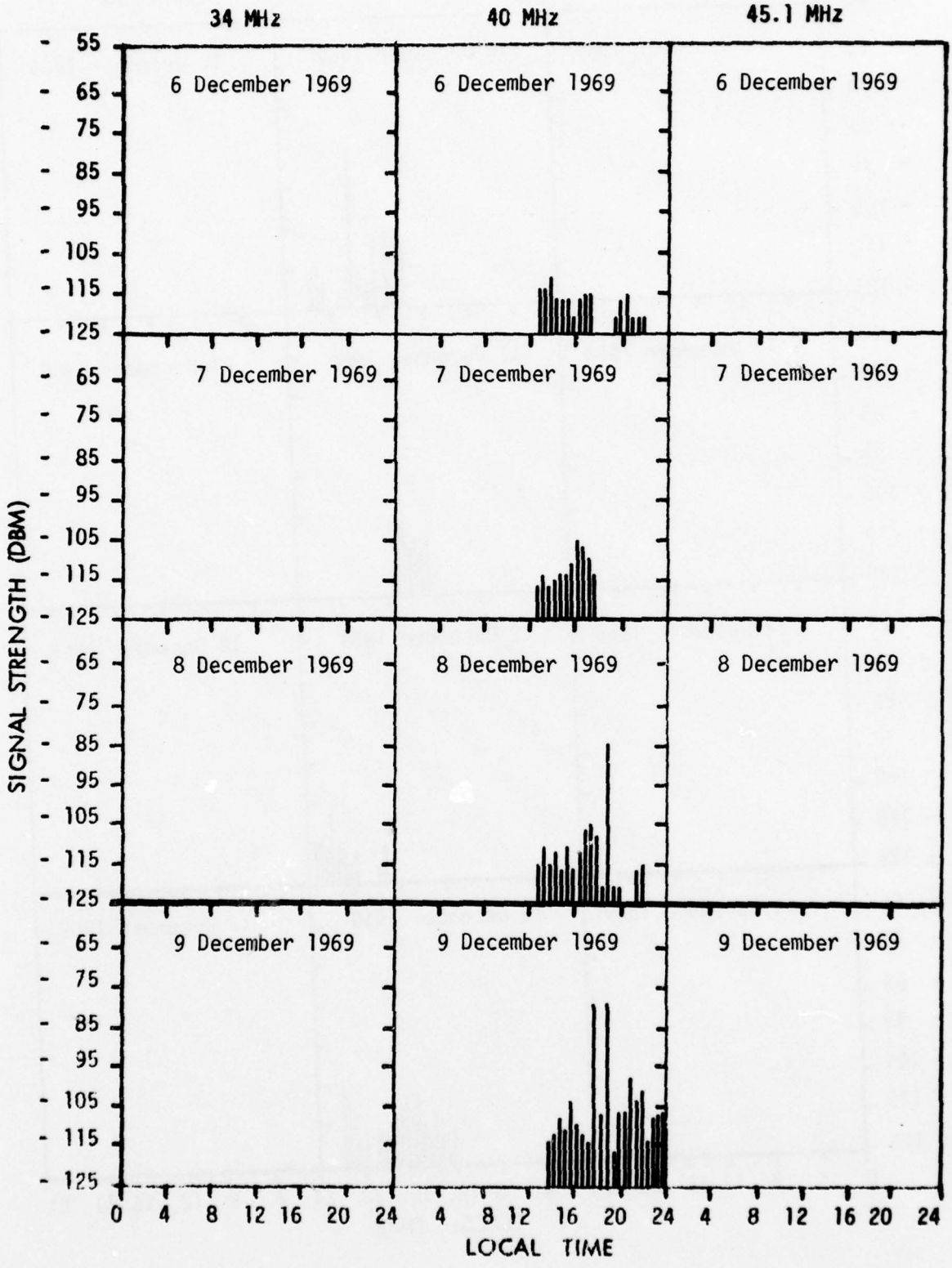

Fig. 56 — 34, 40 and 45.1 MHz Reception at Rome

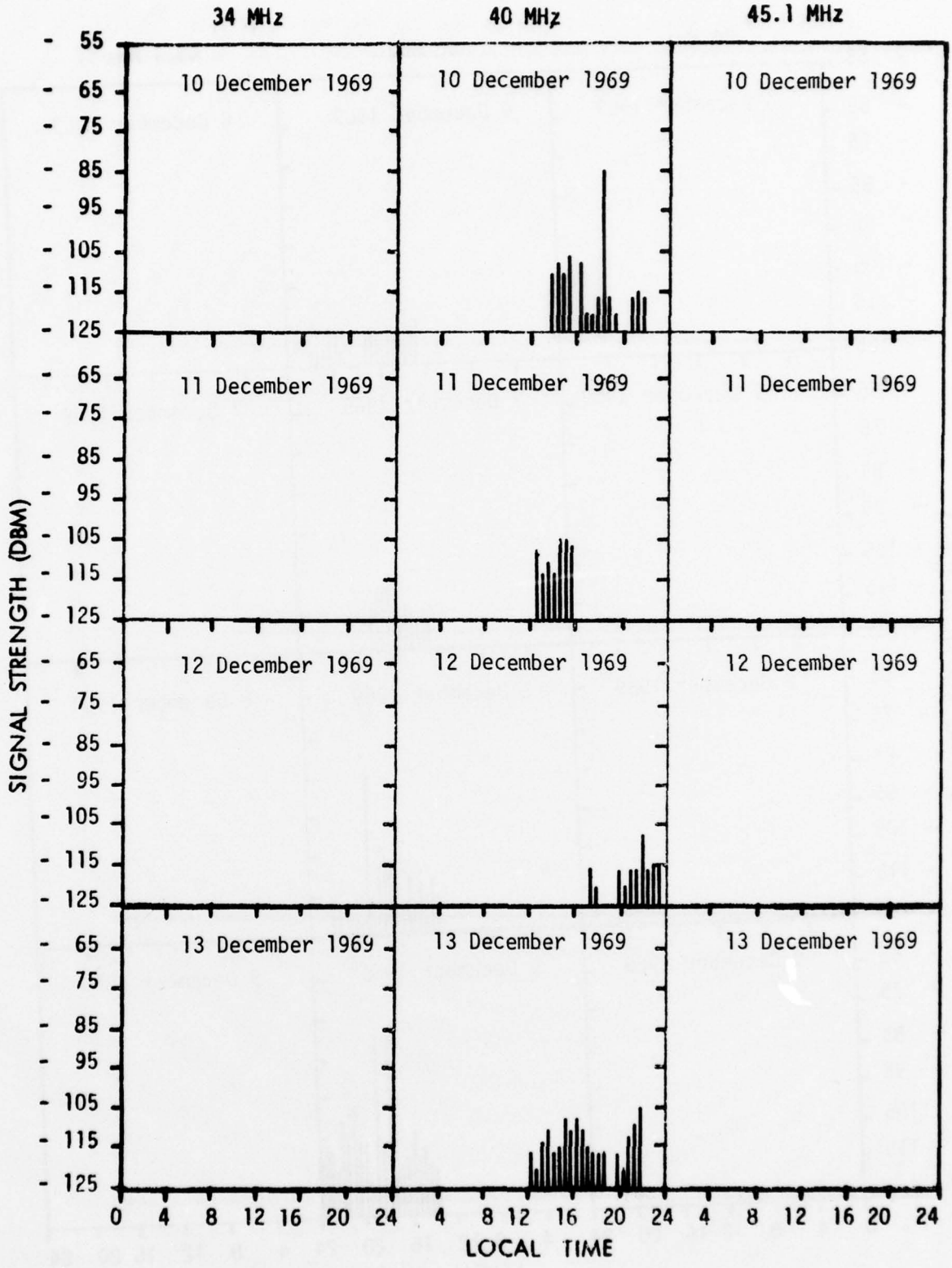

Fig. 57 – 34, 40 and 45.1 MHz Reception at Roma

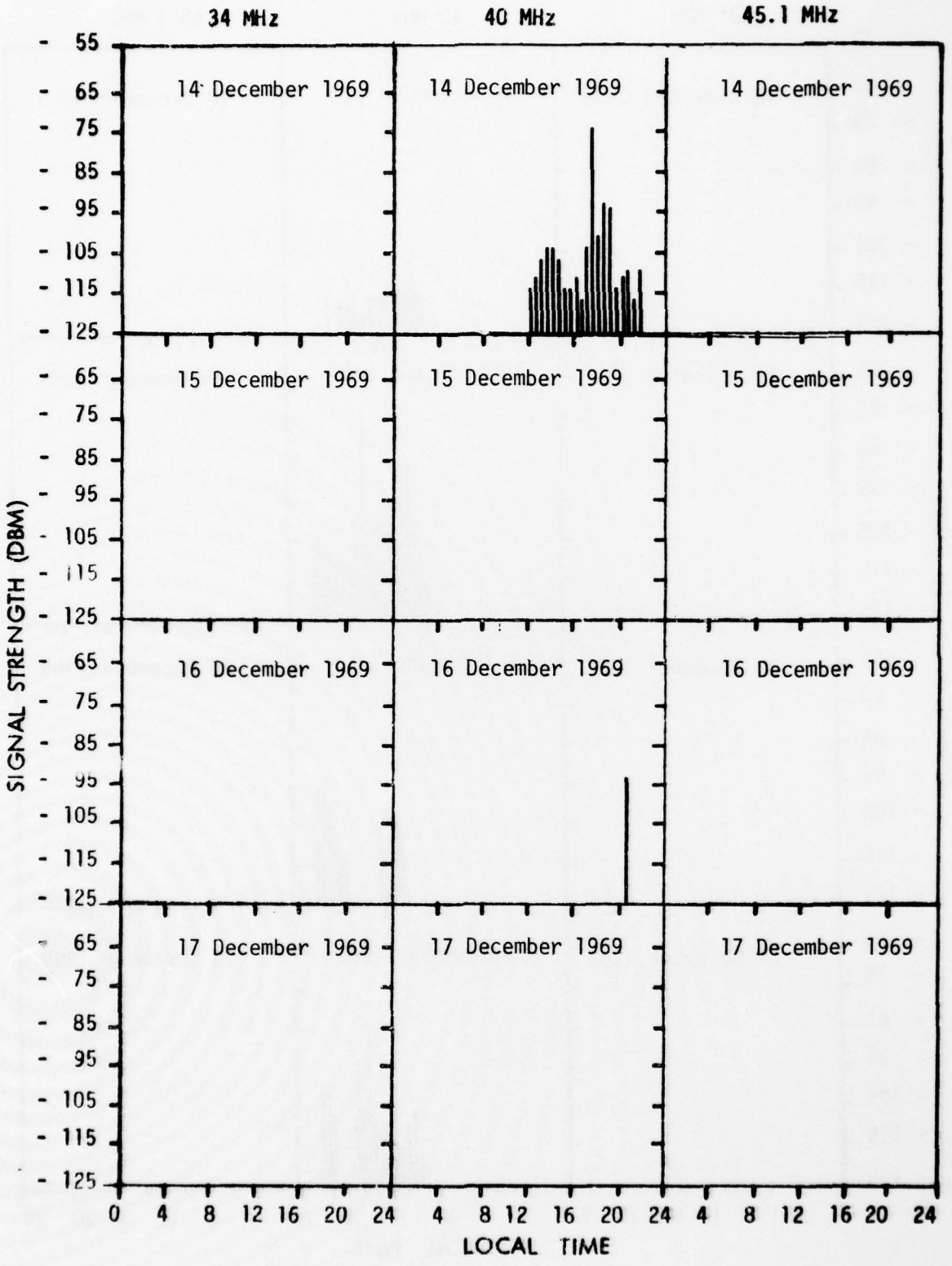

Fig. 58 – 34, 40 and 45.1 MHz Reception at Roma

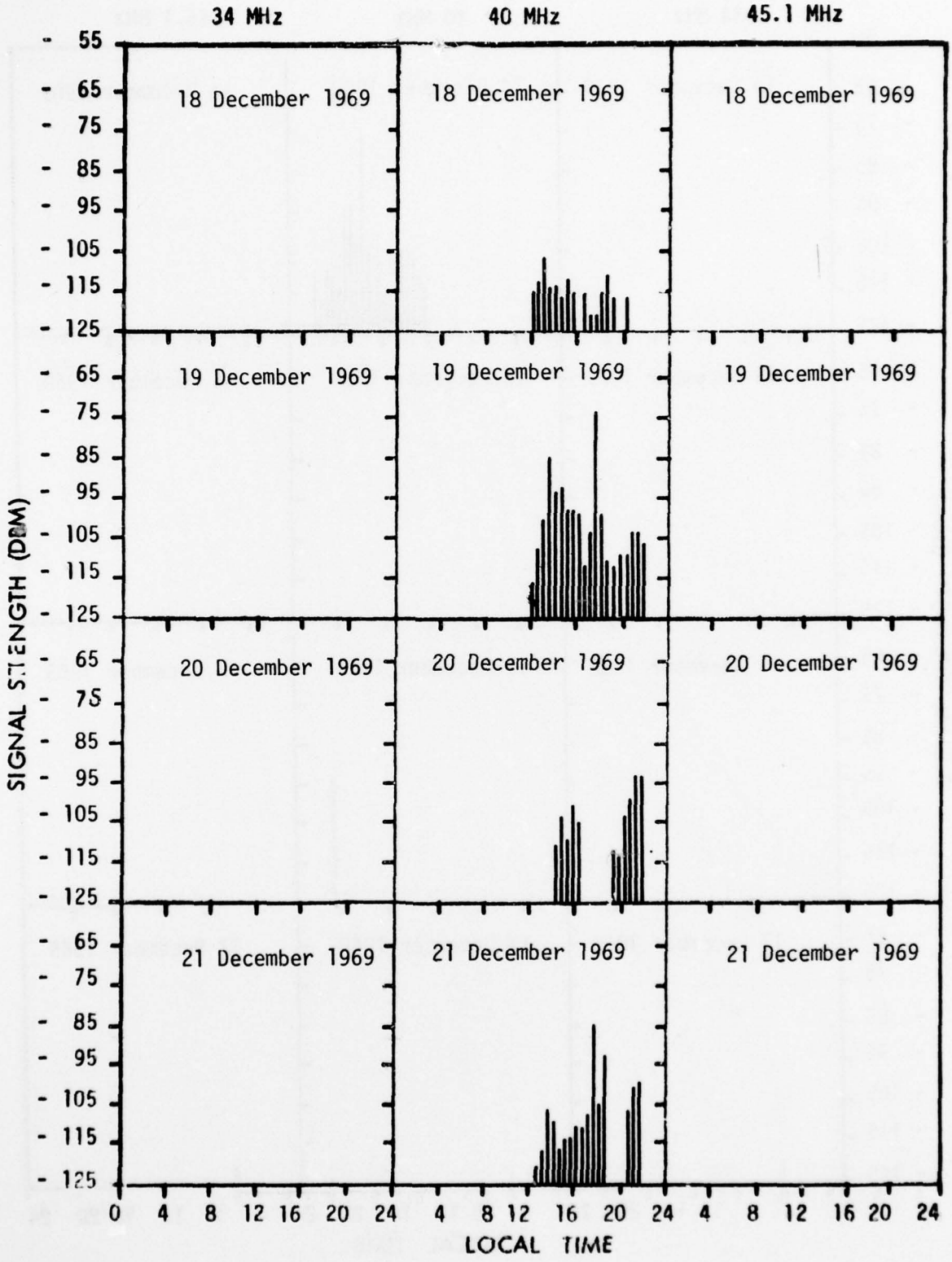

Fig. 59 – 34, 40 and 45.1 MHz Reception at Roma

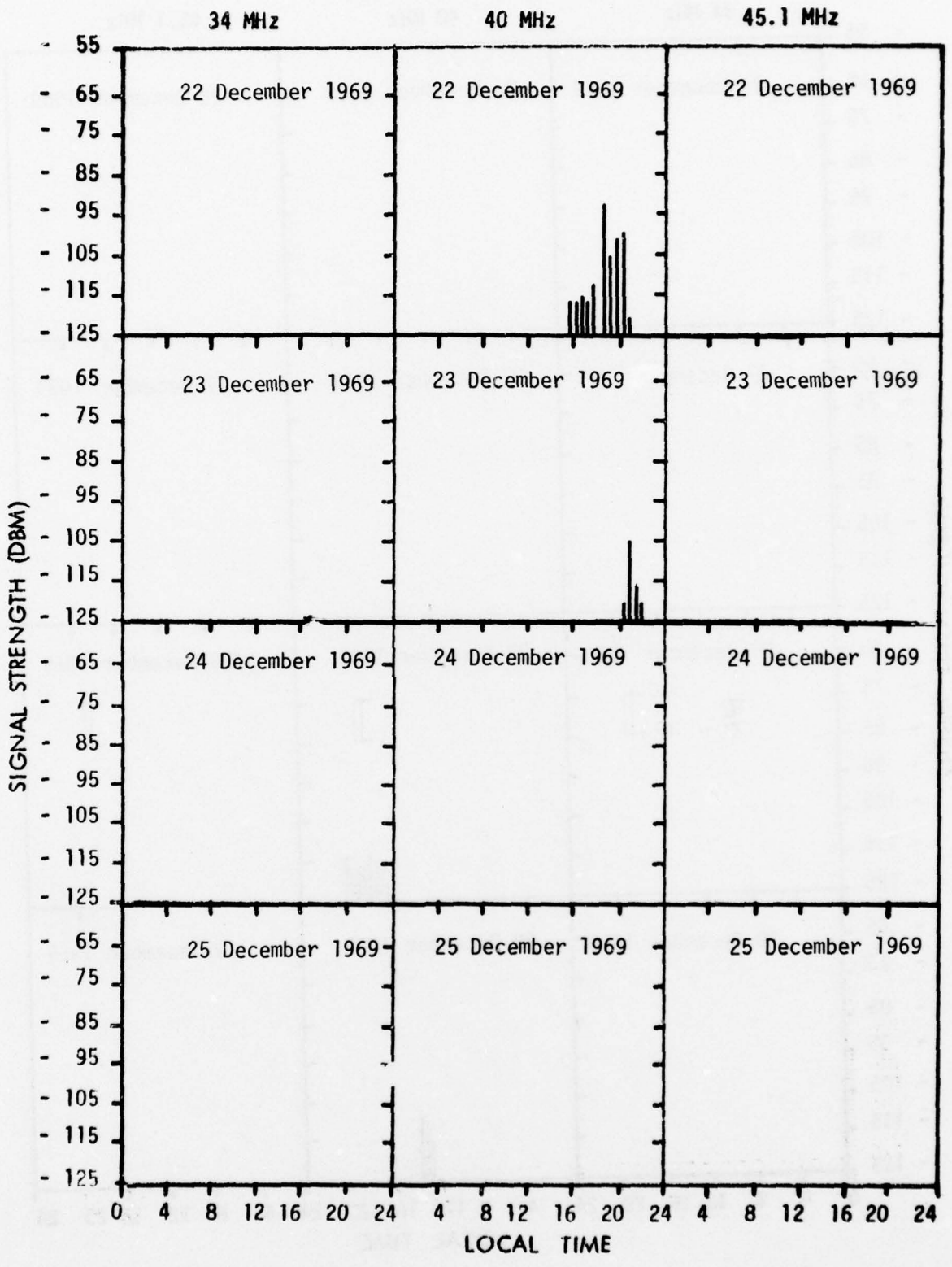

Fig. 60 – 34, 40 and 45.1 MHz Reception at Roma

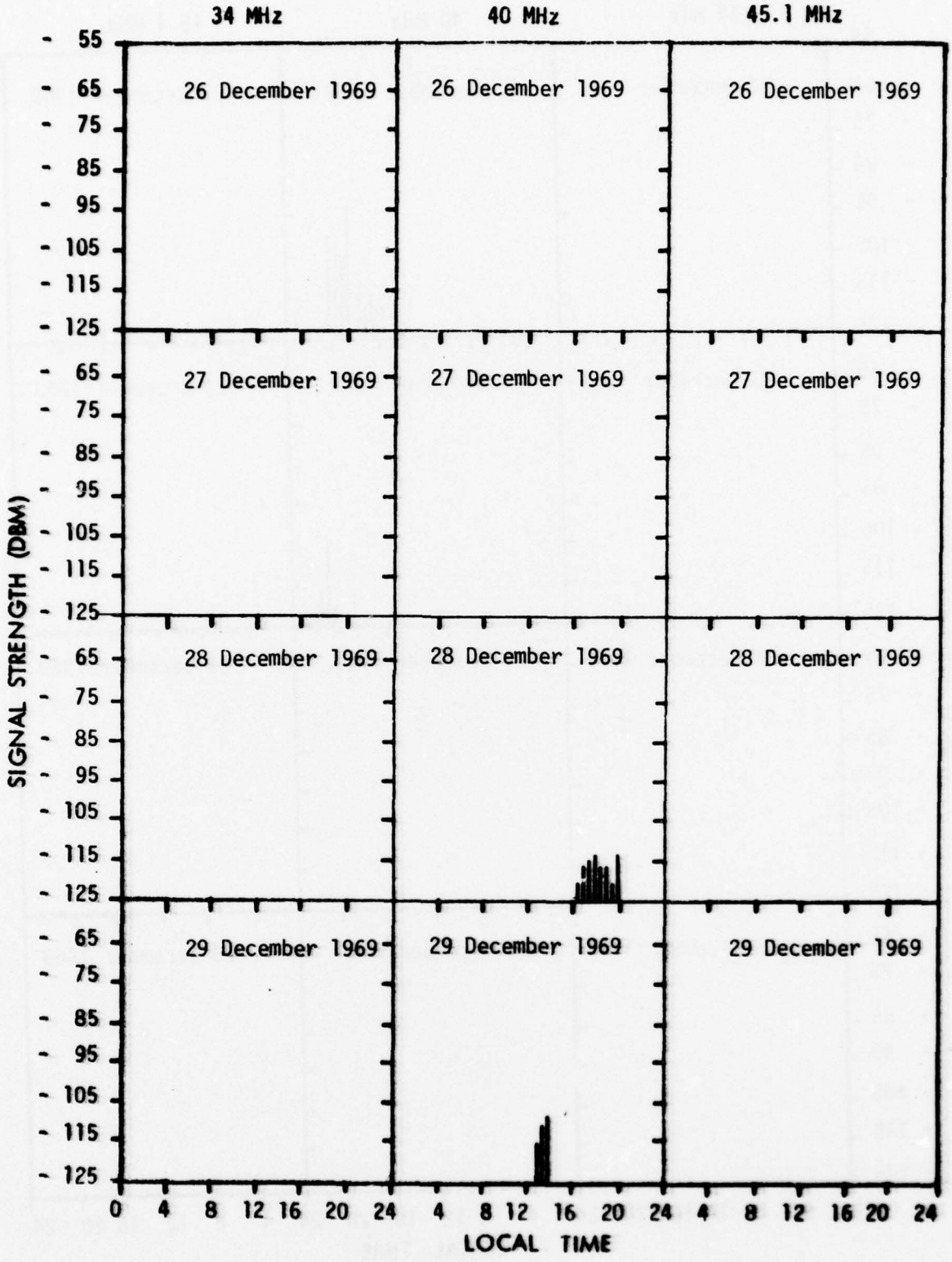

Fig. 61 – 34, 40 and 45.1 MHz Reception at Rome

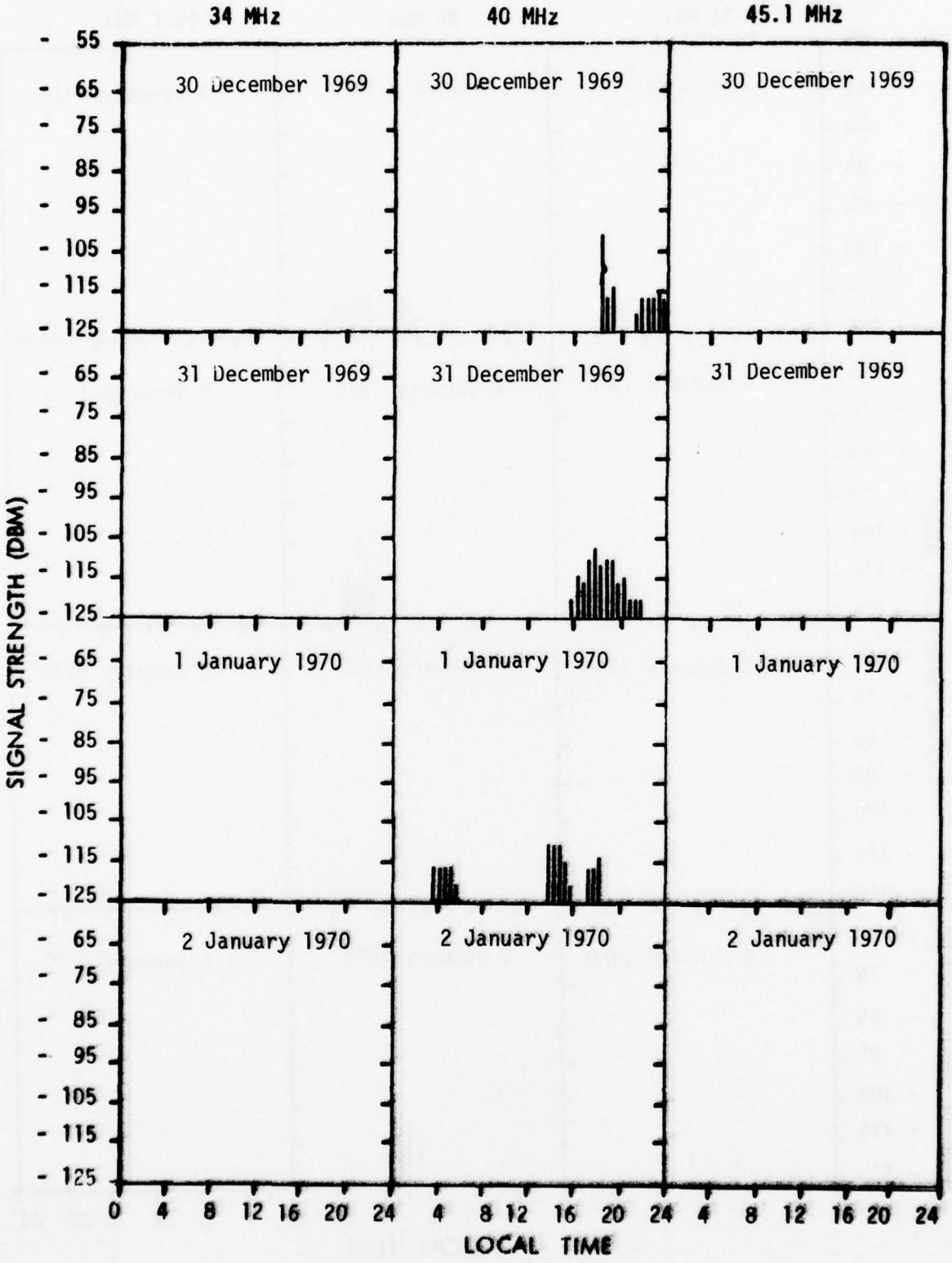

Fig. 62 – 34, 40 and 45.1 MHz Reception at Rome

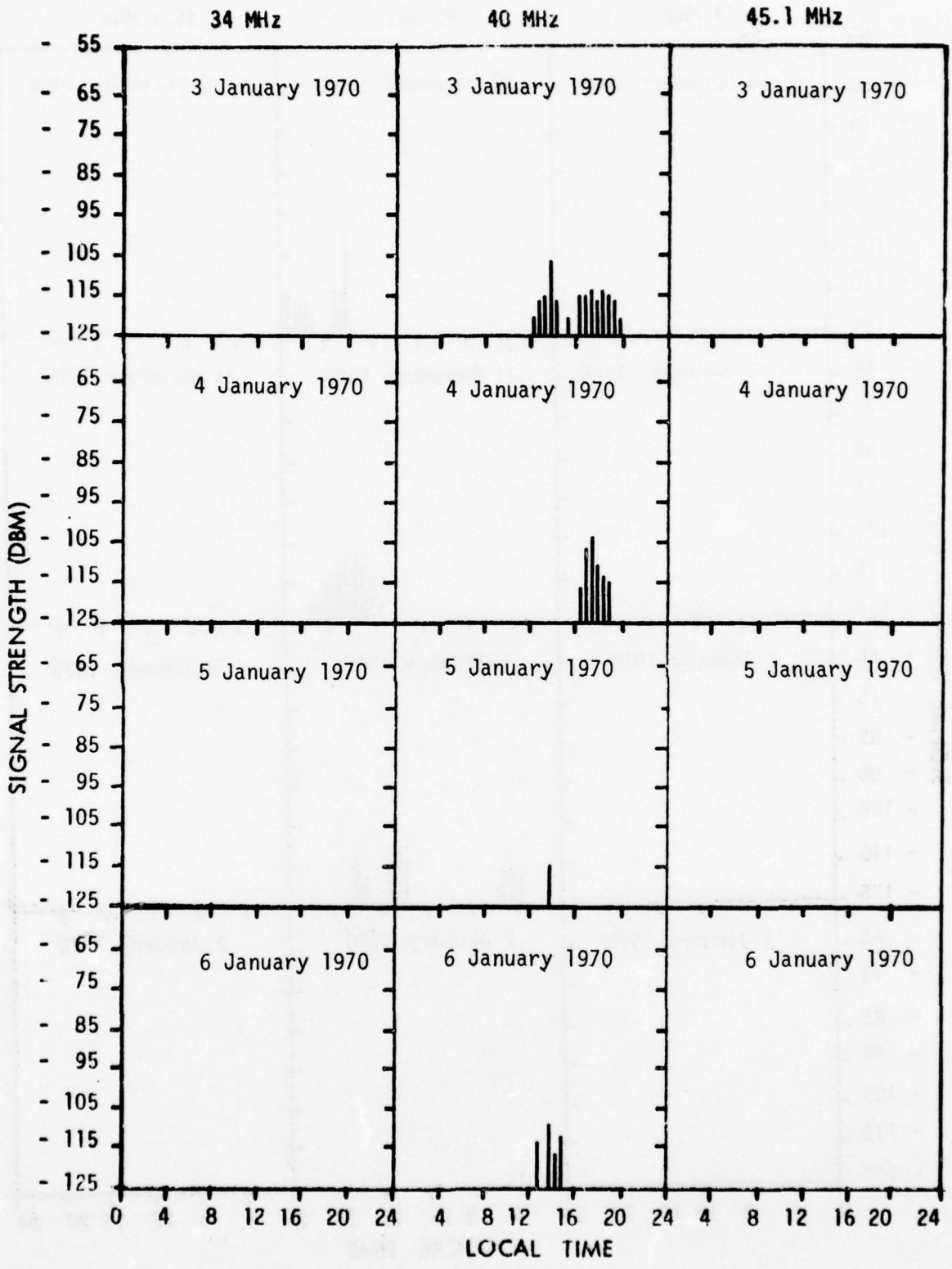

Fig. 63 – 34, 40 and 45.1 MHz Reception at Roma

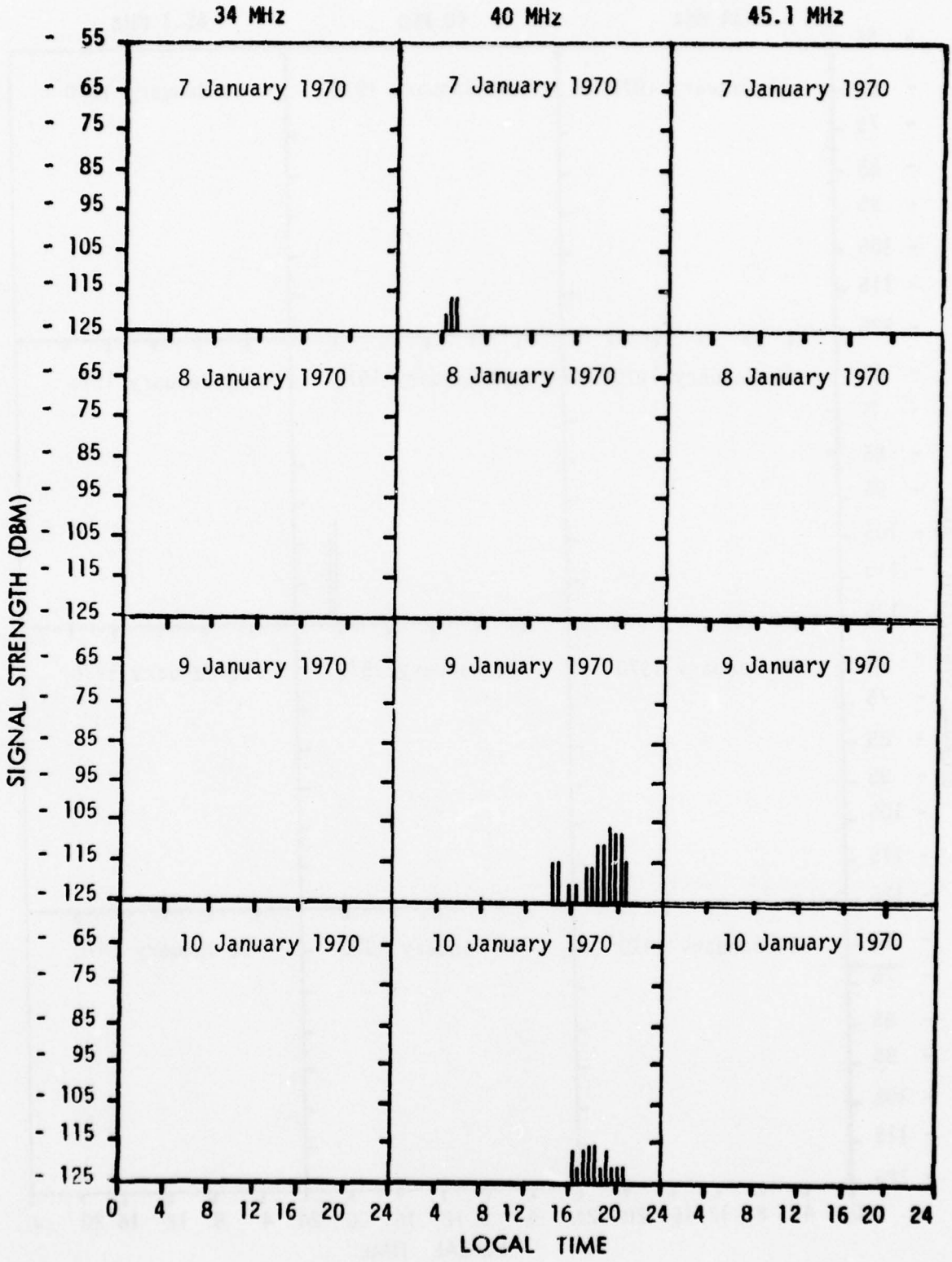

Fig. 64 – 34, 40 and 45.1 MHz Reception at Roma

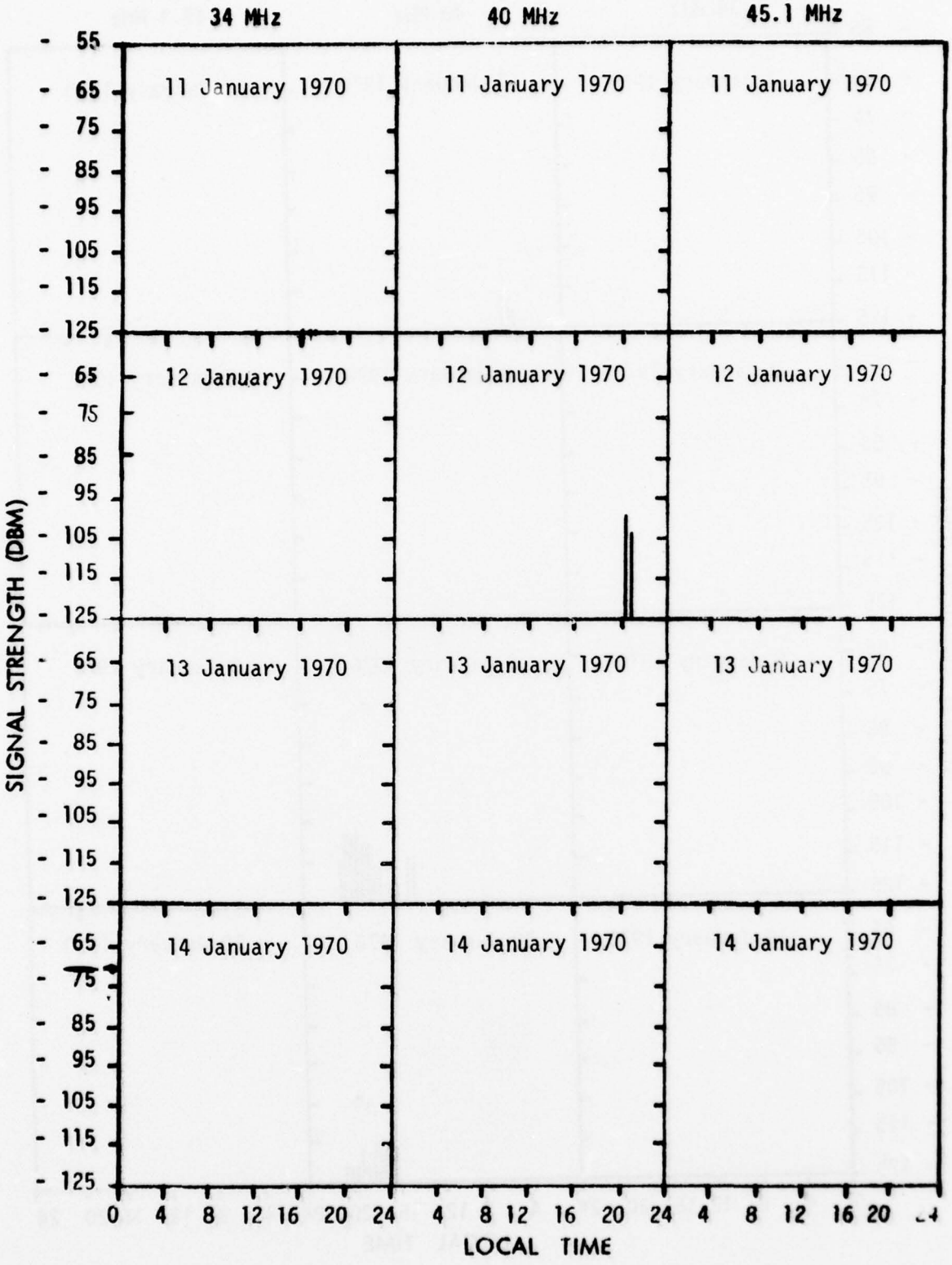

Fig. 65 – 34, 40 and 45.1 MHz Reception at Roma

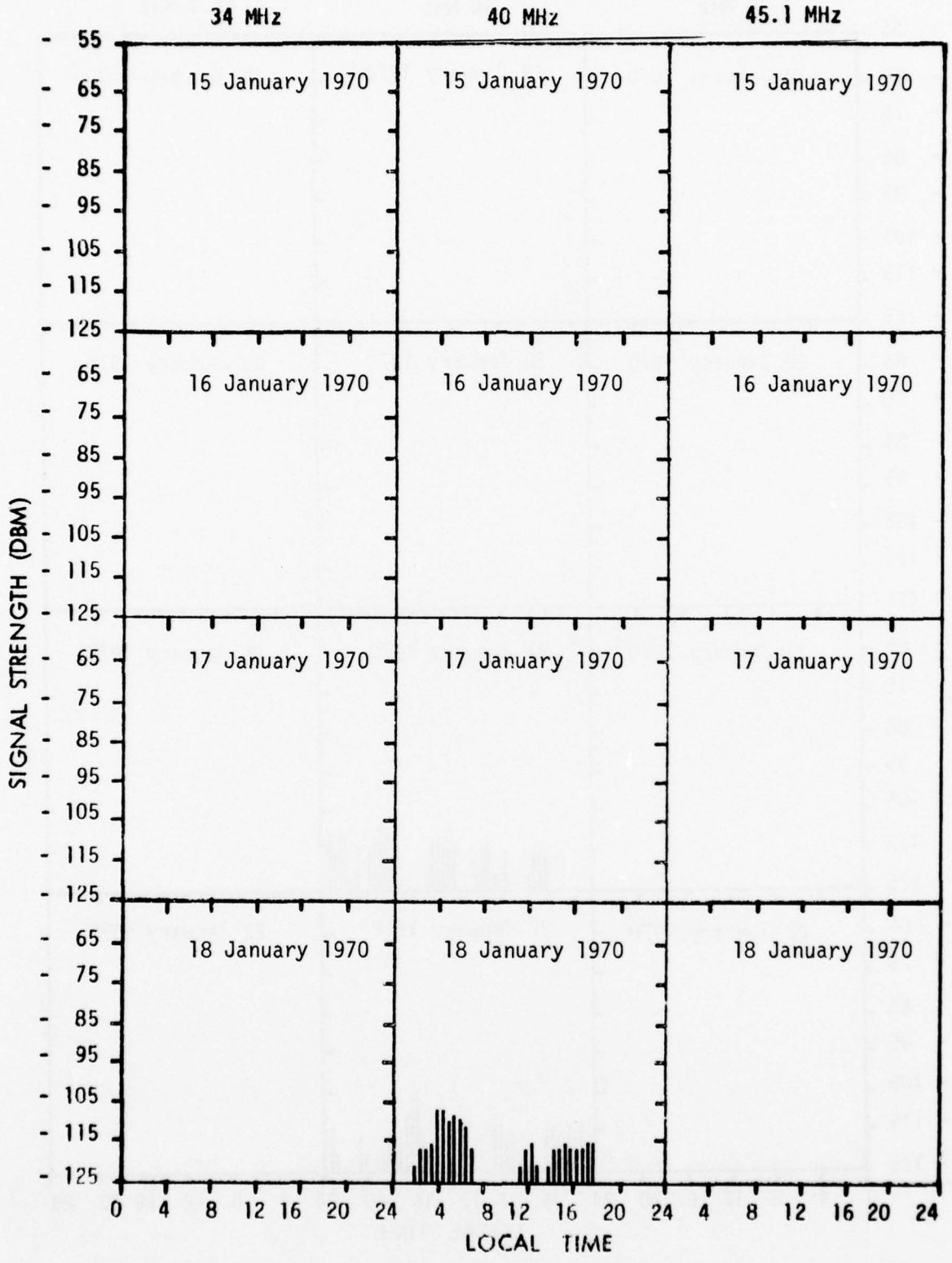

Fig. 66 – 34, 40 and 45.1 MHz Reception at Roma

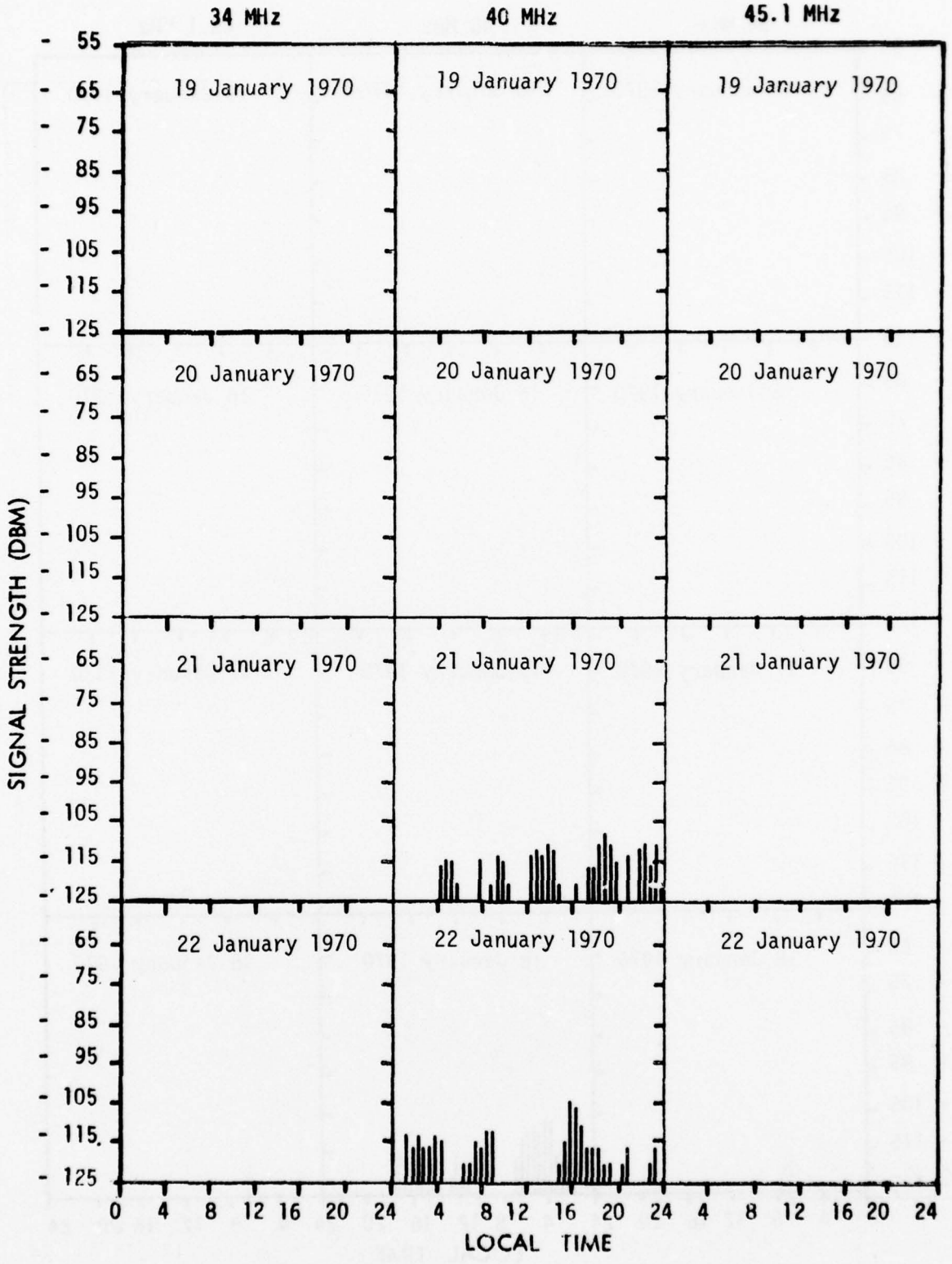

Fig. 67 – 34, 40 and 45.1 MHz Reception at Roma

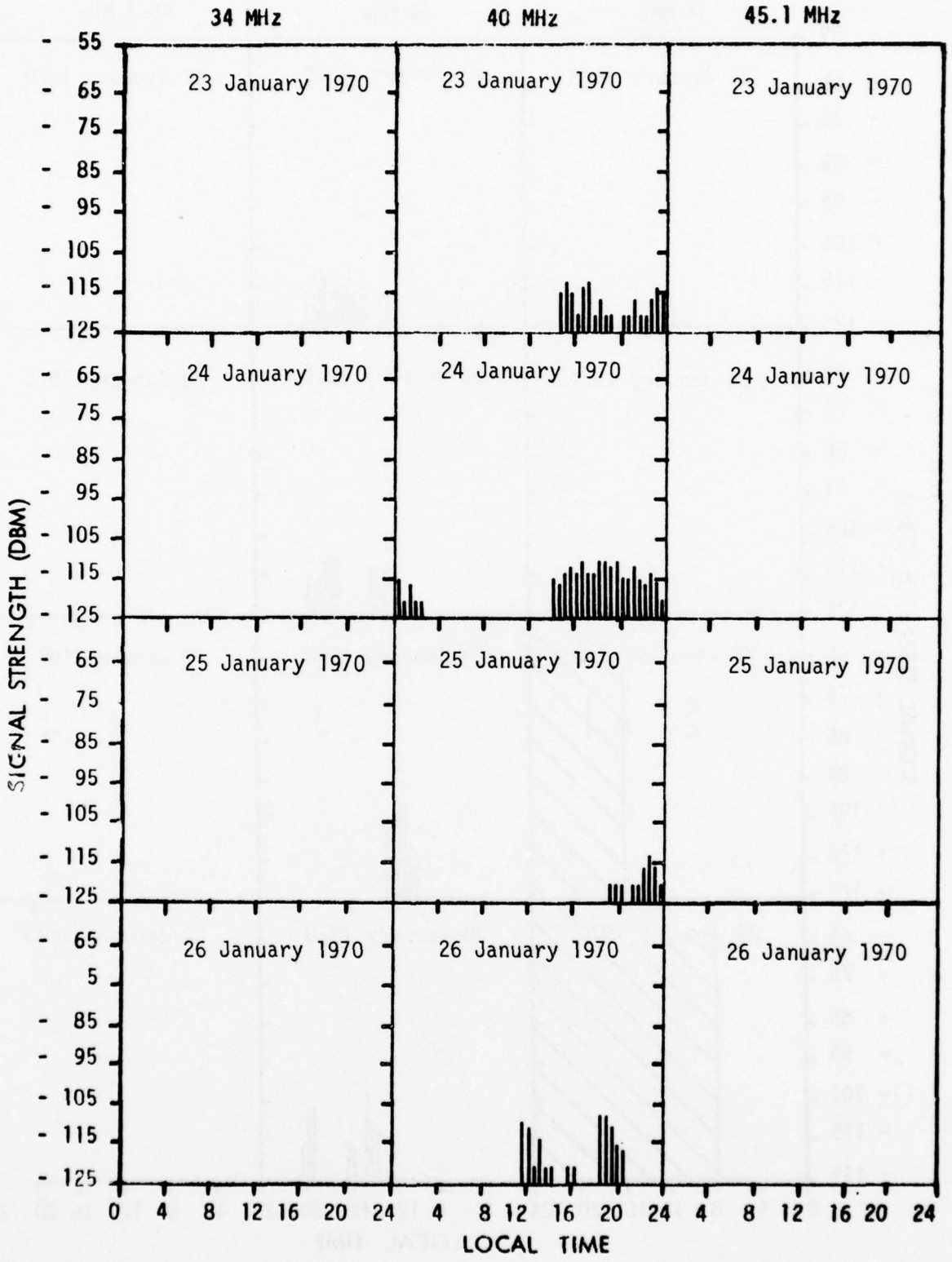

Fig. 68 – 34, 40 and 45.1 MHz Reception at Roma

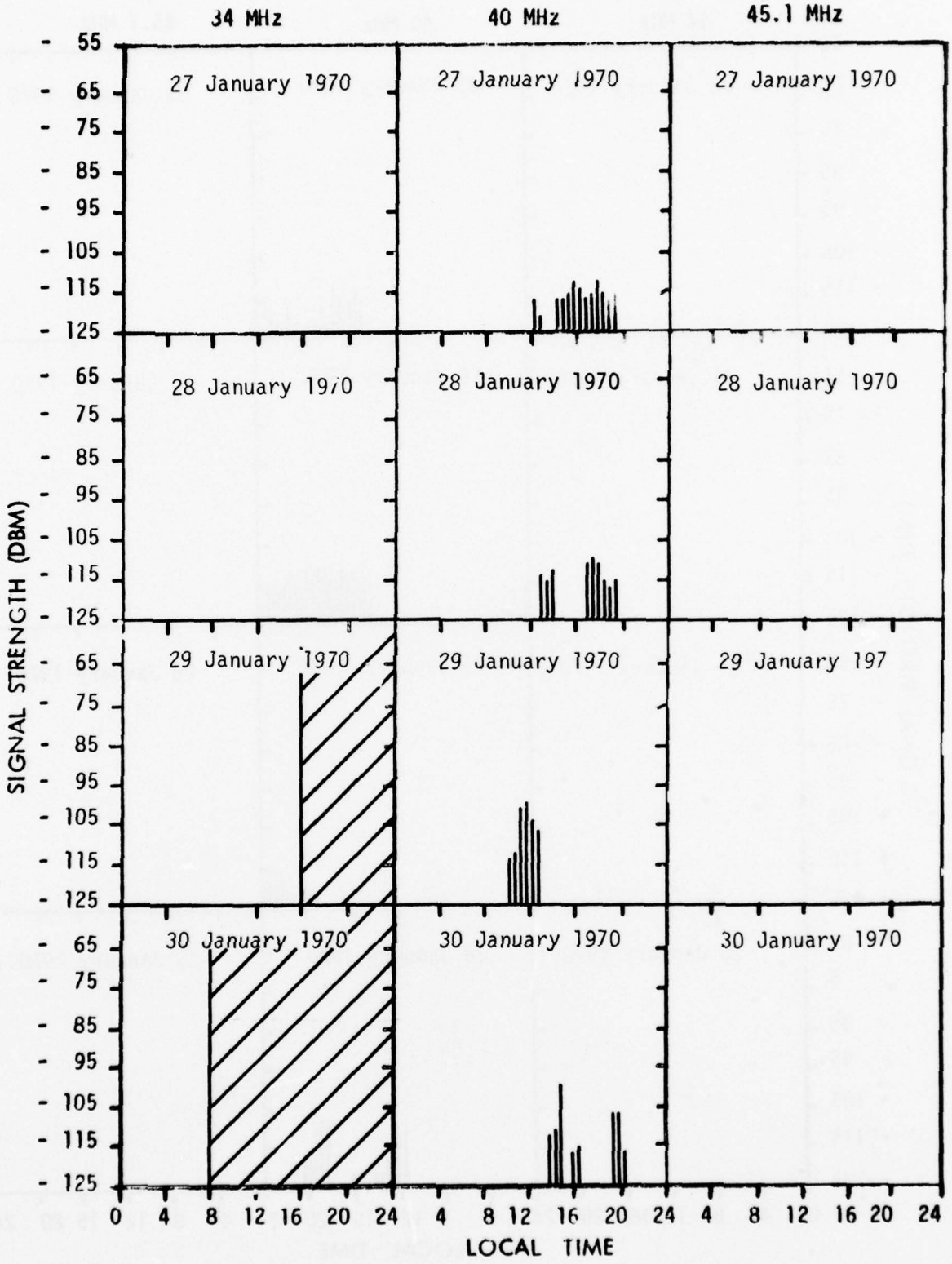

Fig. 69 – 34, 40 and 45.1 MHz Reception at Roma

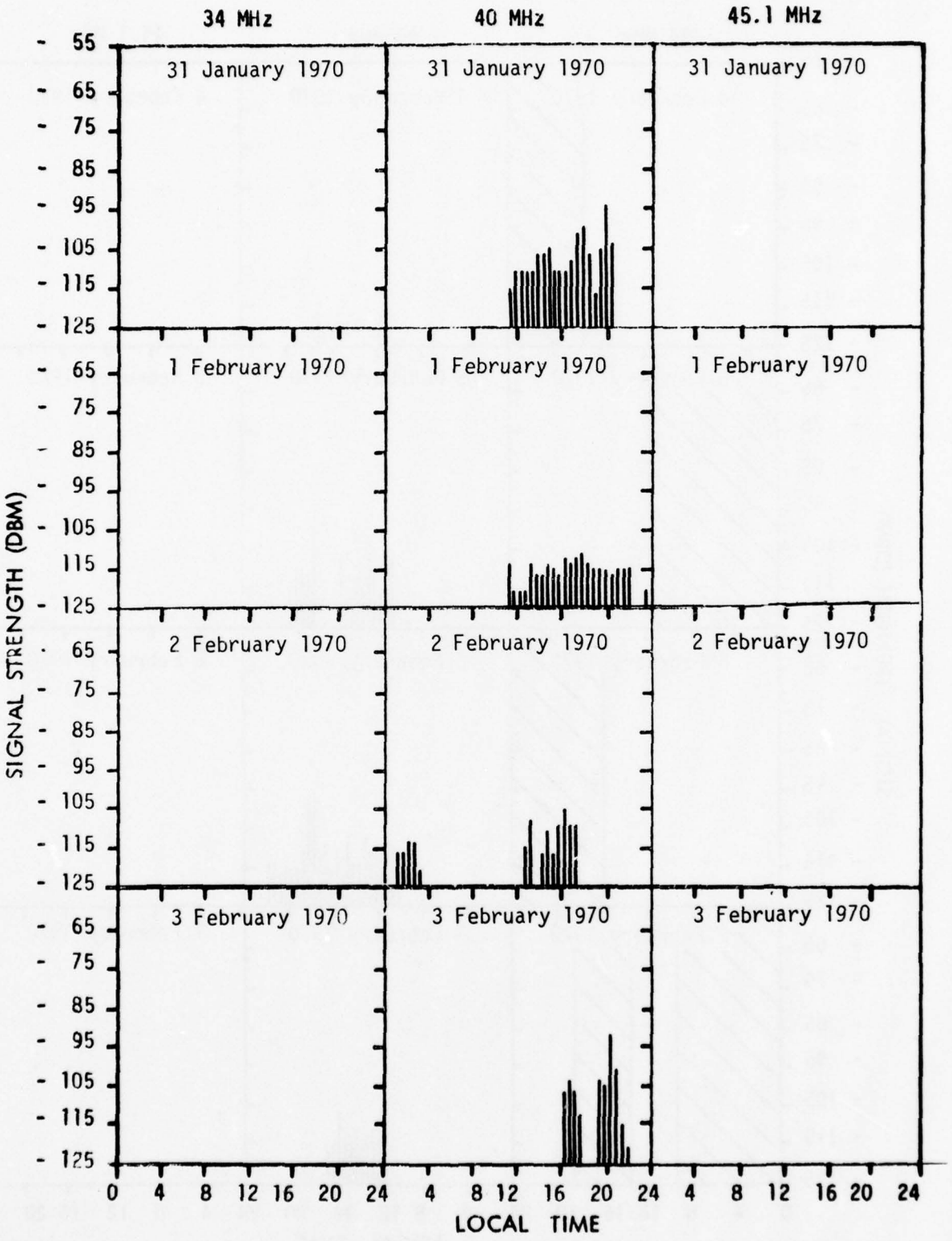

Fig. 70 – 34, 40 and 45.1 MHz Reception at Roma

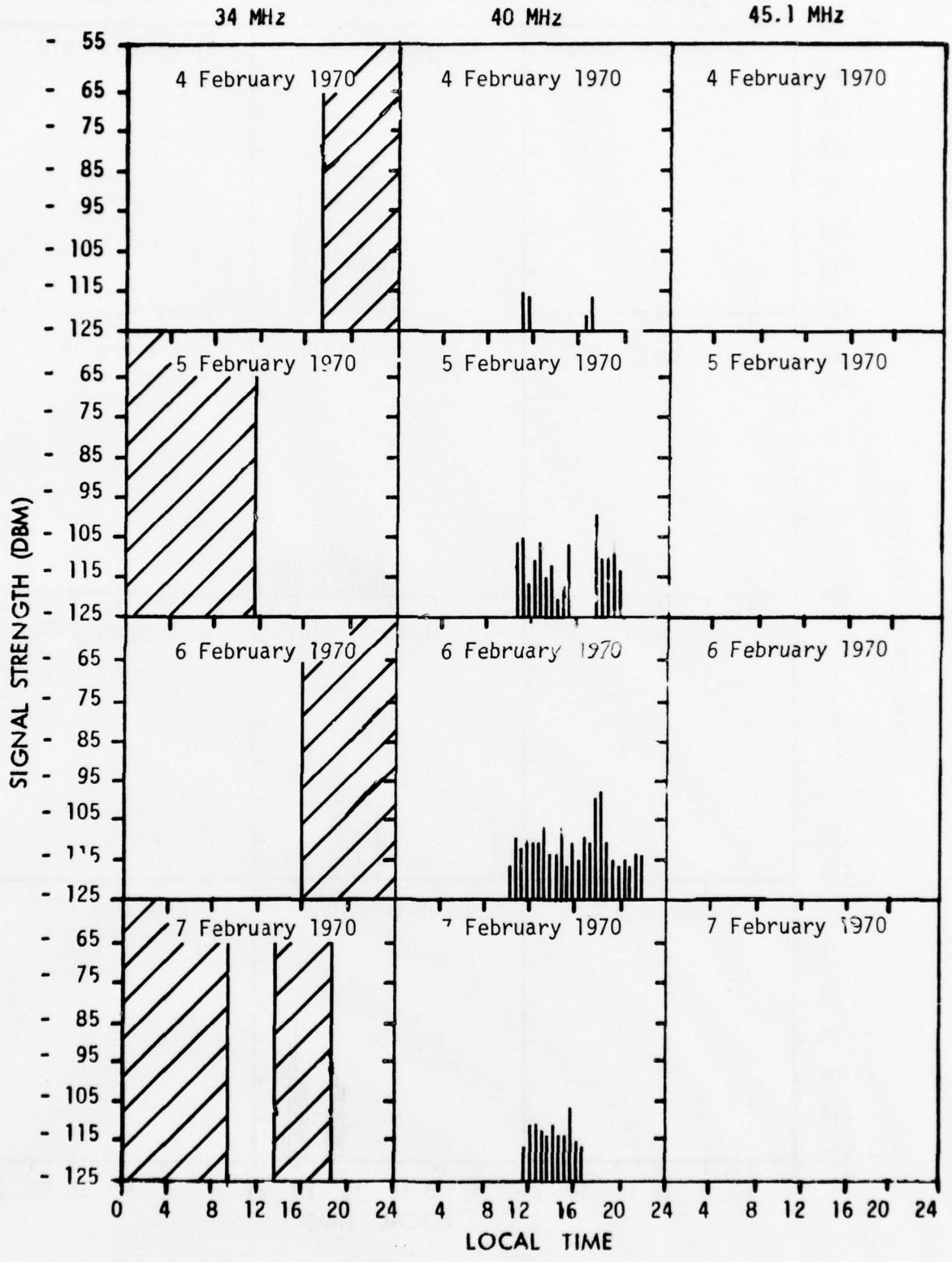

Fig. 71 – 34, 40 and 45.1 MHz Reception at Roma

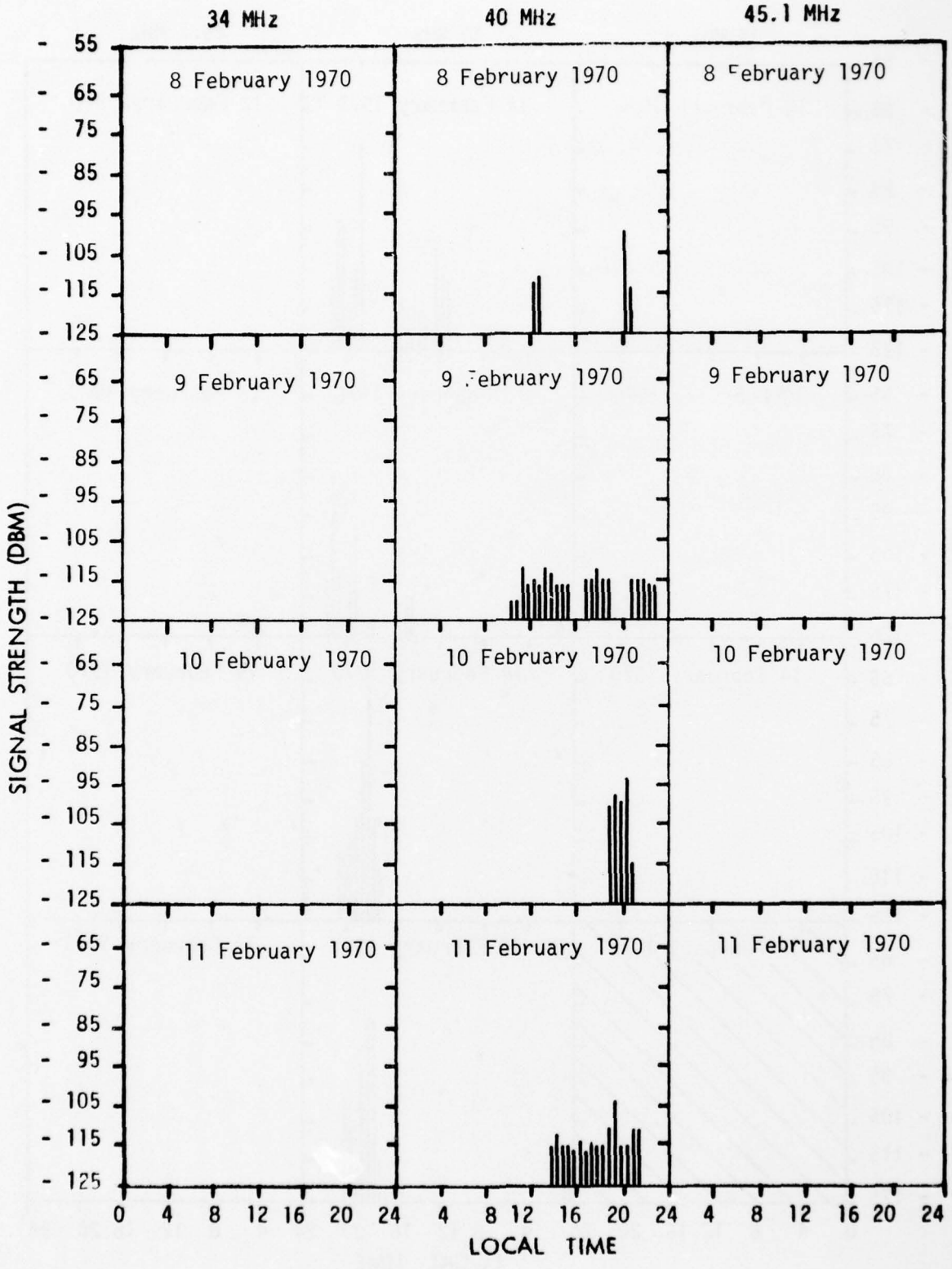

Fig. 72 – 34, 40 and 45.1 MHz Reception at Roma

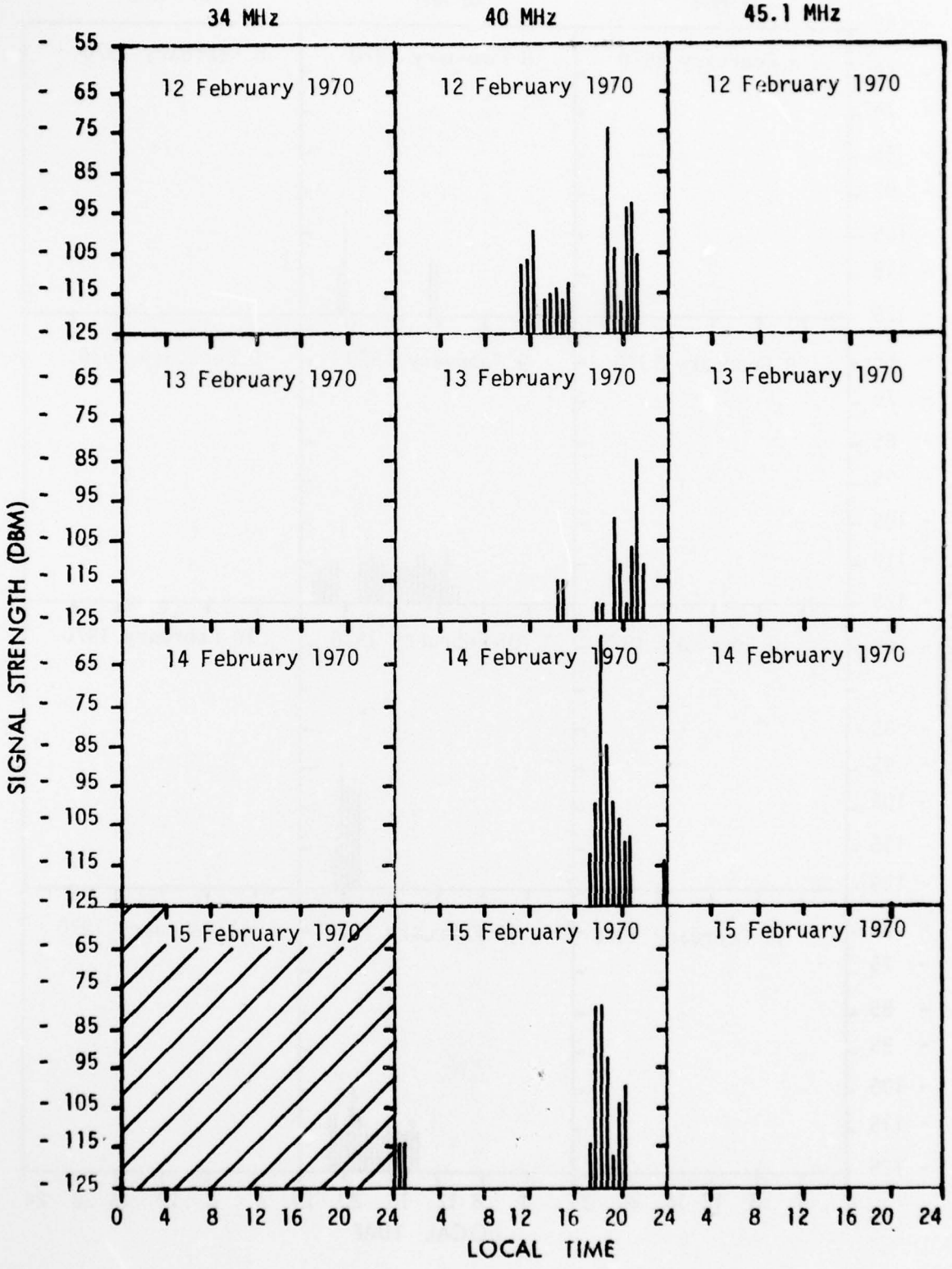

Fig. 73 – 34, 40 and 45.1 MHz Reception at Roma

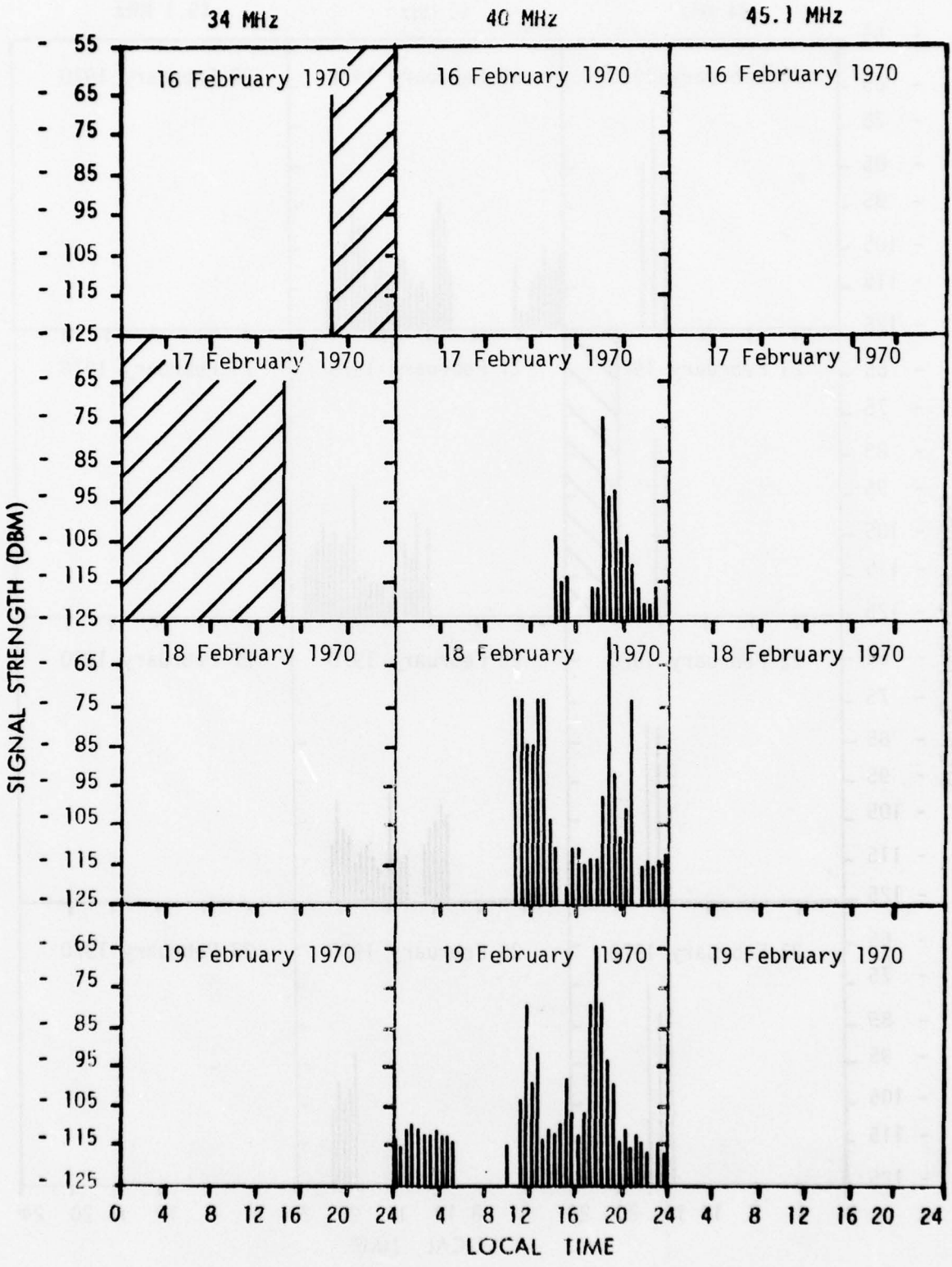

Fig. 74 – 34, 40 and 45.1 MHz Reception at Roma

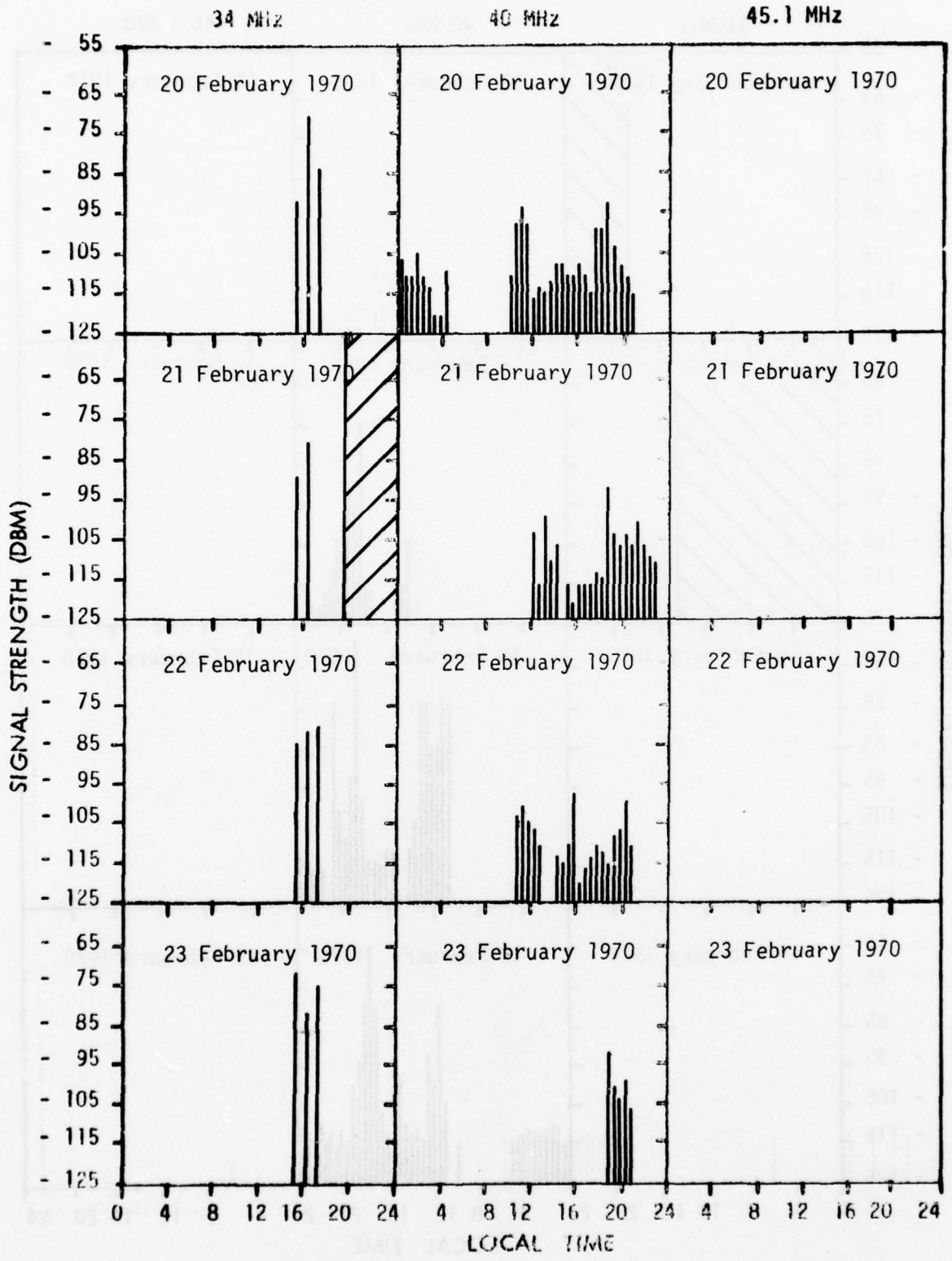

Fig. 75 – 34, 40 and 45.1 MHz Reception at Roma

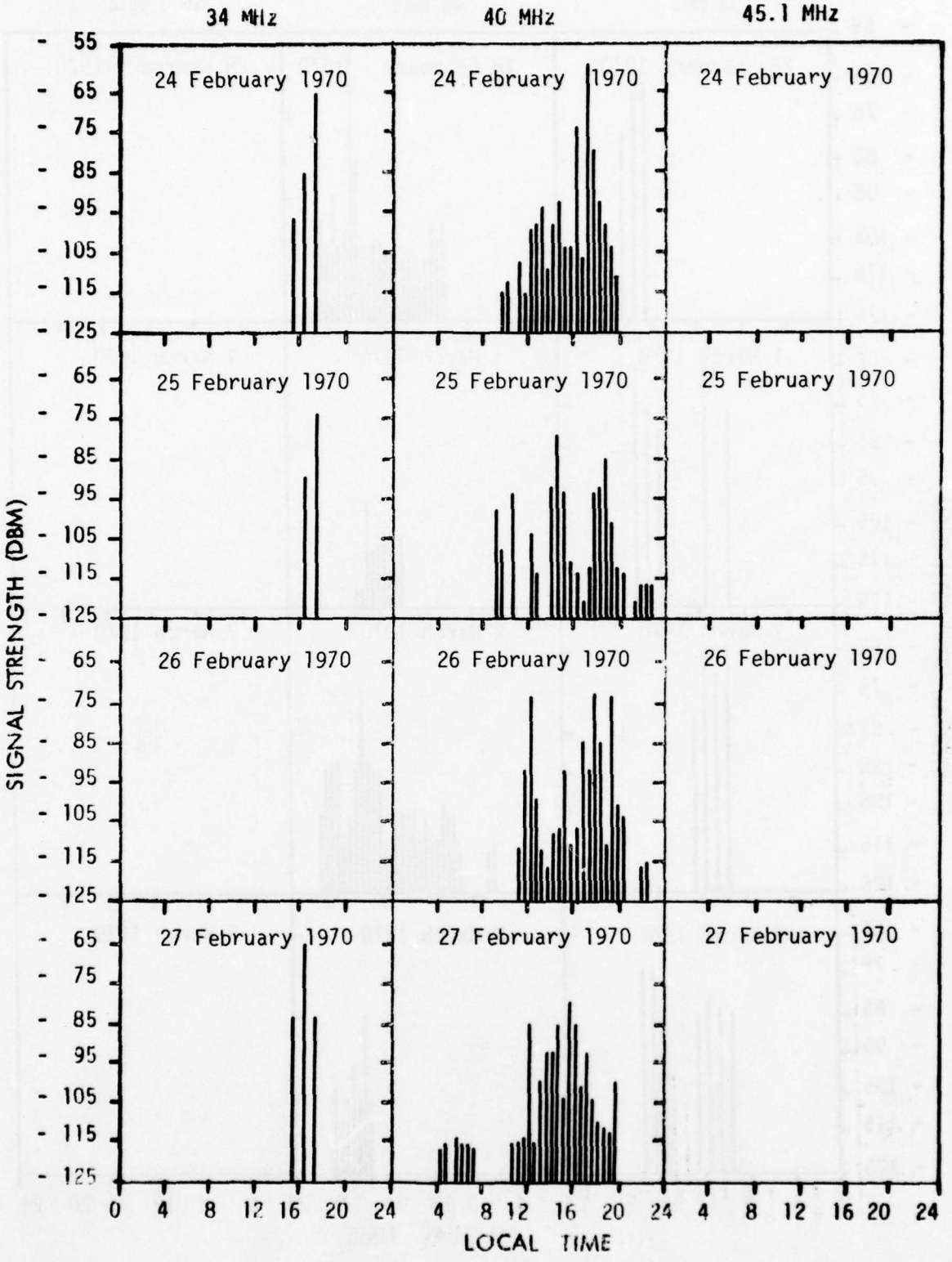

Fig. 76 – 34, 40 and 45.1 MHz Reception at Roma

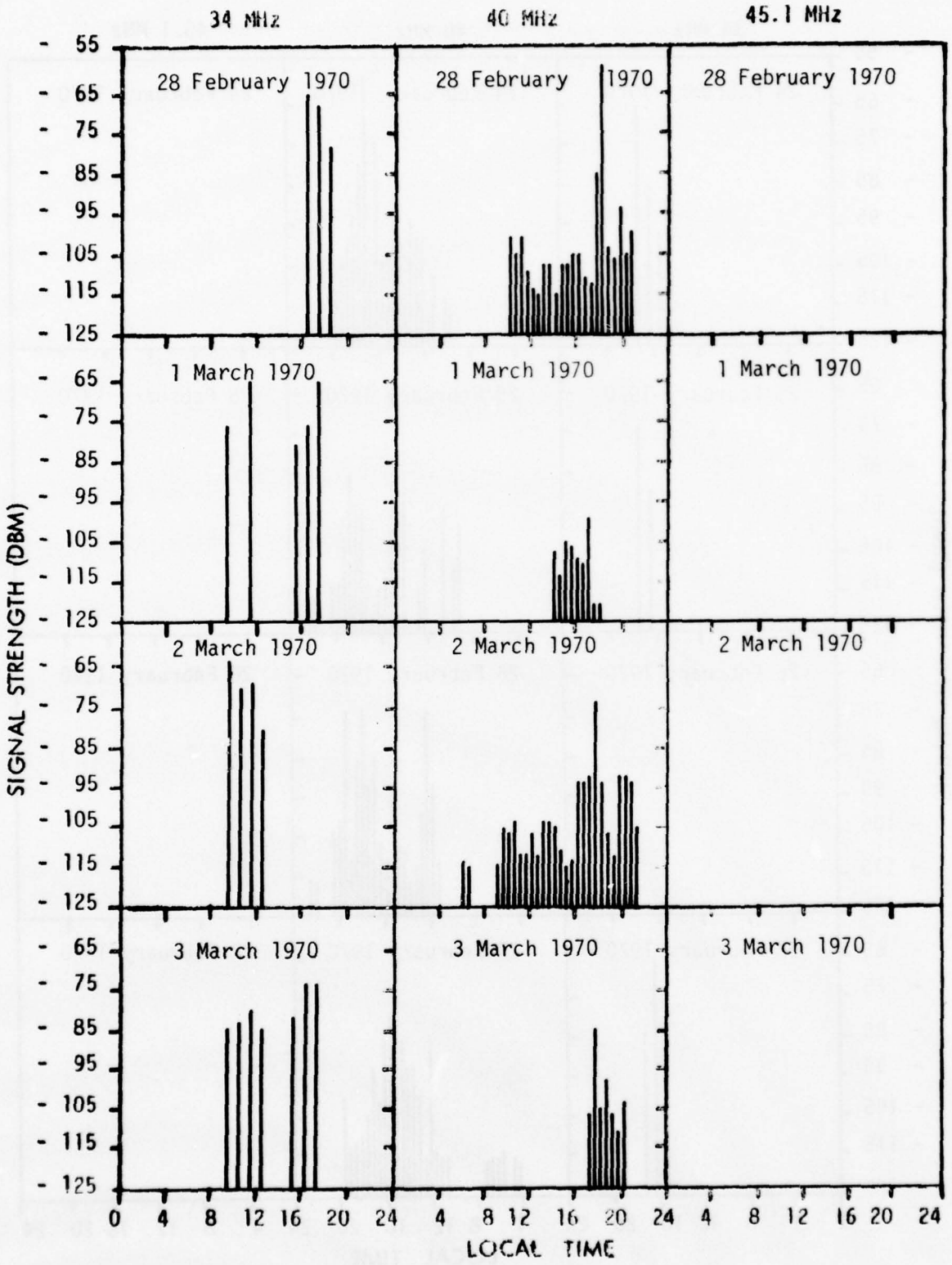

Fig. 77 – 34, 40 and 45.1 MHz Reception at Roma

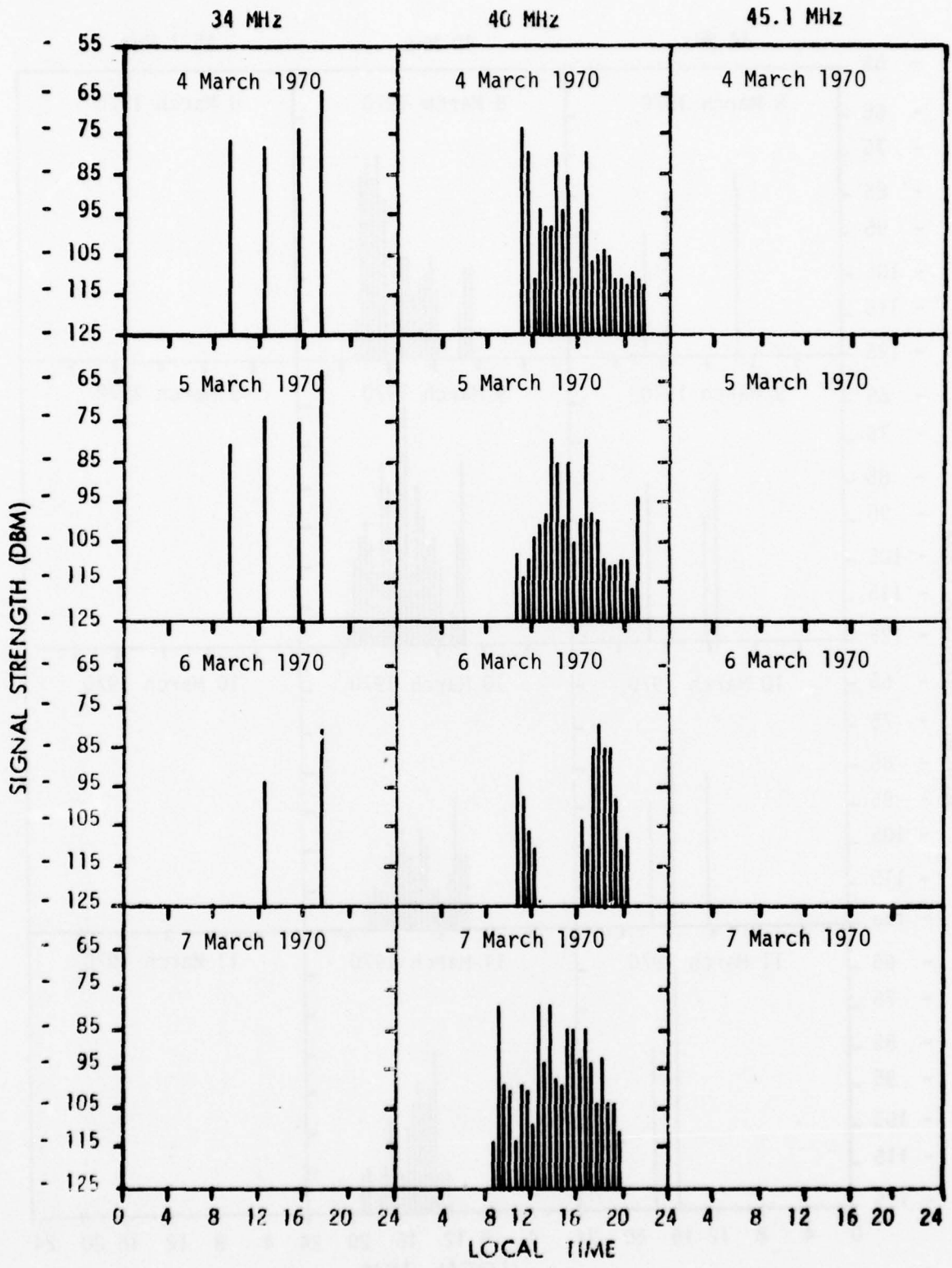

Fig. 78 – 34, 40 and 45.1 MHz Reception at Roma

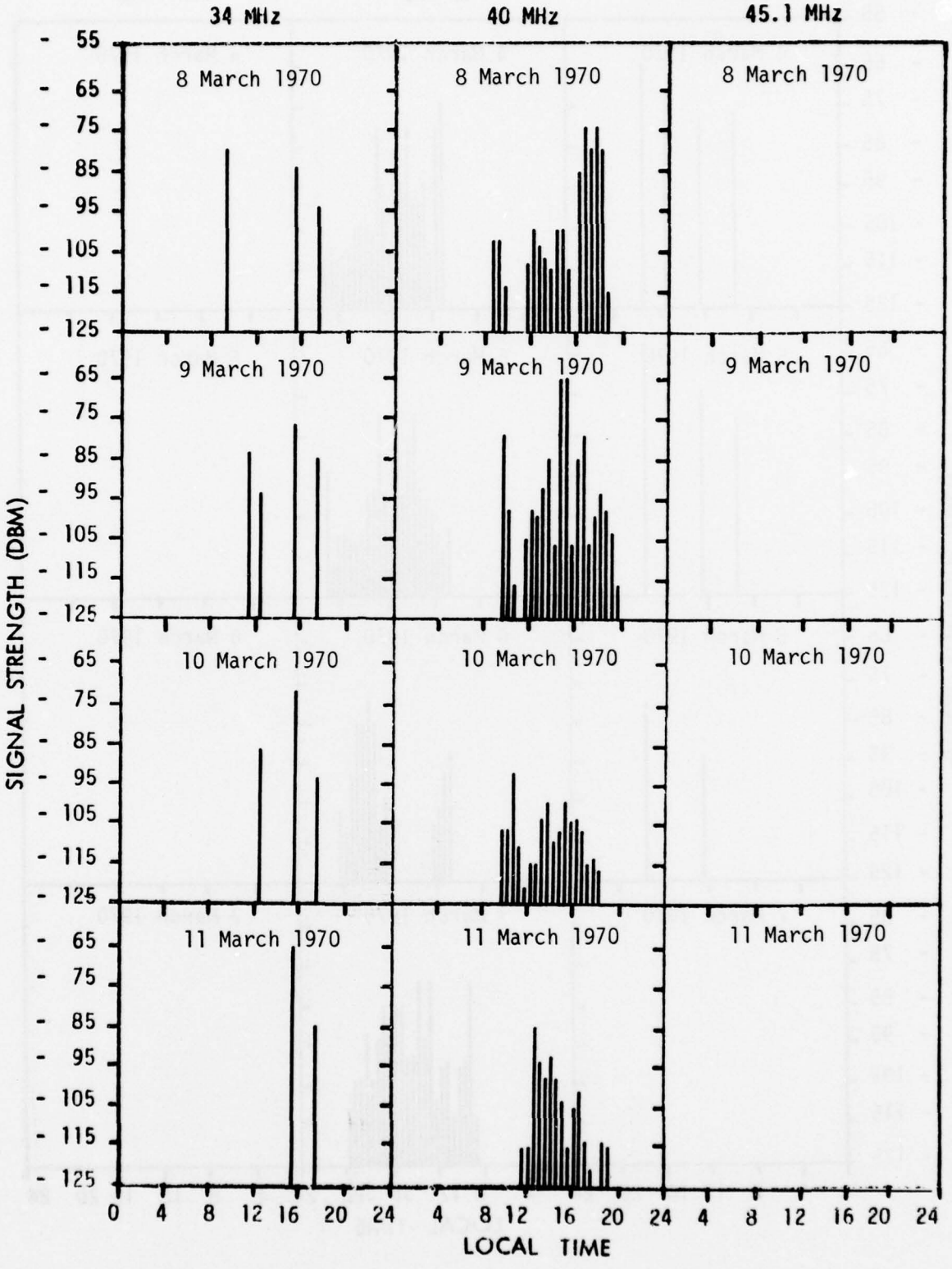

Fig. : 79 – 34, 40 and 45.1 MHz Reception at Roma

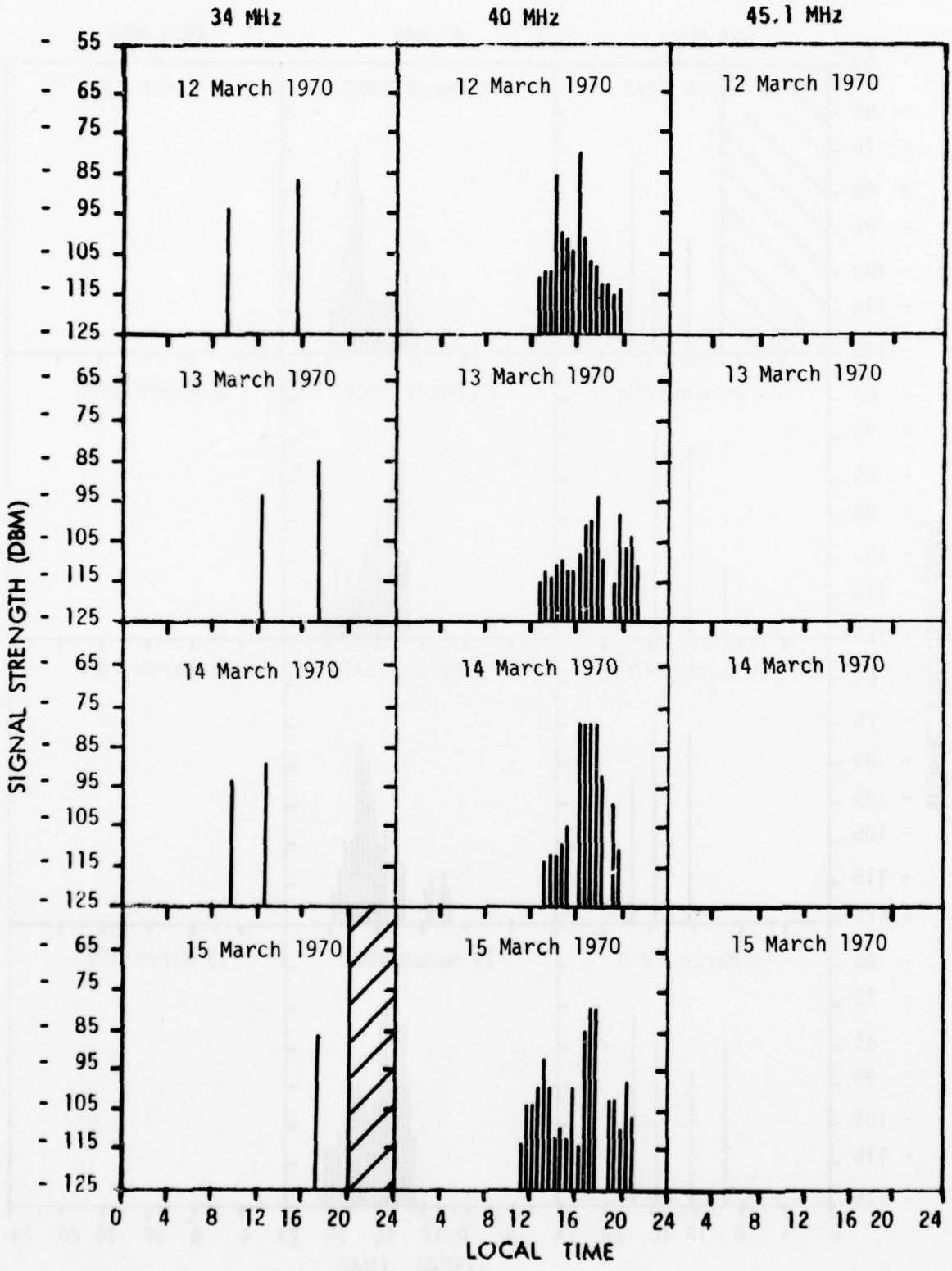

Fig. 80 – 34, 40 and 45.1 MHz Reception at Roma

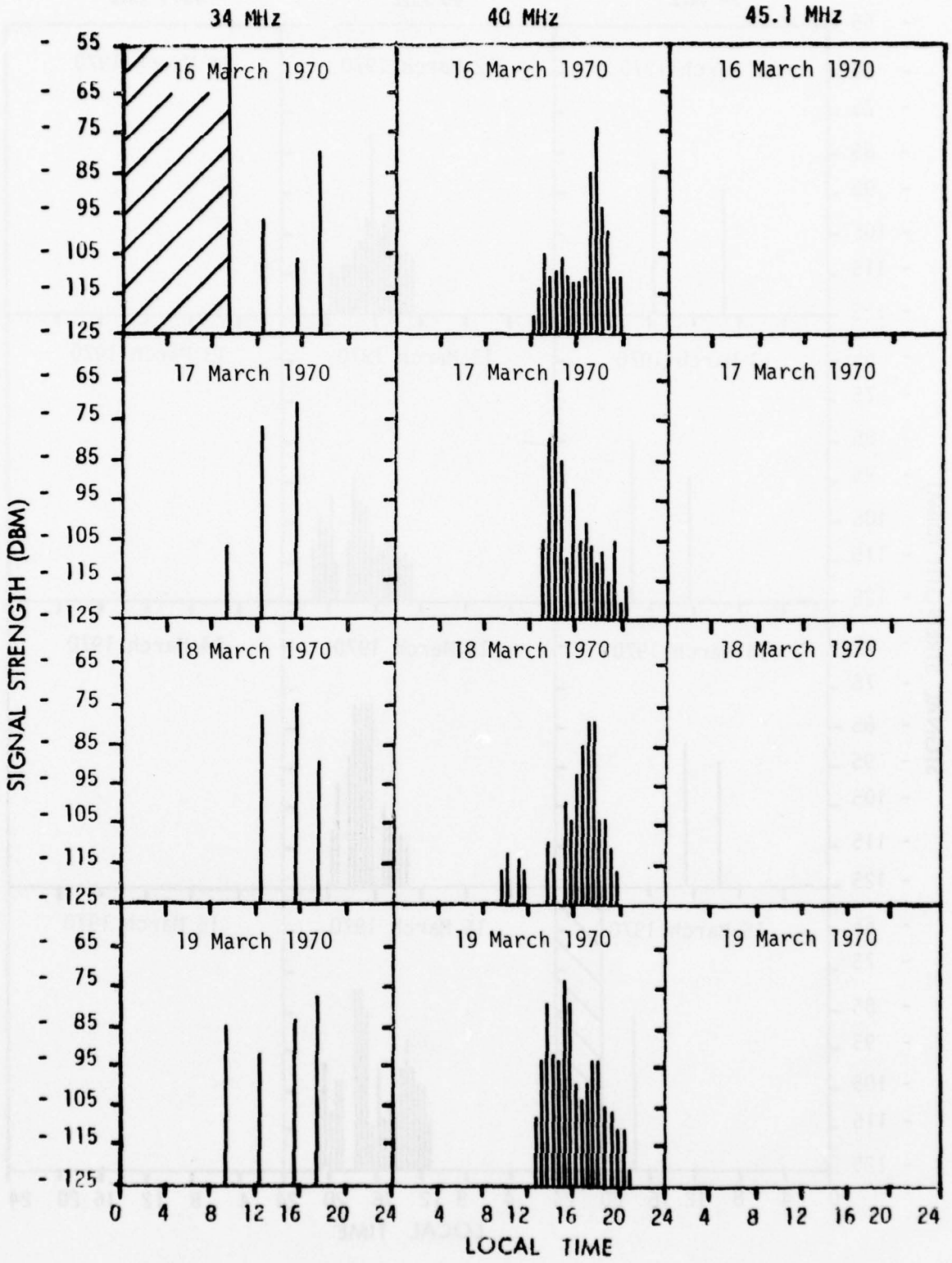

Fig. 81 – 34, 40 and 45.1 MHz Reception at Roma

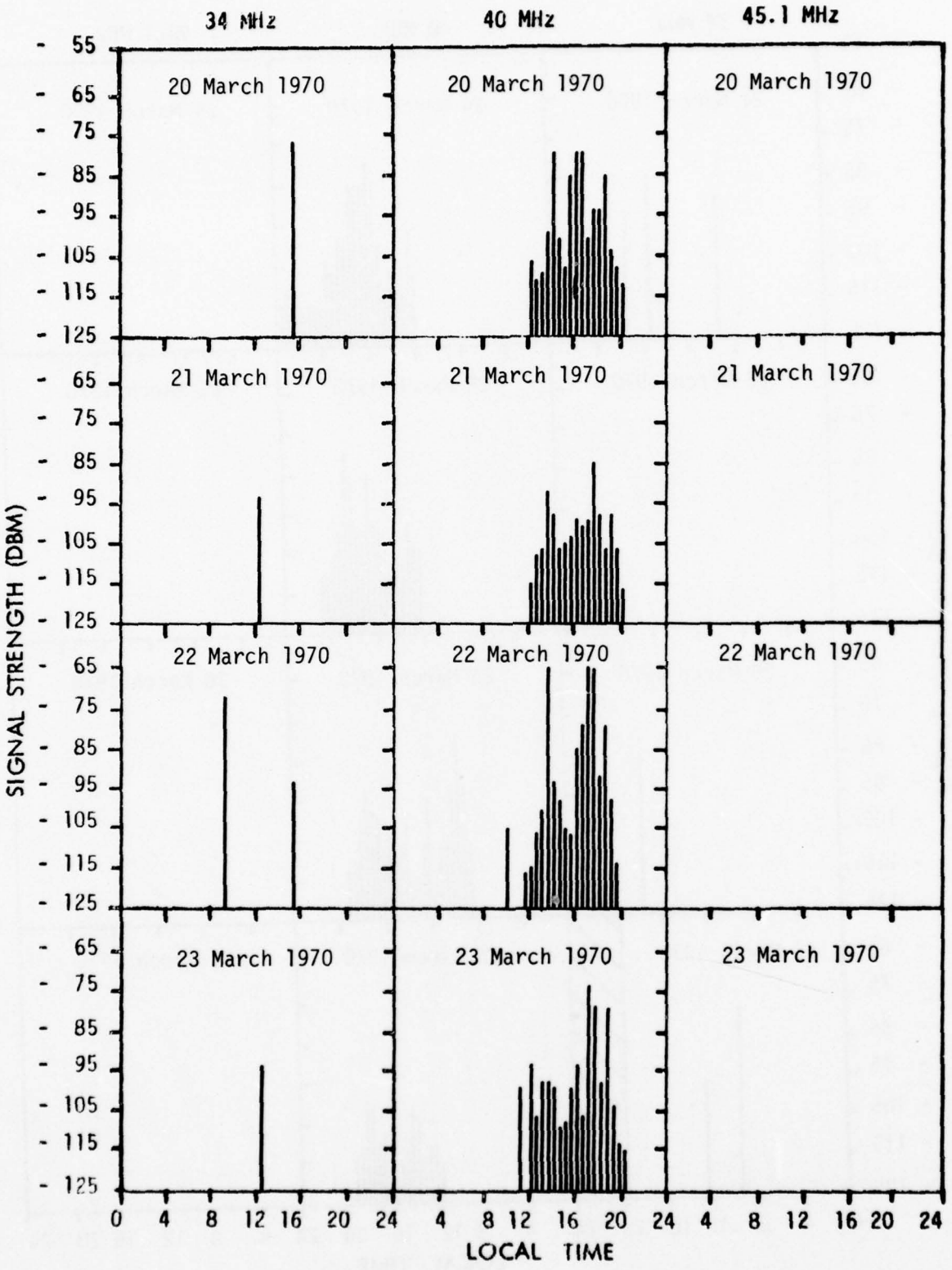

Fig. 82 – 34, 40 and 45.1 MHz Reception at Rome

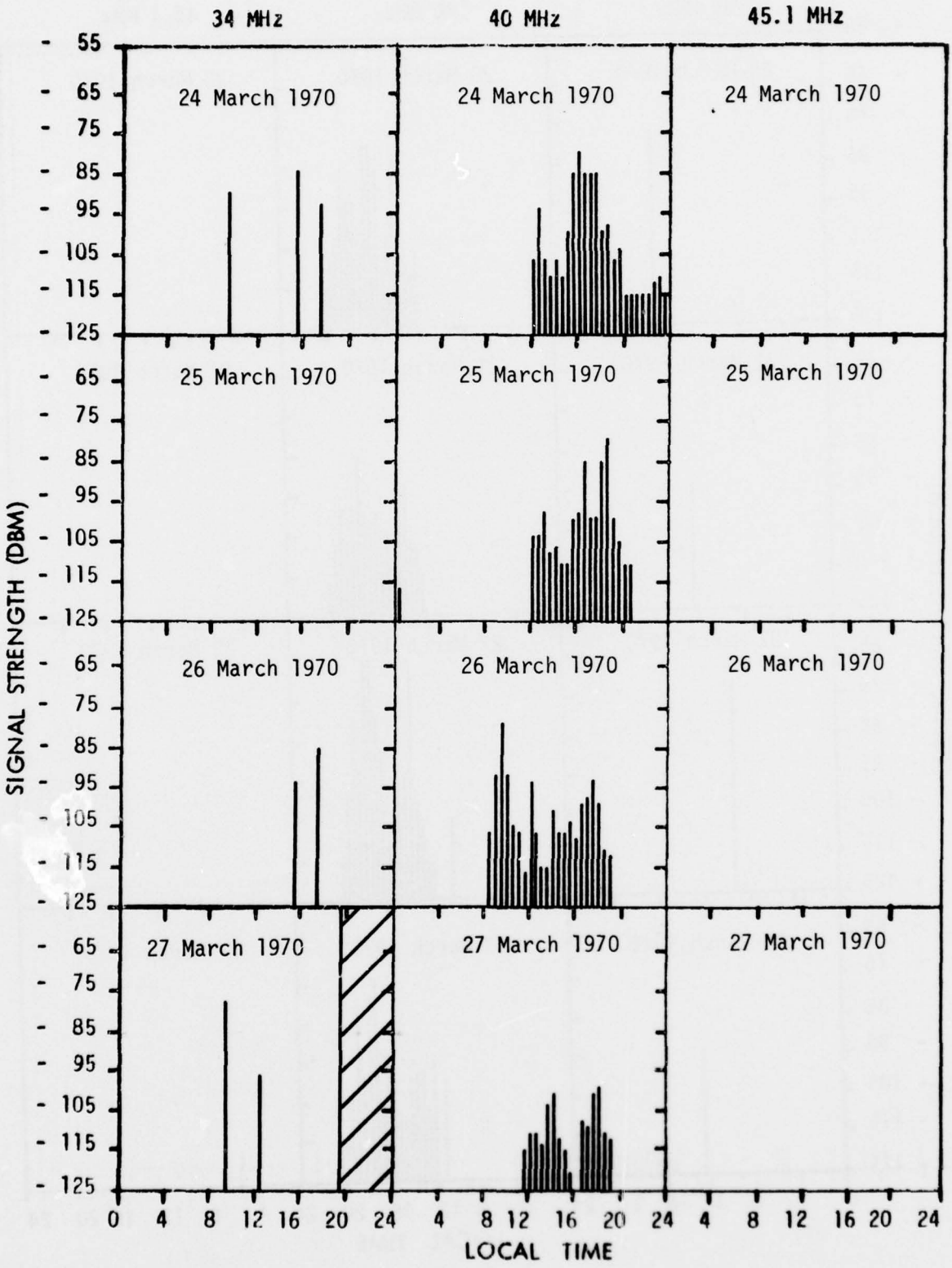

Fig. 83 – 34, 40 and 45.1 MHz Reception at Roma

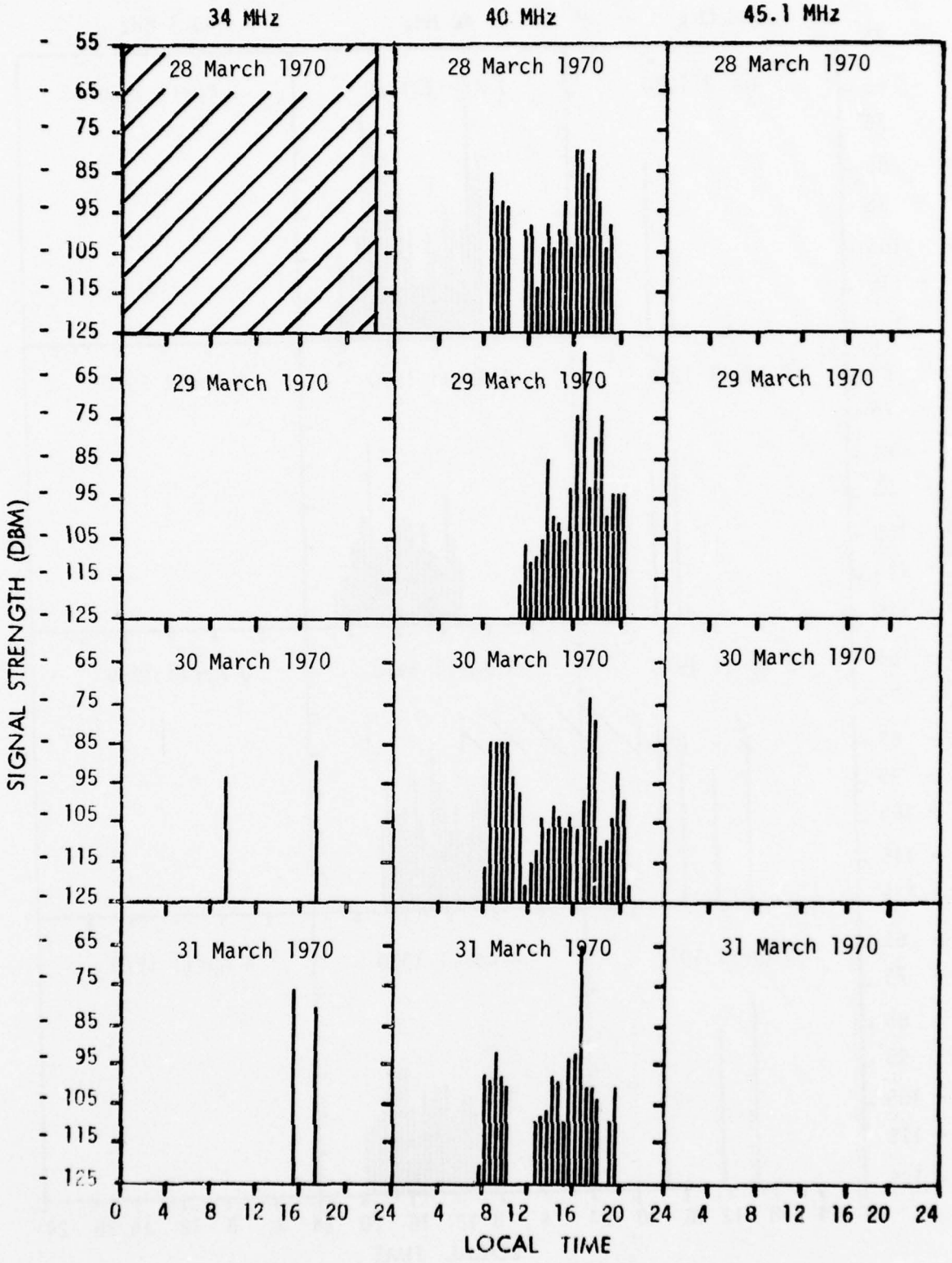

Fig. 84 – 34, 40 and 45.1 MHz Reception at Roma

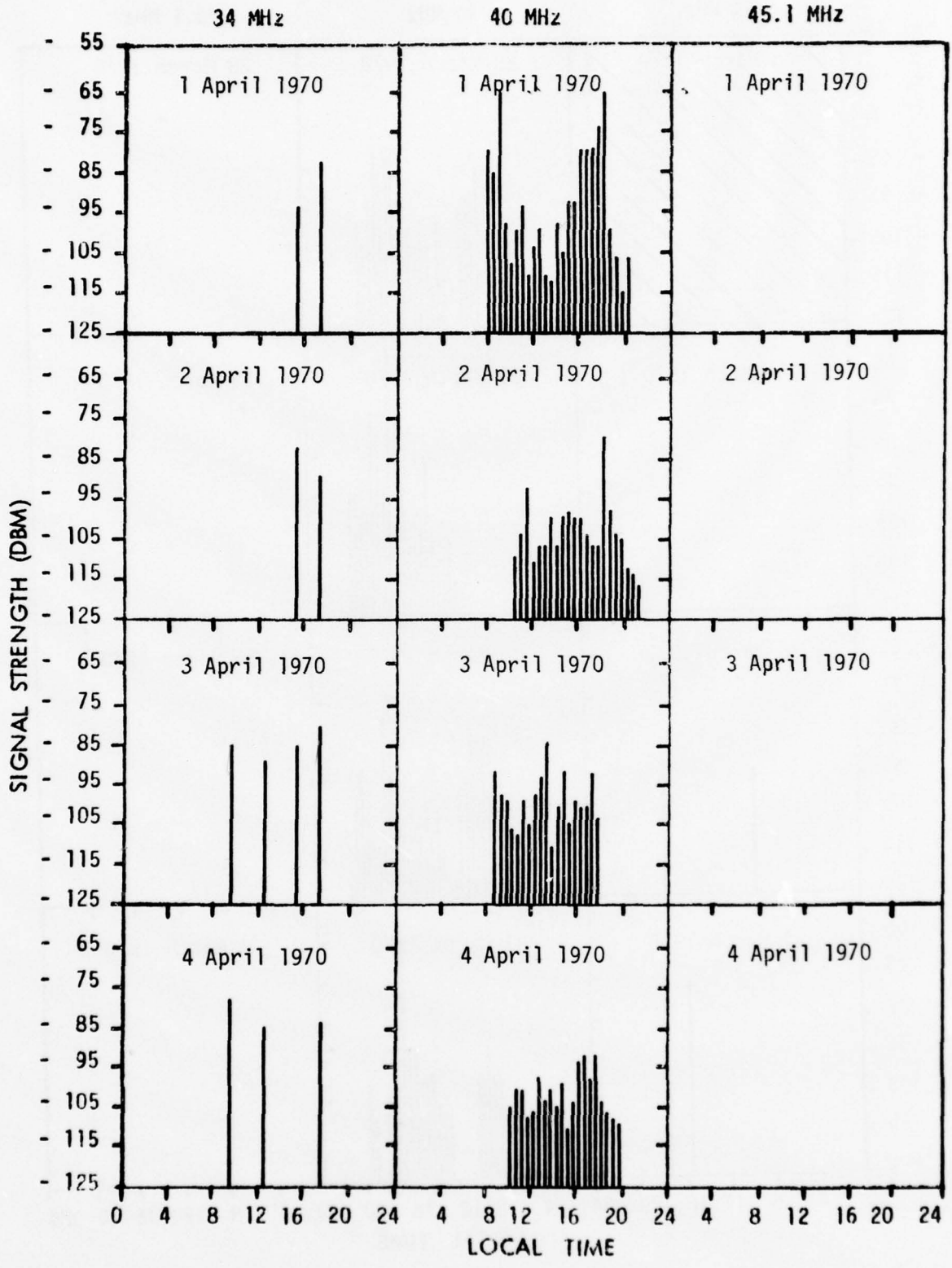

Fig. 85 – 34, 40 and 45.1 MHz Reception at Roma

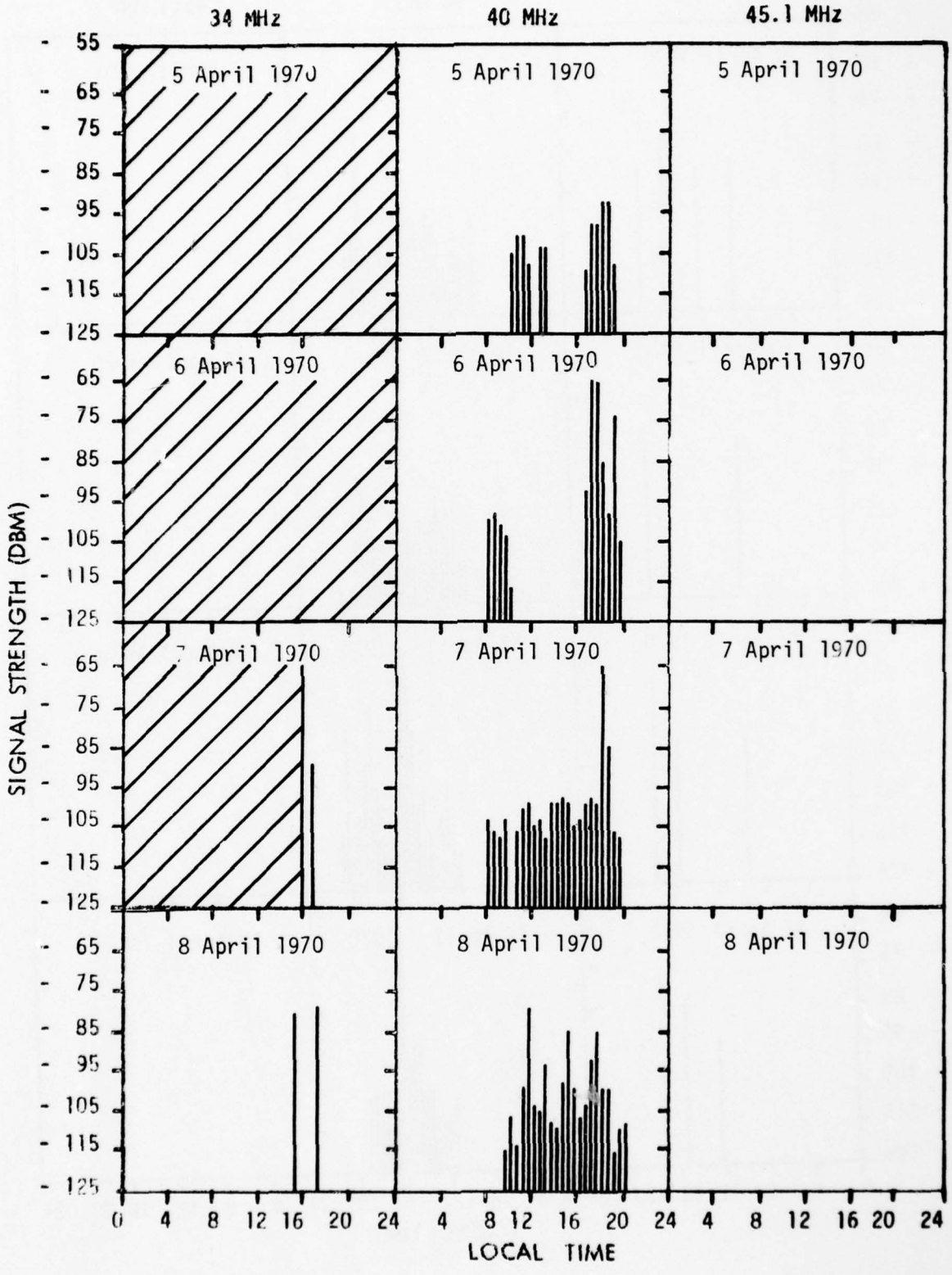

Fig. 86 – 34, 40 and 45.1 MHz Reception at Roma

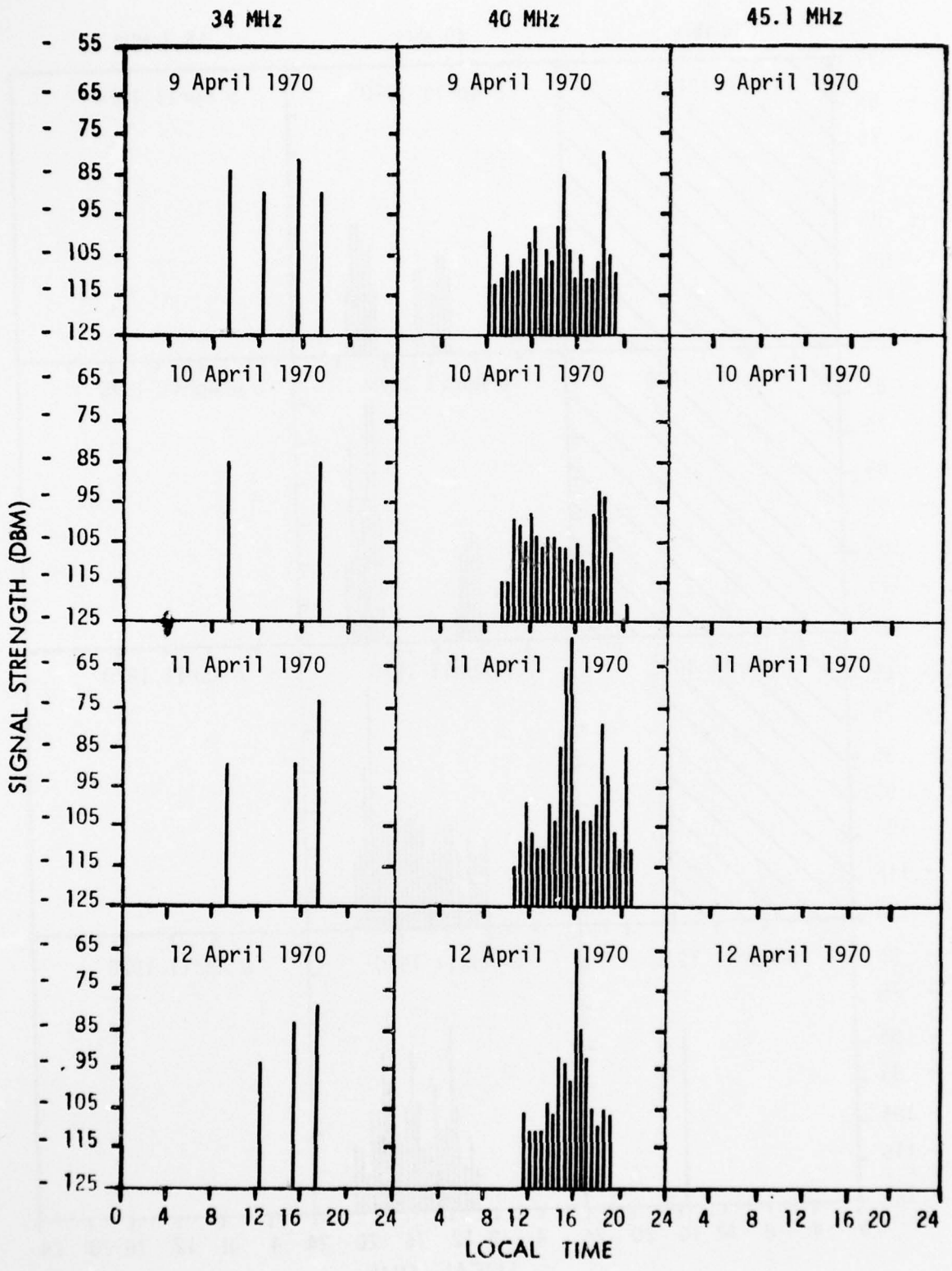

Fig. 87 – 34, 40 and 45.1 MHz Reception at Roma

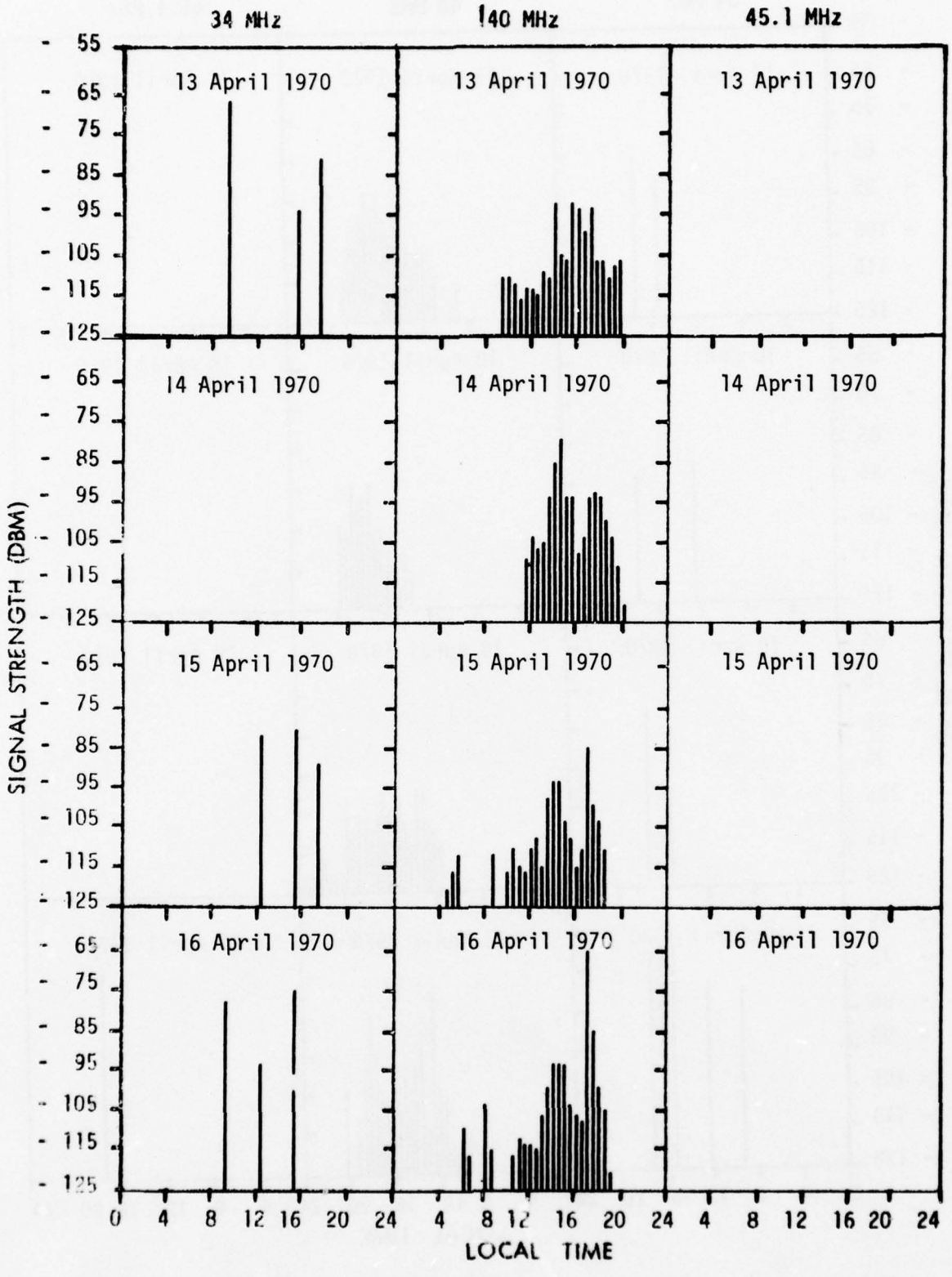

Fig. 88 – 34, 40 and 45.1 MHz Reception at Roma

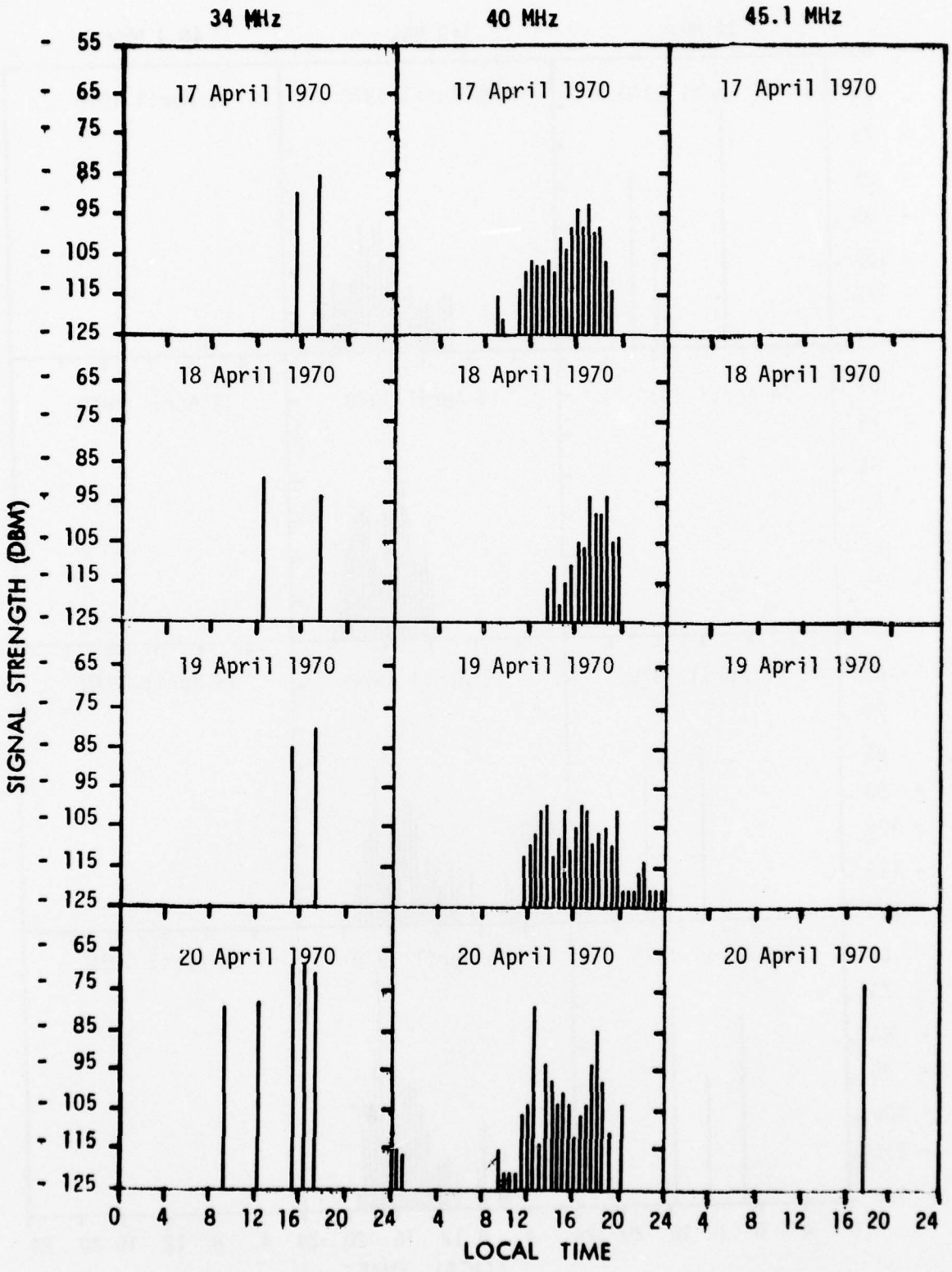

Fig. 89 – 34, 40 and 45.1 MHz Reception at Roma

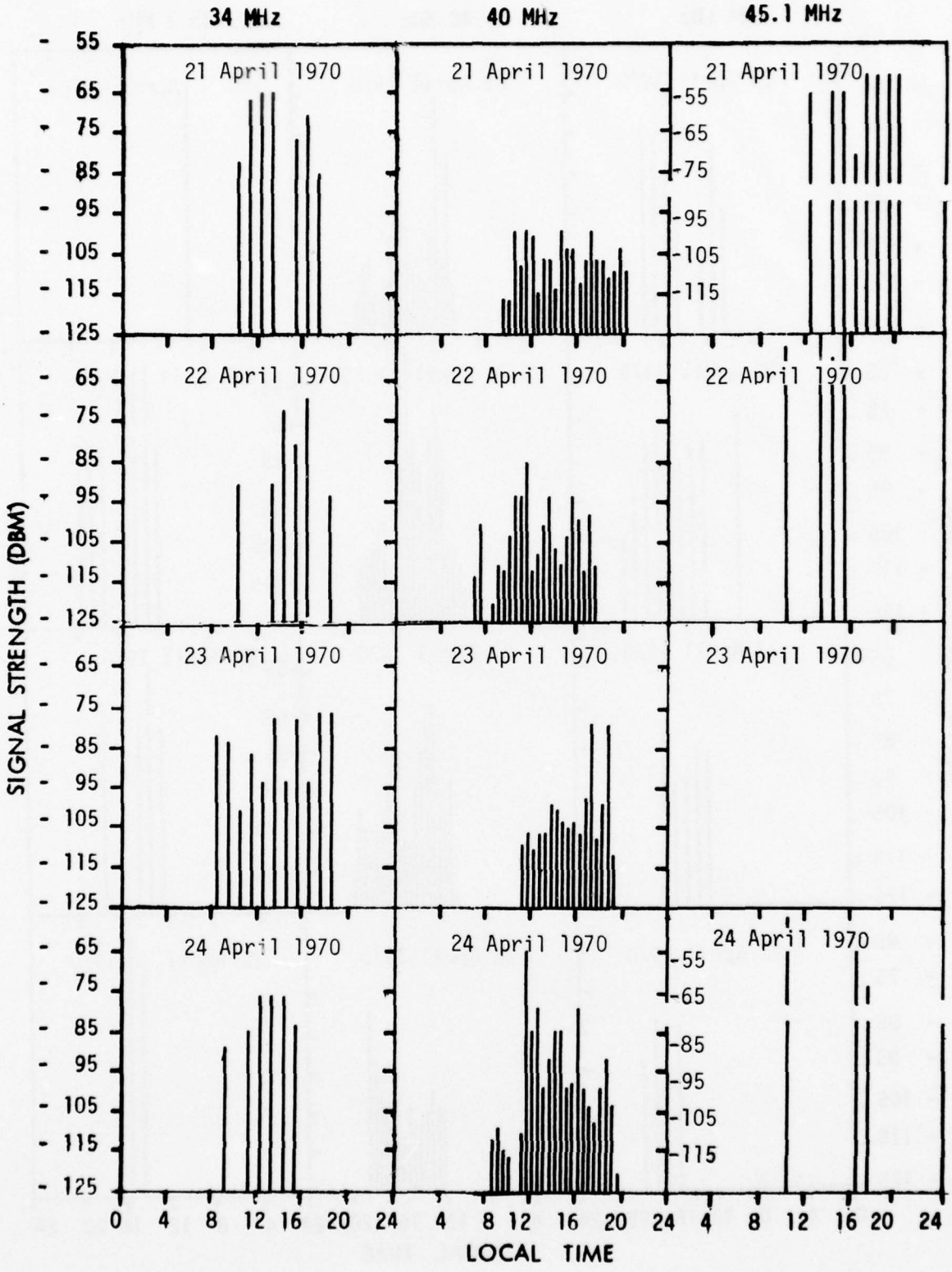

Fig. 90 – 34, 40 and 45.1 MHz Reception at Roma

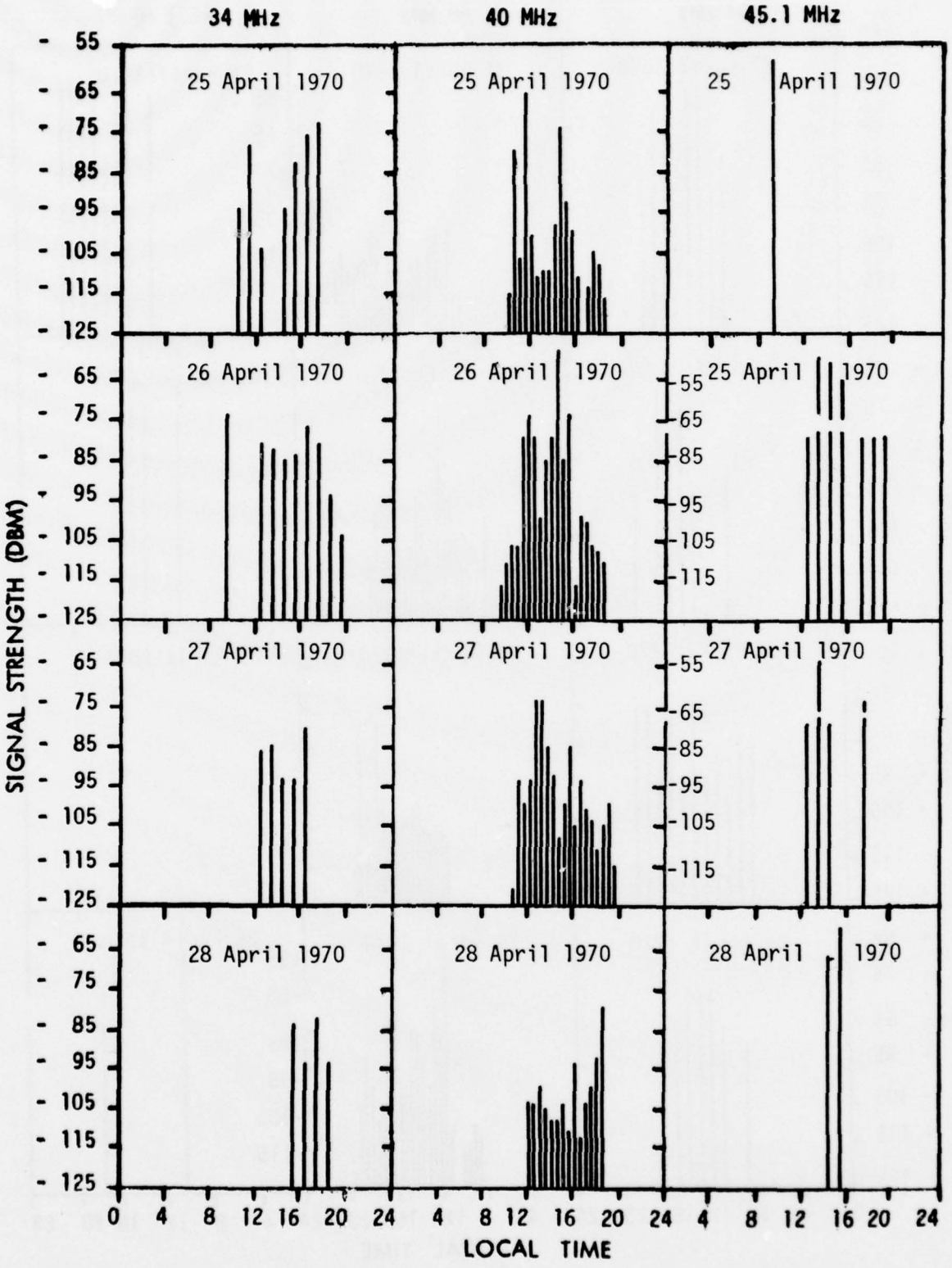

Fig. 91 – 34, 40 and 45.1 MHz Reception at Roma

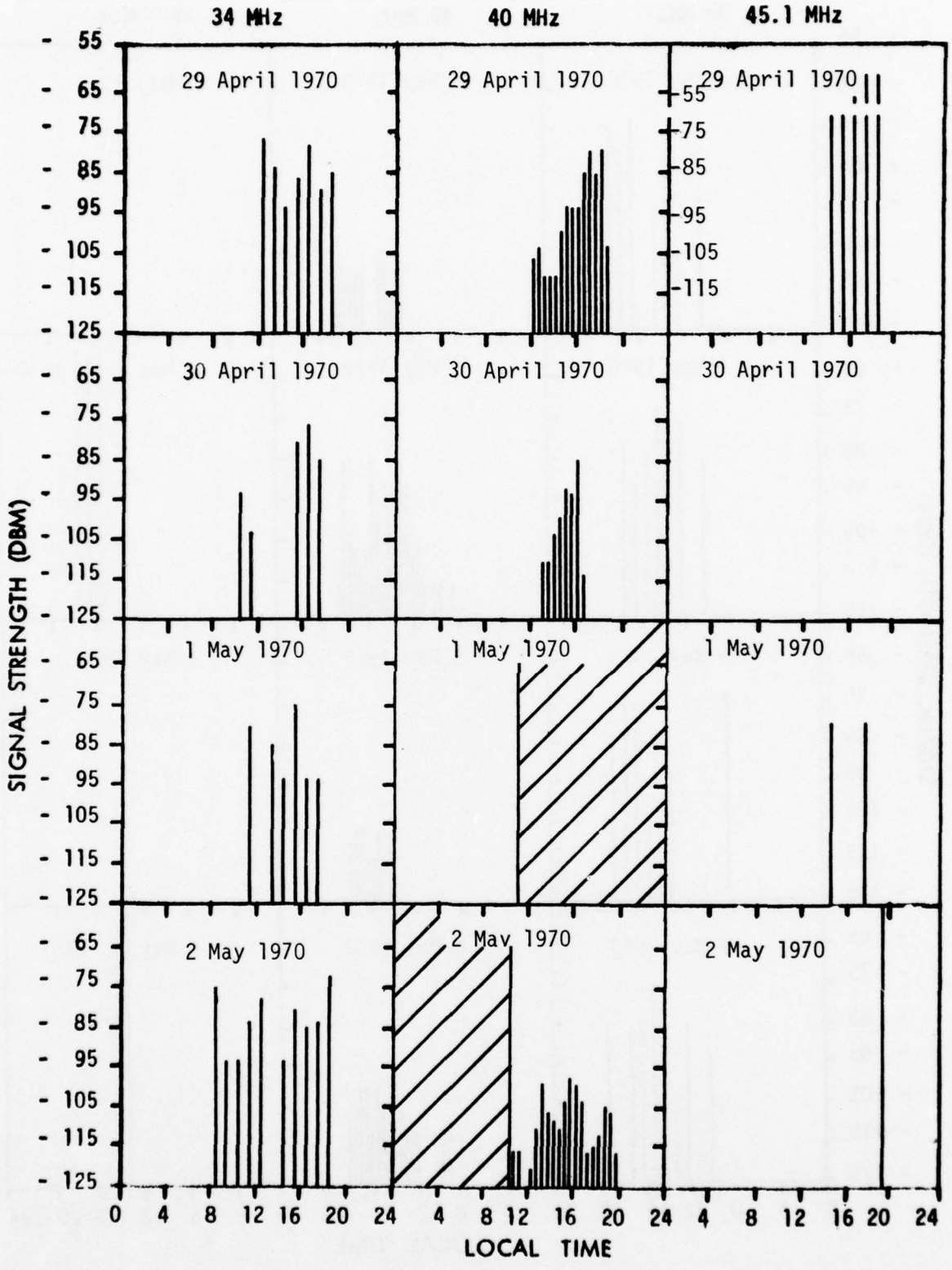

Fig. 92 – 34, 40 and 45.1 MHz Reception at Roma

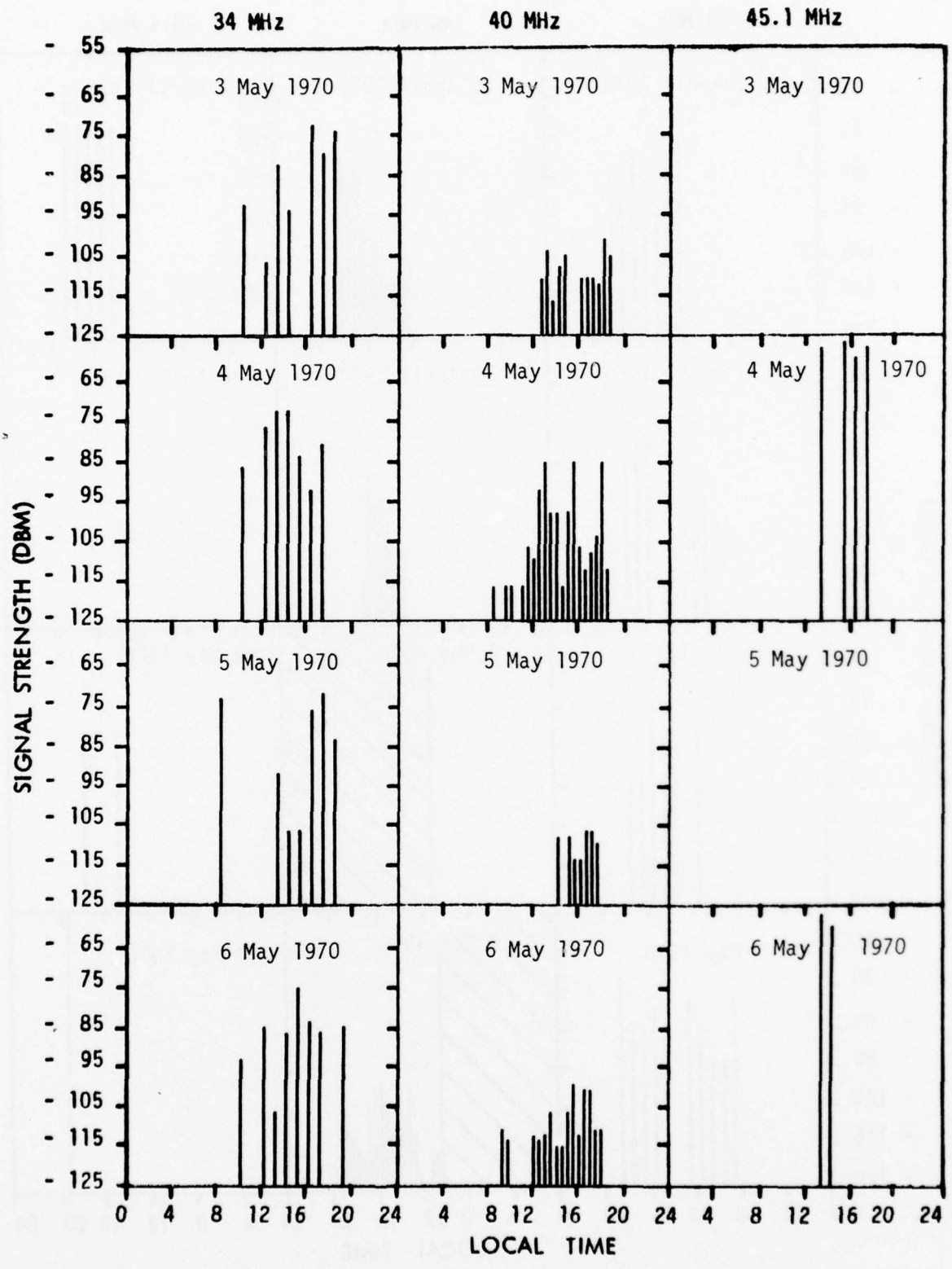

Fig. 93 – 34, 40 and 45.1 MHz Reception at Roma

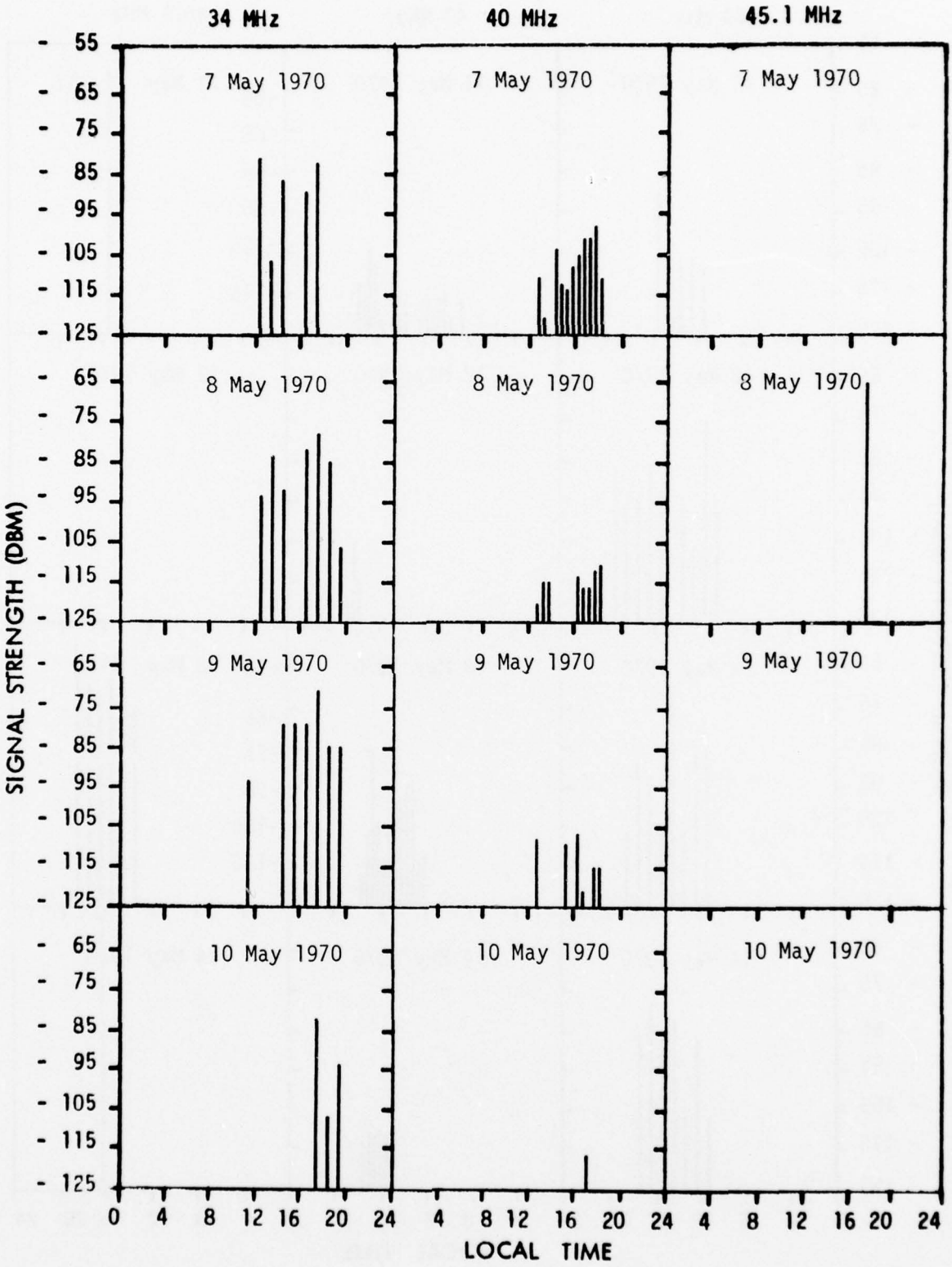

Fig. 94 – 34, 40 and 45.1 MHz Reception at Roma

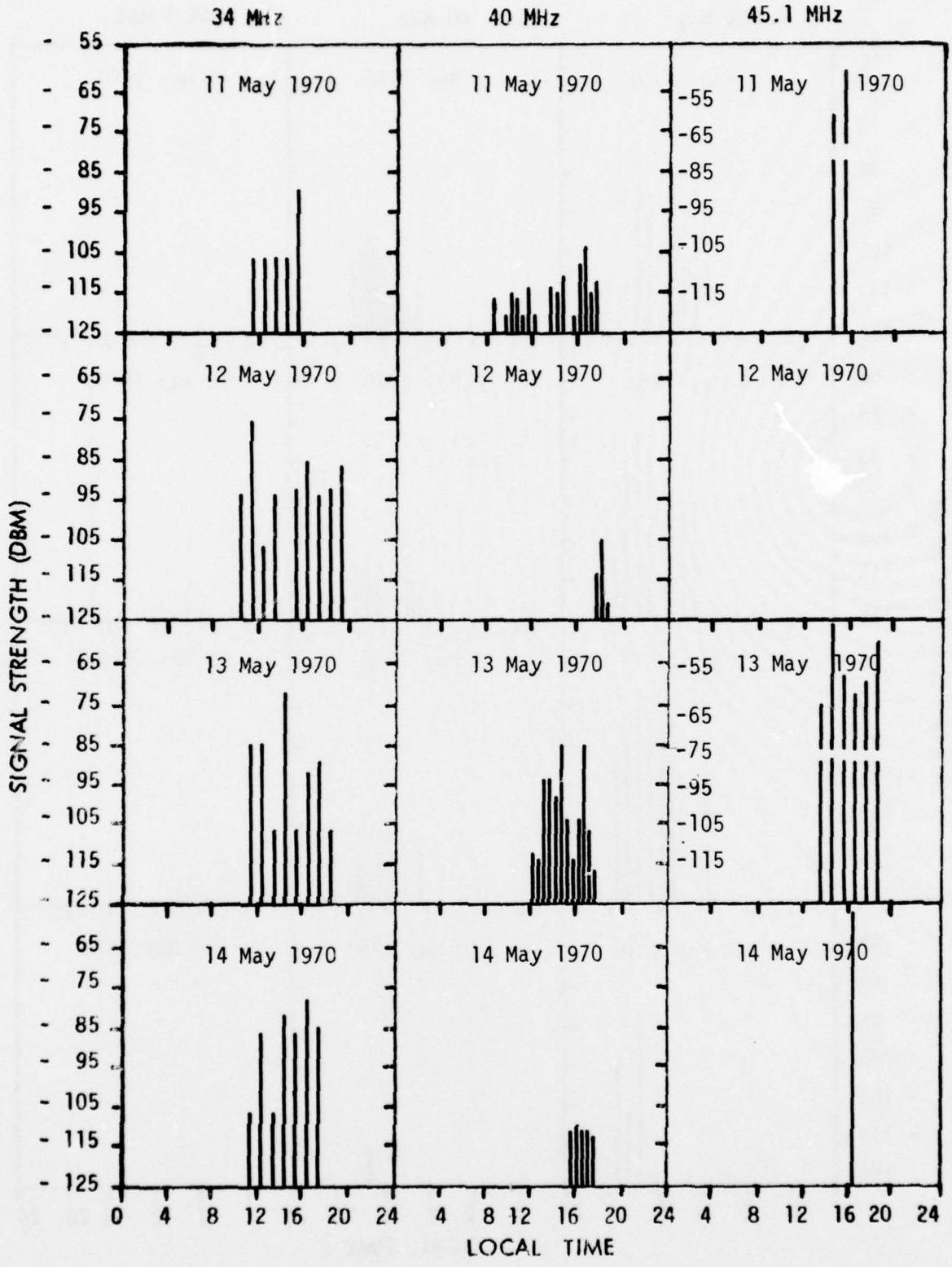

Fig. 95 – 34, 40 and 45.1 MHz Reception at Roma

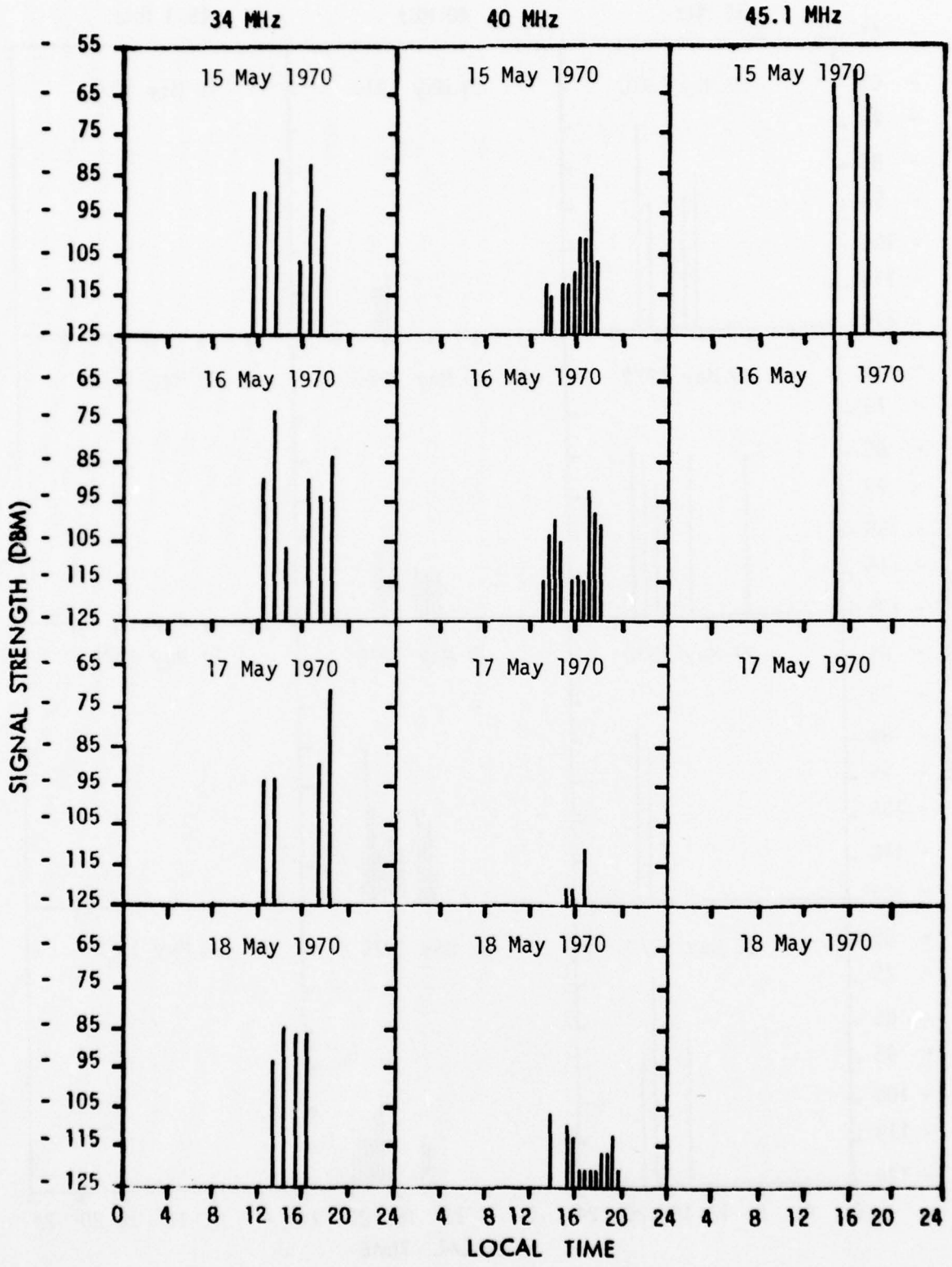

Fig. 96 – 34, 40 and 45.1 MHz Reception at Roma

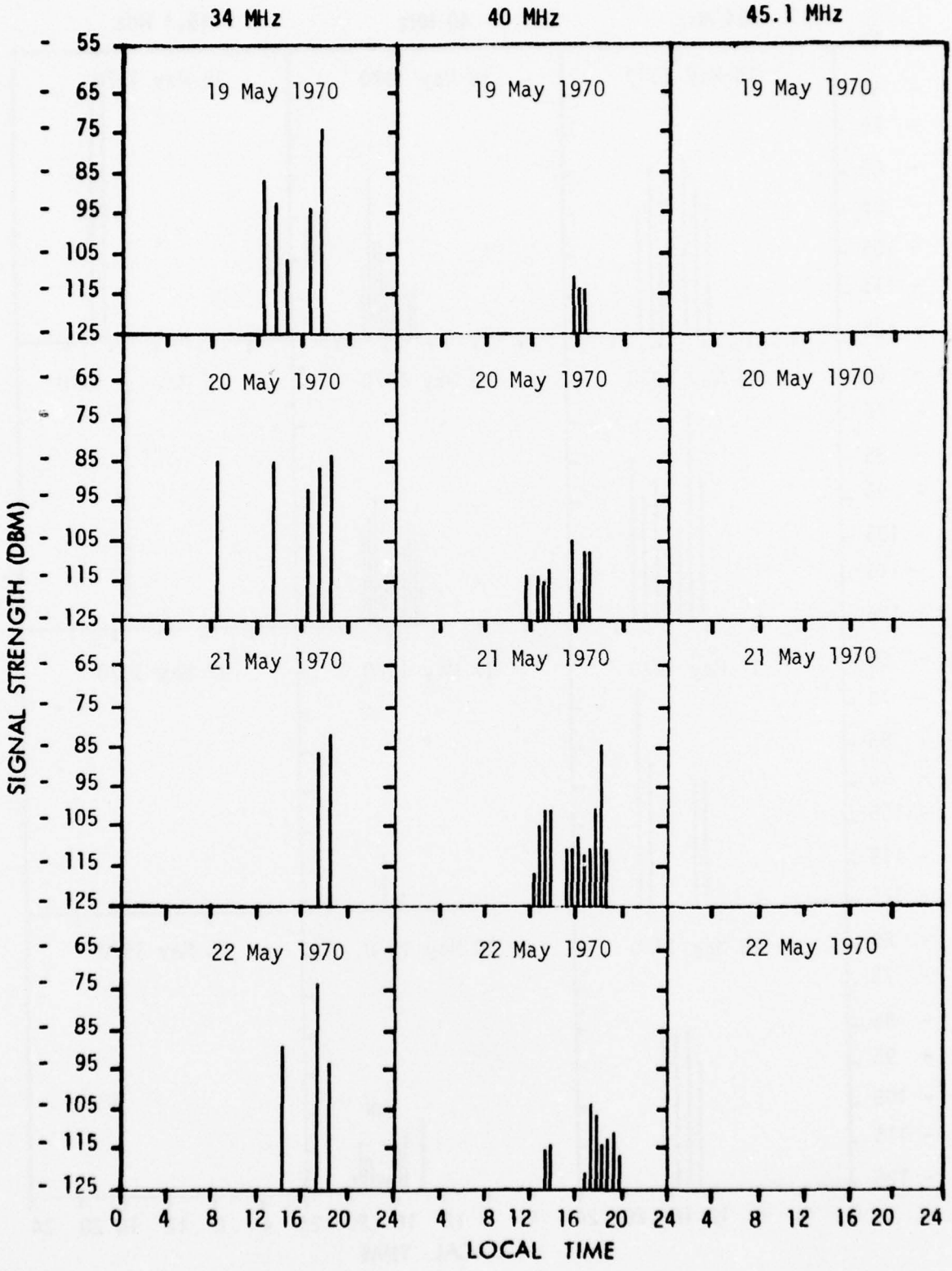

Fig. 97 – 34, 40 and 45.1 MHz Reception at Roma

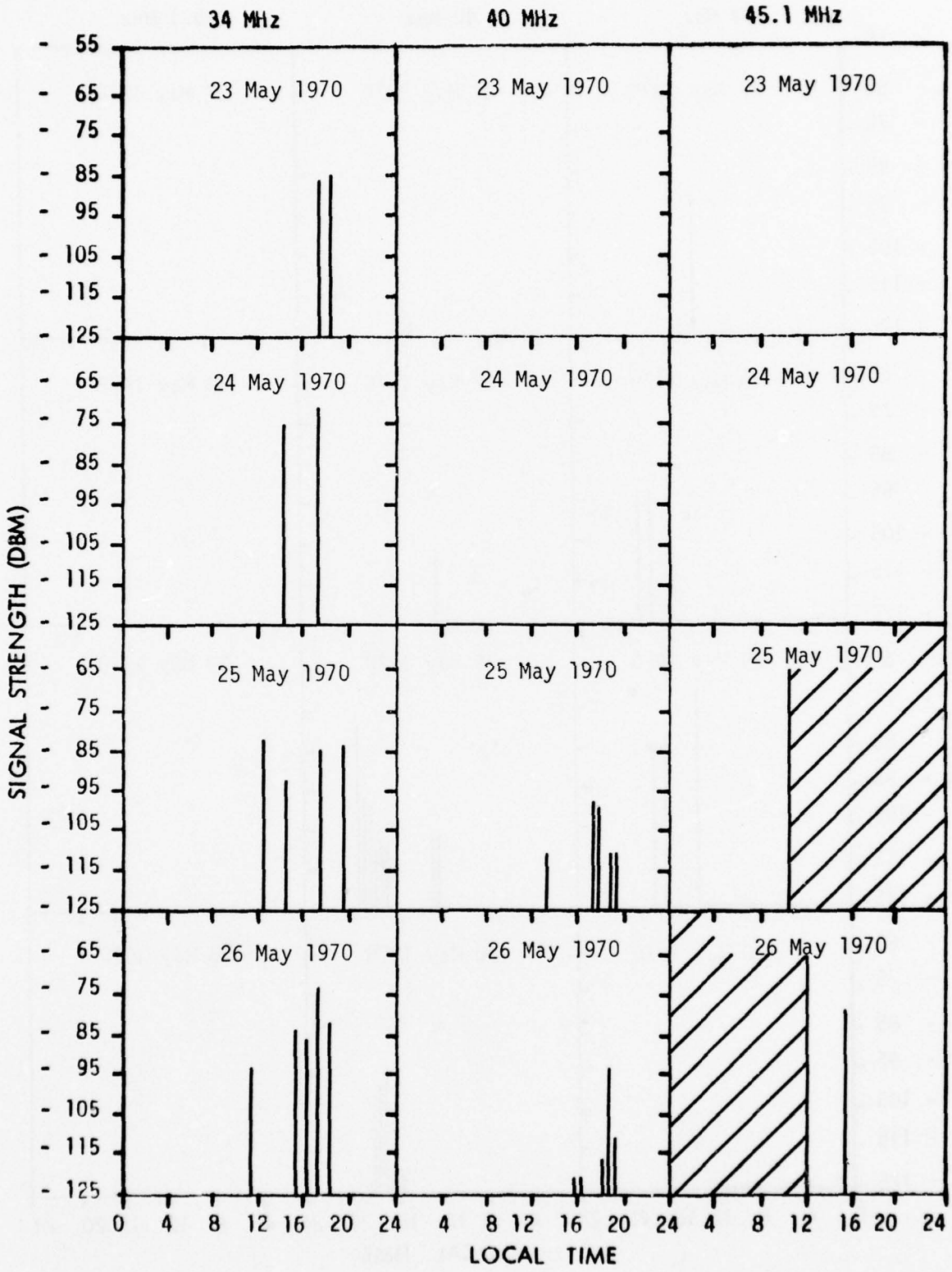

Fig. 98 – 34, 40 and 45.1 MHz Reception at Roma

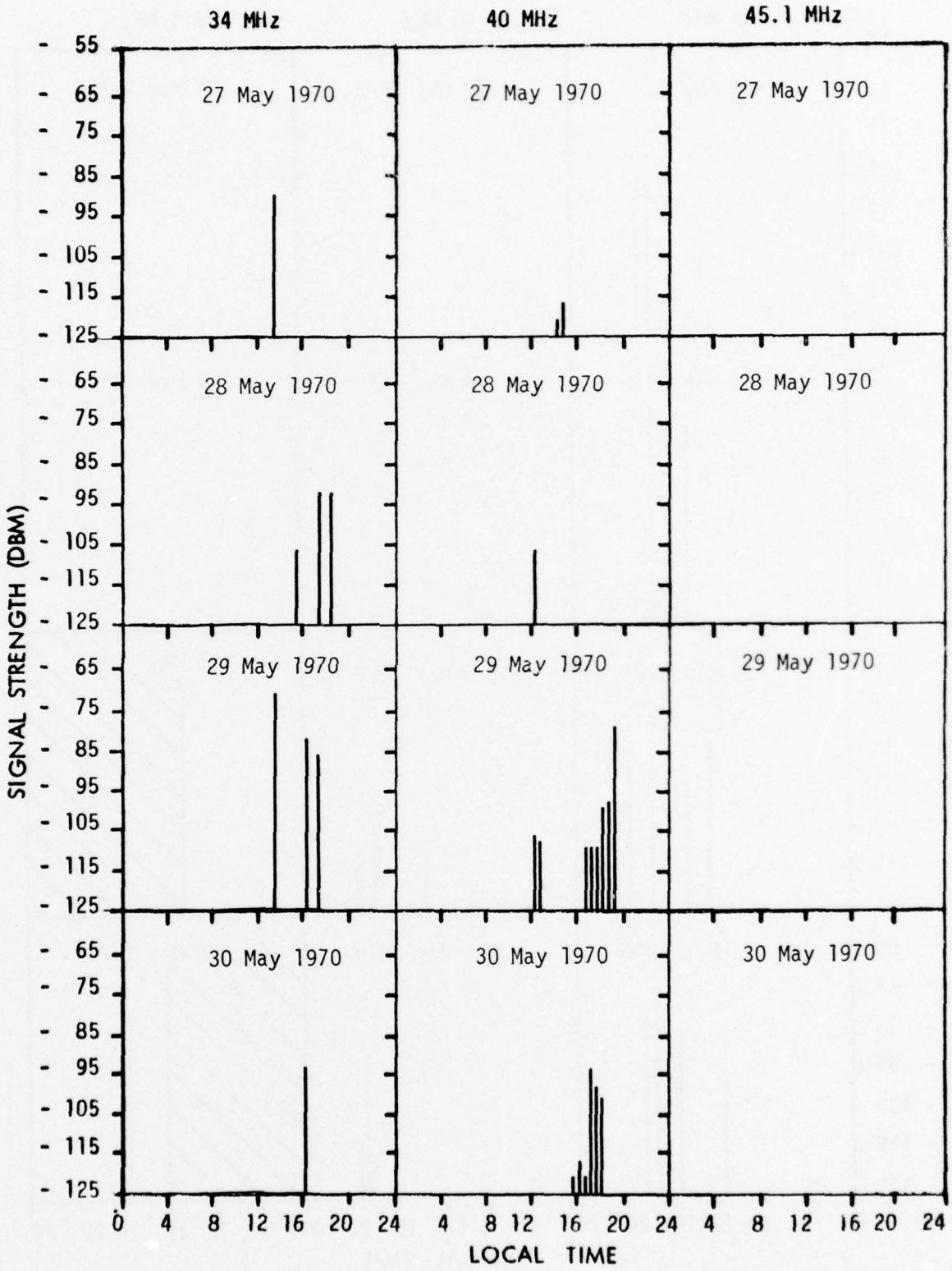

Fig. 99 – 34, 40 and 45.1 MHz Reception at Roma

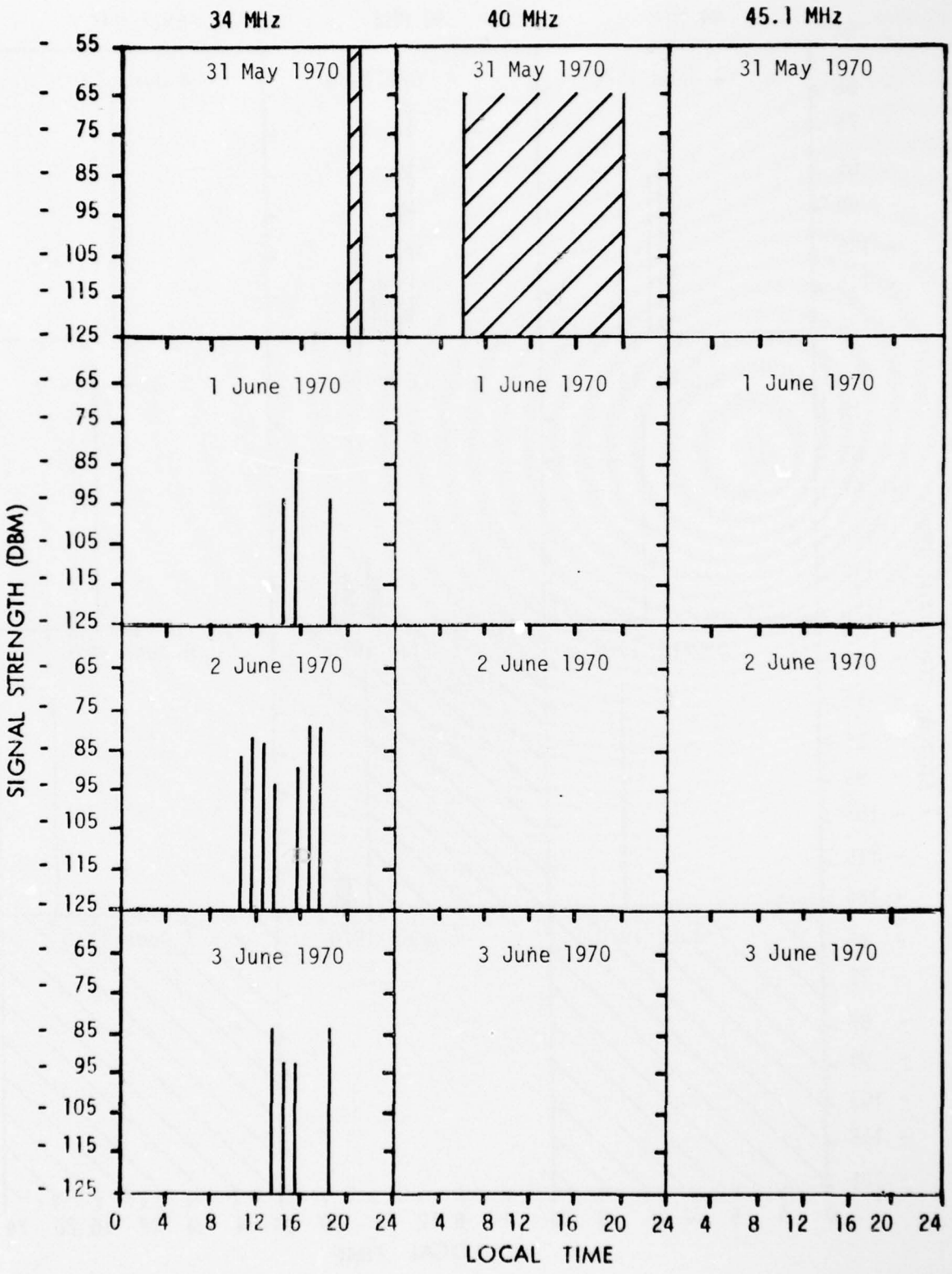

Fig. 100 – 34, 40 and 45.1 MHz Reception at Roma

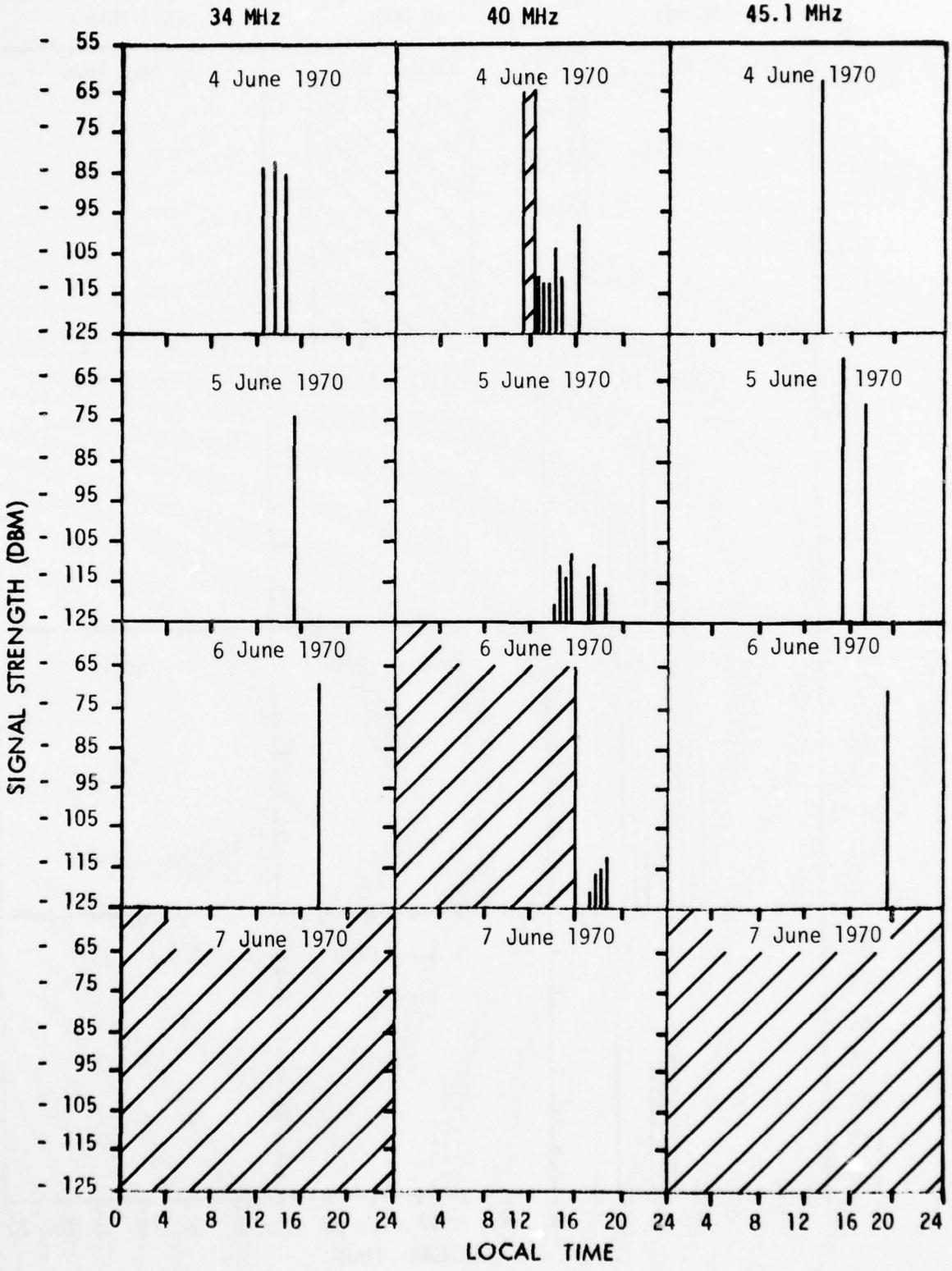

Fig. 101 – 34, 40 and 45.1 MHz Reception at Roma

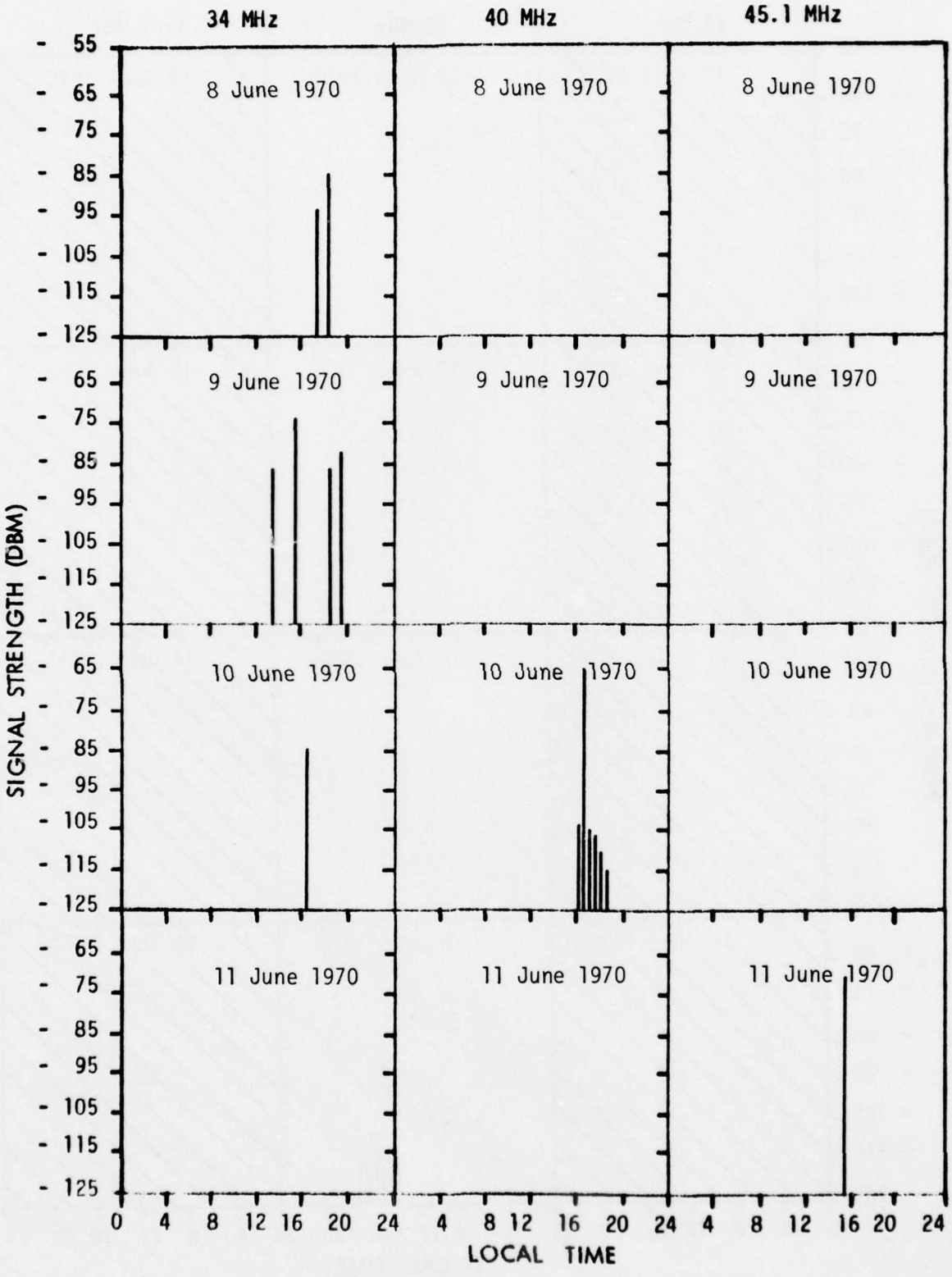

Fig. 102 – 34, 40 and 45.1 MHz Reception at Roma

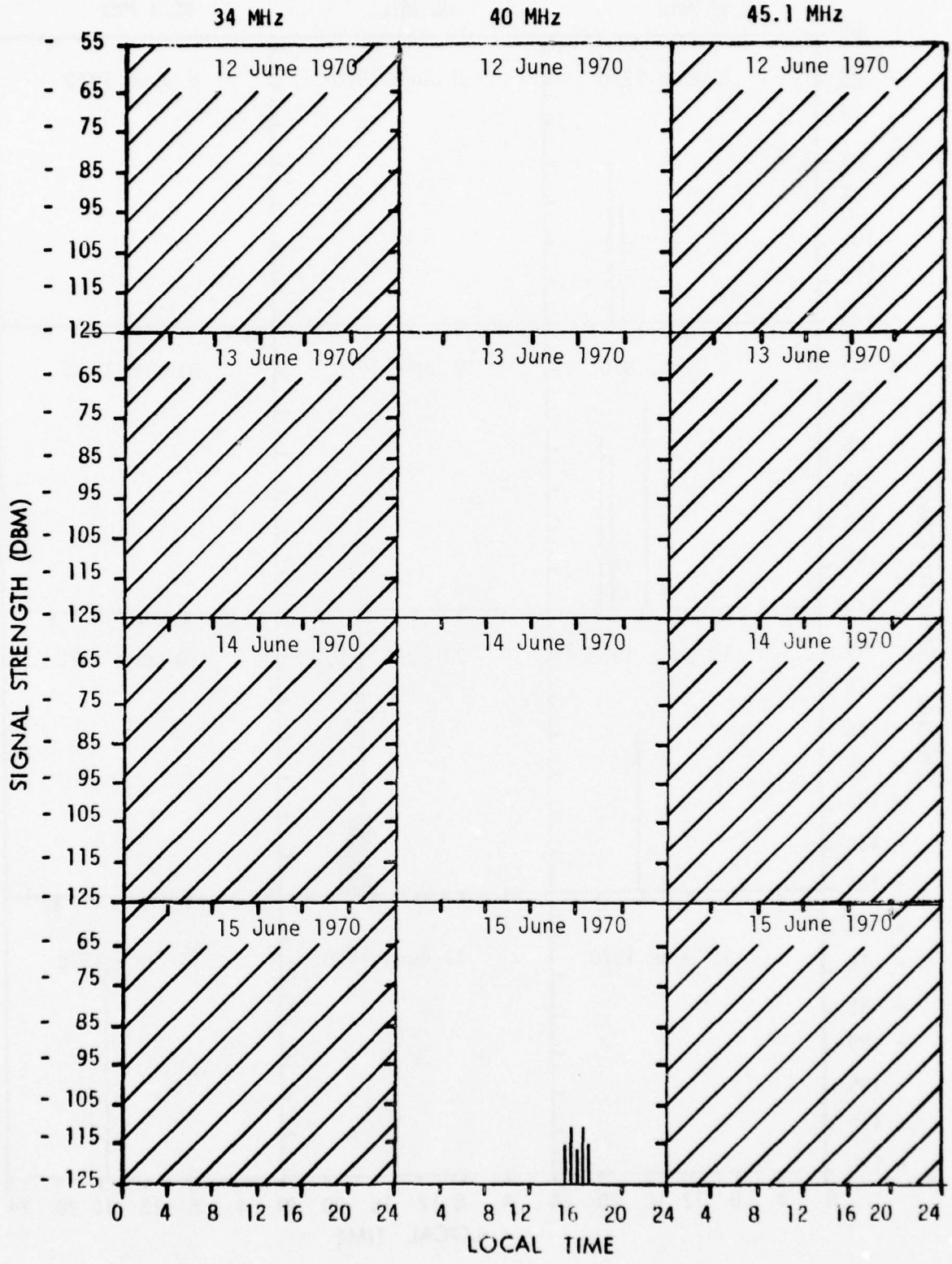

Fig. 103 – 34, 40 and 45.1 MHz Reception at Roma

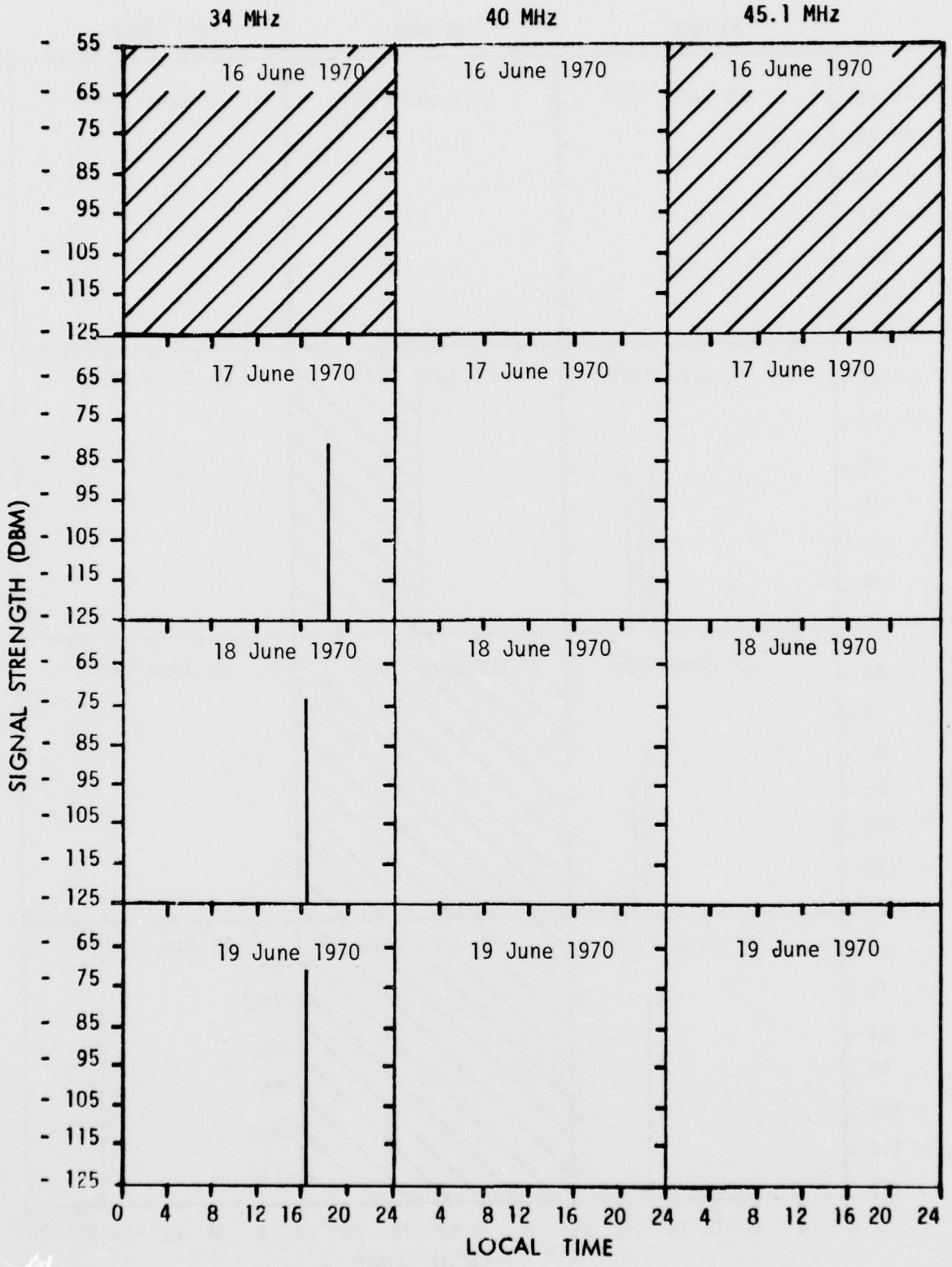

Fig. 104 – 34, 40 and 45.1 MHz Reception at Roma

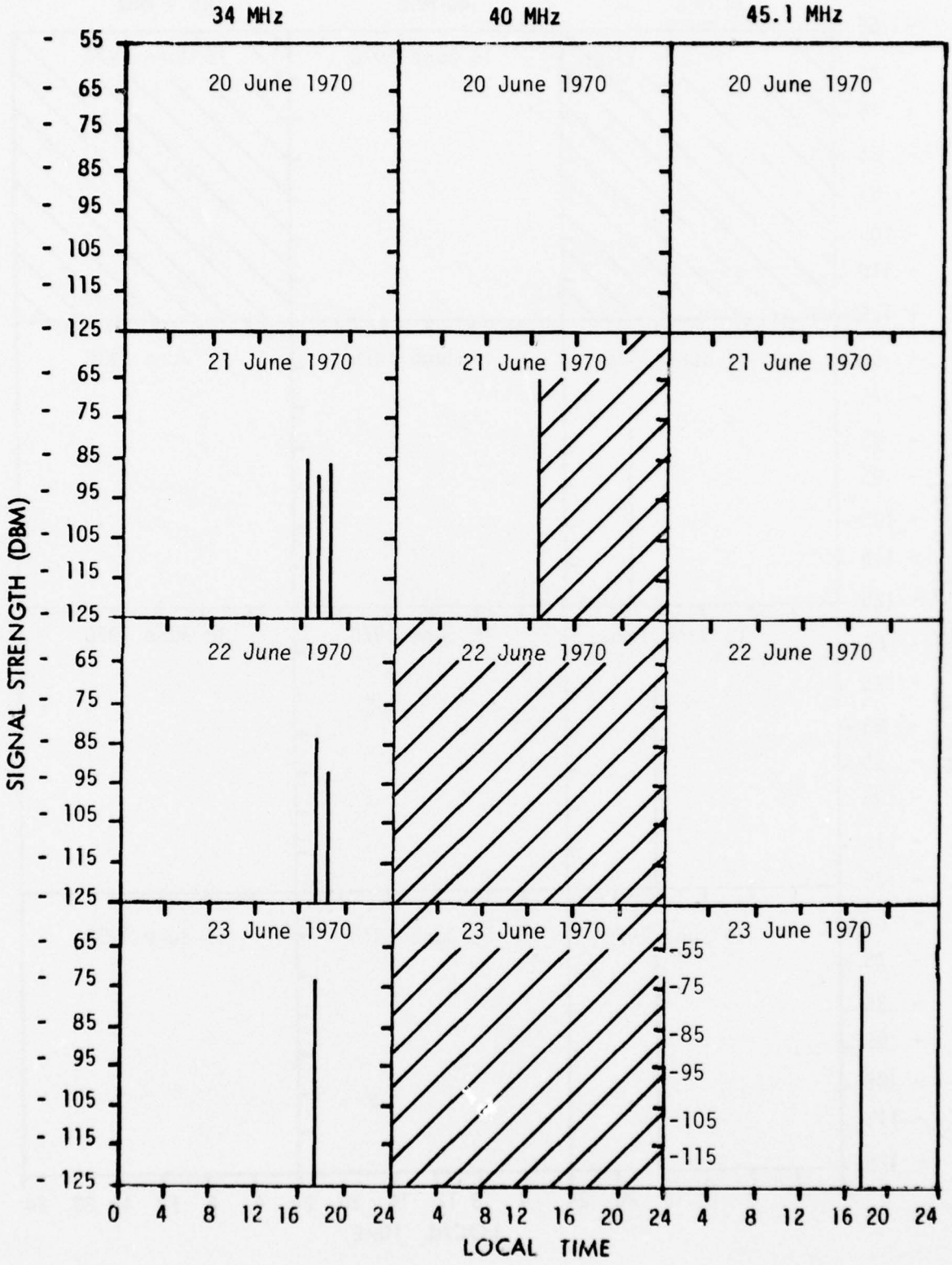

Fig. 105 – 34, 40 and 45.1 MHz Reception at Roma

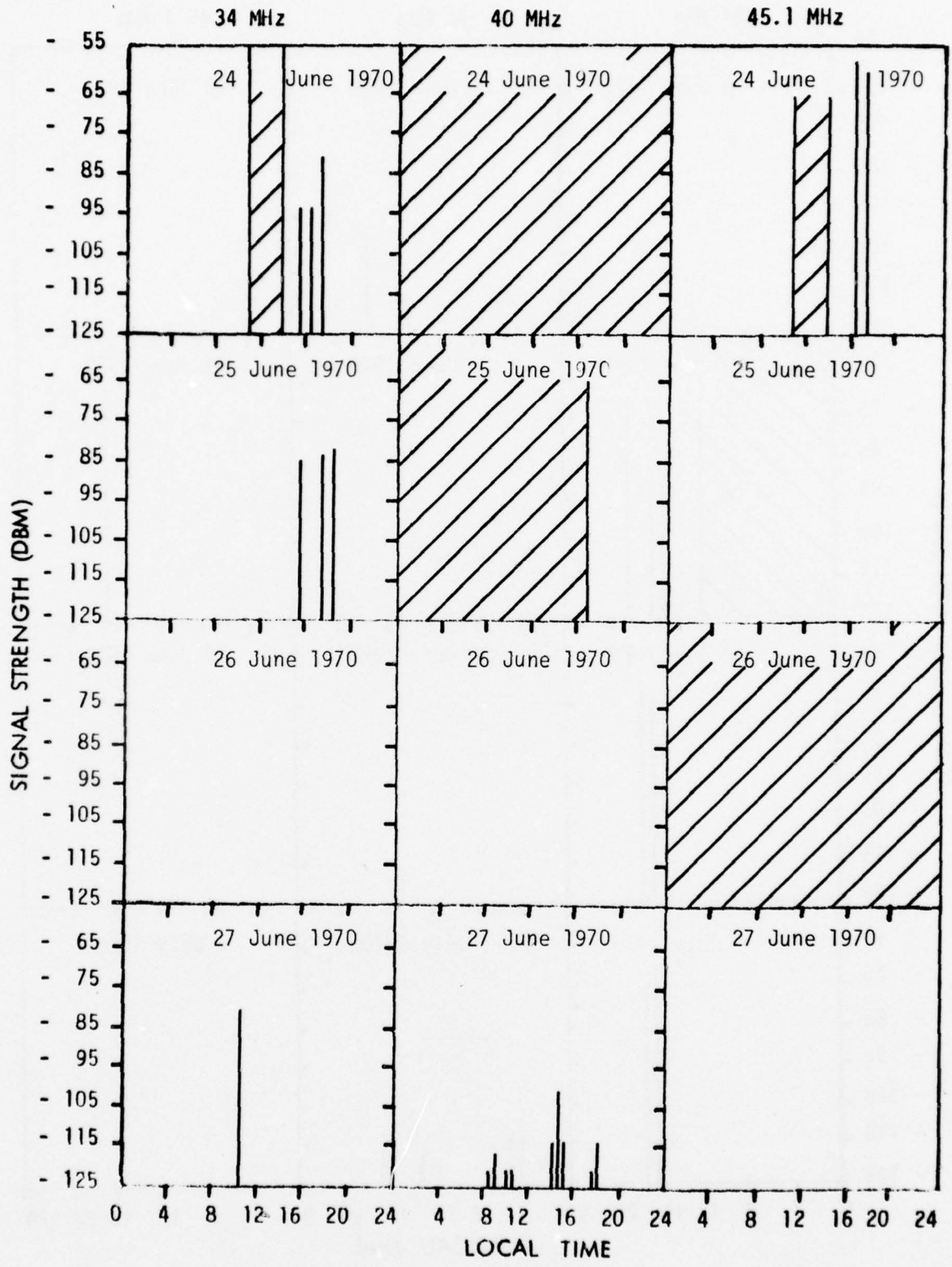

Fig. 106 – 34, 40 and 45.1 MHz Reception at Roma

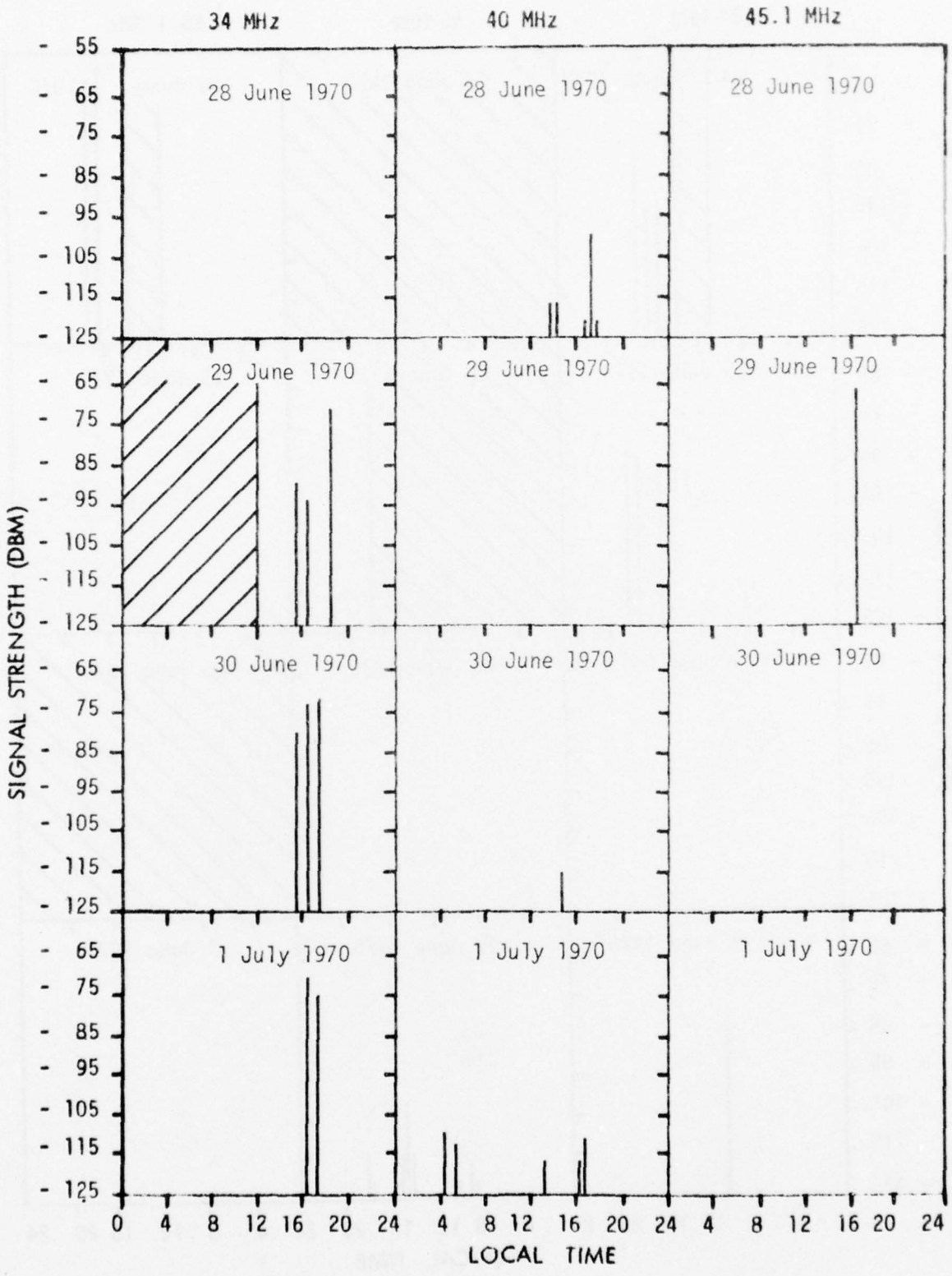

Fig. 107 – 34, 40 and 45.1 MHz Reception at Roma

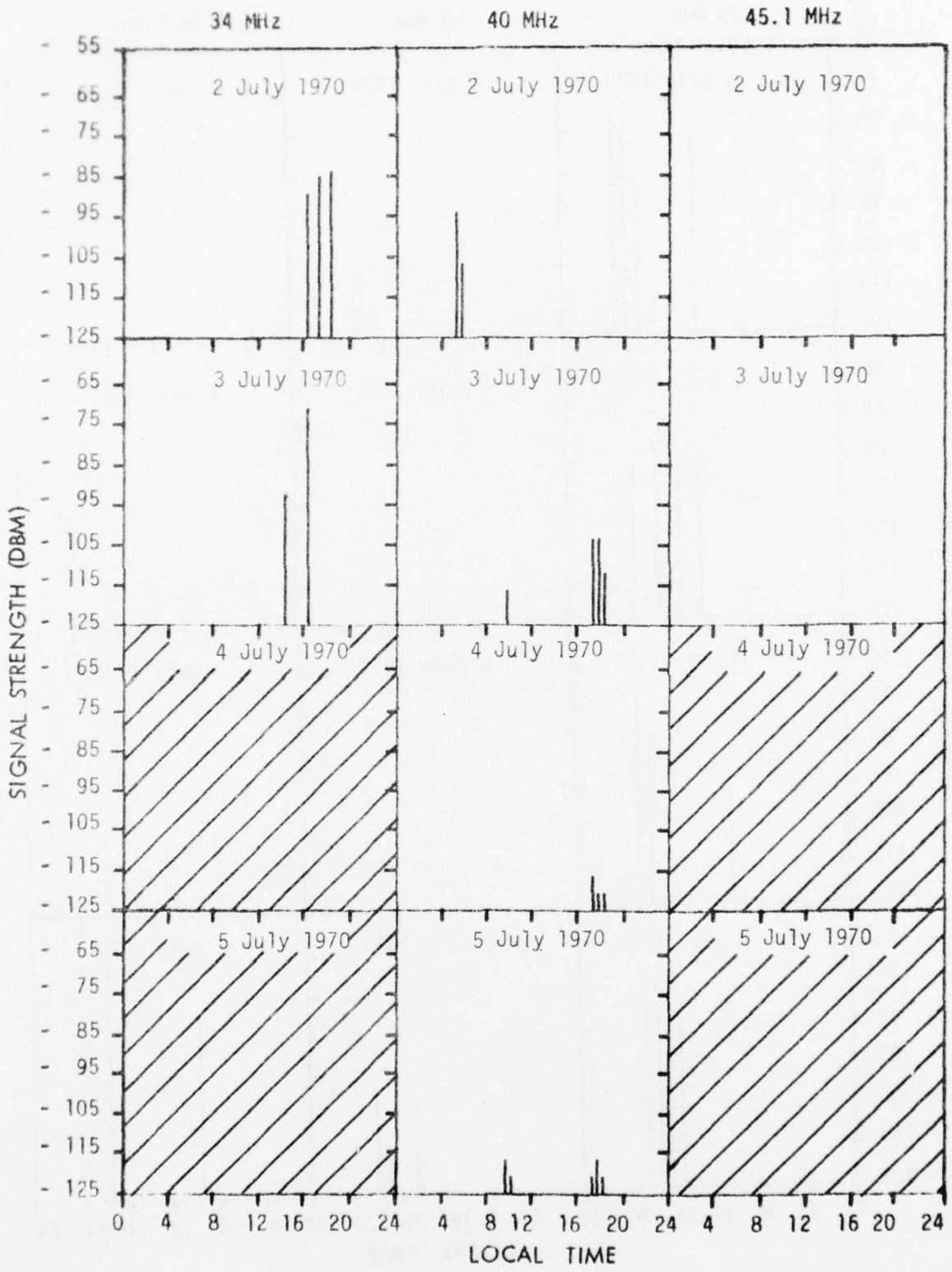

Fig. 108 – 34, 40 and 45.1 MHz Reception at Roma

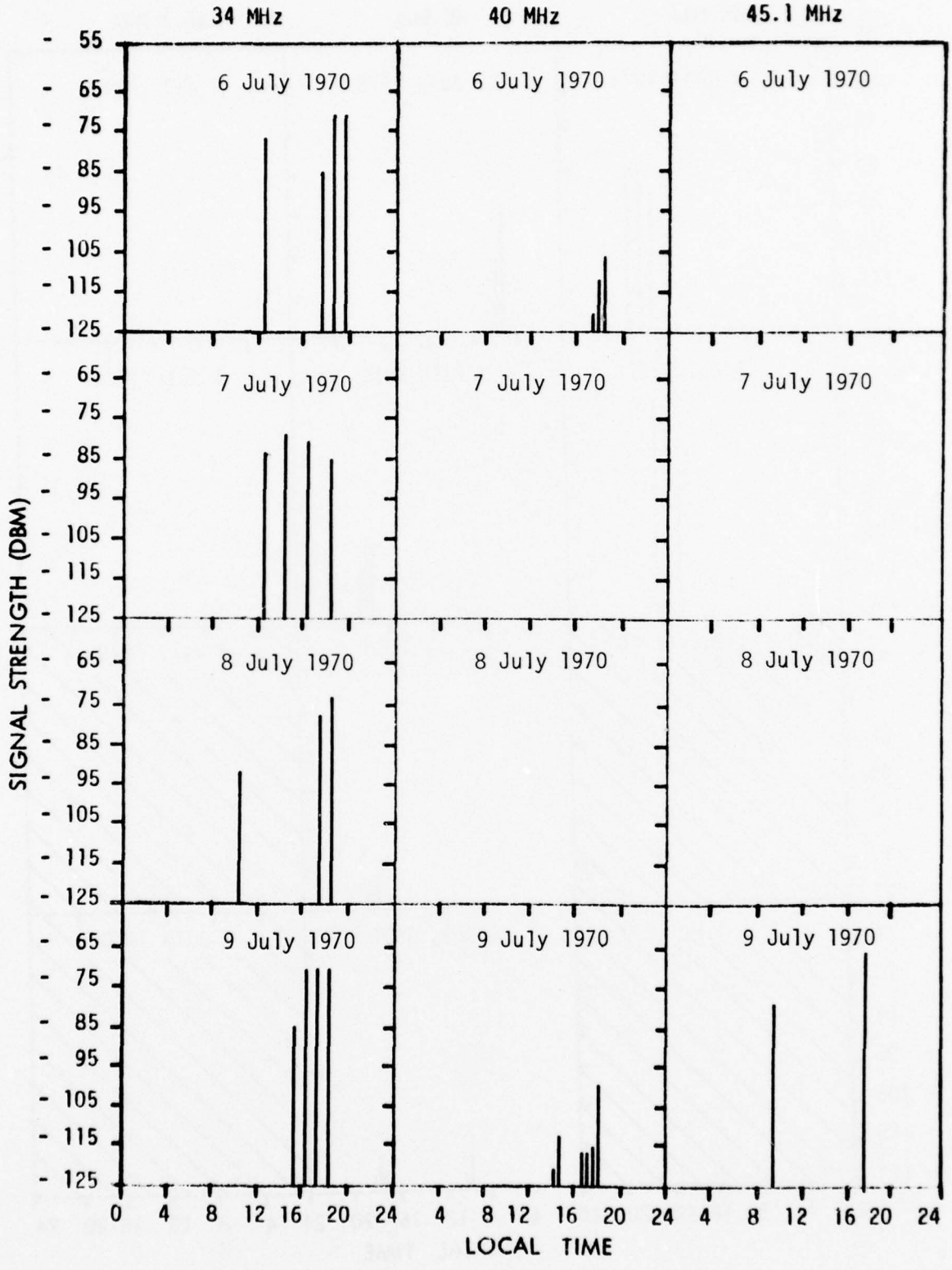

Fig. 109 – 34, 40 and 45.1 MHz Reception at Roma

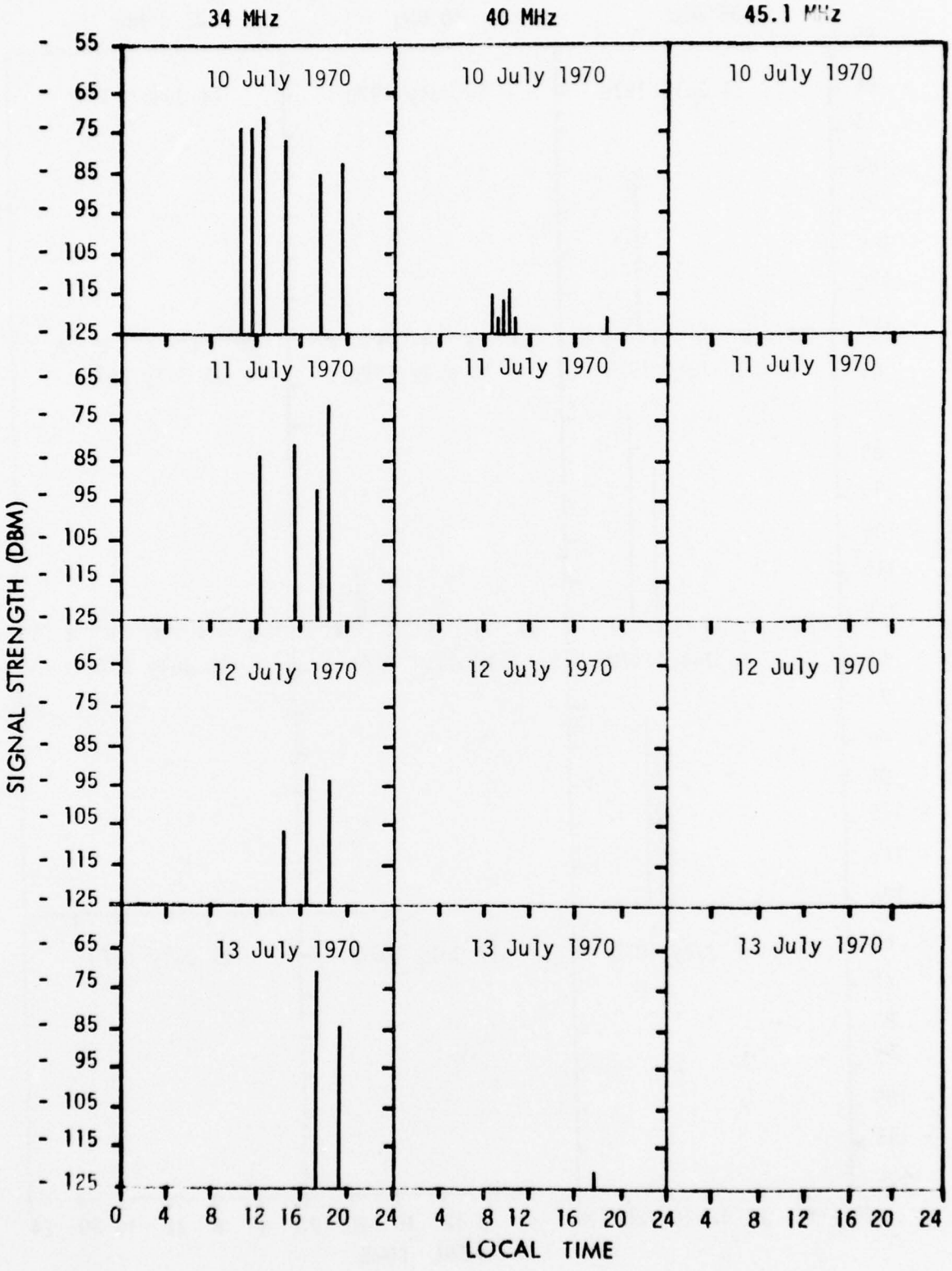

Fig. 110 – 34, 40 and 45.1 MHz Reception at Roma

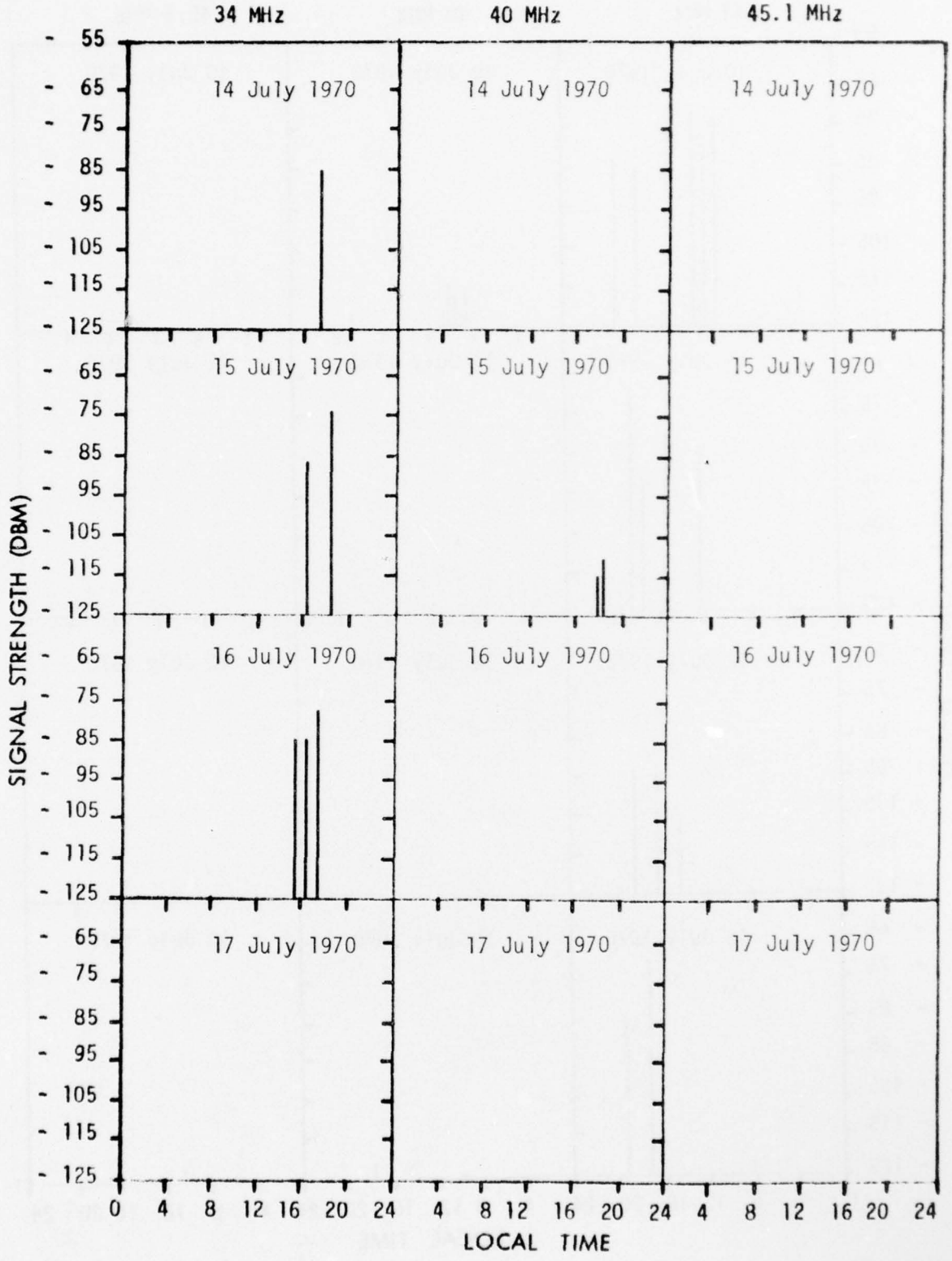

Fig. 111 – 34, 40 and 45.1 MHz Reception at Roma

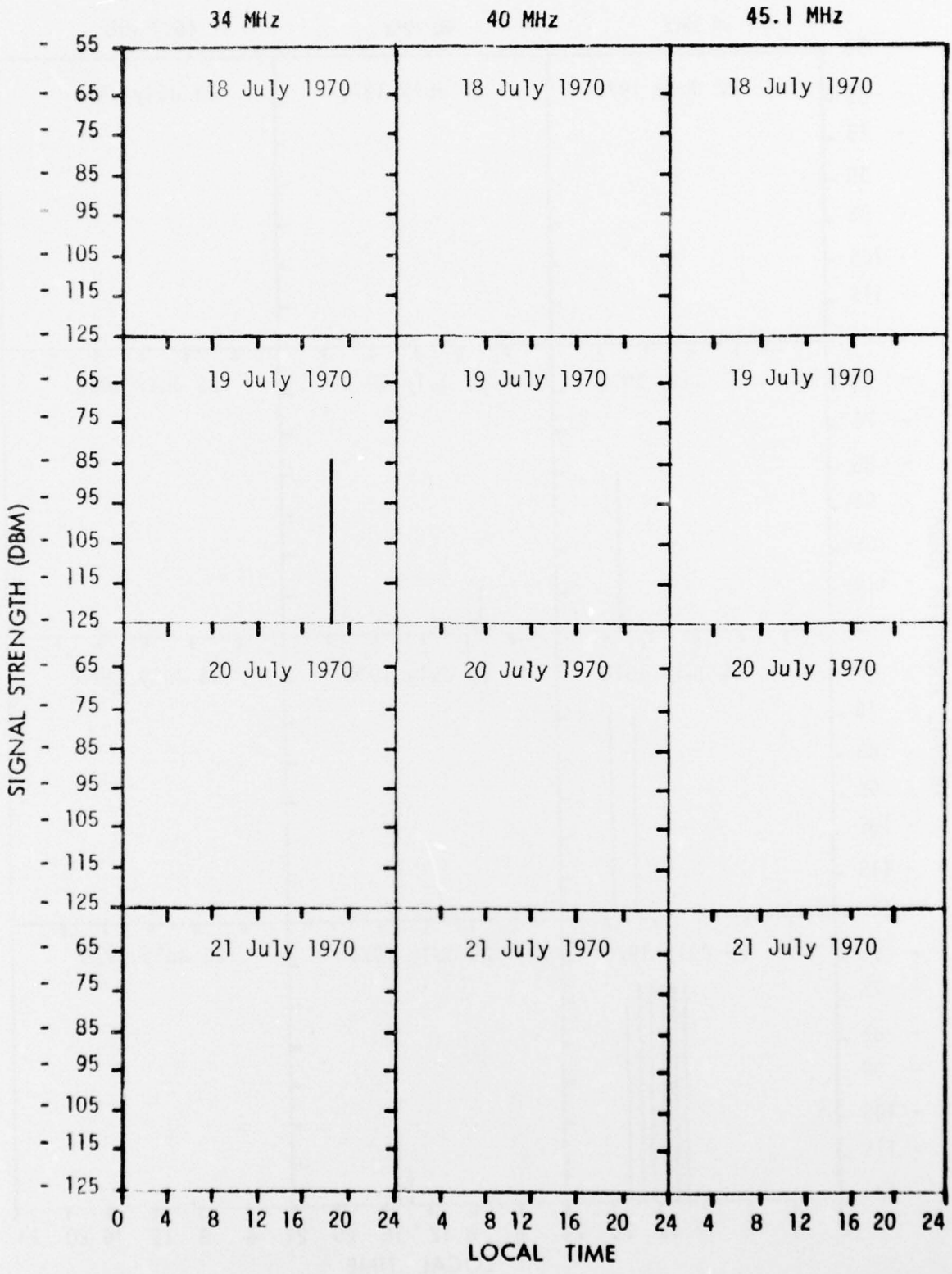

Fig. 112 – 34, 40 and 45.1 MHz Reception at Roma

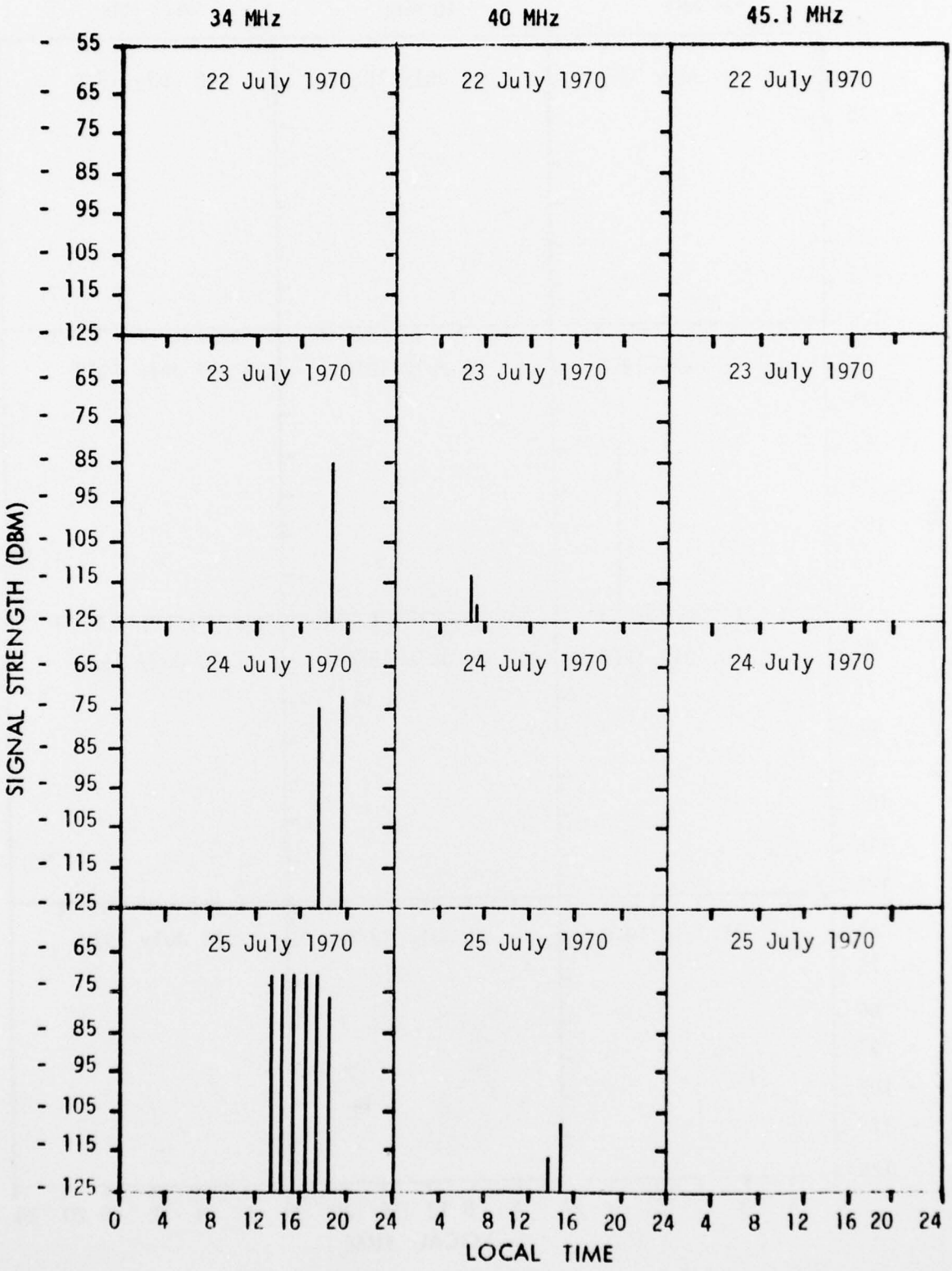

Fig. 113 – 34, 40 and 45.1 MHz Reception at Roma

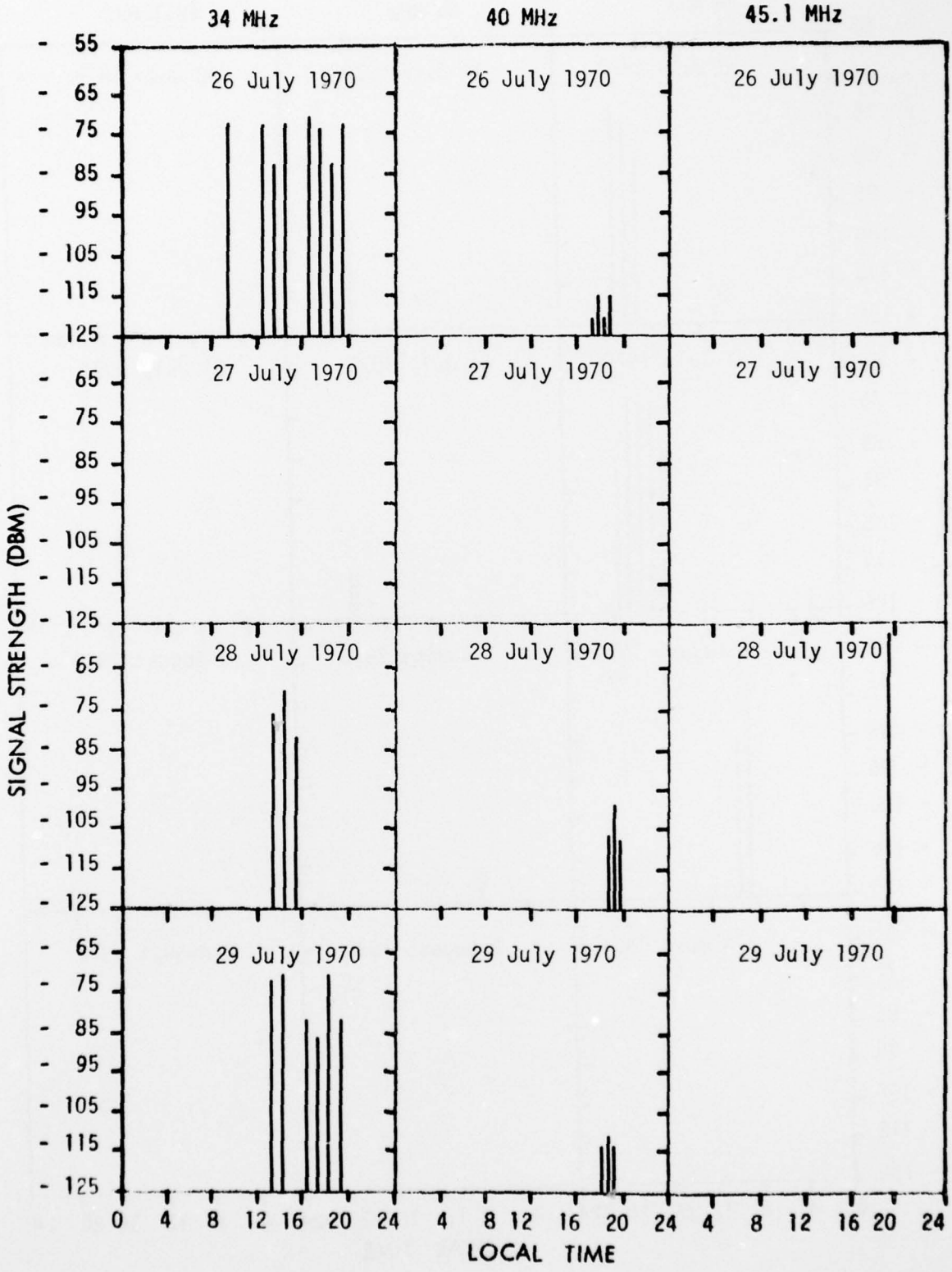

Fig. 114 – 34, 40 and 45.1 MHz Reception at Roma

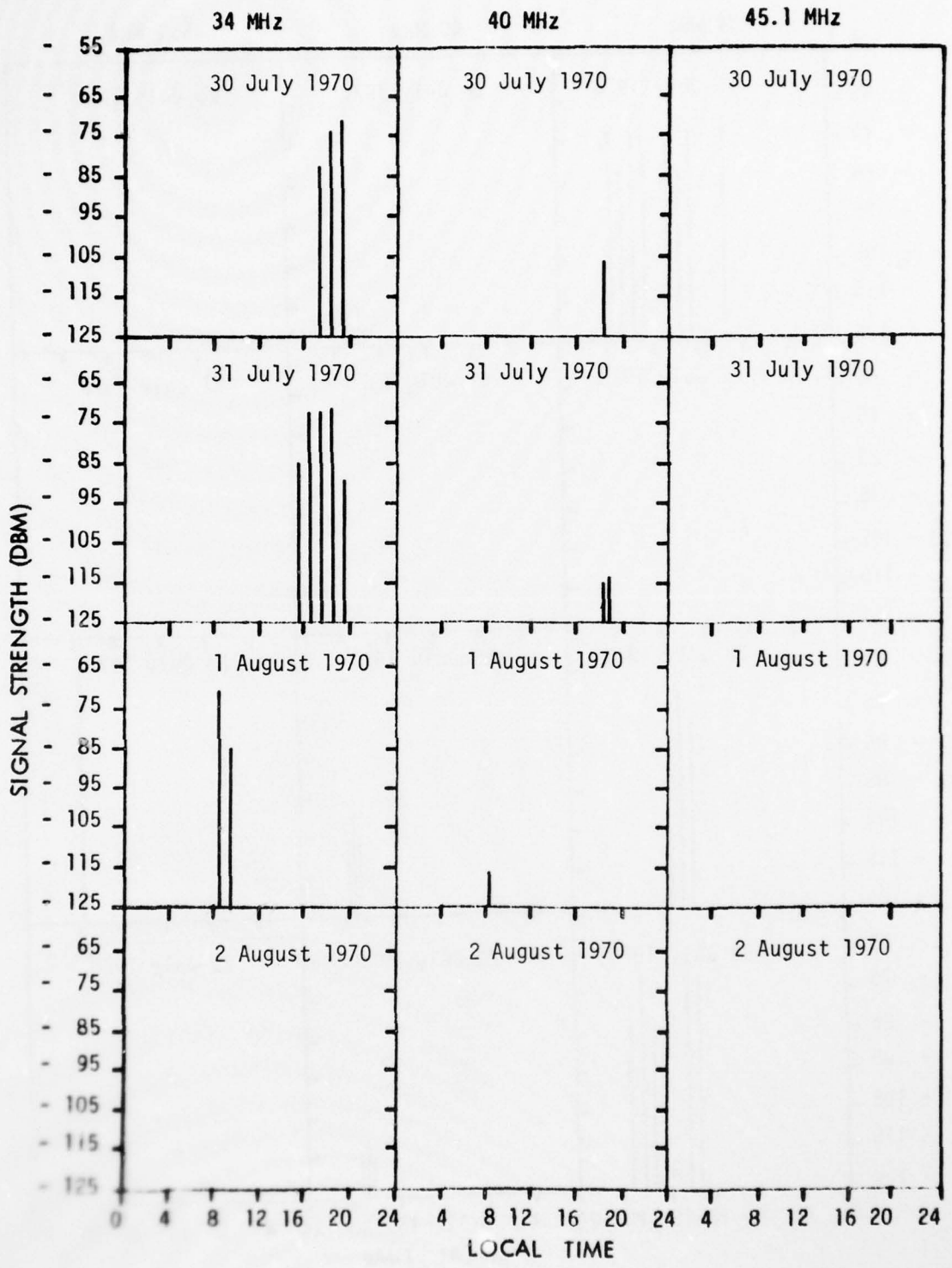

Fig. 115 – 34, 40 and 45.1 MHz Reception at Roma

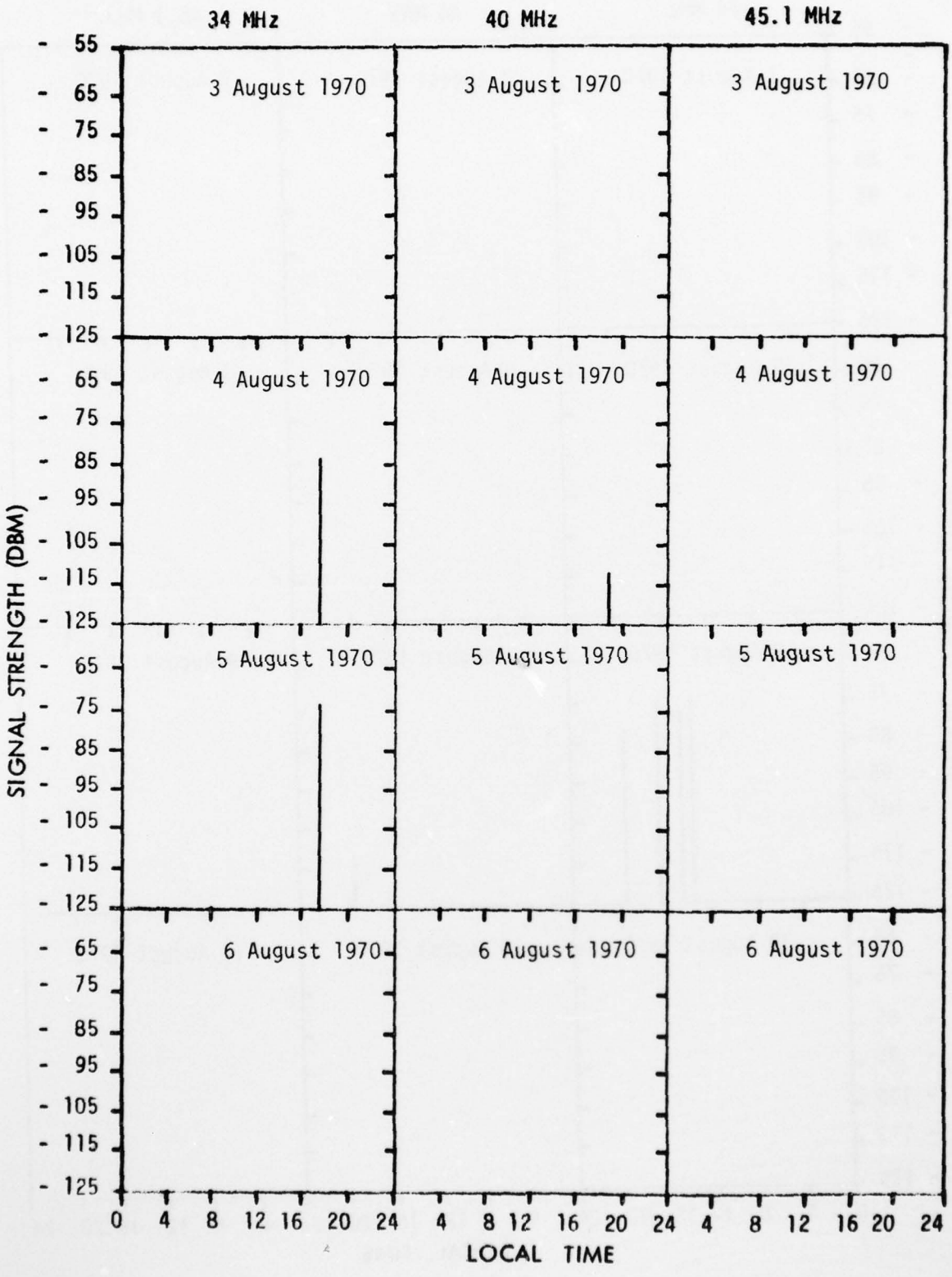

Fig. 116 – 34, 40 and 45.1 MHz Reception at Roma

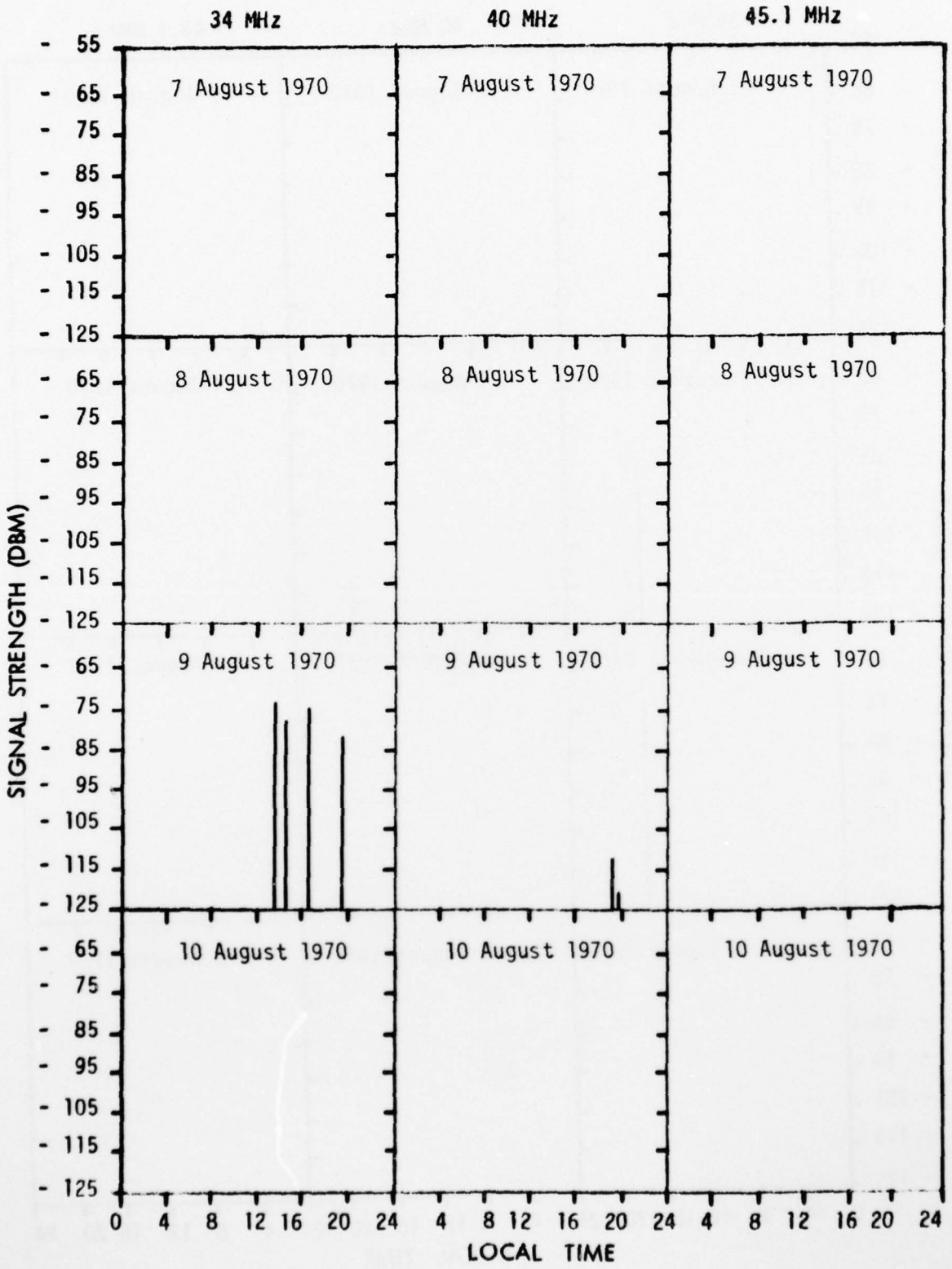

Fig. 117 – 34, 40 and 45.1 MHz Reception at Roma

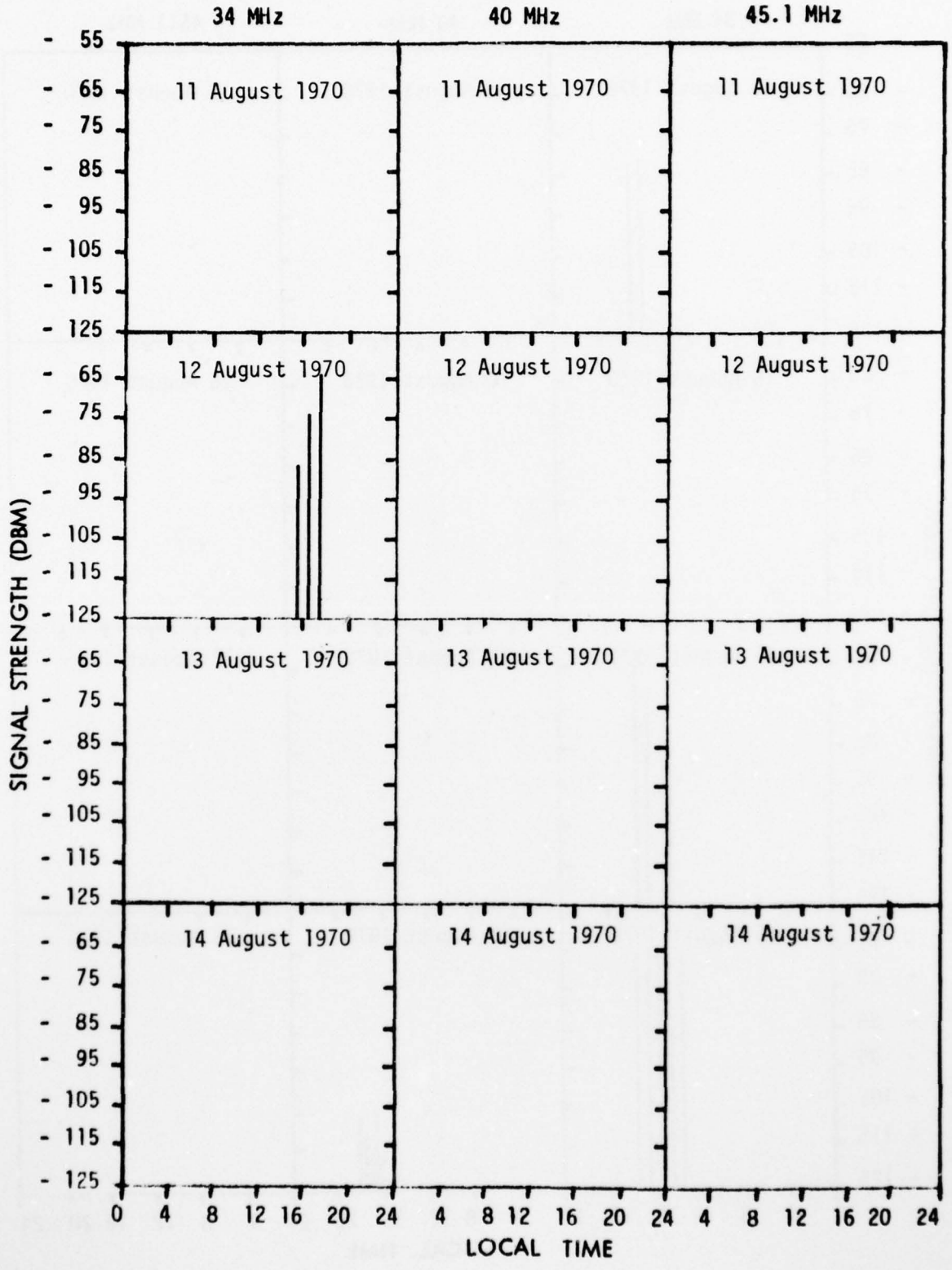

Fig. 118 – 34, 40 and 45.1 MHz Reception at Roma

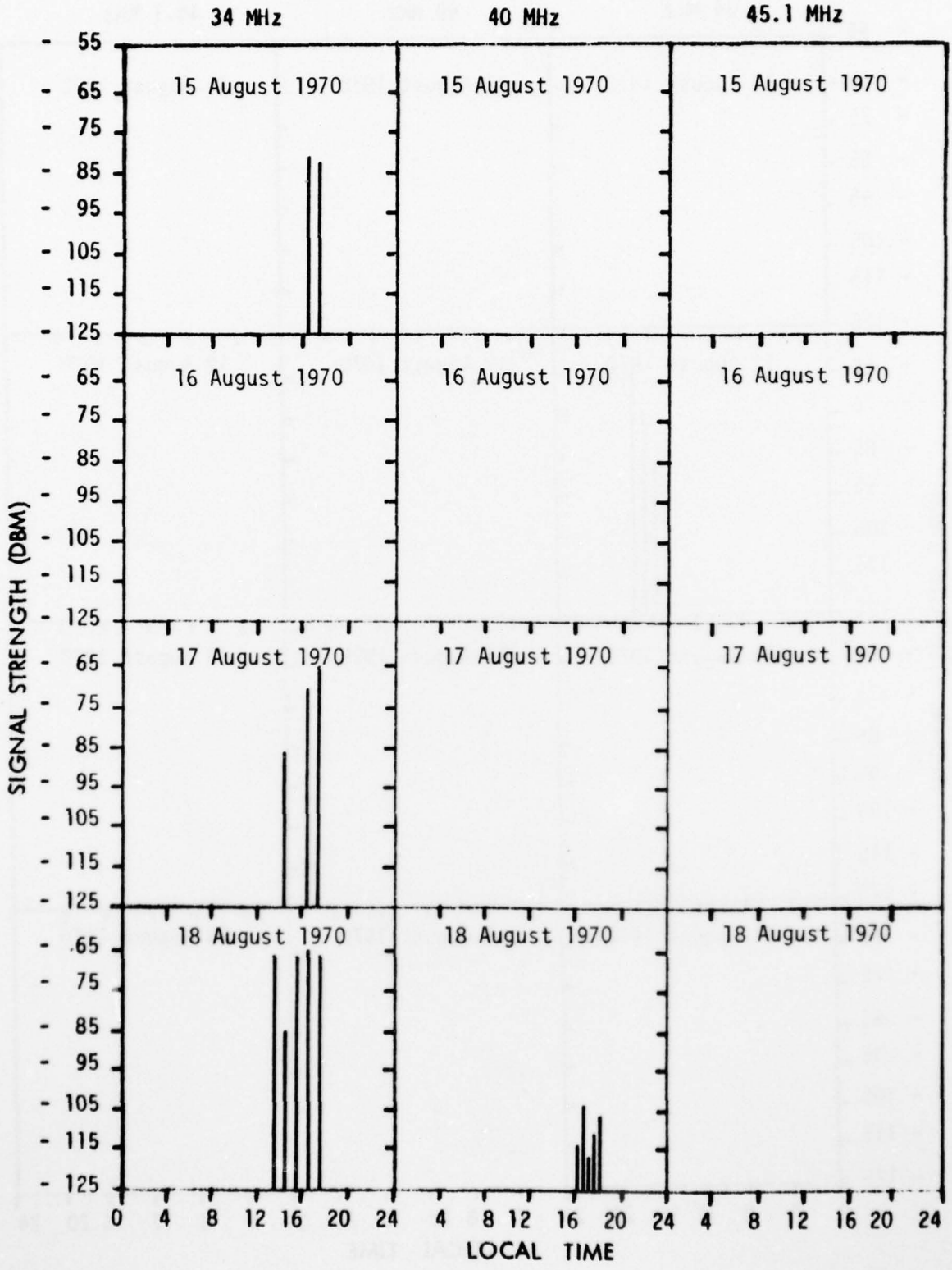

Fig. 119 – 34, 40 and 45.1 MHz Reception at Roma

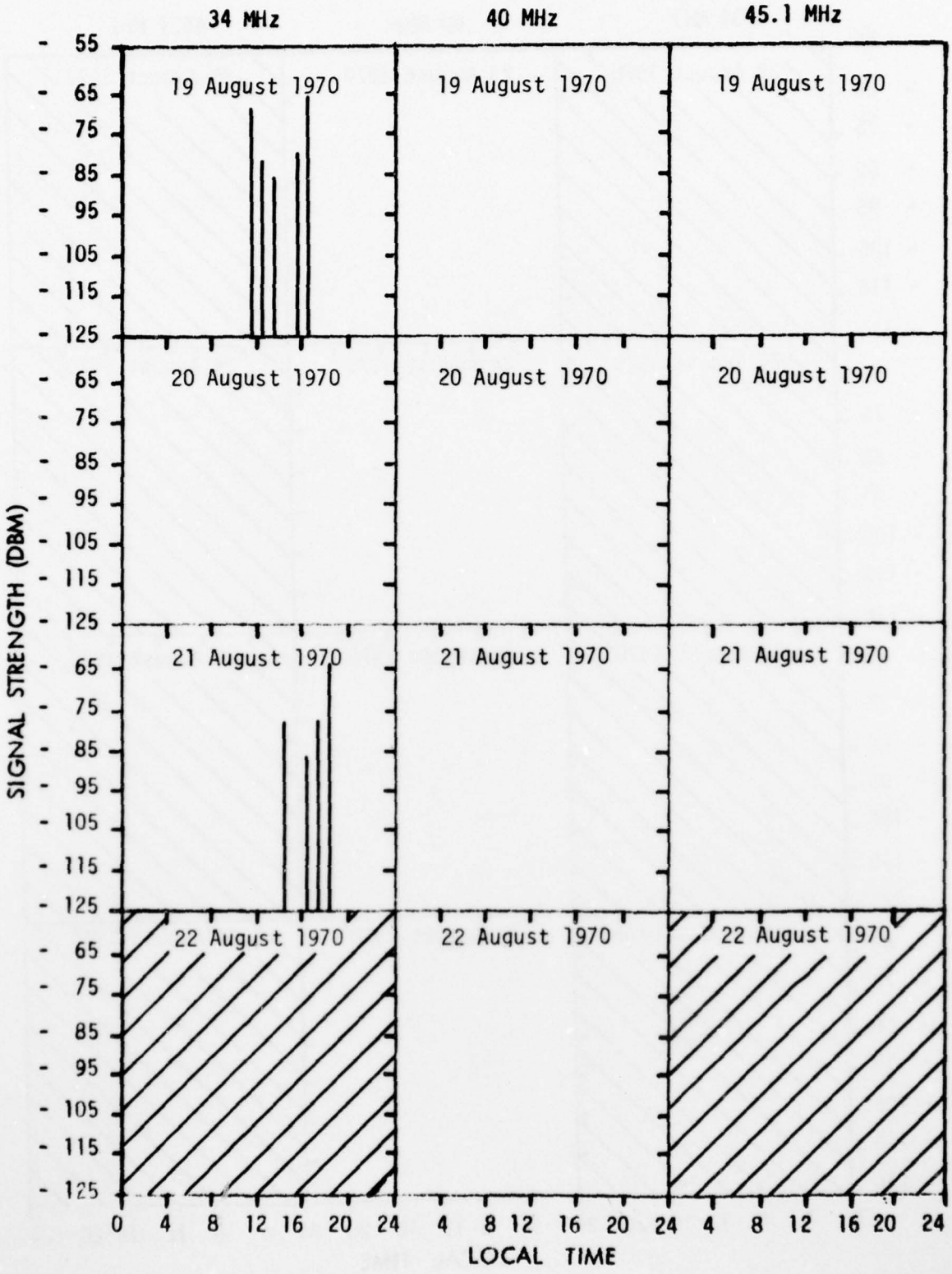

Fig. 120 — 34, 40 and 45.1 MHz Reception at Roma

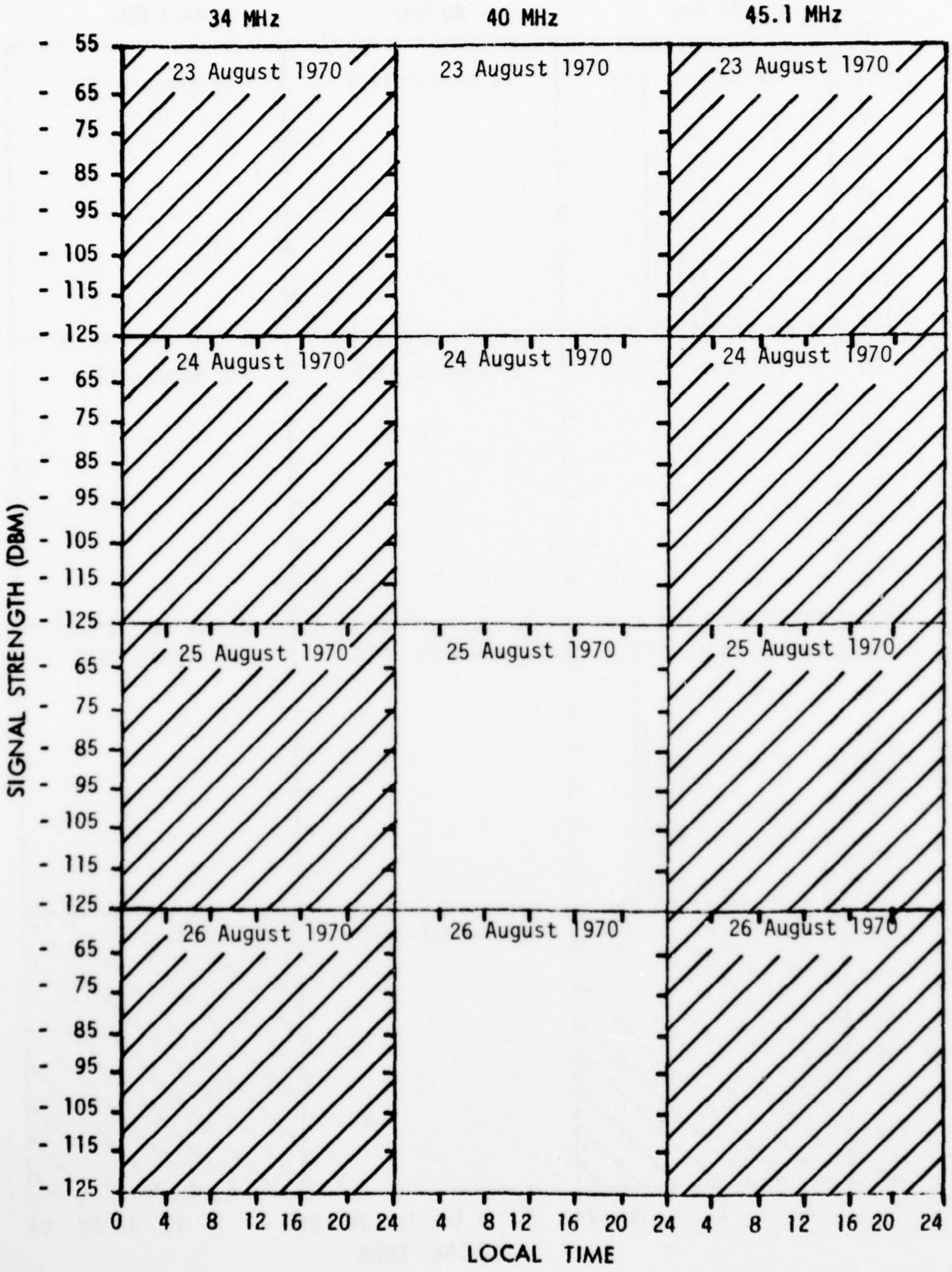

Fig. 121 – 34, 40 and 45.1 MHz Reception at Roma

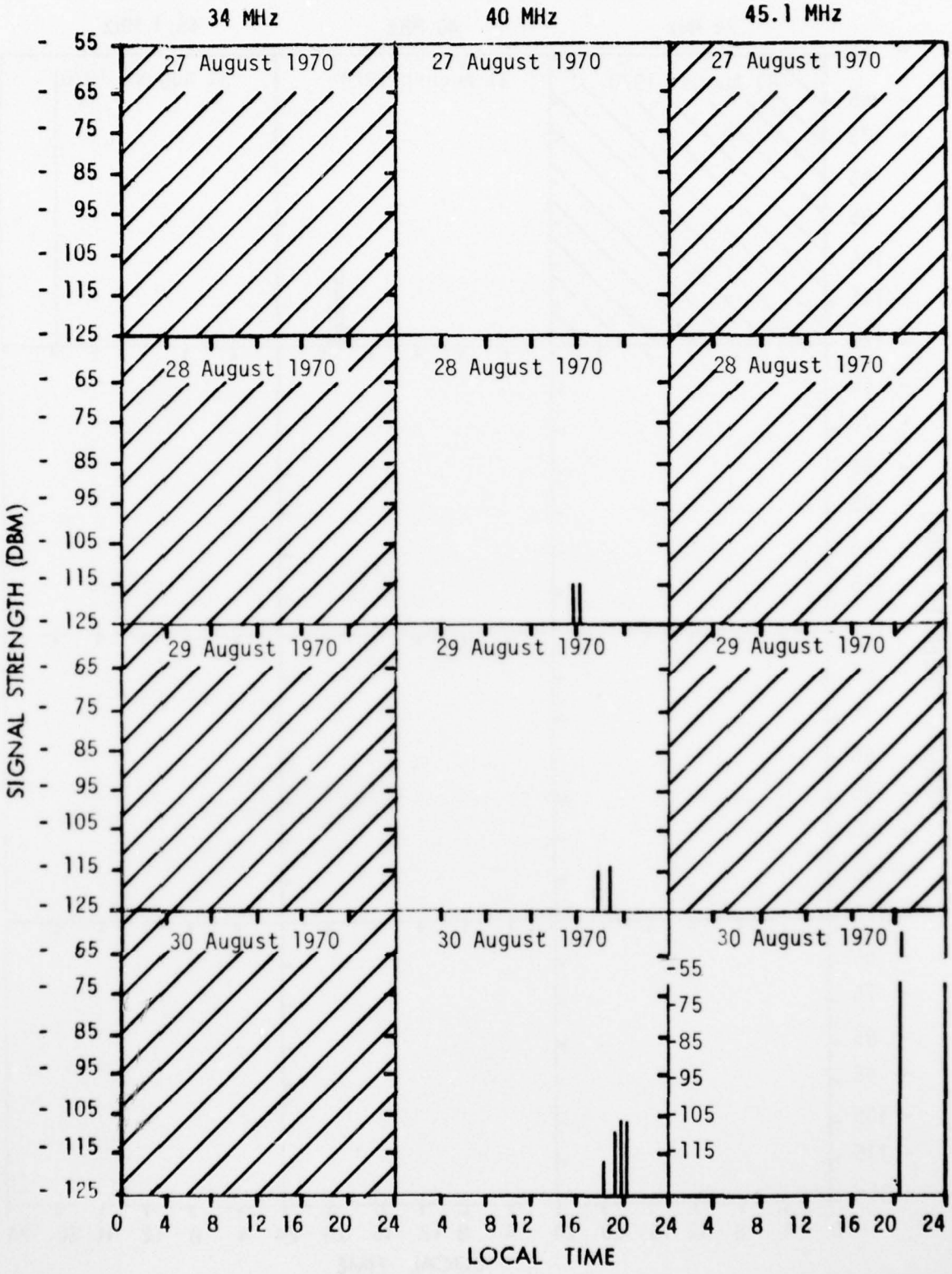

Fig. 122 – 34, 40 and 45.1 MHz Reception at Roma

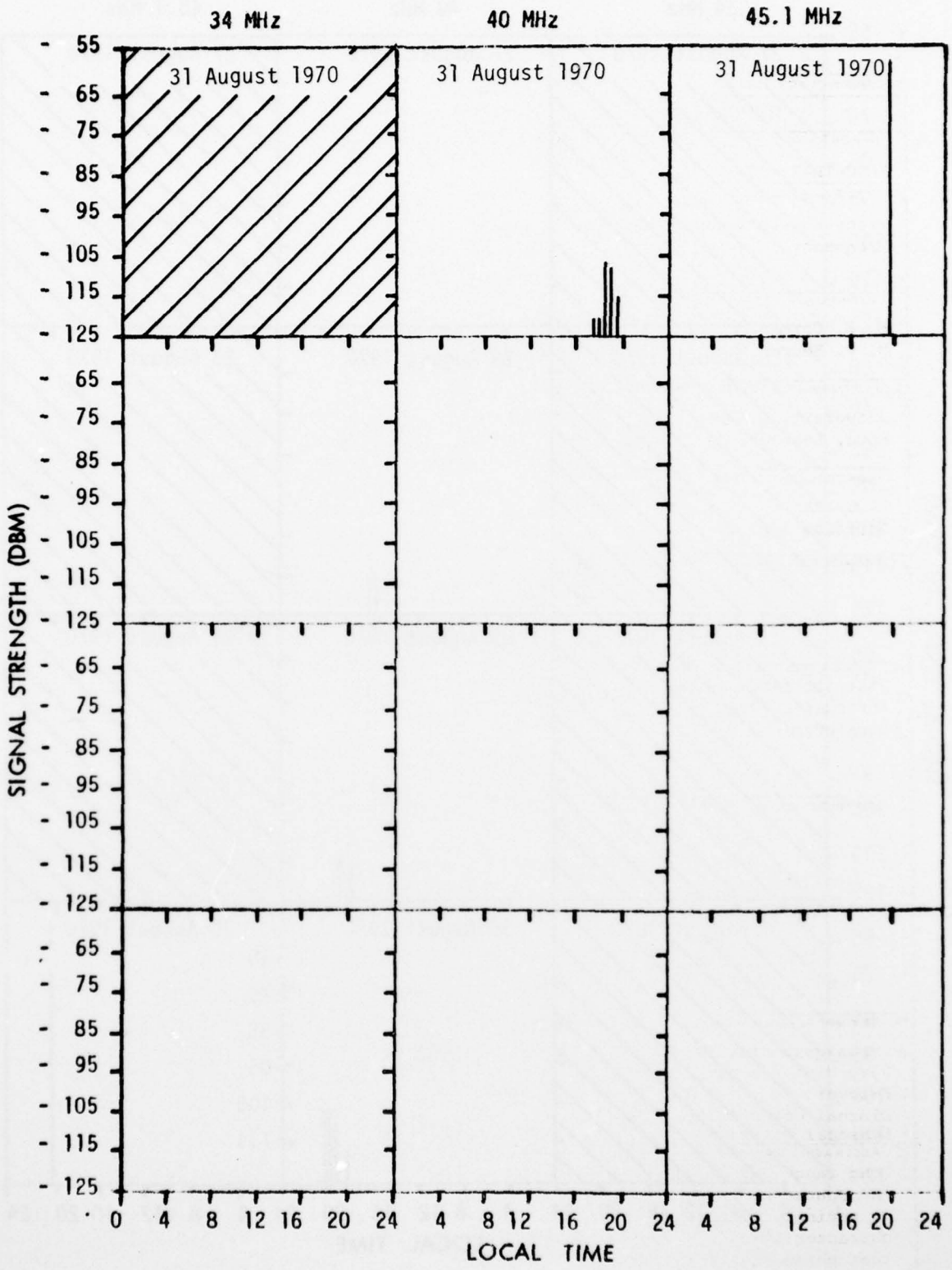

Fig. 123 – 34, 40.and 45.1 MHz Reception at Roma

UNCL

SECURITY CLASSIFICATION OF THIS PAGE *(When Data Entered)*

REPORT DOCUMENTATION PAGE

READ INSTRUCTIONS BEFORE COMPLETING FORM

1. REPORT NUMBER: RADC-TR-73-383	2. GOVT ACCESSION NO.
3. RECIPIENT'S CATALOG NUMBER	
4. TITLE *(and Subtitle)*: Trans-Equatorial Transmissions at Very High Frequency	5. TYPE OF REPORT & PERIOD COVERED: Final, 1 Sep 69 - 18 Apr 72
	6. PERFORMING ORG. REPORT NUMBER: - - -
7. AUTHOR(s): **E. H. Carman**, **M. P. Heeran**	8. CONTRACT OR GRANT NUMBER(s): F61052-67-C-0003
9. PERFORMING ORGANIZATION NAME AND ADDRESS: University of Botswana, Lesotho, and Swaziland, Roma, Lesotho, Africa	10. PROGRAM ELEMENT, PROJECT, TASK AREA & WORK UNIT NUMBERS: Proj 4505, Task 450504
11. CONTROLLING OFFICE NAME AND ADDRESS: RADC/IRAA, Griffiss AFB, NY	12. REPORT DATE: **September 1973** 13. NUMBER OF PAGES: 177
14. MONITORING AGENCY NAME & ADDRESS *(if different from Controlling Office)*: N/A	15. SECURITY CLASS. *(of this report)*: UNCL 15a. DECLASSIFICATION/DOWNGRADING SCHEDULE: N/A

16. DISTRIBUTION STATEMENT *(of this Report)*

DISTRIBUTION STATEMENT A
Approved for public release; Distribution Unlimited

17. DISTRIBUTION STATEMENT *(of the abstract entered in Block 20, if different from Report)*

18. SUPPLEMENTARY NOTES: N/A

19. KEY WORDS *(Continue on reverse side if necessary and identify by block number)*

Transequatorial Transmission
Very High Frequency
F-layer
Diurnal Occurrence
Seasonal Occurrence
Signal Strength
Sunspot Number
Fading
Path Loss
Path Analysis
Equatorial Anomaly
Electron Density Profiles
Airglow
Sudden Ionospheric Disturbances
Irregularities

20. ABSTRACT *(Continue on reverse side if necessary and identify by block number)*

Long range VHF transequatorial propagation (TEP) experiments between Greece and Southern Africa on 34, 40 and 45.1 MHz, in progress since 1967, have an equinoctial character regarding occurrence and strength. Studies of fading characteristics and topside electron density profiles lead to the conclusions that phase coherent signals are most likely at least 2-hop great-circle F-transmissions, while other afternoon and evening types, including flutter, which is strongly related to equatorial spread-F, are off great-circle super-modes involving two reflections from the F-layer without intermediate ground

DD FORM 1 JAN 73 1473 EDITION OF 1 NOV 65 IS OBSOLETE

(see reverse)

UNCL

SECURITY CLASSIFICATION OF THIS PAGE *(When Data Entered)*